

https://dspace.org/

Effects of the environment on the conformational stability of the chloride intracellular channel protein CLIC1

McIntyre, Sylvia

2008-05-20T07:24:15Z
http://hdl.handle.net/10539/4853

Downloaded from a DSpace repository. https://dspace.org/

EFFECTS OF THE ENVIRONMENT ON THE CONFORMATIONAL STABILITY OF THE CHLORIDE INTRACELLULAR CHANNEL PROTEIN CLIC1

Sylvia McIntyre

A thesis submitted to the Faculty of Science, University of the Witwatersrand, Johannesburg, in fulfilment of the requirements for the degree of Doctor of Philosophy

Johannesburg, 2007

DECLARATION

I declare this thesis is my own, unaided work. It is being submitted for the degree of Doctor of Philosophy to the University of the Witwatersrand, Johannesburg. It has not been submitted before for any other degree or examination at any other University.

_____

Sylvia McIntyre

_____ day of _____ 2007

This work is dedicated to the people I love;

To Mom and Dad

To Sonia and Dario

Ai miei Nonni

And to my husband, Robbie

"To see what everybody else has seen, and think what nobody else has thought". Dr. Albert Szent-Györgyi

ABSTRACT

CLIC1 is an intracellular membrane protein that is unusual in that it can exist in both a soluble and an integral membrane form. The manner in which this protein inserts into membranes is unknown although it is proposed to undergo a change in structure whereby it initially experiences a degree of unfolding and then refolds into its new membrane-bound conformation. This study focuses on the characterisation of CLIC1 in terms of its secondary, tertiary and quaternary structure, the determination of its conformational stability at equilibrium and the establishment of its unfolding kinetics, all under conditions of varying pH, polarity, redox conditions, temperature and ionic strength. CLIC1 was found to be most stable at pH 7.0 / 20^{o}C. The unfolding process is two-state and cooperative, producing a $\Delta G(H_2O)$ of ~10 kcal/mol and a *m*-value of ~2 kcal/mol per molar urea. A decrease in pH to 5.5 or an increase in temperature to 37^{o}C resulted in the stabilisation of an equilibrium intermediate species under mild denaturing conditions and a destabilisation of the native state. This was further evidenced by an increase in the rate of unfolding of CLIC1 from the native state to the denatured state under these conditions. A state with similar properties to the intermediate species was detected in the absence of urea at pH 5.5 / 37^{o}C and under non-reducing conditions at both pH 7.0 / 20^{o}C and pH 5.5 / 20^{o}C. The intermediate species is more hydrophobic than either the native or denatured state; it is stabilised by salts, has a reduced secondary structure, increased flexibility and a buried Trp35 relative to the native state. The rate of formation of the intermediate species is a slow process which may involve an oligomerisation step. The results from this study provide an interpretation for the structure and mechanism of CLIC1 pore formation *in vivo* by comparing the effects of the environment on the structure and stability of the protein.

ACKNOWLEDGEMENTS

I would like to express my sincere thanks to Professor H. Dirr for his constant guidance, help and support, for inspiring me, motivating me and for helping me to appreciate and share in his passion for protein biochemistry.

Thank you to all the members of the Protein Structure-Function Research Unit and especially to Chris Nathaniel, Stoyan Stoychev, Diane Kuhnert, Samantha Gildenhuys and Portia Lutya for the stimulating discussions, assistance, encouragement and friendship throughout our studies together.

And, of course I am extremely grateful to the National Research Foundation of South Africa and the University of the Witwatersrand for their financial assistance without which, this work would not have been possible.

TABLE OF CONTENTS

ABSTRACT ..... **IV**

ACKNOWLEDGEMENTS ..... **V**

ABBREVIATIONS ..... **X**

LIST OF FIGURES ..... **XII**

LIST OF TABLES ..... **XV**

CHAPTER 1. INTRODUCTION **1**

1.1. Electrostatic Contributions to Protein Stability **2**

1.1.1. Electrostatic Interactions 2
1.1.2. The Effect of pH on Protein Stability 3
1.1.3. The Effect of Ionic Strength on Protein Stability 5
1.1.4. The Role of Charged Amino Acid Residues 10

1.2. Protein Stability and Folding: Thermodynamics and Forces Involved **11**

1.2.1. Introduction 11
1.2.2. Van der Waals Forces 11
1.2.3. Hydrogen Bonds 12
1.2.4. The Hydrophobic Effect 14
1.2.5. The Entropic and Enthalpic Effects 15

1.3. Conformational States Available to a Protein **17**

1.3.1. Introduction 17
1.3.2. Mechanisms of Protein Folding 17
1.3.3. The Native State 20
1.3.4. The Denatured State 22
1.3.5. Detecting Intermediates 25
1.3.6. The Molten Globule State 26

1.4. CLIC1 and Other Soluble Membrane Proteins **29**

1.4.1. Chloride Intracellular Channels 29

1.4.2. Structure of CLIC1 39
1.4.3. Stability and Folding of Members of the GST Superfamily . 49
1.4.4. Stability and Folding of Membrane Proteins 56
1.5. Objectives 78

CHAPTER 2. EXPERIMENTAL 79

2.1. Materials 79

2.2. Methods 79

2.2.1. Plasmid Verification 79
2.2.2. CLIC1 Expression and Purification 80
2.2.3. SDS-PAGE 82
2.2.4. Protein Concentration Determination 83
2.2.5. SEC-HPLC 84
2.2.6. Dynamic Light Scattering 84
2.2.7. Changing pH, Polarity, Ionic Strength, Temperature and Redox Conditions 85
2.2.8. Circular Dichroism Measurements 87
2.2.9. Fluorescence Measurements 89
2.2.10. Reversibility Studies 91
2.2.11. Urea - Induced Equilibrium Unfolding 92
2.2.12. Unfolding Kinetics 100

CHAPTER 3. RESULTS 103

3.1. CLIC1 Purification 103

3.1.1. Plasmid Verification 103
3.1.2. CLIC1 Expression and Purification 103

3.2. Structural Characterisation of CLIC1 108

3.2.1. Effect of pH on CLIC1 Structure 108
3.2.2. Effect of Salt on CLIC1 Structure 119
3.2.3. Effect of Temperature on CLIC1 Structure 126
3.2.4. Effect of Non - Reducing Conditions on CLIC1 Structure . 131
3.2.5. Effect of Change in Polarity of Solvent on the Structure of CLIC1 137

3.3. Urea – Induced Equilibrium Unfolding of CLIC1 141

3.3.1. Reversibility Studies 141
3.3.2. Concentration Dependence Studies 143
3.3.3. Effect of pH on Stability 145
3.3.4. Effect of Salts on Stability 161
3.3.5. Effect of Temperature on Stability 166
3.3.6. Effect of Non - Reducing Conditions on Stability 170
3.4. Binding of ANS 171
3.4.1. Effect of pH on ANS Binding..... 173
3.4.2. Effect of Salt on ANS Binding 176
3.4.3. Effect of Temperature on ANS Binding..... 179
3.4.4. Effect of Non - Reducing Conditions on ANS Binding 181
3.5. Unfolding Kinetics of CLIC1 181
3.5.1. Effect of pH on Unfolding Kinetics 181
3.5.2. Effect of Salt on Unfolding Kinetics..... 191
3.5.3. Effect of Temperature on Unfolding Kinetics 196
3.5.4. Effect of Non - Reducing Conditions on Unfolding Kinetics198
3.5.5. Summary of Kinetic Parameters 199
3.6. Properties of the Intermediate 202
3.6.1. Secondary Structure of the Intermediate 202
3.6.2. Tertiary Structure of the Intermediate State..... 203
3.6.3. Hydrodynamic Diameter of the Intermediate State 205
3.6.4. ANS Binding to the Intermediate 208
3.6.5. Kinetics of Formation of the CLIC1 Intermediate 208
CHAPTER 4. DISCUSSION..... 210
4.1. Equilibrium Unfolding: Two-State *versus* Three-State..... 210
4.1.1. CLIC1 is Most Stable at pH 7.0 / 20^{o}C..... 210
4.1.2. CLIC1 Forms an Intermediate at pH 5.5 / 20^{o}C 214
4.1.3. At 37^{o}C an Intermediate-Like Species is Detectable at pH 7.0 Under Mild Denaturing Conditions and at pH 5.5 in the Absence of Denaturant..... 219
4.2. The CLIC1 Intermediate..... 223
4.2.1. Conditions Required for the Intermediate to Form..... 223

4.2.2. Structure of the Intermediate 224
4.2.3. Stability of the Intermediate 228
4.3. Mechanism of CLIC1 Unfolding 229
4.3.1. Unfolding of the Native State 229
4.3.2. Unfolding of the Intermediate State 232
4.3.3. Slow Formation of the Intermediate State 232
4.3.4. Unfolding Pathway of CLIC1 233
4.4. Different Electrostatic Conditions Influence the Structure and Stability of CLIC1 237
4.4.1. NaCl Stabilises the Native and Intermediate States of CLIC1 239
4.4.2. CLIC1 Amino Acid Distribution 242
4.4.3. Na_2SO_4 and KSCN Stabilise the Intermediate State 246
4.4.4. NaF Interacts Specifically with CLIC1 248
4.4.5. A Decrease in the Polarity Increases the Helical Content of CLIC1 251
4.4.6. The Absence of Reducing Conditions has a Major Impact on the Structure and Stability of CLIC1 253
4.5. Implications for CLIC1 Function 257
4.5.1. Is the Intermediate a Membrane-Competent Form? 257
4.5.2. Linkage Between Stability and Membrane Cooperativity .. 258
4.5.3. Proposed Mechanism of Membrane Insertion 259
CHAPTER 5. CONCLUSIONS 263
CHAPTER 6. REFERENCES 267

ABBREVIATIONS

ANS	8-anilino-1-napthalene sulphonate
CFTCR	Cystic fibrosis transmembrane conductance regulator
CLIC	Chloride intracellular channel
ClC	Chloride channel
D	Denatured state
DLS	Dynamic light scattering
DTNB	5, 5'-dithiobis-2-nitrobenzoic acid
DTT	Dithiothretol
$\Delta G(H_2O)$	Change in Gibbs free energy upon unfolding in the absence of denaturant
ε_{280}	Molar extinction coefficient at 280 nm
E_{222}	Ellipticity measured at 222 nm
ERK7	Extracellular signal-regulated kinase 7
F_{345}	Fluorescence intensity at 345 nm
F_{356} / F_{345}	Ratio of the fluorescence intensity at 356 nm to the fluorescence intensity at 345 nm
F_{max}	Maximum intensity of the fluorescence emission spectrum
Far-UV CD	Far ultraviolet circular dichroism
Grx2	Glutaredoxin-2
GSH	Reduced glutathione
GSSG	Oxidised glutathione
GST	Glutathione transferase

GST A1-1	Alpha class glutathione transferase
GST B1-1	Beta class glutathione transferase
GST O1-1	Omega class glutathione transferase
I	Intermediate state
IAA-94	Indanyloxyacetic acid 94
IPTG	Isopropyl β-D-thiogalactoside
kDa	Kilodalton
λ_{max}	The wavelength at which the fluorescence spectra show maximum emission
m-value	Susceptibility of protein to denaturant
MAPK	Mitogen activated protein kinase
M_u	Obtained by multiplying the kinetic parameter "m_u" by RT. It gives a measure of the amount of surface area exposed in the transition state as the protein unfolds
N	Native state
Near-UV CD	Near ultraviolet circular dichroism
NEM	N-ethyl maleimide
OD_{600}	Optical density at 600 nm
PDB	Brookhaven Protein data bank
r.p.m.	Revolutions per minute
SDS-PAGE	Sodium dodecyl sulphate polyacrylamide gel electrophoresis
SEC-HPLC	Size exclusion high pressure liquid chromatography
*Sj*26GST	*Schistosoma japonicum* glutathione transferase
Ure2p	Yeast prion protein

LIST OF FIGURES

Figure 1: Debye-Hückel screening by counterions at high ionic strengths 7
Figure 2: The Hofmeister series 9
Figure 3: A representative folding funnel 21
Figure 4: Schematic comparing some states available to proteins 23
Figure 5: Dendrogram of the GST superfamily 33
Figure 6: Comparison of the structures of soluble CLIC1 and CLIC4 38
Figure 7: CLIC1 sequence 41
Figure 8: Crystal structure of CLIC1 42
Figure 9: Charged surface of CLIC1 45
Figure 10: CLIC1 active site 46
Figure 11: Structure of the CLIC1 dimer 48
Figure 12: Alignment of CLIC1 with GST O1-1 and Grx2 illustrating charged residues 51
Figure 13: Schematic of toxin insertion and infection 61
Figure 14: Comparison of CLIC1 topology with that of pore-forming proteins .. 69
Figure 15: Restriction map of pGEX-4T-1 104
Figure 16: SDS-PAGE gel showing a representative CLIC1 purification 106
Figure 17: Elution off the DEAE-Sepharose anion exchange column 109
Figure 18: pH dependence of the far-UV circular dichroism spectra of CLIC1. 111
Figure 19: Comparison of the circular dichroism spectra at pH 7.0 and pH 5.5 112
Figure 20: Comparison of the fluorescence spectra at pH 7.0 and pH 5.5 114
Figure 21: pH dependence of the fluorescence spectra of CLIC1 116
Figure 22: Comparison of the SEC-HPLC elution profiles at pH 7.0 and pH 5.5118
Figure 23: pH dependence of the hydrodynamic diameter of CLIC1 120
Figure 24: Effect of salts on the circular dichroism spectra of CLIC1 at pH 7.0 and pH 5.5 122
Figure 25: Effect of salts on the fluorescence spectra of CLIC1 at pH 7.0 and pH 5.5 123
Figure 26: Salt dependence of the hydrodynamic volume occupied by CLIC1 using SEC-HPLC and DLS as probes 125
Figure 27: Melting curve of CLIC1 at pH 7.0 and pH 5.5 using circular dichroism and dynamic light scattering as probes 128

Figure 28: The effect of temperature on the circular dichroism spectra at pH 7.0 and pH 5.5 130
Figure 29: Fluorescence spectra at 20°C and 37°C at pH 7.0 and pH 5.5..... 132
Figure 30: Effect of non-reducing conditions on circular dichroism spectra at pH 7.0 and pH 5.5 133
Figure 31: Effect of non-reducing conditions on the fluorescence spectra of CLIC1 at pH 7.0 and pH 5.5 135
Figure 32: Effect of redox conditions on the hydrodynamic size of CLIC1..... 136
Figure 33: Circular dichroism spectra of CLIC1 at pH 7.0 and pH 5.5 in the presence of increasing concentrations of TFE 139
Figure 34: Fluorescence spectra of CLIC1 in the presence of TFE..... 140
Figure 35: Recovery of secondary and tertiary structure of CLIC1..... 142
Figure 36: Protein concentration dependence study 144
Figure 37: pH dependence of CLIC1 unfolding at equilibrium using circular dichroism as a probe..... 146
Figure 38: pH dependence of CLIC1 unfolding at equilibrium using the maximum fluorescence emission intensity as a probe 150
Figure 39: pH dependence of CLIC1 unfolding at equilibrium using the wavelength of maximum emission as a probe 151
Figure 40: Raleigh scatter to detect aggregation..... 152
Figure 41: Comparison of equilibrium unfolding curves of CLIC1 at pH 7.0 and pH 5.5 using circular dichroism, fluorescence and light scattering as probes 154
Figure 42: Equilibrium unfolding of CLIC1 at pH 8.2 to pH 4.5 using circular dichroism and fluorescence as probes..... 158
Figure 43: pH dependence of thermodynamic parameters 159
Figure 44: Equilibrium unfolding of CLIC1 at pH 7.0 and pH 5.5 in the presence of NaCl, NaF and Na_2SO_4..... 163
Figure 45: KSCN-induced unfolding of CLIC1 at pH 7.0 and pH 5.5 166
Figure 46: Comparison of unfolding at 37°C and 20°C 169
Figure 47: Equilibrium unfolding of CLIC1 in the presence and absence of 1 mM DTT at pH 7.0 and pH 5.5..... 172
Figure 48: The structure of ANS..... 174
Figure 49: Binding of ANS to CLIC1 at pH 8.2, pH 7.0 and pH 5.5 along the equilibrium unfolding transition 175
Figure 50: ANS binding to CLIC1 in the presence of different salts and increasing urea concentrations 178
Figure 51: Effect of temperature on ANS binding to CLIC1..... 180

Figure 52: ANS binding to CLIC1 under non-reducing conditions 182
Figure 53: Unfolding kinetics using fluorescence and circular dichroism as probes 183
Figure 54: Urea dependence of the unfolding rates of CLIC1 at pH 8.2, 7.0, 5.5 and 5.3 185
Figure 55: Unfolding kinetics of the CLIC1 equilibrium intermediate 187
Figure 56: Urea dependence of the unfolding rate constants of CLIC1 - comparison of the N → D and I → D transitions 188
Figure 57: Kinetics of formation of the equilibrium intermediate 190
Figure 58: Urea dependence of the rate constants for the N → I transition 192
Figure 59: Comparison of unfolding kinetics of CLIC1 in the presence and absence of NaCl 193
Figure 60: Unfolding kinetics in the presence of NaF 195
Figure 61: Unfolding kinetics of CLIC1 at pH 7.0 / 37°C 197
Figure 62: Unfolding kinetics when under reducing and non-reducing conditions 200
Figure 63: Far-UV circular dichroism spectra of the CLIC1 native state and intermediate species 204
Figure 64: Fluorescence spectra of the CLIC1 native state and intermediate species 206
Figure 65: Near-UV circular dichroism spectra of CLIC1 at pH 7.0 and pH 5.5 in the presence and absence of 3.8 M urea 207
Figure 66: ANS binds to the equilibrium intermediate at 20°C and 37°C 209
Figure 67: Dimensions of CLIC1, Grx2 and GST A1-1 212
Figure 68: Proposed scheme for the unfolding pathway of CLIC1 235
Figure 69: Alternative unfolding pathway for CLIC1 238
Figure 70: Residue distribution on the surface of CLIC1 244
Figure 71: Schematic illustrating CLIC1 interaction with the membrane 260
Figure 72: Summary of the effect of different environmental conditions on the structure, stability and unfolding kinetics of CLIC1 264

LIST OF TABLES

Table 1: Comparison of the equilibrium and kinetic unfolding mechanisms and parameters of certain members of the GST superfamily 55

Table 2: Table comparing the properties of CLIC1 to some soluble pore-forming proteins 63

Table 3: Comparison of the thermodynamic parameters obtained from equilibrium unfolding curves of CLIC1 at different pH 160

Table 4: Comparison of the equilibrium thermodynamic parameters obtained under different environmental conditions 167

Table 5: Parameters for the unfolding kinetics of CLIC1 under different environmental conditions 201

Chapter 1. Introduction

Crystal structures of proteins now widely available may advocate a misconception that proteins are static entities. This could not be further from the truth. Proteins are extremely complex and dynamic molecules whose structure and properties at any given moment are dependent on their environment. A protein molecule may fluctuate between various altered conformations depending on its *milieu,* which includes extrinsic features of the environment such as the temperature and pressure as well as the properties of the protein solution such as the pH, polarity and ionic strength. *In vivo* a further complication as to how a protein will exist and behave is the crowded environment within the cell.

The perspective of this project can be divided into three main aspects. These include: (1) The effect of the environment on a protein. This includes electrostatic effects (specifically the effect of pH, ionic strength and polarity), temperature and redox potential. (2) The conformational stability of a protein. This is a broad field but I feel it is necessary to deal with two aspects of this topic in the context of this project and they are the conformational states available to a protein and the forces involved in either maintaining or disrupting these states. (3) The model system used for the study, namely the chloride intracellular channel protein, CLIC1. Here a description of the structure and properties of this protein will be given in the context of other members of the superfamily to which it belongs as well as in the context of other membrane proteins in order to add more pieces to the puzzle of how structure relates to function.

1.1. Electrostatic Contributions to Protein Stability

1.1.1. Electrostatic Interactions

Electrostatic interactions take place between charged groups. Since proteins are polyampholytes and contain a number of electrically charged residues, (including the carboxy- and amino termini) electrostatic forces play an imperative role in defining the stability of a protein molecule. The energy (U) for the association of two charges (q_1 and q_2) is derived from Coulomb's law as follows:

$$U = \frac{kq_1q_2}{\varepsilon r^2} \qquad \mathbf{1}$$

where ε is the dielectric constant of the medium that varies inversely with temperature and r is the distance separating the two charges. From this relationship, it can be seen that as the dielectric constant is increased, so less energy is required to separate the electrostatic interactions. Therefore over a certain distance, the electrostatic attractions and repulsions will be weaker in a medium with a high dielectric constant such as water, than in a more apolar environment such as the interior of protein molecules. The strong electrostatic interactions in the protein interior are not believed to have a substantial effect on the stability of proteins however, since they are not very common. The Born energy (W_B) is defined as the free energy of transfer in moving a molecule with charge q and radius r from a region of dielectric strength ε_2 to a region of dielectric strength ε_1 (Born, 1920). It is defined by the equation:

$$W_B = \left(\frac{q^2}{2r}\right)\left(\frac{1}{\varepsilon_1} - \frac{1}{\varepsilon_2}\right) \qquad \mathbf{2}$$

Ion pairs (distance between charges of approximately 4 Å) or salt bridges (distance between charges ≤ 3.5 Å and can result in hydrogen bonds) are formed when two protein residues of opposite charge associate with each other. They can also be formed between a charged protein residue and ions in solution. These charge-charge interactions are stronger than dipole interactions (section 1.2) and conserved ion pairs in particular, could contribute significantly towards stabilising the native state (Barlow and Thornton, 1983; Dill, 1990) They also assist in the uniqueness of the protein fold or ligand-binding geometry due to their specificity (Hendsch and Tidor, 1994). The net electrostatic free energy resulting from the interaction of charged groups on the surface of a protein is in the range of 10 kcal/mol (Honig *et al.,* 1986). However, whereas ion pairs are not directional, the total electrostatic free energy contribution of a salt bridge to the stability of a protein depends on two things: the geometry of the salt-bridge which includes the positioning of the side chains relative to one another; and the location of the salt-bridge within the protein (Kumar and Nussinov, 2002). The contribution of salt bridges towards the stability of a protein appears to be dependent on the accessibility of the salt bridge to solvent, with salt bridges that are 100% accessible only contributing marginally to stability, while those that are 100% inaccessible contribute approximately 2.1 kcal/mol to the stability of the protein (Takano *et al.*, 2000).

Electrostatically driven processes depend on pH and/or ionic strength. The pH of the solution will determine the total charge on the protein while the salt present in the solution will regulate the extent to which these charges interact.

1.1.2. The Effect of pH on Protein Stability

It is well considered that protein function is dependent on the pH of the solution, hence enzymes, for example, only function effectively within a very narrow pH range. Therefore it is apparent that the association and interactions

of protons on the surface of a protein play very important roles in determining and maintaining both the structure and function of proteins. By varying the pH of a protein solution, the ionization states of the amino acid side chains will be altered. This changes the distribution of charge over the entire protein molecule and can alter the hydrogen bonding requirements of many residues.

The dependence of the stability of a protein on the pH of the solution is determined by the difference in the H^+ binding affinity of the native and denatured states of the protein (Tan *et al.,* 1995; Whitten and García-Moreno, 2000; Shaw *et al.,* 2001). The state of the protein with the higher affinity for protons will be stabilised as the concentration of H^+ ions is increased. Therefore a high dependence of stability on pH, particularly a drop in the stability of the native state with a drop in pH, means that on average the acidic residues in the denatured state will have a higher affinity for the binding of protons than in the native state. Conversely an increase in stability with a drop in pH means that the acidic residues in the native state will have a higher proton affinity than in the denatured state.

Numerous studies have been conducted on numerous proteins to determine the effect of altering the pH on the equilibrium stability of the proteins. In an early study, Goto *et al.* (1990) unfolded three separate proteins: β-lactamase, apomyoglobin and cytochrome *c* to a relatively unfolded state by adding HCl to the solution. They found that decreasing the pH even further caused the proteins to regain a degree of their secondary structure and form a "molten globule"-like conformation (see section 1.3.6). This refolding was proposed to be due to binding of the chloride anion to the proteins, which minimised the charge repulsion that had caused the unfolding in the first place. The molten globule state of apomyoglobin was studied further by Barrick and Baldwin (1993b) to determine the energy required in creating this state. Additional studies of the effect of pH on proteins have been conducted on diphtheria toxin (Blewitt *et al.,* 1984; Jiang *et al.,* 1991; Chenal *et al.,* 2002); barnase (Pace *et al.,* 1992; Oliveberg *et al.,* 1994); chymotrypsin inhibitor 2 (Tan *et al.,* 1995);

human prion protein (Swietnicki *et al.*, 1997; Jackson *et al.,* 1999); annexin V (Beerman ofm cap *et al.,* 1998); ubiquitin (Makhatadze *et al.,* 1998); β-lactoglobulin (Renard *et al.,* 1998); pheromone-binding protein from *Bombyx mori* (Wojtasek and Leal, 1999); the N-terminal domain of L9 (Kuhlman *et al.,* 1999); myoglobin (Kao *et al.,* 2000); staphylococcal nuclease (Whitten and García-Moreno, 2000); thioredoxin (Setterdahl *et al.*, 2003); the cytolytic δ-endotoxin, Cyt1A (Manceva *et al.,* 2004); the apoptosis regulating protein Bcl-$_{XL}$ (Thuduppathy and Hill, 2005) and the lipid-binding protein, ostreolysin (Berne *et al.,* 2005) to name a few. Theoretical estimates of the pK_a- and pH-dependent stabilities of proteins, particularly of the pore-forming domains of colicin, have been made by Warwicker, (1999). All these studies have proven that *pH is an essential component in determining the stability of a protein.* This effect is often achieved by fine-tuning the microenvironment surrounding certain ionisable residues.

1.1.3. The Effect of Ionic Strength on Protein Stability

When small diffusible ions are present in a protein solution, they will affect the inherent charge interactions present on the protein surface by surrounding each charged residue with a cloud of counterions. This enrichment of ions enveloping each charge will prevent the intrinsic ion pairs or charge interactions between charged residues from occurring on the protein surface. This screening effect was quantified by Debye and Hückel in terms of the radius of counterions surrounding each charged molecule and has become known as Debye-Hückel screening (Debye and Hückel, 1923) (Figure 1). Intuitively it is obvious that this screening effect depends on the concentration of counterions present in the solution. The ionic strength (I) of a solution is a function of the ion concentration and is defined as

$$I = \tfrac{1}{2} \sum_i \left(M_i Z_i^2 \right) \qquad \textbf{3}$$

taken in a solution containing a number, *i*, of ions where *M* is the molarity of each ion and *Z* is the stoichiometric charge on each ion.

The shielding effects of salt on ionised residues are only truly effective at low salt concentrations. High salt concentrations will saturate the charged residues and thus will exert their effects on the solvent properties of the solution rather than on the protein (Dill, 1990). These effects (known collectively as the Hofmeister effect) include a reduction in the volume of water surrounding a charged protein molecule and a reorienting and ordering of the adjacent water dipoles at particularly high salt concentrations.

Not all salts have the same effect on the stability of a protein. In fact some ions are able to interact specifically with and stabilise proteins, some have little effect and others destabilise proteins. These interactions may be specific to the protein and to the particular condition of the environment such as the pH or temperature (Baldwin, 1996).

The Hofmeister series (Figure 2) gives a measure of the salt effects on the stability of proteins (Hofmeister, 1888). The effects of these ions are generally independent of the specific protein under study. Here one can see that sulphate ions are the most stabilising anions and ammonium ions are the most stabilising cations, while thiocyanate, calcium and barium are tremendously chaotropic. Both sodium and chloride ions fall in the neutral region of the series and therefore do not independently affect protein stability. Thus sodium chloride is a highly successful salt to use when studying the effect of changes in ionic strength on a certain protein, since any changes will not be due to the specific ions in the salt but rather to changes in electrostatic interactions on the protein surface.

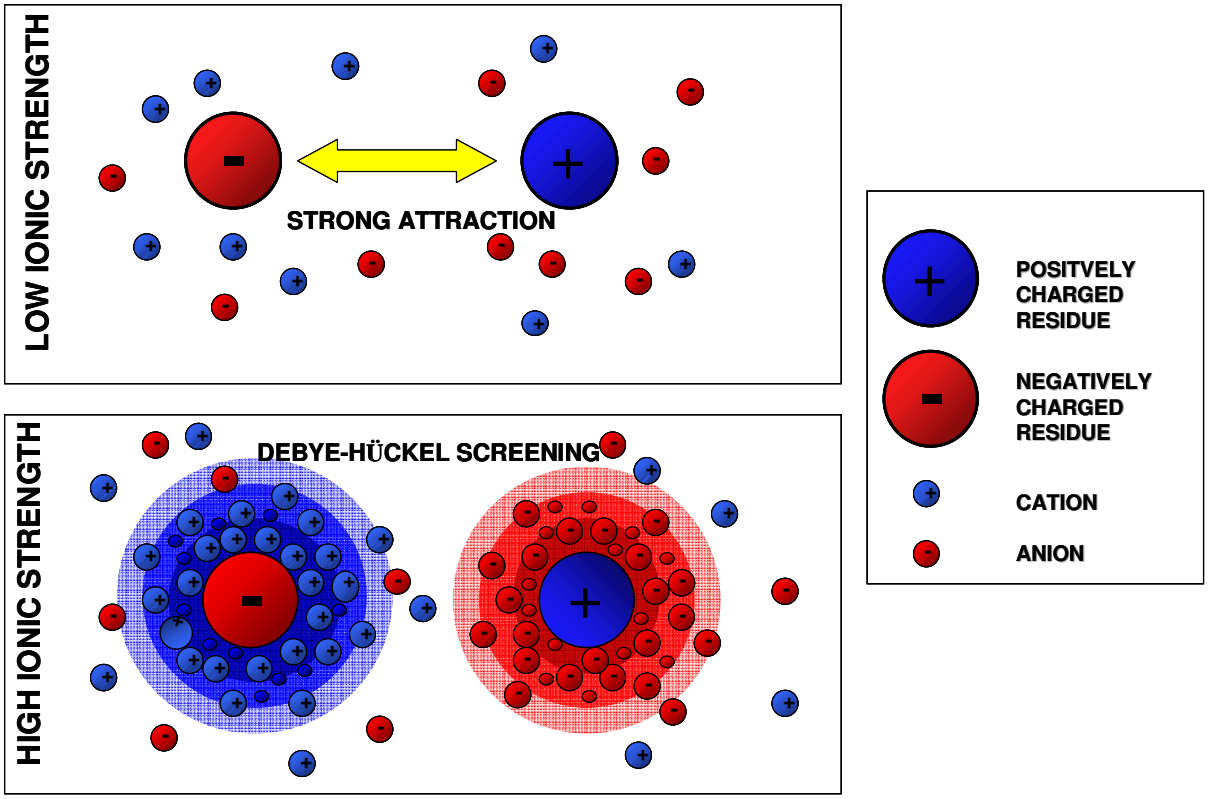


Figure 1: Debye-Hückel screening by counterions at high ionic strengths

Schematic illustrating the effect of ionic strength on the attractive forces between two oppositely charged groups, such as amino acid residues, on the surface of a protein (adapted from Mathews and van Holde, (1995)).

The effect of ionic strength (Stigter and Dill, 1990; Barrick and Baldwin, 1993a; La Brake *et al.,* 1993; Oliveberg *et al.*, 1994; Tan *et al.,* 1995; Szeltner and Polgar, 1996; Lusitani *et al.,* 1998; Makhatadze *et al.,* 1998; Renard *et al.,* 1998; Kuhlman *et al.*, 1999; Kao *et al.,* 2000; Pace *et al.*, 2000; Stevens *et al.,* 2000; Whitten and García-Moreno, 2000; Shaw *et al.,* 2001; Lee *et al.,* 2002; Yassin *et al.,* 2003; Manceva *et al.,* 2004) and salt bridges (Kohn *et al.,* 1997; Pace *et al.,* 2000; Strop and Mayo, 2000; Takano *et al.,* 2000; Shaw *et al,* 2001; Kumar and Nussinov, 2002) on proteins and protein stability has been studied extensively on many different model systems with many different outcomes. The general inferences drawn from these studies are that salt effects cannot be overlooked as they are responsible for changes in the overall structure, function and stability of proteins as well as in their physicochemical properties such as their solubility (Carbonnaux *et al.,* 1995) and the pK_a of their residues (Abe *et al.*, 1995).

The pK_a of an acid can be defined as the pH at which the acid will release its bound proton. The pK_a values of ionisable residues of proteins are sensitive to their local environments. Therefore the pK_a values of residues in highly charged proteins are often influenced by the net charge on the protein. This makes them extremely sensitive to the ionic strength of the solution. Under conditions of high ionic strength, the charged form of the ionisable residue will be preferentially selected over the neutral form. Thus the pK_a of basic groups will increase and the pK_a of acidic groups will decrease as the ionic strength of the solution is increased (Tan *et al.,* 1995).

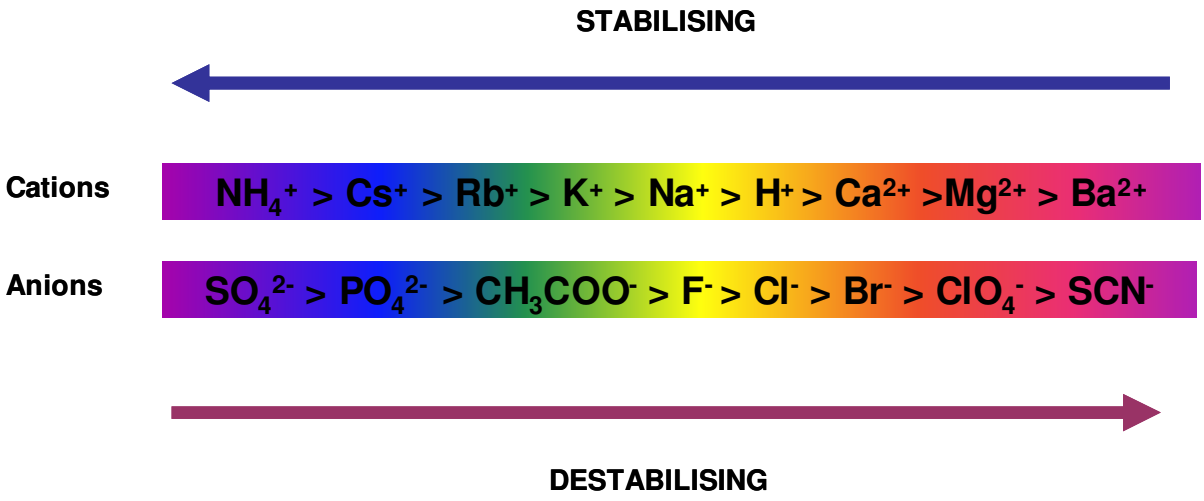


Figure 2: The Hofmeister series

The Hofmeister series showing the effect of ions on protein stability. The red colours indicate the most destabilising ions while the most stabilising ions are shown in blue.

1.1.4. The Role of Charged Amino Acid Residues

Proteins contain two types of acidic amino acid residue, namely aspartate and glutamate. These residues have a carboxyl group as their functional group. The pK_a of these side chain carboxyl groups is around 4 in model compounds (that is: short peptides containing specific amino acids), with the pK_a of aspartate being slightly lower than the pK_a of glutamate. These residues should thus be negatively charged at pH values greater than 4. The two basic amino acid residues found in proteins are arginine (pK_a of guanidino group is 12.5) and lysine (pK_a of epsilon amino group is 10.5). These residues are positively charged at pH values below 10.5. Histidine is unique among the amino acids in that it is the only amino acid that has a side chain with a pK_a value that lies within the physiological pH range (pK_a of the imidazole group is 6.1). This amino acid can therefore be either neutral or basic depending on the pH of the solution. The histidine residues within a protein therefore play an important role in the electrostatic effects that govern the stability of the protein.

The pK_a values of the charged amino acid residues in proteins are not fixed at the values found in model compounds and can easily fluctuate over a range of 2 to 3 pH units from the value found in the model compounds (Matthew, 1985). An example of this is the pK_a of the catalytically active Tyr9 in class Alpha glutathione transferase. The pK_a of this residue has been experimentally determined as 8.1, which is 2.2 units lower than the value of 10.3 reported for tyrosine residues in model compounds (Bjornestedt *et al.,* 1995; Gustafsson *et al.*, 1999). In fact, the pK_a values of the charged residues of a protein are a reflection of the macromolecular environment surrounding that residue and the effect that this environment has on the energy difference between the charged and neutral forms of the residue (Whitten and Garcia-Moreno, 2000). Therefore these charged residues provide an essential electrostatic contribution towards the stability of a protein. By investigating the electrostatic nature of the macromolecular *milieu* surrounding each of the residues, one can predict

whether or not the pK_a of that residue will be sensitive towards the ionic strength of the solution.

1.2. Protein Stability and Folding: Thermodynamics and Forces Involved

1.2.1. Introduction

The stability of a protein molecule refers to the energetic competency of that protein to remain in its native folded state. It can be defined as the difference between the free energies (ΔG) of the native and denatured states of a protein. This value therefore represents a rather small difference in energy between the many interactions that favour the folded protein and the unfavourable entropic forces that favour the unfolded state of the protein.

The principal forces involved in stabilising the native three-dimensional structure of a folded protein are: van der Waals forces, electrostatic interactions and most significantly, hydrogen bonds and hydrophobic interactions (Matthew, 1985; Dill, 1990, Pace *et al.,* 1996). It is a subtle combination of these forces, a delicate balance of interactions; that results in the network of stabilising contacts on the protein surface in addition to the packing interactions within the hydrophobic core of the protein (Dill, 1990). These non-covalent forces can be up to 100 times weaker than covalent bonds. It is their very weakness that results in the dynamic behaviour observed in most macromolecules which is essential for functional protein systems and for life in general.

1.2.2. Van der Waals Forces

Van der Waals forces occur as non-covalent interactions (either permanent or induced dipoles) between electrically neutral residues. These dipole moments provide a measure of the magnitude of the polarity of a molecule. Permanent

dipoles are often formed between backbone moieties of a protein's secondary structure. These are weak interactions that attenuate considerably with the distance separating them. Therefore, since these forces are only functional over very short distances, the correct packing of a protein molecule is imperative to ensure its stability. When van der Waals interactions are present in the interior of a protein they are essential forces, either stabilising or destabilising the native state (Takano *et al.*, 2003).

London dispersion forces are extremely weak van der Waals interactions that arise from attractive forces present in nonpolar molecules. These attractive forces are due to fluctuations of the electrons in these molecules that give rise to a small induced dipole moment at any instant. These forces attenuate even more drastically with distance than the permanent dipole forces, making them only significant in atoms that actually make contact with one another. Nevertheless, the close packing of the amino acid residues that leads to London forces plays an important role in stabilising the folded state of proteins (Chakravarty *et al.,* 2002).

1.2.3. Hydrogen Bonds

Over the years there has been a shift in thinking as to the importance of hydrogen bonds in the stabilisation of the folded protein structure (reviewed in Pace *et al.,* 1996). Initially, Pauling's group could "not overemphasise the importance of hydrogen bonding in protein structure" (Mirsky and Pauling, 1936). However in 1959, Kauzmann put forward a convincing argument for the significance of "hydrophobic bonds" rather than hydrogen bonds in stabilising protein structure (Kauzmann, 1959). The recent view, though, is that both hydrogen bonds and the hydrophobic effect are the major stabilising forces in a protein (Pace *et al.,* 1996; Baldwin, 2003).

Hydrogen bonds are noncovalent interactions that are formed between a hydrogen atom bonded to a highly electronegative and weakly acidic donor atom and another highly electronegative acceptor atom such as oxygen, nitrogen or sulphur that bears a lone pair of electrons. The peptide backbone and polar amino acid side chains within a protein contain potential hydrogen bond donor and acceptor sites. Hydrogen bonds, like van der Waals forces, are a result of dipole-dipole interactions. These directional, mostly linear bonds have a bond distance between the donor hydrogen and the acceptor atom, in the range of 2.7 – 3.1 Å and their strength lies in the range of 2 – 10 kcal/mol depending on the orientation of the bonding atoms (Dill, 1990) and the degree of solvation of the peptide group, for example (Baldwin, 2003). Although individually these interactions would impart an almost insignificant stabilising force upon the protein molecule in its entirety, their strength lies in their numbers and thus even a negligible contribution per hydrogen bond results in an energetically significant amount when multiplied by the total number of hydrogen bonds in the protein (Kim and Baldwin, 1990). Furthermore, both peptide – peptide (Baldwin, 2003) and side-chain – side-chain (Ragone, 2003) hydrogen bonding have recently been shown to provide a substantial contribution towards protein stability. In fact, the underlying structural element of both helices and β-sheets is the peptide – peptide hydrogen bond (Baldwin, 2003).

The hydrogen bonding network within the protein provides a constrained geometry in which peptide dipoles may align and give rise to a macrodipole. This is particularly evident in the α-helical structures. This helix dipole moment can contribute up to 20 kcal/mol of stabilisation energy to interhelix packing interactions (Matthew, 1985)! A relationship has been detected between the formation of peptide hydrogen bonds and the burial of non-polar surface area (Krantz *et al.*, 2002). This burial of non-polar surface area will provide favourable free energy for hydrogen bond formation. Polyalanine alone can form a helix in water (Marqusee *et al.*, 1989), this observation coupled with the fact that the change in heat capacity upon unfolding of the polyalanine

helix is zero (Baldwin, 2003) implies that helix formation is not driven by the hydrophobic effect (an alanine helix will not bury much non-polar surface area) but rather by peptide hydrogen bonding and solvation of the peptide bond (Baldwin, 2003).

Protein structures are organised in such a way that approximately 70% of all possible hydrogen bonds are formed (Baldwin, 2003). Hydrogen bonds can potentially be buried within the protein interior but the desolvation penalty for burial is around 2.5 kcal/mol. Therefore hydrogen bonds are far more common on the solvent-exposed surface of the protein (Takano *et al.,* 1999; Baldwin, 2003).

When a protein is denatured in a polar solvent, its hydrogen bonding requirements will be satisfied by bonding with water molecules over and above the polar residues in the denatured state. It therefore follows that the stabilisation free energy conferred on a native protein by its hydrogen bonds is simply the difference in the hydrogen bonding capability between the native and denatured states.

1.2.4. The Hydrophobic Effect

The hydrophobic effect is seen when hydrophobic substances tend to minimise their relationship with water and with any polar solvent. This effect is apparent when amphipathic molecules form micelles in aqueous solutions. The hydrophobic effect is observed in proteins since the polar and charged residues commonly exist on the surface of the molecule while the nonpolar residues associate away from the aqueous environment to form the nonpolar globular core. This effect, which can be attributed to the unique properties of water-including its high dielectric constant, must therefore be of great significance in the process that drives the folding of a protein. Non-polar side chains in particular will interact significantly due to the hydrophobic effect, even when in contact with water. This force thus provides important stabilising energetics

towards protein folding via the folding of partially formed intermediate species that have exposed hydrophobic patches (Kim and Baldwin, 1990).

The hydrophobic effect has been proposed to assist the folding process by bringing surfaces that are relatively close in sequence together, thereby resulting in the principal formation of loosely associated secondary structures through long range hydrophobic forces, and in so doing, by excluding water from the protein core (Parker and Marqusee, 1999). These hydrophobic forces are non-directional and extremely abundant in protein molecules and hence contribute immensely to the global stability of the molecule.

The free energy obtained from the hydrophobic effect confers approximately 60 kcal of energy per mol of protein (Dill, 1990) and, along with hydrogen bonds, is the main source of stabilising free energy for a protein (Kim and Baldwin, 1990).

1.2.5. The Entropic and Enthalpic Effects

While all the forces mentioned thus far generally act to stabilise proteins, there is an opposing force, the configurational entropy (Spolar *et al.,* 1994). As the protein unfolds, so the degrees of freedom available to the unfolding molecule increase. The residues that previously formed relatively inflexible structures such as α-helices or β-sheets, or even the hydrophobic residues that were conformationally restrained within the interior of the native protein, gain considerable plasticity upon unfolding. This entropic force favours the unfolding of proteins and results in reduced stability. The amino acid content of a protein will influence its configurational entropy. Proteins containing a high percentage of the inflexible residue proline, for example, will have lower configurational entropy than proteins with a high content of flexible glycine residues (Murphy, 1995). The destabilising free energy conferred by the entropic effect is approximately 50 kcal/mol protein (Dill, 1990). Therefore,

since the stabilising energy is about 60 kcal/mol, the net stability of a protein is the small difference between these two relatively large free energy values.

The thermodynamic forces that collectively result in the folded protein structure of given stability can be related by the following equation:

$$\Delta G_{stabilisation} = \Delta H_{bonds} - T\left(\Delta S_{conformational} + \Delta S_{solvation}\right) \qquad \textbf{4}$$

This equation indicates that there are two thermodynamically opposing entropic contributions to protein stability. While the conformational entropy opposes folding, the entropy of solvation of the residues promotes folding and is strongly linked to the hydrophobic effect. This is because when in the folded state, the hydrophobic side chains will not be exposed to the solvent and this is thermodynamically more favourable than when hydrophobic residues are in contact with the aqueous environment in the unfolded state.

The enthalpic effect involves the formation of bonds and the configuration and formation of interactions as the protein folds. The greater (more negative) the enthalpy, the greater the free energy required to stabilise a protein. In other words, the free energy of stabilisation is maximised by molecular interactions. The compact nature of the tertiary structure of globular proteins and the many hydrogen bonds and van der Waals interactions in the tightly packed structure, function to make the enthalpy value as negative as possible by increasing side-chain – side-chain interactions and hence by increasing the total interaction energy in the molecule (Privalov, 1992).

1.3. Conformational States Available to a Protein

1.3.1. Introduction

The synthesis of a linear polypeptide chain off the ribosome is followed by the folding of this polypeptide into its correct three-dimensional configuration. The manner in which the protein rapidly adopts precisely its correct fold despite the huge number of conformational states available to the newly folding protein has intrigued scientists for years (Levinthal, 1968; reviewed by Dill, 1990; Dobson and Karplus, 1999; Clementi *et al.,* 2000; Rumbley *et al.,* 2001) and has become known as "the protein folding problem". Clearly, protein folding cannot solely be predicted from the primary sequence of the protein's amino acids as was proposed by Anfinsen, 1973. Many factors including the environment of the protein, the existence of molecular chaperones to assist folding, and the many stabilising and destabilising forces present within the protein itself will contribute towards the final folded state.

Proteins are in dynamic equilibrium within the cell. In other words they are able to unfold and refold and once they are formed off the ribosome there is no guarantee that they will remain in that particular folded state (Dobson, 2000). This process, coupled with the fact that the cellular environment is highly crowded, may lead to proteolysis, incorrect folding, aggregation or fibril formation (reviewed in Ellis and Hartl, 1999; Dobson and Karplus, 1999). These developments may lead to diseases such as Alzheimer's disease, prion-associated spongiform encephalopathies, many cancers, Parkinson's disease and others. Therefore an understanding into the correct mechanisms of protein folding is vital, if not only to cure many fatal diseases.

1.3.2. Mechanisms of Protein Folding

A variety of theories have been proposed in an attempt to explain the mechanisms of protein folding (Chan *et al.*, 1995; Dobson and Karplus, 1999;

Rumbley *et al.*, 2001; Clark, 2004). These postulations include many models that range from the *classical theory* of protein folding where the protein follows predetermined pathways cluttered with intermediate species (Englander, 2000; Krishna and Englander, 2007) to the *"new view"*, which is based mainly on computer simulations and proposes that proteins fold by tumbling along a downhill energy landscape consisting of an unlimited continuum of undefined intermediates (Baldwin, 1994; Wolynes *et al.,* 1995). Furthermore, many theoretical studies have been conducted with the aim of predicting the outcome of the folding process (Govindarajan and Goldstein, 1998; Laurents and Baldwin, 1998; Dobson and Karplus, 1999; Clementi *et al.*, 2000; Chakravarty *et al.*, 2002; Pande, 2003; Clark, 2004; Vu *et al.*, 2004).

An early model to explain protein folding, the *side-chain packing model* (Shakhonovich and Finkelstein, 1989) propounds that folding cooperativity arises from "jigsaw puzzle-like packing and interdigitaition among side chains". Cooperativity is explained in terms of the unfolding of a protein molecule: as the chain expands it reaches a critical disjuncture point at which the side chains will be released from their compact arrangement. This model does not account for the fact that as the protein unfolds, the degrees of freedom gained by the residues are initially acquired very rapidly but then start to decelerate while the protein continues to expand.

The *hydrophobic collapse model* (Dill and Stigter, 1995) uses the fact that when exposed to an aqueous environment, hydrophobic molecules will cooperatively form hydrophobic cores away from the water. This nonpolar association in water is strong and this model offers more credibility than the side-chain packing model, although it is unable to give a convincing elucidation of the elementary principles governing protein folding, since structural preferences due to the sequence of the protein are difficult to explain with this model (Roder and Colon, 1997).

The fundamental mechanism of protein folding can be described by the *nucleation-condensation* model in which the entire structure condenses around

a small number of key amino acid residues that form the "folding nucleus" in a native-like environment early on in the folding process (Fersht, 2000; Vendruscolo *et al.,* 2001). If these key interactions are not formed the protein usually is unable to fold to its stable globular structure.

To this effect, synergy of theory and experiment is vital to procure a clear and concise understanding of protein folding events (reviewed in Pande, 2003; Dobson, 2004). Many of the earlier conceptual models are combined in the *"new view"* which represents protein folding by a funnel-like energy landscape known as a *protein folding funnel* (Figure 3) (Dill and Chan, 1997). The unfolded protein moves along this landscape, altering its conformations by forming stabilising native contacts. The energy of the system and the number of accessible conformations available to the folding protein decreases until eventually, by avoiding stable minima that could encourage aggregation (the "double funnel" theory (Clark, 2004)), the protein acquires the state with the least energy and thereby assumes its native state (reviewed by Dobson and Karplus, 1999; Ozkan *et al.,* 2002; Clark, 2004). This model therefore allows for several possible routes to reach the native state from the denatured state and also accounts for intermediate species as local minima that may hinder or promote the folding process depending on the funnel surface.

The final state of folding is independent of the pathway taken to reach the folded state, however. "Protein folding is thus a simple mechanistically uniform process, not dependent on the fine details of sequence but rather on the global equilibrium properties" (Plaxco *et al.*, 1998; Clementi *et al.*, 2000; Plaxco *et al.*, 2000; Makarov *et al.*, 2001).

Kinetics

The unfolding and folding kinetics of many small globular proteins are deceptively simple. The transition often occurs as a first order reaction involving two states separated by a single free-energy barrier (Roder *et al.*,

2000). It is expected that the folding process is, in fact far more complex often involving a number of transient intermediate species on pathway to the native state (for a recent review see Wallace and Matthews, 2002). Proteins fold in this way by utilising a "diffusion-collision" mechanism where native-like secondary structure is formed in the denatured state. (Myers and Oas, 2001). Small single-domain proteins may be more prone to folding in a two-state manner than larger proteins, however, because there is less hydrophobic surface area available to stabilise a collapsed intermediate state (Dobson *et al*, 1998).

The rates of protein folding have been found to vary drastically (Laurents and Baldwin, 1998). They range from the submillisecond and millisecond time range such as the B-domain of staphylococcal A with a folding rate constant of 120 000 s^{-1} making it one of the fastest folding proteins known (Myers and Oas, 2001) to much slower rates especially for multimeric proteins and proteins containing disulphide bonds (Kim *et al.,* 2000; Spooner *et al.,* 2004). However, since aggregation is a slow process, proteins have evolved to fold relatively rapidly so as to minimise competing reactions that could favour aggregation (Kiefhaber, 1995). The fastest known process in protein folding is α-helix formation (Laurents and Baldwin, 1998; Vu *et al.*, 2004) and therefore the rate at which a protein folds is dependent on its secondary structural content.

1.3.3. The Native State

The native state of a protein (Figure 4) is the term used to describe its compact, biologically active conformation. In contrast to the many non-native conformations that a protein may assume, the native state is unique and has highly distinct characteristics. The native state structure is extremely tightly packed, with many of the residues (mostly hydrophobic) buried within the interior.

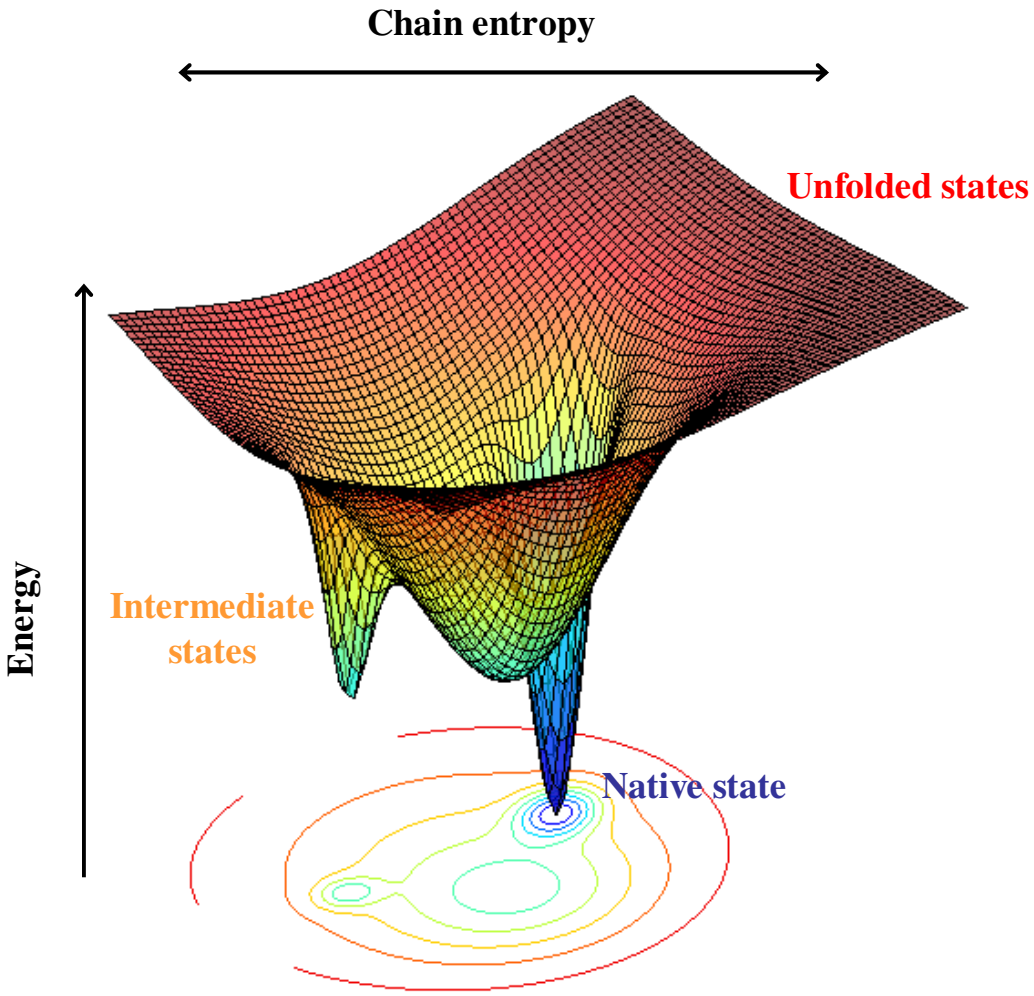


Figure 3: A representative folding funnel

A representation of the paths available to a folding protein. Each point on the surface of the funnel represents a potential conformational state available to the folding polypeptide chain and its corresponding energy value. Initially there are many conformations available to the unfolded protein but these decrease as the protein moves towards its native conformation. The breadth of the funnel represents all possible conformations of the chain while the separation between the top and bottom of the funnel signifies energy contributions (such as solvent entropy and enthalpy) to each chain conformation. There is only one correctly folded native state and it is represented by the point of lowest energy on the funnel. However the folding protein may become trapped in energy minima *en route* to the native state. These minima may prevent the protein from reaching the native folded structure or they could be intermediate states on the pathway to the native state. The image was generated using the programme MATLAB v7..

These buried side chains are fairly inflexible and fixed in specific locations. This is unlike the side chains of the exposed, (mainly polar), residues on the protein surface, approximately 50% of which are extremely disordered (Dobson, 2000). These local fluctuations may contribute to the stability of the protein. In fact the native state of a protein consists of a number of transient interconverting yet closely related states that on average embody the configuration represented by its crystal structure (Whitten *et al.,* 2005). The backbone of a protein in the native state is somewhat rigid however, and the secondary and tertiary structures are kept in place by an elusive balance of stabilising and opposing forces bestowing a degree of global cooperativity upon the molecule. As the protein becomes denatured so the buried residues become exposed to the solvent and the intrinsic interactions between the buried residues in the native state are disrupted and replaced, in many cases, by interactions with the solvent.

1.3.4. The Denatured State

The denatured state (Figure 4) can be defined as any state occupied by a protein that is not its native conformation. However the protein is only considered to be completely denatured when it has lost its secondary, tertiary and quaternary structure and exists essentially as a random coil of polypeptide. In practise this process rarely occurs to completion and residual structure is often present in the denatured state.

Proteins can be denatured by changing various external conditions such as using extreme pH or temperature, changing the pressure or using chemical denaturants.

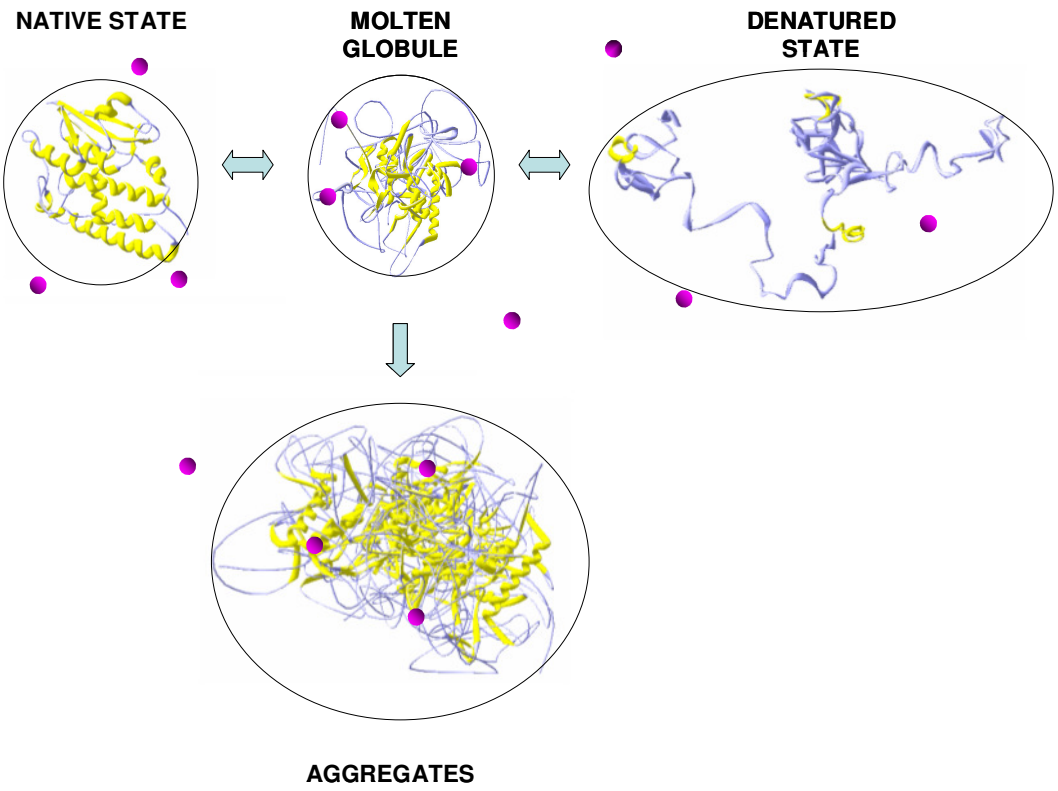


Figure 4: Schematic comparing some states available to proteins

Illustration of the native, intermediate (specifically molten globule) and denatured states occupied by a single monomeric protein. The aggregate structure that may form by accumulation of the molten globule species via their exposed hydrophobic patches is also shown. The hydrodynamic volume occupied by each species is represented by the sphere surrounding them (see text). The pink spheres symbolize the hydrophobic dye ANS (see text). All secondary structure is shown in yellow.

Chaotropic chemicals such as urea and guanidine hydrochloride denature proteins either directly by forming hydrogen bonds with the peptide backbone and with the π electrons of aromatic residues, or indirectly by affecting the structure of the water molecules in the solvent thereby affecting the hydration of protein groups and diminishing the hydrophobic effect (Bennion and Daggett, 2003). Denaturants are predicted to be able to solvate non-polar groups better than water does. Therefore during the denaturation process, the hydrophobic core of the native state will initially be solvated by water to form the transition state and then the transition state will be solvated by denaturant, which interacts preferably with these non-native states, to form the denatured state (Bennion and Daggett, 2003). It is likely that urea is only effective in increasing the solubility of larger hydrophobic residues however, and it may not be able to solvate the smaller hydrophobic residues such as alanine. This could result in the presence of residual hydrophobic clustering of the smaller non-polar residues in the denatured state (Shimizu and Chan, 2002).

Denatured states of many proteins are thus not simply a random coil of completely unfolded protein showing no secondary structure as was once believed (Tanford *et al.*, 1967). Denatured states have since been defined as "dynamic ensembles of rapidly interconverting species of similar energies" (Brockwell *et al.*, 2000) and even at urea concentrations of up to 8 M, nuclear magnetic resonance studies have shown that native-like orientations still remain in the denatured state (Whitten and Garcia-Moreno, 2000; Plaxco and Gross, 2001; Shortle and Ackerman, 2001). Thus, when the hydrophobic interactions and hydrogen bonds that stabilise the native state are disrupted, the unfolded polypeptide chain will still form favourable long-range electrostatic interactions, often resulting in compact structures and contributing towards a *denatured state ensemble* rather than a completely unfolded polypeptide chain (Pace *et al.*, 2000).

1.3.5. Detecting Intermediates

Although the folding of small globular proteins has often been proved to be a two-state process (Grantcharova *et al.,* 2001), intermediate species have been found to populate the folding pathway of most proteins greater than 100 amino acids long under certain conditions such as high salt concentrations and low pH. There is an amount of controversy as to whether these intermediates form an off-pathway kinetically trapped species that slows down the folding process (Bhuyan and Udgaonkar, 2001; Rumbley *et al.,* 2001) or whether they are productive and do not hinder the folding process. In fact, they have frequently been seen to accelerate the rate of folding, or at least to assist the protein in achieving the native state (Roder *et al.*, 2000; Jemth *et al.,* 2004). These intermediate states differ, not only in their functional significance towards the folded state, but also in the mechanism of their formation. Some intermediates are believed to be a collapsed form of the denatured state (Qi *et al*., 1998) while others are understood to be distinct species separated from the denatured state ensemble by an energy barrier (Shastry and Roder, 1998).

Luque *et al.* (2002) propose the existence of at least one intermediate state in all denaturation processes, however in certain instances when the denaturant dependence of the intermediate state is low; it may never become significantly populated and hence will not be detected.

As a protein proceeds from the denatured state to the native state, it occurs as a transient, somewhat nebulous intermediary state, known as the *transition state*. The transition state is defined as the peak in the energy barrier between the native and denatured states (Daggett and Fersht, 2000) and thus consists of all intermediate states (either transiently or significantly populated) *on pathway* to the native state (Dobson and Karplus, 1999). These states have been detected and characterised using a combination of protein engineering and molecular dynamics simulations (Daggett and Fersht, 2000) and are believed to be stabilised by the amino acid sequence of the protein and formed via the

cooperative secondary structural elements of the native state (Rumbley *et al.*, 2001). These intermediates function in searching for critical interactions thereby limiting the conformational space available to the folding protein. Their formation therefore constitutes the rate-limiting step in protein folding.

Often intermediate species accumulate in a "burst phase" which precedes the rate-limiting step in the formation of the native state. An example of a protein that folds via a burst phase intermediate is β-lactoglobulin (Kuwajima *et al.,* 1996). These early intermediates which are compact albeit dynamic species along the folding pathways of proteins are formed primarily as a result of the hydrophobic effect. This was seen in a number of intermediates that displayed an inverted temperature dependence of their stability which is consistent with the hydrophobic effect (Roder and Colon, 1997).

A survey of the literature reveals that many intermediate states have been detected both at equilibrium (Goto *et al.,* 1990; Ogasahara *et al.*, 1993; Barrick and Baldwin, 1993a,b; Carra *et al.*, 1994; Guha and Bhattacharyya, 1995; Ionescu *et al.,* 1997; Swietnicki, *et al.,* 1997; Baskakov and Bolen, 1998; Bilsel *et al.,* 1999; Gualfetti *et al.*, 1999; Fujiwara *et al.,* 1999; Ionescu *et al.,* 2000; Whitten *et al.*, 2001) and on pathway to the folded state (Ogasahara *et al.*, 1994; Guha and Bhattacharyya, 1995; Engelhard and Evans, 1995; Ionescu *et al.,* 1997; Fujiwara *et al.,* 1999; Parker and Marqusee, 1999; Ionescu *et al.,* 2000; Cobos and Radford, 2006). These intermediates often require certain conditions to be detected. These conditions include mild denaturing conditions, extremes of pH and temperature and reasonably high ionic strengths.

1.3.6. The Molten Globule State

The molten globule state (Figure 4) can be defined as a compact hydrophobic intermediate state assumed by many globular proteins under certain conditions (Fink, 1995). The hydrophobic core of the molten globule state is often highly

hydrated resulting in the molten globule being more expanded and swollen than the native state (Uchiyama *et al.,* 1995; Kharakoz and Bychkova, 1997) although a solvent-inaccessible core still remains (Chalikian *et al.,* 1995). The molten globule species has been detected both at equilibrium and as a transient kinetic intermediate species (Van der Goot *et al.*, 1991, Ogasahara *et al.,* 1994; Guha and Bhattacharyya, 1995; Ionescu *et al.,* 1997; Fujiwara *et al.*, 1999; Ionescu *et al.,* 2000). Thus the equilibrium molten globule states can often be considered as stable models for the transient kinetic intermediates (Roder and Colon, 1997).

It is believed that the molten globule state is a general species found in all proteins (reviewed by Kim and Baldwin, 1990; Fink, 1995). It is able to form from the native state under conditions where the native state loses its tight packing arrangement. It is not always detected because it requires certain specific conditions to form. These conditions include one or a combination of high salt concentrations (Fink *et al.*, 1994; Prajapati *et al.,* 1998), mild denaturant concentrations (Ogasahara *et al.*, 1993; Carra *et al.,* 1994; Gualfetti *et al.*, 1999), high temperatures (Zhao and London, 1986; Ionescu *et al.,* 2000 Ulrih *et al.,* 2004), decreased polarity (Shiraki *et al.,* 1995; Bychkova *et al.,* 1996; Konno *et al.,* 2000; Fatima *et al.,* 2006) and extreme pH (Zhao and London, 1986; Carra *et al.,* 1994; Bychkova *et al.*, 1996; Ulrih *et al.,* 2004).

There are four properties that define a molten globule state: Firstly this species has a *dense core* and a degree of compactness that is closer to the compactness of the native state than the denatured state (only 10-30% larger than the native state, (Kuwajima and Arai, 2000)). Secondly when in the molten globule state, the protein will have *defined secondary structure* as detected by far-UV circular dichroism (Vassilenko and Uversky, 2002). Thirdly, the *tertiary structure* as detected by near-UV circular dichroism will be *indistinct* with merely loosely packed side chains, and fourthly the molten globule state will have a significant amount of *exposed hydrophobic surface* and thus a greater propensity to form aggregates (Figure 4). The greater amount of exposed

hydrophobic surface, understood to occur as a result of hydrophobic collapse (Kim and Baldwin, 1990), can be detected experimentally by the high capacity of the molten globule state to bind to the hydrophobic part of the dye ANS, compared to the native and the denatured states (Semisotnov *et al.*, 1991) (Figure 4).

The molten globule state and other non-native states of proteins have been shown to be involved in some physiological processes such as protein penetration into membranes (Van der Goot *et al.,* 1991), release of protein bound ligands (Celej *et al.*, 2003) and protein recognition by chaperones (Van der Vies *et al.*, 1992; Dobson and Karplus, 1999). Cells have evolved molecular chaperone mechanisms in order to shield the exposed hydrophobic surfaces in partly folded proteins so as to assist in the folding process by avoiding aggregation (Ellis and Hartl, 1999).

Not all techniques used to measure protein unfolding are capable of detecting the molten globule state and could therefore simply show either the native ⇨ molten globule transition or the native ⇨ denatured transition, thereby advocating a misconception that the unfolding of the protein is two-state in nature. The molten globule state can be distinguished from the native state by the increase in the exposure of non-polar residues and a lack of the hydrophobic interactions that are present in, and stabilise the native state.

The molten globule state most likely does contain a small degree of tertiary structure (Kim and Baldwin, 1990), despite the hypothesis that it is rapidly fluctuating. It is proposed to be composed of a number of compact, ordered "sub states" that retain an amount of tertiary structure but are joined by extremely flexible, disordered, mostly hydrophobic links (Nishii *et al.,* 1995). The molten globule can thus be explained in terms of a protein state consisting of rapidly interchanging tertiary structure due to packing interactions being broken and reformed which creates a number of enthalpic barriers along the

folding funnel towards the native state. This explains why there is variety in the structures of experimentally determined molten globules, why some molten globule states have a higher proportion of tertiary structure than others and why the molten globule state may not be detected in smaller proteins that have a minimal number of tertiary interactions in the native state.

1.4. CLIC1 and Other Soluble Membrane Proteins

1.4.1. Chloride Intracellular Channels

The chloride intracellular channels or CLICs are a family of chloride ion channel proteins that are fairly unusual in that they can exist either in a membrane bound state or in a soluble state (for reviews, see Berryman and Bretscher, 2000; Cromer *et al.*, 2002; Ashley, 2003). The CLIC nomenclature was proposed by Heiss and Poustka (1997) based on the channel forming activity of the first members of this family although despite their sequence similarity, many of the recent members have failed to exhibit pore-forming activity.

CLICs are one of the four major classes of chloride channels. The other chloride channels- which share no sequence homology with the CLIC family (Dutzler *et al.,* 2002), include the ligand gated anion channels (GABA receptors), the cystic fibrosis transmembrane conductance regulators (CFTCRs), and chloride channels (ClCs) (Jentsch *et al.*, 2001; Dutzler, 2006). The functions of these channels include transepithelial transport, regulation of intracellular pH and regulation of cell volume (reviewed by Jentsch *et al.,* 2001; Dutzler, 2006).

CLICs can localise to the plasma membrane or to most organelle membranes, they are distributed in various tissues and cells (Chuang *et al.,* 1999, Duncan *et al.,* 1999; Edwards, 1999; Valenzuela *et al.,* 2000) and are involved in diverse

functions such as kidney function (Tulk and Edwards, 1998), bone resorption (Schlesinger, 1997), water secretion (Nishizawa *et al.,* 2000), spermatozoa function (Myers *et al*., 2004), signal transduction (Qian *et al.,* 1999; Berryman and Goldenring, 2003; Saeki *et al.,* 2005), cell division (Tonini *et al.,* 2000; Warton *et al.*, 2002), cell cycle regulation (Valenzuela *et al.,* 2000; Berryman and Goldenring, 2003) and apoptosis (Fernandez-Salas *et al.,* 2002; Suh *et al.,* 2005) where they control cellular ion concentrations, possibly through the formation of channels.

Whether CLICs actually form membrane channels or whether they simply modulate them has been a matter of some speculation (Duncan *et al.,* 1997; Valenzuela *et al.,* 1997; Nishizawa *et al.,* 2000; Tonini *et al.,* 2000; Proutski *et al.,* 2002; Tulk *et al.,* 2002; Warton *et al.,* 2002; Ashley, 2003; Friedli *et al.,* 2003), particularly since these proteins are relatively small and only form one putative transmembrane domain which is highly unusual for ion channels. For example the ClC channels form dimers with ten to twelve transmembrane domains each and create two effectively independent pores (Dutzler *et al.,* 2004; Dutzler, 2006), CFTCRs also have twelve transmembrane domains and GABA receptors have four transmembrane domains which combine to form pentameric channels (Jentsch *et al.,* 2001; Weinreich and Jentsch, 2001). Some CLICs may therefore simply be anion channel regulators while others may genuinely form anion channels and yet others may be involved in both functions (Suginta *et al.,* 2001).

Another property of the CLICs that is atypical of ion channel proteins is that more than 50% of the protein present in the cell exists in a *soluble form* either in the cytoplasm or in intracellular compartments and thus only small amounts of the protein are actually localised to the membrane. However it is understood that p64 (CLIC5B) (Landry *et al.,* 1993), CLIC4 (Chuang *et al.,* 1999), CLIC1 (Tonini *et al.*, 2000) and CLIC5A (Berryman *et al.,* 2004) form membrane-resident channels in their own right by facilitating ion efflux, and recently CLIC1 has been shown both to insert into phospholipid vesicles and to form

chloride sensitive channels in the absence of ancillary subunits or accessory proteins (Tulk *et al.*, 2000; Harrop *et al.*, 2001; Tulk *et al.*, 2002).

The CLIC family consists of seven members to date whose sequences are highly conserved across species ranging from humans to frogs to zebra fish to *Drosophila* to yeast (Ashley, 2003; Shorning *et al.,* 2003) and they are: CLIC1; CLIC2; CLIC3; CLIC4 and CLIC5A which are all approximately the same size (~240 amino acid residues); and two larger variants, p64 (CLIC5B in humans) and Parchorin (CLIC6 in humans) that contain additional unrelated N-terminal domains that are not evolutionarily conserved. These acidic proteins (with p*I* values less than 5.4 except for CLIC3 which has a slightly higher p*I* value) all have a conserved hydrophobic core as determined by Kyte-Doolittile hydropathy plots (Kyte and Doolittle, 1982). They have a high sequence identity (47-76% identity) and therefore although only the crystal structures of CLIC1 and CLIC4 have been solved (Harrop *et al.*, 2001; Littler *et al.*, 2005), it is most likely that all the members of the CLIC family share a similar canonical fold. The CLIC family appear to belong to the glutathione transferase (GST) superfamily of proteins (Figure 5) although their highest sequence identity with GSTs is only approximately 16% with Omega class GST (see Figure 12).

CLIC1 was first proposed to be a member of the GST superfamily based on its primary sequence by Dulhunty *et al.*, (2000); and then was proven to be a member of this superfamily when Harrop *et al.* obtained the crystal structure the following year. Like all members of this superfamily, reduced CLIC1 has two domains: an N-terminal domain containing a thioredoxin fold (Holmgren, 1985; Martin, 1995) and an all-helical C-terminal domain (see Figure 8).

The fold common to the GST superfamily comprises five families (Figure 5): The largest is the class of glutathione transferases. These are soluble homodimeric enzymes that have a variety of functions, the most common of

which is the detoxification of cells (reviewed in Sheehan *et al.*, 2001; Oakley 2005). These proteins are ubiquitous in mammalian, plant, fungal, insectal, helminth and bacterial systems (Sheehan *et al.*, 2001). The second member of the GST superfamily is glutaredoxin 2 (Grx2) from *Escherichia coli*. This monomeric protein is involved in redox reactions particularly under stress conditions and is structurally related to the ancient GSTs (Xia *et al.,* 2001). The yeast prion protein, Ure2p is the third member (Bousset *et al.,* 2001). The CLIC family including CLIC1 (Harrop *et al.,* 2001) and CLIC4 (Littler *et al.,* 2005) is the fourth member, and most recently, a domain of yeast elongation factor 1-gamma (Jeppesen *et al.,* 2003) is the latest member of this superfamily to have its crystal structure solved (SCOP: Murzin *et al.*, 1995).

CLIC1 was first isolated in the human myelomonocytic cell line, U937 by Valenzuela *et al.* in 1997 and was described as being not only the first human member of the CLIC family of proteins to be cloned (of which the bovine p64 (Redhead *et al.,* 1992; Landry *et al.,* 1993) and rat brain p64H1 (Howell *et al.*, 1996) were the only other known members at that stage), but also as being the first chloride ion channel to be discovered that localises to the nuclear membrane. Hence it was named NCC27 (nuclear chloride channel of 27 kDa).

Subsequent studies have revealed that CLIC1 is widely distributed in tissues and cells (Valenzuela *et al.,* 2000; Tulk *et al.,* 2002; Warton *et al.,* 2002; Myers *et al.*, 2004; Novarino *et al.,* 2004) but is mostly localised to the nucleoplasm, and nuclear membrane and is most abundant in kidney, heart and placental cells (Tulk and Edwards, 1998) where it is believed to play a role in the cell cycle, particularly in cell division, by forming ion channels (Valenzuela *et al.,* 2000; Tulk *et al.* 2002; Warton *et al.*, 2002).

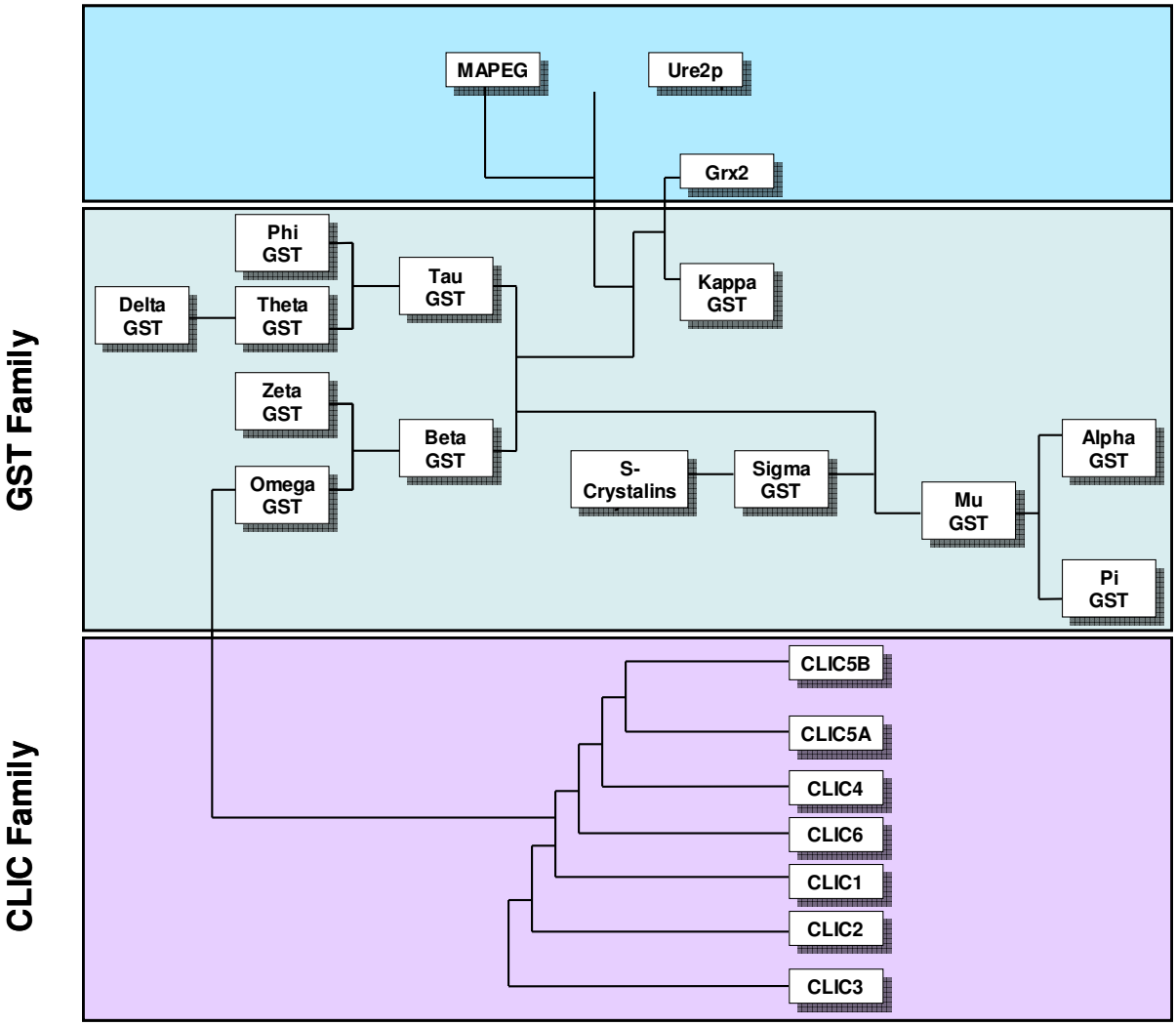


Figure 5: Dendrogram of the GST superfamily

Sequence relatedness between the members of the CLIC family (adapted from Berryman and Bretscher, 2000) and the members of the GST family (adapted from Sheehan *et al.,* 2001).

In contrast to ClC channels where the Cl^- ion is believed to bind specifically to the channel and influence the probability of it being open (Dutzler *et al.,* 2002; Dutzler, 2006), the latest understanding is that CLIC1 does not form channels specific towards chloride ions or even towards anions in general. Rather it functions as a non-selective membrane pore, allowing for the passage of several different ions across the membrane (Singh and Ashley, 2006).

he fact that CLIC1 is well conserved across unrelated species, that its mRNA tissue distribution is practically ubiquitous and that the gene encoding CLIC1 is active from early on in embryogenesis throughout adult life suggests that the biological role of CLIC1 must be a fundamental process common to most, if not all cells (Valenzuela *et al.,* 2000). An interpretation of CLIC1 biological activity offered by Valenzuela *et al.* (2000) and Warton *et al.* (2002) states that, since CLIC1 channel activity can be observed on the plasma membranes of cells that are in the process of dividing or have just completed division (Tonini *et al.,* 2000), cytoplasmic (and/or nucleoplasmic) CLIC1 likely localises to the plasma (and/or nuclear) membrane during the G2/M phase of the cell cycle. After it localises to the membrane, CLIC1 may regulate the "swelling" of the cell (and/or the nucleus) during mitosis and hence allow cell division to occur by providing a means for the cell to change its volume through the modification of the cellular (and/or nuclear) concentration of chloride ions.

Recently a link has been found between the functional expression of CLIC1 in microglial cells in the brain and the activation of these cells by the β-amyloid protein that is a major factor in Alzheimer's disease (Novarino *et al.,* 2004). Furthermore, blockade of CLIC1 channel activity by the CLIC1 specific inhibitor, indanyloxyacetic acid 94 (IAA-94) was found to inhibit proliferation of the microglial cells, to hamper neuronal toxicity formed as a result of β-amyloid-induced activation of microglial cells and to reduce production of tumour necrosis factor-α and nitrite which are upregulated by the presence of

β-amyloid and are implicated in the disease (Novarino *et al.,* 2004). Thus CLIC1 should be considered as a therapeutic target for inflammatory diseases.

The other members of the CLIC family are also associated with chloride channels but their biological roles are somewhat diverse (reviewed by Ashley, 2003). CLIC2 (243 amino acids in size), which shares 60% overall identity with CLIC1, is possibly involved in diseases associated with chromosome Xq28 such as X-linked epilepsy (Heiss and Poustka, 1997). Until recently no information about the subcellular location or function of CLIC2 was available. Board *et al.* (2004) have found that CLIC2 is widely distributed in human tissue, being most abundant in the spleen and lung. Despite its Cys-X-X-Cys redox motif, the protein unexpectedly does not exhibit thiol transferase activity which is characteristic of the glutaredoxins that display the same redox pattern. CLIC2 interacts with cardiac ryanodine receptors where it inhibits Ca^{2+} release from internal stores (Dulhunty *et al.,* 2005). This role of CLIC2 provides a further link between the CLICs and the GSTs- in particular class Omega GST (Dulhunty *et al.,* 2001; Board *et al.,* 2004).

CLIC3 (208 residues) shares slightly lower sequence identity with CLIC1 (49%) and with the CLIC family in general. It has been shown to interact with the C-terminal of ERK7, a member of the mitogen activated protein (MAP) kinase pathway although CLIC3 is not a direct substrate of ERK7 (Qian *et al.,* 1999). Like CLIC1, CLIC3 localises predominantly to the nuclear membrane and is expressed in human placenta (Money *et al.,* 2006). By stimulating chloride conductance it helps activate MAP kinase signal transduction and therefore possibly has a function in the regulation of cell growth (Qian *et al.*, 1999). CLIC3 has a limited hydrophobic domain, however, and thus likely multimerises if it forms part of a membrane channel.

Human CLIC4 (253 residues and 67% sequence identity with CLIC1) was first identified in nephron and proximal tubule cells of human kidney (Edwards,

2000). As with the other members of the CLIC family, the subcellular distribution of CLIC4 varies according to the cell type and the cell function (Berryman and Bretscher, 2000). Cytotoxic stimuli, DNA damage and over-expression of p53 and tumour necrosis factor-α (Suh *et al.,* 2005) result in the upregulation of CLIC4 and ultimately lead to apoptosis which causes pH changes in the cell and is associated with alterations in the mitochondrial membrane and the release of cytochrome *c* to the cytoplasm (Fernandez-Salas *et al.,* 1999; Fernandez-Salas *et al.*, 2002). CLIC4 is believed to have the ability to form an integral membrane protein that contains a large cytoplasmic C-terminal domain, a single membrane-spanning portion and a small N-terminal domain that pokes into the lumen of the endoplasmic reticulum (Duncan *et al.,* 1997) or other intracellular organelles. The crystal structure of a mutant form of soluble human CLIC4 with a C-terminal extension referred to as CLIC4(ext) shows this protein to be monomeric with the only significant difference to the CLIC1 structure localised to the α2 helix (Littler *et al.,* 2005). The crystal structure of wild type human CLIC4 has also been resolved (Li *et al.,* 2006) and interestingly reports the soluble protein to exist as a homotrimer where the monomeric subunits are associated by hydrophobic and hydrogen bond contacts! As in the CLIC4(ext) monomer, the subunits of the trimer differ from CLIC1 in the α2 helix (Figure 6). These results imply that α2 could be a flexible hinge region involved in the structural transition of these CLIC proteins from their soluble state to the membrane-associated form.

CLIC5A (251 amino acids and 63% sequence identity with CLIC1) associates with microvilli and interacts with the actin cytoskeleton in polarised epithelial cells in heart and skeletal muscle (Berryman and Bretscher, 2000). This protein is distinguished from the other members of the family by its ability to remain tightly bound to the cytoskeleton (Berryman and Bretscher, 2000). CLIC5A, like many of the CLICs, has been shown to conduct dose-dependent chloride efflux across artificial liposomes. This conductance is sensitive to the channel blocker, IAA-94 (Berryman *et al.,* 2004).

p64 (437 amino acids long) was the first member of the CLIC family to be discovered (Redhead *et al.,* 1992; Landry *et al.,* 1993) and is a bovine protein that plays a role in kidney function (Tulk and Edwards, 1998) while its avian homologue, p62, is involved in osteoclast formation (Schlesinger *et al.*, 1997*).* The C-terminal domain of p64 shares 60% sequence identity with CLIC1. The human homologue of p64, CLIC5B, is a 46-kDa splice variant of CLIC5A that localises to the osteoclast Golgi apparatus (Shanks *et al.,* 2002; Friedli *et al.,* 2003; Edwards *et al.,* 2006). p64 and its homologues function in the acidification of intracellular organelles and the regulation of acid transport via the formation of ion channels containing two putative transmembrane domains both found in the C-terminal part of the molecule (Edwards, 1999; Ashley, 2003).

Parchorin (637 amino acids) was discovered predominantly to localise to rabbit parietal cells and the choroid plexus, which is how it got its name (Nishizawa *et al.,* 2000). These proteins exist in the cytoplasm of water-secreting cells and are translocated to the plasma membrane only when the level of chloride ions in the cell is low (Nishizawa *et al.*, 2000). Unlike other members of the CLIC family, the N-terminal part of Parchorin is highly charged and the protein has no predicted membrane-spanning domains in its hydropathy profile. This protein might, therefore, simply be an activator or regulator of a chloride channel. The human homologue of Parchorin, CLIC6, consists of 704 amino acids, and is the longest identified member of the family to date. It is further different from CLICs 1-5 in that it contains a six amino acid motif in its N-terminal domain repeated 15 times (Friedli *et al.,* 2003; Griffon *et al.*, 2003).

CLIC6 is expressed in water-secreting cells and in endocrine cells where it forms a multimeric complex with a dopamine receptor and with scaffolding proteins (Griffon *et al.,* 2003). Therefore, it is plausible that CLIC6 and Parchorin are involved in the regulation of secretion, probably by controlling chloride ion transport (Urushidani *et al.,* 1999; Griffon *et al.,* 2003) however whether they actually form transmembrane channels remains to be proved.

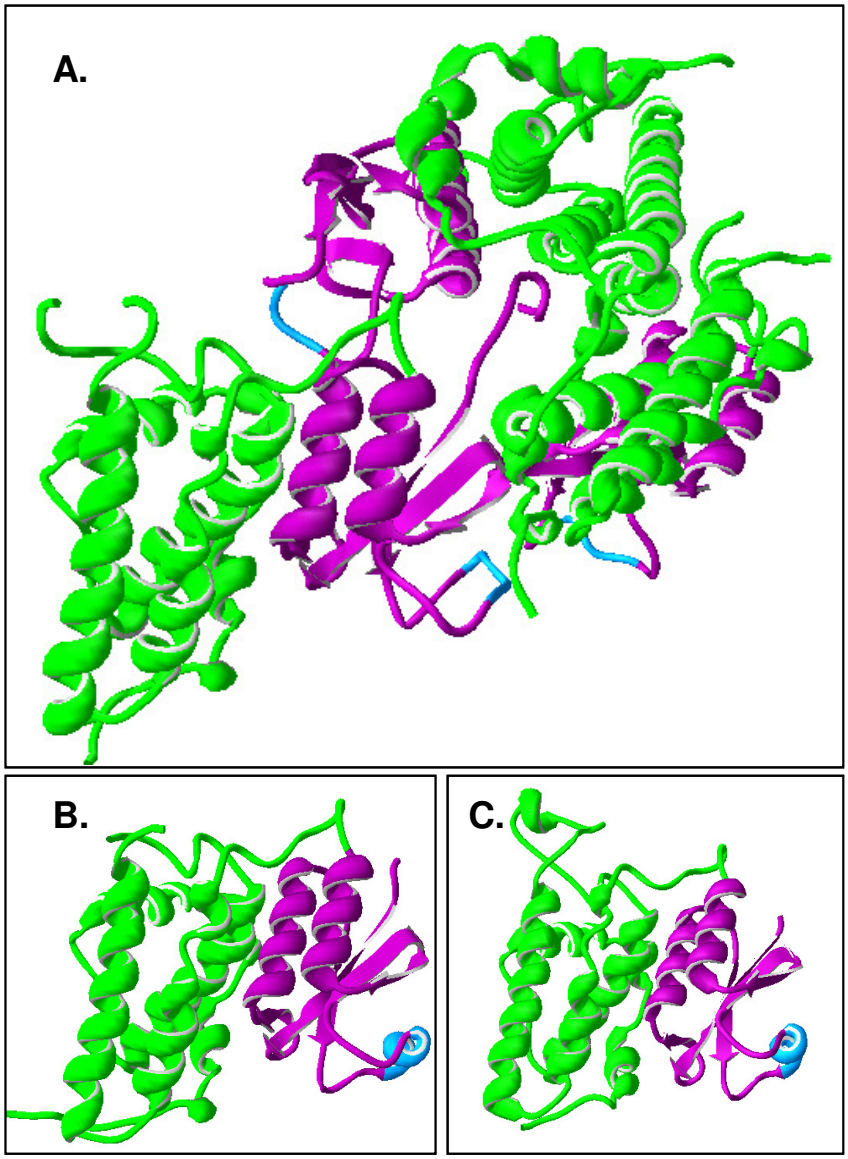


Figure 6: Comparison of the structures of soluble CLIC1 and CLIC4

(A) The structure of soluble CLIC4 is a trimer made of three identical subunits. **(B)** Mutant CLIC4(ext) with a C-terminal extension crystallises as a monomer. **(C)** The CLIC1 crystal structure is monomeric and very similar in structure to the monomeric subunits of CLIC4 except for the region surrounding the α2 helix (indicated in blue). The N-terminal domain of each subunit is indicated in purple while the C-terminal domain is green. The flexible loop region that is present in the CLIC1 structure was not captured in the CLIC4 structure due to its extremely flexible nature. The model was generated with Swiss PDB viewer (Guex and Peitsch, 1997) using the PDB files 2d2z (Li *et al.,* 2006), 2ahe (Littler *et al.,* 2005) and 1k0m (Harrop *et al.*, 2001) for the CLIC4 trimer, CLIC4(ext) monomer and CLIC1 monomer respectively.

Although the members of the CLIC family have similar structures and related functions, they display remarkable differences in their locations within the cell, hence the hypothesis that these proteins are "functionally redundant and their co-expression is simply to ensure that essential cellular functions are fulfilled" (Berryman, and Bretscher, 2000).

1.4.2. Structure of CLIC1

Primary and secondary structure: The CLIC1 protein sequence

Reduced CLIC1 is a monomeric protein consisting of 241 amino acids. It has a molecular weight of 26.9 kDa and a p*I* of 4.85 as estimated by the DNAStar software (Lasergene) (Valenzuela *et al.,* 1997; Ashley, 2003). This protein has a 47.7% helical content and an 8.3% sheet content according to the crystal structure (Harrop *et al.,* 2001). The sequence contains putative protein kinase and cAMP phosphorylation sites, mainly in the N-terminal domain (Valenzuela *et al.*, 1997) and contains a potential protein interaction domain in the C-terminal part of the protein (Ashley, 2003).

There is only one tryptophan residue in the CLIC1 sequence (Figure 7): Trp35, present in the N-terminal domain, and eight tyrosine residues scattered throughout the protein but predominantly in the C-terminal domain. The protein contains six cysteine residues, one of which, Cys24, is found in the active site. The CLIC1 sequence contains 35 acidic residues and 27 basic residues (Figure 7) signifying that the protein has an imbalance in charge (net charge of -7) and could have a strong dipole nature depending on how the residues are arranged in the tertiary structure.

Tertiary structure of CLIC1

Until the structure of CLIC4 was published in 2005 (Littler *et al.,* 2005), CLIC1 was the only member of the CLIC family of proteins to have its crystal structure solved. The crystal structure of the soluble and reduced form of

CLIC1 has been determined at 1.4 Å resolution at pH 5.0 (Harrop *et al.*, 2001) (Figure 8). CLIC1 is a relatively flat protein (see dimensions Figure 8) that folds into two domains linked by a proline-rich loop that is believed to confer an amount of plasticity on the domain interface (Harrop *et al.*, 2001). The N-terminal domain accommodates a characteristic thioredoxin fold (βαβαββα motif) (Martin, 1995). The larger C-terminal domain is all α-helical in nature. CLIC1 forms a highly negatively charged loop between helix 5 and 6 (Pro147 – Gln164). This loop is unique to the CLIC structure and is not found in other members of the GST superfamily (see Figure 12). This negatively charged loop, structurally adjacent to the proline-rich loop connecting the two domains, is extremely flexible and possibly is involved in protein – protein interactions or even membrane insertion (Harrop *et al.*, 2001, Cromer *et al.,* 2002).

The fact that membrane-bound CLIC1 was found to be resistant to alkaline extraction implied that the protein spans the membrane (Tulk and Edwards, 1998). And in 2000, Tonini *et al.* demonstrated conclusively that CLIC1 can exist as an *integral membrane protein* that not only associates with membranes but inserts into and spans the membrane, directly forming ion channels either on its own in monomeric form or else by aggregating to form larger oligomers.

Harrop *et al.* (2001) were the first to propose that in order for CLIC1 to form a channel in membranes, the *N-terminal* domain of the protein must undergo rapid unfolding and refolding so that the helix can be correctly inserted into the membrane. Confirming this assumption, hydrogen exchange studies have shown the N-terminal domain of CLIC1 to be more flexible and less stable than the C-terminal domain (Nathaniel PHD thesis, in preparation). The N-terminal domain is thus more likely to undergo the structural rearrangements required for the transition from the soluble to membrane-bound state.

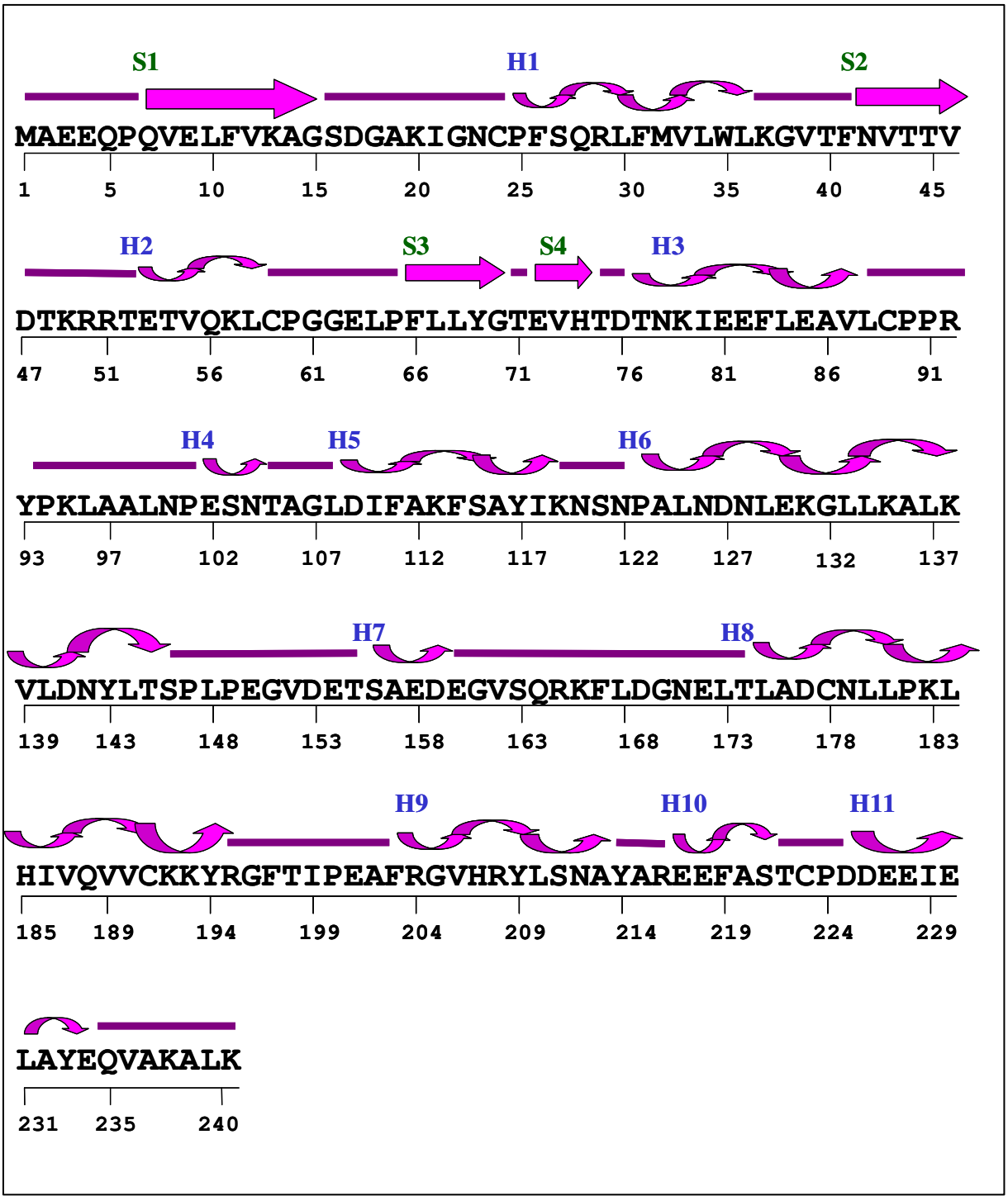


Figure 7: CLIC1 sequence

The CLIC1 sequence illustrating its primary and secondary structure. Helices are indicated with a blue H and β strands with a green S. This image was adapted from the PDBsum database (Laskowski *et al.*, 1997)

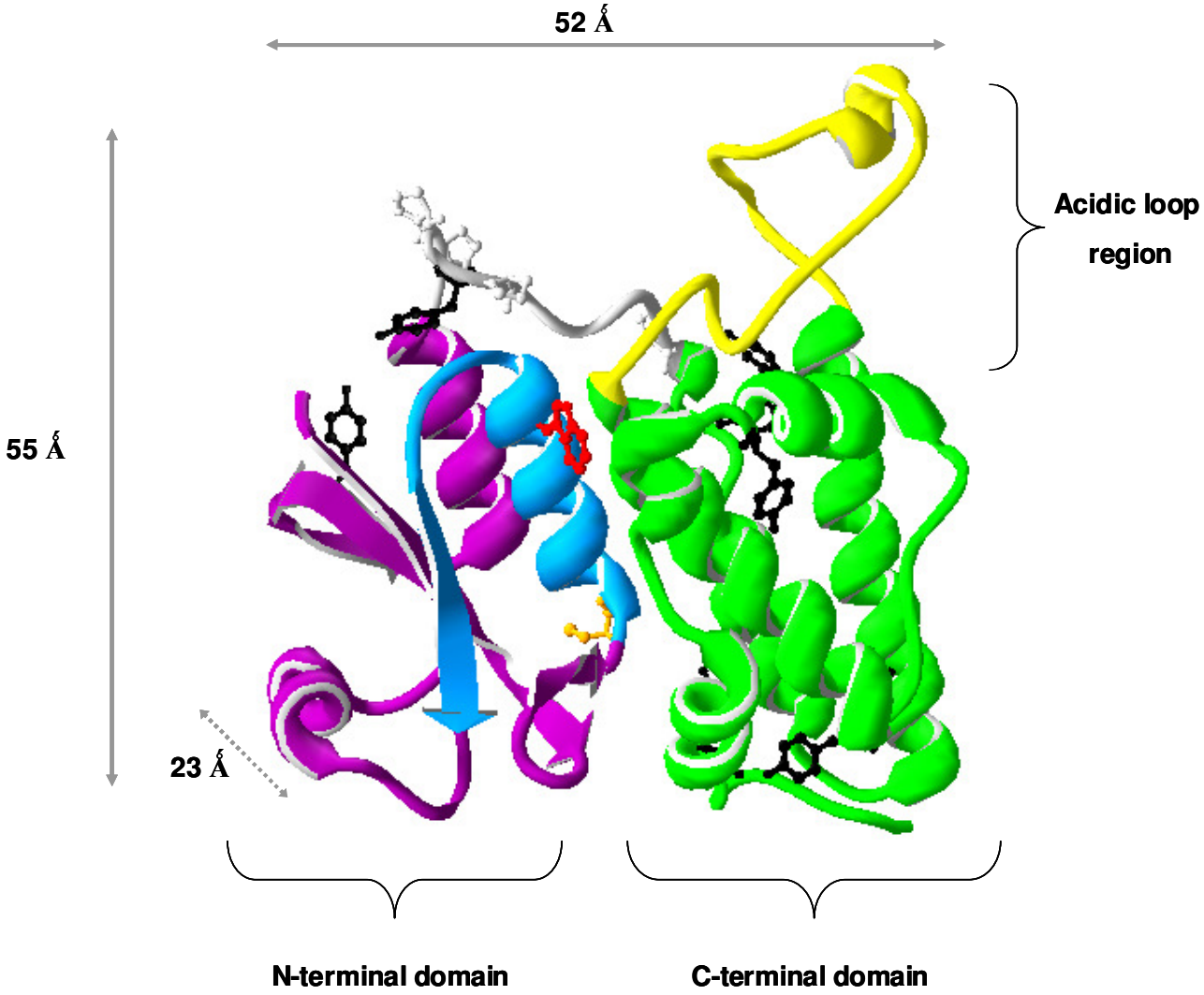


Figure 8: Crystal structure of CLIC1

Crystal structure of reduced CLIC1. The N-terminal domain containing the thioredoxin fold is indicated in purple and blue and the all α-helical C-terminal domain is indicated in green and yellow. The proline-rich loop connecting the two domains is indicated in grey. The active site Cys24 is indicated in orange. The single tryptophan residue, Trp35 is red and the 8 tyrosines (2 in the N-terminal domain and 6 in the C-terminal domain) are black. The negatively charged loop is shown in yellow and the helix that is considered likely to traverse the membrane is indicated in blue. The model was generated with Swiss PDB viewer (Guex and Peitsch, 1997) using the PDB file 1k0m (Harrop *et al.*, 2001).

A 22-residue segment in the N-terminal domain encompassing the α1 helix and β2 strand and extending from Pro25 to Val46 (indicated in blue in Figure 8) is considered likely to form the *helix that traverses the membrane*, placing Cys24 directly at the membrane interface. Not only is this region highly exposed on one face of the molecule and a suitable length for membrane insertion (31 Å) but the α1 helix and β2 strand that form this segment are strikingly hydrophobic and distinguish CLIC1 from other members of the GST superfamily that have a far more polar α1 helix and β2 strand despite the fact that they are closely related in sequence and structure to CLIC1 (Harrop *et al.,* 2001) (see Figure 12). Furthermore, this region has a high propensity to form a helix and has a strong N- and C- capping motif (according to the helix-coil algorithm AGADIR (Lacroix *et al.,* 1998)) that is conserved across the CLIC family but is not found in the other members of the GST superfamily (Nathaniel PHD thesis, in preparation). There is a conserved positively charged motif from Lys49 to Arg51 (CLIC1 numbering) that is located at the C-terminal end of the CLIC family's putative transmembrane region (see Figure 12). This motif is considered likely to act as a "plug", preventing the protein from inserting further into the negatively charged membrane (Nathaniel PHD thesis, in preparation).

The overall charge distribution of CLIC1 is asymmetrical and there are hotspots of both negative and positive charge evident in the three-dimensional structure that bestow an acute dipole character upon the molecule (Figure 9). There are two highly significant negatively charged patches in the CLIC1 structure that appear to be unique to CLICs. The first is the negatively charged flexible loop region (Pro147 – Gln164) that extends from the C-terminal domain. This region contains seven acidic residues. The second negatively charged patch is the α9 helix comprising six acidic residues found precisely at the C-terminus of the molecule (Figure 9). These regions that have high concentrations of charge will be exquisitely sensitive to changes in pH and could be important for membrane insertion.

CLIC1 contains a glutathione (GSH) binding site within its N-terminal domain (Figure 10). This region has four residues that are conserved in the GSH binding sites of the GST superfamily and they are (CLIC1 numbering): Lys13; Cys24; Leu64 and Thr77 (Cromer *et al.,* 2002). GSH covalently binds to Cys24, forming a mixed disulfide bridge. Therefore, although CLIC1 is redox active, it is dependent on GSH. This is unlike CLIC2, CLIC3 and Grx2 (another monomeric member of the GST superfamily) that contain the Cys-X-X-Cys redox motif. The interactions between GSH and CLIC1 are fewer than with the GSTs. Thus GSH binding in CLIC1 is much weaker than it is in GSTs except for class Kappa GST that also possesses less extensive interactions with GSH than the other GSTs (Ladner *et al.,* 2004). It has been suggested that CLIC1 could use its GSH-binding site to target this ion channel protein to specific locations within the cell (Harrop *et al.*, 2001). Consequently this GSH-dependent redox mechanism would maintain an equilibrium between the soluble and membrane-bound forms of the protein (Littler *et al.,* 2004). CLIC1 contains six cysteine residues (Figure 7) and therefore has intra- and inter-domain disulphide bond-forming potential. A recent theory proposes that when the protein is bound to the membrane under oxidising conditions, the disulphide bonds that form result in the "closure" of the channel which can be reopened upon reduction to allow the passage of ions through the membrane (Singh and Ashley, 2006).

CLIC1 has been observed to form a non-covalent dimer *in vitro* upon oxidation by hydrogen peroxide (Littler *et al.,* 2004). This transition, which is reversible upon reduction, is due to the formation of an intramolecular disulphide bond between Cys24 and Cys59 and results in a major structural transition, particularly in the N-terminal domain, to an all-helical protein with a great amount of hydrophobic surface exposed at the dimer interface (Figure 11).

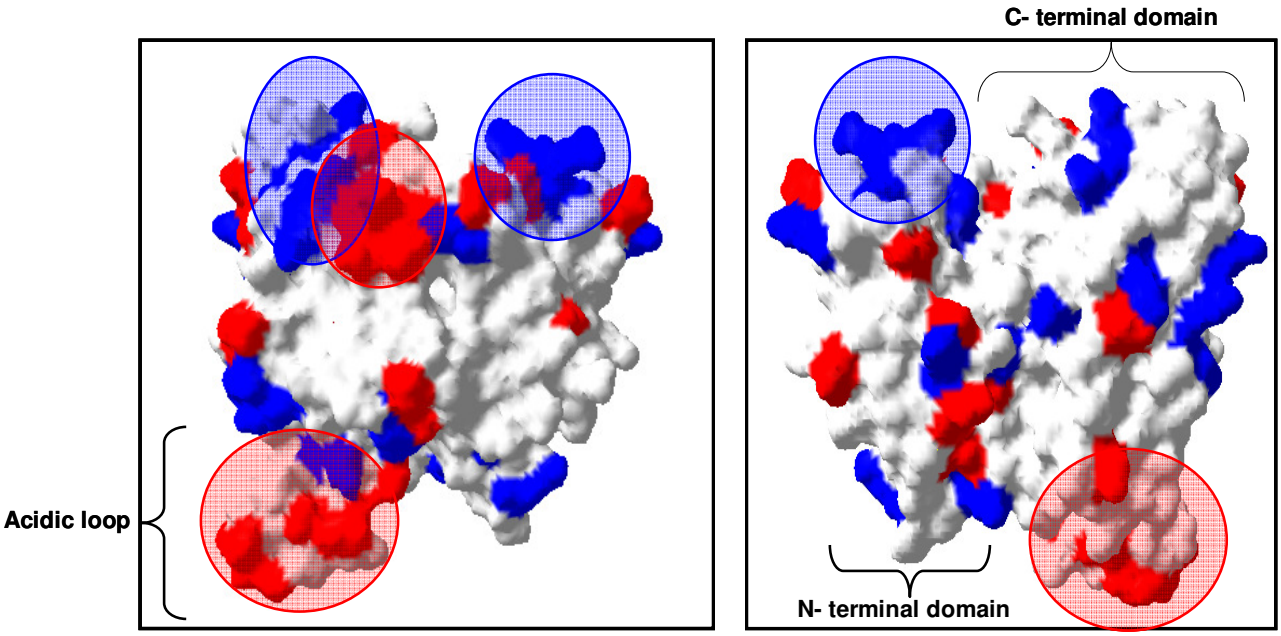


Figure 9: Charged surface of CLIC1

The distribution of charged residues on the surface of CLIC1. Both faces are shown. Acidic residues are indicated in red, basic residues are shown in blue. The regions of the protein containing hotspots of negative and positive charge are ringed. The images were rendered with Swiss PDB viewer, (Guex and Peitsch, 1997) using the PDB code 1k0m (Harrop *et al.*, 2001).

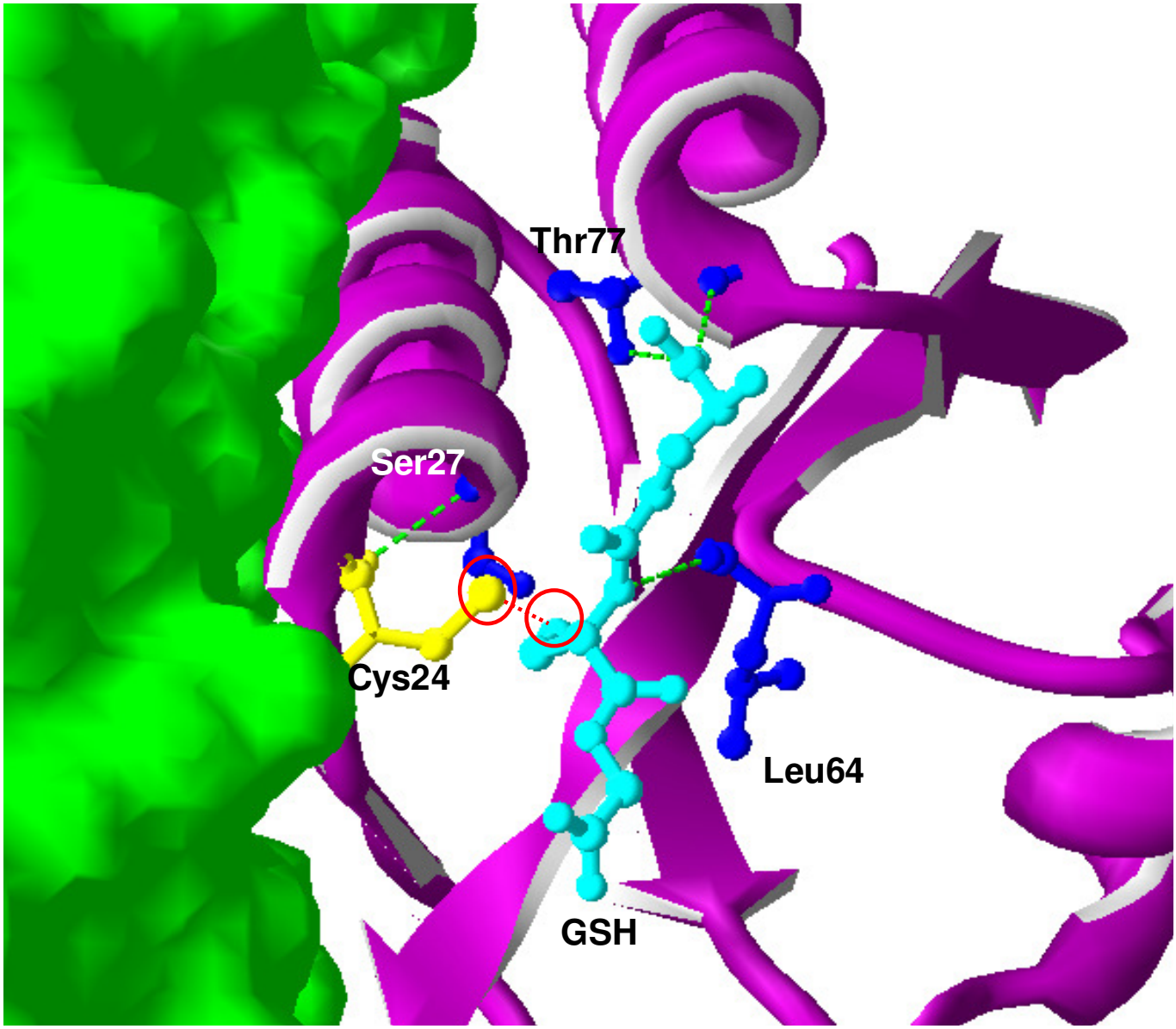


Figure 10: CLIC1 active site

The glutathione binding site of CLIC1. GSH is indicated in turquoise. Hydrogen bonds are shown with a green dotted line. Cys24 is shown in yellow. Ser27, Leu64 and Thr77 are blue. The sulphur atoms from Cys24 and GSH are ringed in red and the mixed disulphide bond is indicated with a red dotted line. The C-terminal domain is shown as a green surface while the N-terminal domain is a purple ribbon structure. The image was generated with Swiss PDB viewer (Guex and Peitsch, 1997) using the PDB file 1k0n (Harrop *et al.*, 2001).

This hydrophobic surface may represent the membrane-docking interface *in vivo* where the monomer is believed to undergo similar alterations to its N-terminal domain before interacting with the membrane. Even *in vitro* the N-terminal domain of monomeric CLIC1 will occasionally transit to this altered conformation but is unstable and prone to aggregation due to the increased surface hydrophobicity (Littler *et al.,* 2004). Only in the absence of lipid will oxidised CLIC1 form the dimer whereas in the presence of lipid the oxidised protein is proposed to interact favourably with the membrane (Littler *et al.*, 2004).

When present in its soluble form in the cytoplasm however, it is unlikely that CLIC1 will spontaneously form the oxidised dimer, considering the cytoplasm contains up to 10 mM GSH (Hwang *et al.,* 1992) and thus presents a particularly reducing environment to the protein. Therefore, should this dimer be significant, there must be some signal, possibly as a result of the changing phases of the cell cycle, which results in the oxidation of the protein.

The CLIC1 dimer is less globular than the dimers formed by other members of the GST superfamily and can be compared with the unusual elongated dimer of the class Kappa enzyme (Ladner *et al.,* 2004). The oxidised CLIC1 dimer can still form chloride channels as can the reduced protein, and both Cys24 and Cys59 were shown to be essential for CLIC1 channel formation (Littler *et al,* 2004).

Cys59, found at the C-terminal end of the α2 helix in CLIC1 is not conserved across the CLIC family, and corresponds to a conserved alanine in most other members of the family (Littler *et al.,* 2004). Therefore if this disulphide bond is involved in the interaction of CLIC1 with the membrane, it seems unlikely that an identical mechanism would be utilised by the other members of the family.

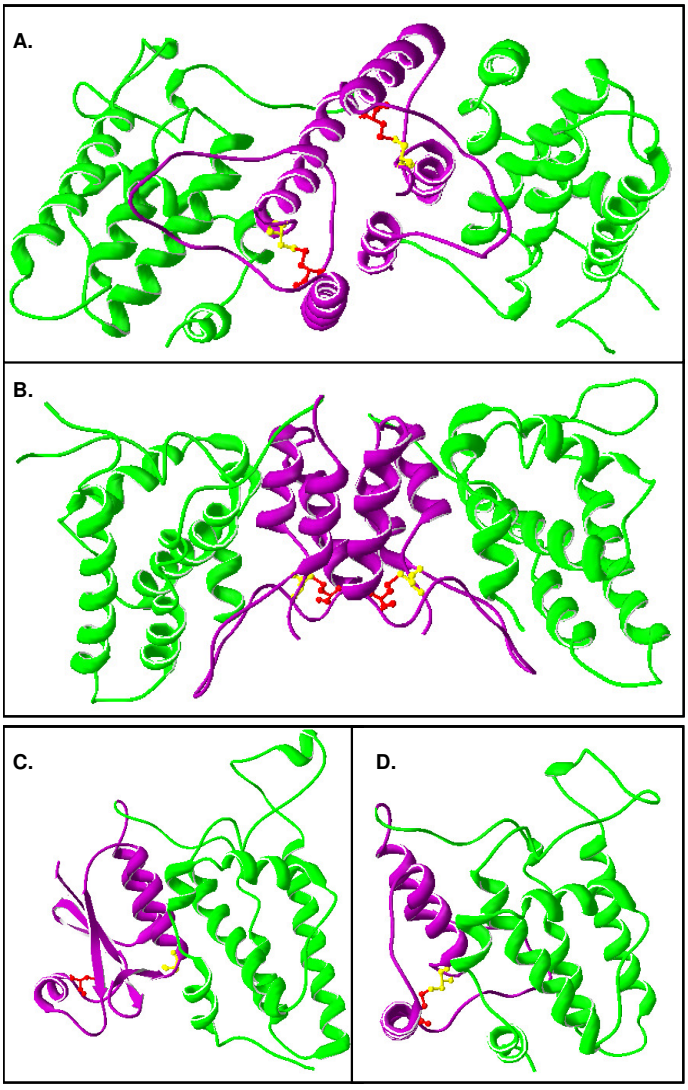


Figure 11: Structure of the CLIC1 dimer

(A) and **(B)** represent the crystal structure of the non-covalent dimeric form of oxidised CLIC1 when viewed in different orientations (Littler *et al.,* 2004). The structure of monomeric, reduced CLIC1 is shown in **(C)** and is compared with the structure of a single subunit of the oxidised dimer **(D)**. Residues 1-21 and 235-241 are excluded from this structure. Notice that there is only slight variation in the C-terminal domain while the N-terminal domain has undergone a major structural rearrangement to an all-helical conformation with the formation of an intrasubunit disulphide bond. In all four images the N-terminal domain of each subunit is purple; the C-terminal domain of each subunit is green; Cys24 is shown in yellow and Cys59 is red. The models were generated with Swiss PDB viewer (Guex and Peitsch, 1997) using the PDB file 1rk4 (Littler *et al.,* 2004) and 1k0m (Harrop *et al.*, 2001) for the dimer and monomer respectively.

Furthermore an increase in channel activity has been detected with an increase in the reducing agent; DTT, while an increase in the concentrations of the sulphyldryl modifying agents; GSH and NEM inhibits channel conductance from the *trans* side of the membrane (although not in the C24A mutant) (Tulk *et al.*, 2002; Singh and Ashley, 2006) suggesting that reduced sulphyldryls, particularly reduced Cys24, may be favourable for channel conductance. Although this may be true for vertebrate CLICs, the active site cysteine residues are believed to be unnecessary for invertebrate CLIC function (Berry and Hobert, 2006).

The only other member of the CLIC family that is known to form a homodimer is CLIC6 (Griffon *et al.*, 2003). This protein dimerises in solution at its GST-like C-terminus but nothing else is known about the structure or properties of the CLIC6 dimer. CLIC4 has been shown to form a homotrimer under non-reducing conditions (Li *et al.,* 2006). This trimer is formed in the absence of disulphide bonds and proves that hydrogen bonds and hydrophobic contacts may be all that is required for a CLIC protein to muiltimerise (Figure 6).

1.4.3. Stability and Folding of Members of the GST Superfamily

The glutathione transferases (GSTs) (EC 2.5.1.18) are typically a family of soluble dimeric enzymes (~50 kDa) involved in catalysing the conjugation of GSH to electrophilic substrates (reviewed by Sheehan *et al.,* 2001; Oakley, 2005). The members of the GST superfamily are related by their common fold, not necessarily by their functions which can vary quite dramatically.

Most of the soluble GSTs are cytosolic although the class Kappa enzymes exist in the mitochondrion (Oakley, 2005). Furthermore there is a separate microsomal, membrane-bound family of GSTs that is only associated with the cytosolic enzymes by its interaction with GSH. These enzymes are known as

membrane-associated proteins in eicosanoid and glutathione metabolism (MAPEG) (Jakobsson *et al.,* 1999). These proteins have GST-like (MGST2 and MGST3) and peroxidase-like (MGST1) activity but are not structurally related to the GST superfamily of proteins. They are relatively small for membrane proteins (137-161 amino acids) and are believed to exist as a trimer with four helical membrane-spanning segments per monomer (Herbert *et al.,* 1997). They exist in the mitochondrion and, along with class Kappa GST, are involved in the detoxification of products of lipid oxidation.

CLIC1 most closely resembles human class Omega GST (GST O1-1) (Figure 12) and bacterial class Beta GST (GST B1-1). All three of these proteins have a single cysteine residue in their active sites and are capable of forming a mixed disulphide bond with glutathione (Figure 10) (Rossjohn *et al.*, 1998; Board *et al.*, 2000; Harrop *et al.,* 2001; Caccuri *et al.*, 2002).

CLIC1 and monomeric Omega GST show similarities in the length of their sequences both being approximately 241 amino acids long. Additional similarities between these proteins include the fact that they are both abundant in the nucleoplasm and that their α4 and α5 helices are exceptionally straight. Furthermore the active site of both CLIC1 and GST O1-1 is a crevice sufficiently wide so as to accept protein ligands (Board *et al.*, 2000). This active site is much broader than that of the other GSTs except for the ancient class Kappa GST which also has a wide active site. The exposed active site surface of class Kappa GST has been proposed to interact with either a protein ligand or a membrane surface (Ladner *et al.,* 2004) and this, too, may be the case with CLIC1.

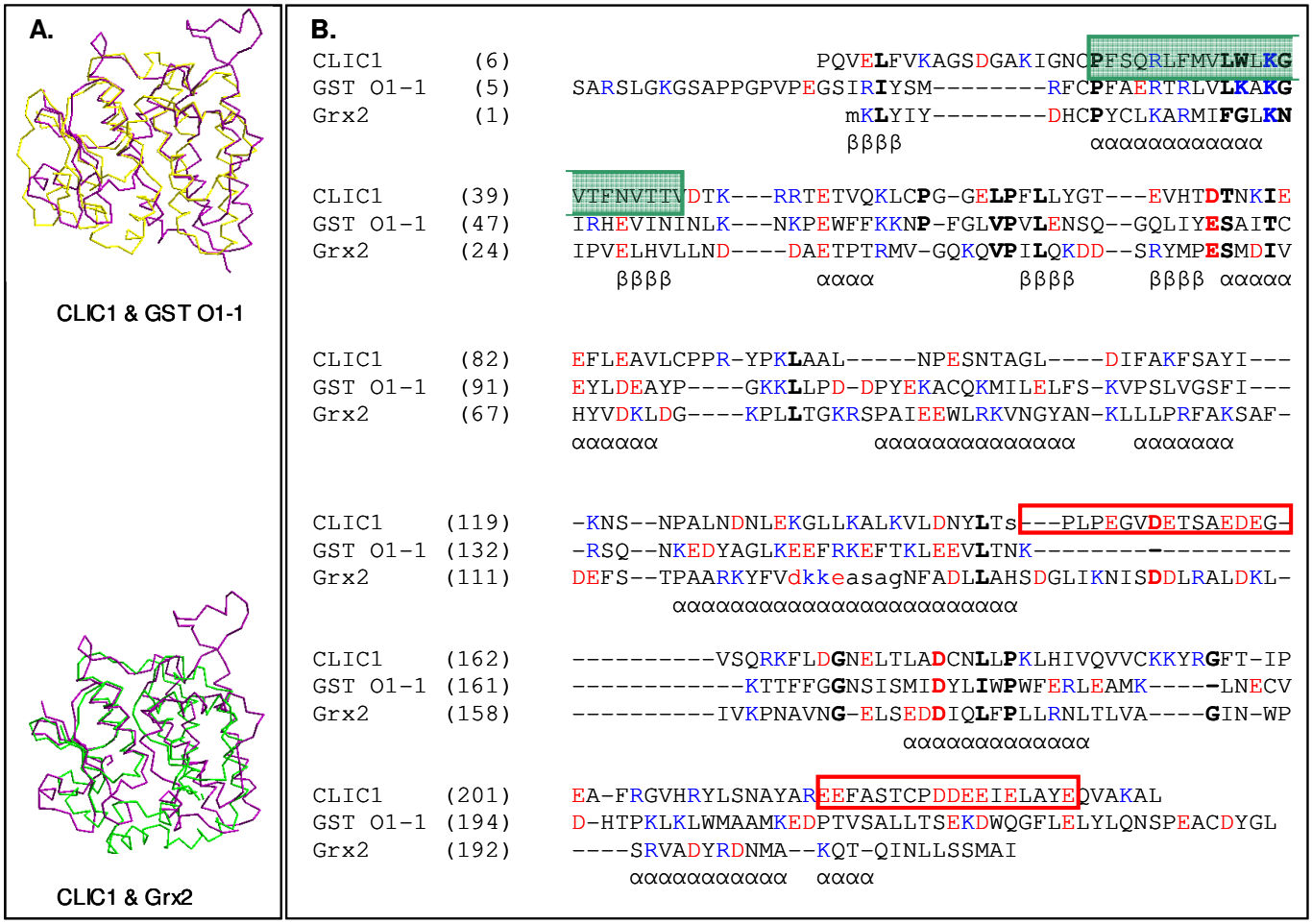


Figure 12: Alignment of CLIC1 with GST O1-1 and Grx2 illustrating charged residues

Structure based alignment of CLIC1 with two close structural neighbours: Omega class GST (GST O1-1) and glutaredoxin 2 (Grx2). **(A)** Alignment of tertiary structure illustrating that the acidic loop is unique to CLIC1 structure. CLIC1 is purple, GST O1-1 is yellow and Grx2 is green. The alignments were performed with Swiss PDB viewer (Guex and Peitsch, 1997). PDB codes 1k0m, 1eem and 1g7o were used for CLIC1, GST O1-1 and Grx2 respectively. The alignment between CLIC1 and GST O1-1 produced an RMS deviation of 1.65 Å (for 452 α carbon atoms) on superposition of the β sheets of the crystal structures while the alignment between CLIC1 and Grx2 produced an RMS deviation of 1.58 Å (for 352 α carbon atoms). **(B)** Structure based sequence alignments. Aligned alpha helices are indicated with an α and aligned beta sheets are indicated with a β. Residues shown in lower case do not form part of

the indicated secondary structure. All highly conserved residues within the species aligned are shown in bold. All basic residues are shown in blue and all acidic residues are shown in red. The proposed transmembrane region in the CLIC1 sequence is highlighted in green. This region does not contain any positive residues. This trend is not conserved in GST O1-1 and Grx2. The two hotspots of negative charge found in CLIC1 that are not conserved in the other members of the GST superfamily are boxed in red. The alignment was done using the COMPARER on-line server.

It has been revealed that GST O1-1 modulates the ryanodine receptor calcium channels (Dulhunty *et al.*, 2001); an analogy with the function of the CLIC family of transmembrane channels (Dulhunty *et al.,* 2005). (Although GST O1-1 does not actually form channels and thus it is likely that the CLICs undergo a major structural rearrangement to change from their soluble GST-like form to their membrane-bound states). Additionally, the inhibitor of the CLICs, indanyloxyacetic acid-94 is a homologue of ethacrynic acid, an inhibitor of the GSTs (Oakley *et al.,* 1997). Furthermore, both the CLICs and the GSTs are known to associate with protein kinases (Qian *et al.*, 1999; Cho *et al.*, 2001; Edwards *et al.,* 2006).

A rather unusual comparison can be drawn between the yeast prion protein, Ure2p and the larger members of the CLIC family, namely CLIC5B and CLIC6. All three of these proteins contain a C-terminal domain that is structurally related to the GST superfamily while their N-terminal domains are relatively unstructured and highly repetitive (Perrett *et al.,* 1999; Friedli *et al.,* 2003). In Ure2p, this unstructured domain is believed to be the prion-determining domain that is involved in the aggregation of the protein (Perrett *et al.,* 1999; Thual *et al.,* 2001) while the function of the flexible, unstructured N-terminal domain in the CLIC family remains unknown.

There are also distinct differences between CLICs and the GSTs, however. Besides Grx2, most GSTs are dimeric while CLICs are monomers. The CLIC family β1 sheet and α2 helix are relatively hydrophobic whereas in many GSTs this region is far more hydrophilic. The position of the α9 helix of CLIC1 results in a more open C-terminal region than in the GST classes that contain this helix (Wallace and Dirr, 1999; Wallace *et al.,* 2000) (Figure 12) Furthermore, perhaps the most striking difference between the CLICs and GSTs is that the CLICs contain a highly negatively charged loop region that is not found in GSTs and is possibly involved in membrane insertion, a property of CLICs that is not shared with the GSTs.

The equilibrium unfolding mechanisms of certain members of the GST superfamily have been elucidated (Table 1). Four of these: class Alpha GST (Wallace *et al.*, 1998b; Wallace and Dirr, 1999); class Pi GST (Dirr and Reinemer, 1991; Erhardt and Dirr, 1995); GST from *Schistosoma japonicum* (Kaplan *et al.,* 1997) and the small monomeric protein, Grx2 (Gildenhuys PHD thesis, 2006) unfold via a two-state process with no stable intermediates detectable at equilibrium. However, the class Mu GST has a three-state equilibrium unfolding mechanism (Hornby *et al.,* 2000) and the class Sigma and Beta GSTs unfold via a four-state process (Sacchetta *et al.,* 1993; Stevens *et al.*, 1998). Ure2p unfolds via a two-state mechanism at pH 8.4 (Perrett *et al.,* 1999). However, at the pH at which this protein is known to form fibrils, namely pH 7.5 and pH 5.5, Ure2p has been shown to be far less stable and to unfold via a multistate process at equilibrium (Thual *et al.,* 2001). Although Ure2p is dimeric in nature, unlike the other dimeric members of the GST superfamily, the extremely unstructured and flexible N-terminal domain does not contribute towards the stability of the molecule and hence its $\Delta G(H_2O)$ value is characteristic of a monomeric protein (Perrett *et al.,* 1999; Thual *et al.,* 2001).

Generally the stability of the dimeric proteins is higher than that of the monomers, indicating that interactions at the subunit interface play a role in stabilising the native state of these dimers. The interface region is not, however, involved in stabilising the monomers (Thompson *et al.,* 2006).

Table 1: Comparison of the equilibrium and kinetic unfolding mechanisms and parameters of certain members of the GST superfamily

	Equilibrium Unfolding Process	$\Delta G(H_2O)$ of unfolding $N \Leftrightarrow U$ (kcal/mol)	*m*-value (kcal/mol/M)	Kinetic Unfolding Pathway
[a]***Sj*26 GST:** 2 µM pH 6.5; 20°C	Two – State $N_2 \Leftrightarrow 2U$	26.0	4.5	
[b]**Class Alpha GST:** 1 µM pH 6.5; 25°C	Two – State $N_2 \Leftrightarrow 2U$	27.6	4.2	Three phases
[c]**Class Pi GST:** 5 µM pH 6.5; 20°C	Two – State $N_2 \Leftrightarrow 2U$	28.3	4.5	Three phases
[d]**Class Omega GST:** 2 µM pH 7.0; 20°C	Two – State $N_2 \Leftrightarrow 2U$	15.5	2.8	Two phases
[e]**Grx2:** 5 µM pH 7.0; 20°C	Two – State $N \Leftrightarrow U$	12.7	2.7	Three phases
[f]**Class Mu GST:** 2 µM pH 7.0; 25°C	Three – State $N_2 \Leftrightarrow 2M \Leftrightarrow 2U$	19.6 (2-state) 27.3 (sum of 3-state parameters)	3.4 (2 state) 4.4 (sum of 3-state parameters)	
[g]**Class Sigma GST:** 1 µM pH 7.0, 0.4 M NaCl; 20°C	Multi – State $N_2 \Leftrightarrow I_2 \Leftrightarrow 2M \Leftrightarrow 2U$	12.5 (first phase)	2.2 (first phase)	
[h]**Class Beta GST**	Multi – State $N_2 \Leftrightarrow I_2 \Leftrightarrow 2M \Leftrightarrow 2U$			
[i]**Ure2p:** 1 µM; 20°C	pH 8.4: Two – State $N_2 \Leftrightarrow 2U$ pH 5.5: Multi – State $N_2 \Leftrightarrow I_2 \Leftrightarrow 2M \Leftrightarrow U$	11.4 (at pH 8.4)	3.9 (at pH 8.4)	

[a] Kaplan *et al.,* 1997; Yassin *et al.,* 2003; [b] Wallace *et al*, 1998a; Wallace and Dirr, 1999; Wallace, *et al.,* 2000; [c] Dirr and Reinemer, 1991; Erhardt and Dirr, 1995; Wallace and Dirr, 1999; Wallace and Dirr, in preparation; [d] Lutya PHD thesis, in preparation [e] Gildenhuys PHD thesis, 2006; [f] Hornby *et al.,* 2000; Luo *et al.,* 2002; [g] Stevens *et al.,* 1998; [h] Sacchetta, *et al.,* 1993; [i] Perrett *et al.,* 1999; Thual *et al.,* 2001

1.4.4. Stability and Folding of Membrane Proteins

Membrane structure and electrostatics

Cell membranes, which include the plasma membrane and organelle membranes, are mostly composed of lipids and proteins. Lipids constitute 50% of the mass of the plasma membrane and proteins make up most of the remainder. The lipid molecules are amphipathic and contain a polar "head group" and a hydrophobic "tail" made up of fatty acids. This amphipathic nature causes the lipid molecules spontaneously to form bilayers in aqueous solution. These bilayers have a self-sealing property and thus form closed structures that establish impermeable barriers towards the passage of most water-soluble molecules. Furthermore, the lipid bilayers are dynamic and it is this fluidity that is essential for the functions of membranes (van Meer, 1989).

The electrical potential of a lipid bilayer is a result of an intricate relationship between its *transmembrane, surface* and *internal potentials* (Honig *et al.,* 1986). The *transmembrane potential* is formed as a result of the difference in charge across the bilayer, with the cytoplasmic side of the membrane invariably being negative relative to the outside. The *surface potential* is the electrostatic potential at the interface between the membrane and the aqueous environment. In biological membranes, this potential is negative due to the negatively charged phospholipids that make up 10 to 20% of the effective lipid area. This negative potential attracts protons from the surrounding solution which results in a decrease in the local pH at the membrane surface by at most two pH units from the pH in the cytoplasm in accordance with Gouy-Chapman theory (Vaz *et al*., 1978; McLaughlin, 1989; Menestrina *et al.,* 1989; Van der Goot *et al.*, 1991; Kraayenhof *et al.,* 1993; Bortoleto and Ward, 1999; Murray *et al.,* 1999). This reduced pH extends for a distance of 5 – 15 Å from the membrane surface (Prats *et al.,* 1986). Counterions are also attracted to the fixed negative charge at the surface of the membrane, forming an electrical double layer at the membrane-aqueous interface (McLaughlin, 1989). The

internal potentials arise from dipoles and charges formed within the low dielectric environment of the membrane interior. Protein molecules, either on the surface of the membrane or spanning the membrane are exposed to these intense electric fields which may regulate the protein structures or functions such as ion transport, energy transduction or even insertion of the protein into the membrane (Honig *et al.,* 1986). Conversely these proteins will also modify the intramembrane potential, with significant implications for the electrostatics.

Biological membranes are 25 – 30 Å wide. They consist of a hydrophobic core flanked by relatively polar "head groups" that measure approximately 10 – 15 Å each (Haltia and Freire, 1995). The dielectric constant at the membrane interface ranges from 10 to 20 while the hydrophobic core of a membrane has a dielectric constant as low as 2. The dielectric constant of the hydrophobic interior of a protein can range from 3 to 5, depending on the flexibility of the peptide backbone although recent experiments have shown it to be more hydrated with dielectric constants of 10 or higher (Karp *et al.,* 2007). Nevertheless, the dielectric constant of water is generally a good deal higher, being 80 at 20^{o}C (White and Wimley, 1994; Haltia and Freire, 1995; Peitzsch *et al.,* 1995).

The lipid membrane is virtually impermeable towards most small inorganic ions such as Na^{+}; K^{+}; Ca^{2+}; Mg^{2+}; Cl^{-} and SO_4^{-}. This is largely due to the Born electrostatic energy barrier (see equation 2) confronted by these ions when attempting to translocate from the high dielectric environment of water to the low dielectric environment within the membrane (Honig *et al.,* 1986). This energy barrier is at least 40 kcal/mol for small ions and the translocation rates are less than 10^{-10} s^{-1}! The Born energy barrier to the translocation of *hydrophobic ions* across the membrane is much lower and thus these nonpolar molecules are able to partition into membranes more favourably. Therefore it is energetically more favourable for hydrophobic segments of proteins to traverse membranes.

The mere fact that membranes are impermeable to polar molecules means that a mechanism is required whereby the polar substances can be transported into and out of the cell and organellar compartments. This is the function of two main classes of membrane protein: *carrier proteins* and *channel proteins*. *Carrier proteins* transport solutes across a membrane by binding to the solute and undergoing conformational changes so as to transport the solute across the bilayers. This process can be "downhill" along the electrochemical gradient or it can be an active "uphill" process that requires energy from ATP (Henderson, 1993). The *channel proteins*, on the other hand, compensate for the loss of aqueous solvation energy by the small inorganic ions, by allowing their passive diffusion across membranes through a hydrophilic pore by means of surrounding the ions with polar groups or charges of the opposite sign. In this way the channel proteins lower the Born energy barrier faced by these ions by raising the dielectric constant of the membrane interior that is accessible to the ions (Honig *et al.*, 1986). The hydrophilic pores are often gated which means they will only open in response to a certain stimulus. These ion channel proteins show selectivity towards ions and only allow ions of appropriate size and charge to pass through (Jentsch, 2001).

Membrane Proteins

A distinction between membrane proteins and soluble proteins is that the amino acids on the surface of the membrane protein are generally less polar than those on the surface of their soluble counterparts. This is because parts of these proteins will be buried within the hydrophobic interiors of membranes. A characteristic of many membrane proteins is that they have α-helices sufficiently long (>20 Å) to span the membrane (White and Wimley, 1999). Furthermore, charged amino acids, especially arginine and lysine are most abundant in the cytoplasmic domains of these proteins and are implicated in membrane binding events for a number of proteins (Gouaux, 1997) while aromatic amino acids such as tyrosine and tryptophan are found at the membrane interface and play a role in modulating protein-membrane interactions (Jacobs and White, 1989; Tilley and Saibil, 2006). These rigid

aromatic residues have limited access to the hydrophobic core, nevertheless a combination of the hydrophobic effect and their aromaticity (which includes their π-electronic structure and quadruple moment) favour their residence in the intricate and electrostatically complex interface environment (Yau *et al.,* 1998). Thus hydrophobic and electrostatic interactions combine at the membrane interface so as to stabilise membrane proteins.

Membrane proteins are rendered stably folded by the interactions of their side chains with each other as well as with water, cofactors, the lipid-water interface and the lipid bilayers (White *et al.,* 2001; White, 2003). Complete hydrogen-bonding of the backbone is required for the protein to reduce the Born energy barrier and traverse the nonpolar membrane. This explains why helices and β-barrels are prevalent in integral membrane structures (White and Wimley, 1999) and why the formation of the internal hydrogen bonding that is so well established in these structures reduces the cost of protein partitioning into the membrane by about 0.5 kcal/mol protein (White, 2003). In fact, there are only two types of channel-forming membrane protein: those that form transmembrane α-helices and do not necessarily need to form oligomers to create a pore, and those that oligomerise into closed β-barrel structures (reviewed in Gouaux, 1997). The predominant factors that control the stability, topology and membrane-insertion of membrane proteins are hydrophobic, electrostatic and polar interactions (Bechinger, 1996).

When a protein binds to a membrane it undergoes significant alterations. It becomes immobilised within the membrane and its flexibility and degrees of freedom are significantly reduced while the fluid membrane itself will structurally adapt to the insertion process. Furthermore, the polarity and dielectric constant within the membrane are reduced compared to the cytoplasm and could lead to strong electrostatic interactions and van der Waals interactions that will become the dominant stabilising forces of the helix-helix interactions of membrane proteins (White and Wimley, 1999; White *et al.,*

2001). Therefore it is obvious that the membrane environment will impose different mechanical constraints on a membrane protein than the aqueous environment will inflict on a soluble protein, and therefore the stability and cooperativity of the membrane protein as determined by its $\Delta G(H_2O)$ and *m*-value are strong functions of the lipid environment (Hong and Tamm, 2004). It is generally recognised that the insertion of a protein into a membrane is driven by the hydrophobic effect and hence by the overall hydrophobicity of the protein (reviewed by Chin *et al.*, 2002), although it must be noted that the hydrophobic effect cannot be responsible for enforcing the compaction of a transmembrane α-helix post insertion. This is because the dehydration effect that is necessary to drive hydrophobic interactions is absent once the protein is immersed within the lipid bilayer (White *et al*, 2001).

Soluble Proteins that insert into membranes

CLIC1 is different from the majority of membrane proteins studied because this protein can exist in both a soluble and integral membrane form. There are other proteins (mostly protein toxins) that exhibit a similar property in that they exist in a water-soluble state but are able to insert into, or in some cases, translocate across cell membranes in order to exert their toxic activity (Table 2). These toxins are produced by different organisms, infect different organisms and their cellular targets vary but they all share the ability to insert into the host membrane (Parker and Pattus, 1993). The fundamental question therefore is how do these water-soluble proteins insert into membranes? They all appear to follow a multi-step process towards membrane insertion and infection according to the scheme in Figure 13 (Gouaux, 1997; Parker and Feil, 2005):

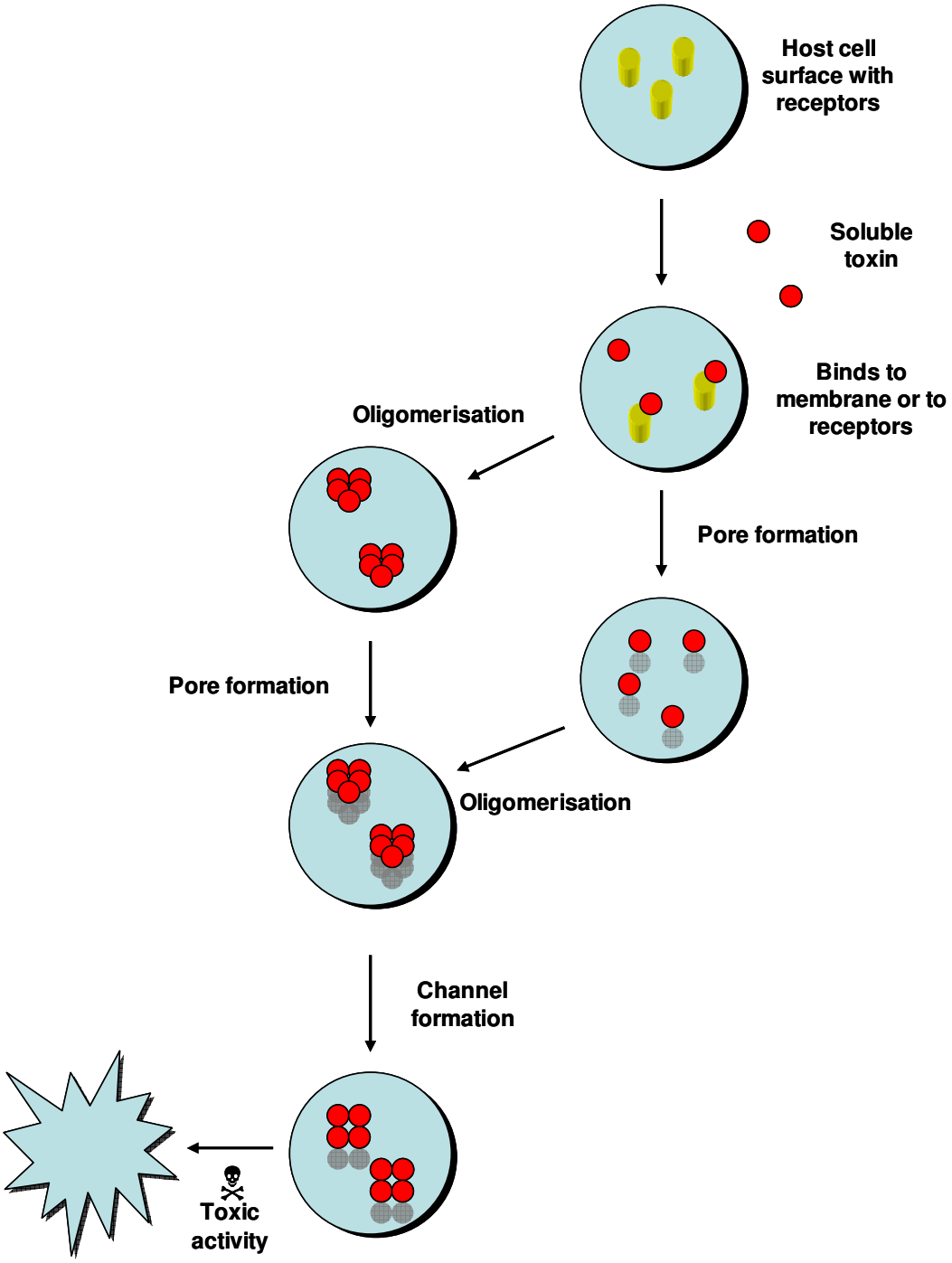


Figure 13: Schematic of toxin insertion and infection

Water-soluble toxins bind to the host cell either directly to the membrane or to receptors on the membrane surface. Depending on the toxin, it may oligomerise before forming a pore or else it may form a monomeric pore and subsequently oligomerise once already inserted into the membrane. The toxin can then form a channel and exert its toxic activity. Schematic adapted from Parker and Feil, 2005.

After an initial binding step that is driven by electrostatic and/or hydrophobic interactions, the mechanism of insertion of the protein toxins into membranes appears to depend on pH to facilitate one of two events: either the *hydrophobicity of the protein is increased* at low pH by the neutralisation of the large number of acidic residues found on the surface, or the protein forms a *molten globule state* at low pH that lowers the energy barrier to membrane insertion. Furthermore, charged residues have been implicated in the insertion mechanisms of many of these toxins (Parker and Pattus, 1993) and thus *electrostatics* is likely also to play a significant role in the insertion process. The insertion of the toxins and other soluble proteins into membranes is different from that of conventional membrane proteins in that these soluble pore-forming proteins will insert into membranes much faster because they will not be inserting from a completely unfolded state, but rather from a partially folded, often molten globule-like conformation (Kleinschmidt and Tamm, 1996).

The pore-forming toxins can be divided into two groups depending on the structure of their pore-forming domains and they are:

1. the α pore-forming toxins including the colicins; exotoxin A; the Cry δ-endotoxins and diphtheria toxin (Figure 14 and Table 2) that form α-helical transmembrane structures
2. the β pore-forming toxins including aerolysin, α-toxin (Table 2); α-hemolysin; cytotoxin; anthrax protective antigen; the cytolytic δ-endotoxins (Table 2) and the cytolysins (Parker and Feil, 2005; Tilley and Saibil, 2006) that form β-barrel transmembrane structures.

Table 2: Table comparing the properties of CLIC1 to some soluble pore-forming proteins

Pore-forming protein	Size of protein	Transmembrane structure	Oligomerisation state	Mechanism of insertion
[a]**CLIC1**	26.9 kDa	Proposed to be α-helical:	Proposed to be monomeric although it can also form oligomers	The results of this study suggest it is likely to form a molten globule
[b]**Colicin A**	~60 kDa	α-helical	Monomer	Molten globule exposes hydrophobic helix. Membrane insertion possibly involves a receptor. Unfolding only proceeds after association with the membrane surface
[c] **δ-endotoxin Cyt1A**	~27 kDa	α-helical	Oligomer	Drop in pH increases surface hydrophobicity and creates a molten globule state
[d]**δ-endotoxin Cry1Ab**	~60 kDa	β-Sheet	Initially the monomers combine to	Binds a receptor before insertion. Highly flexible

Pore-forming protein	Size of protein	Transmembrane structure	Oligomerisation state	Mechanism of insertion
			form a tetramer which then oligomerises into a larger pore-forming structure	oligomeric form inserts into membranes via a "pre-pore" intermediate state. Inserts via a hydrophobic helical hairpin
[e] **Diphtheria Toxin**	~58 kDa	α-helical	Forms a dimer at the membrane surface although higher order oligomers have also been detected	Low pH neutralises acidic residues and reduces hydrophobicity so it can traverse the membrane. Forms a pH-induced molten globule state
[f] **Exotoxin A**	~67 kDa	α-helical		Low pH induces a conformational change from a hydrophilic state to a hydrophobic molten globule state
[g] **Equinatoxin**	~19 kDa	The soluble form has β-sheet structure but the pore-	Oligomer of three to four monomers	Membrane surface causes denaturation and exposes an

Pore-forming protein	Size of protein	Transmembrane structure	Oligomerisation state	Mechanism of insertion
		forming domain is believed to be α-helical		amphipathic helix from the β-sandwich core. The protein then oligomerises via its patch of aromatic residues. Insertion is via a molten globule
[h]Bcl-x_L	~21 kDa	α-helical	Channel formation occurs in the presence of dimers although oligomerisation has been observed	Low pH allows insertion into membranes by protonating certain residues and hence reducing electrostatic repulsion with the anionic lipids. No molten globule is observed
[i]Bax	~21 kDa	α-helical	Oligomerises when in the membrane	Apoptotic signals cause the protein to change from soluble to membrane-bound form. Initially forms an

Pore-forming protein	Size of protein	Transmembrane structure	Oligomerisation state	Mechanism of insertion
				intermediate state while bound to the membrane before arranging to the active pore structure
[j]α-Toxin	~33 kDa	β-sheet	Oligomerises upon binding to the membrane to form a heptameric pore	Binds to a receptor before undergoing a conformational change to a molten globule state with exposed hydrophobic surface to create the membrane-bound form

[a] Harrop *et al.,* 2001; [b] Van der Goot *et al.,* 1991; Tory and Merrill, 1999; Lindeberg *et al.,* 2000*;* Zakharov and Cramer, 2002 and Zakharov *et al.,* 2004; [c] Promdonkoy and Ellar, 2003 and Manceva *et al.,* 2004; [d] Rausell *et al.,* 2004; Parker and Feil, 2005; Tilley and Saibil, 2006; [e] Choe *et al.*, 1992; [f]Jiang and London, 1990; Bell *et al.,* 1997; [g] Tejuca *et al.,* 1996; Ulrih *et al.,* 2004; [h] Schendel *et al.,* 1997; Thuduppathy and Hill, 2005 and Thuduppathy *et al.,* 2006; [i] García-Sáez *et al.,* 2004; [j] Vecsey-Semjen *et al.,* 1996 and Bortoleto and Ward, 1999.

There are a number of pore-forming features that are common to the α pore-forming toxins. Firstly, these proteins are characterised by buried *hydrophobic or amphipathic helices* when in their soluble states. These helices often form large bundles of six to ten helices (Figure 14) that create a hydrophobic "helical hairpin" that inserts into the membrane. This is the case with the colicins (van der Goot *et al.,* 1991; Parker *et al.,* 1992) and diphtheria toxin (Bennett *et al.,* 1994). Other α pore-forming toxins such as equinatoxin only contain one or two helices in their soluble structures (Ulrih *et al.,* 2004). Furthermore, the helices found in some α pore-forming toxins such as exotoxin A and the Cry δ-endotoxins are not particularly hydrophobic and are arranged in a bundle in the membrane-bound structure with the most hydrophobic helix in the centre (Tilley and Saibil, 2006).

Secondly, many of the α pore-forming toxins require *receptors* in order to bind to the cell surface. It is believed that these receptors will concentrate the toxin to a specific location on the membrane surface which will allow for its oligomerisation into a pore-forming structure. There are, however certain α pore-forming toxins that bind directly to the membrane and do not require a receptor, nor do they require an oligomeric state to form a pore (Parker and Feil, 2005). An example of a toxin that binds directly to the membrane is equinatoxin. This protein has a large proportion of aromatic residues clustered on its surface which assist in its membrane binding and/or oligomerisation activity (Parker and Feil, 2005).

Thirdly, it is necessary for the water-soluble toxins to undergo a *conformational change* in order to insert into or translocate across the membrane. This conformational change can be assisted by the presence of *cavities* in the soluble three-dimensional structure of the toxin, as is the case with the colicins (Lazdunski *et al.,* 1988; Zakharov and Cromer, 2002). The most important factor contributing to the conformational change of the α pore-forming toxins is the *low pH found at the membrane surface*. Many of these

proteins have an increased proportion of acidic residues on their surfaces that function as "pH-sensors". This means that these toxins form viable electrostatic interactions with receptors or with the membrane surface. A low pH environment will disrupt many critical interactions on the protein surface such as hydrogen bonds and salt bridges. Due to their pH-sensitivity, many of these toxins (for example colicin A (van der Goot *et al.,* 1991); exotoxin A (Jiang and London, 1990); diphtheria toxin (Jiang *et al.*, 1991; Choe *et al.,* 1992; London, 1992); α-toxin (Bortoleto and Ward, 1999); Cyt1A δ-endotoxin (Manceva *et al.,* 2004) and equinatoxin (Ulrih *et al.,* 2004)) have been shown to form a *molten globule* state at low pH (Table 2). Diphtheria toxin is further influenced by the low pH at the membrane surface or in the lumen of the endosomes because it has a large molecular dipole that extends across the molecule (Choe *et al.,* 1992). This protein interacts with membranes in a specific manner in which hydrophobic interactions are followed by electrostatic interactions involving a highly charged region of the protein (Chenal *et al.,* 2002).

The β pore-forming toxins vary in their pore-forming mechanism, however they all contain a rich β-sheet content and *oligomerisation is essential* in order for them to form their membrane bound structures. There is a high incidence of heptameric pore-forming states in the β pore-forming toxins (Parker and Feil, 2005; Tilley and Saibil, 2006). The cytolysins are the only known toxins that switch secondary structure from soluble α-helical monomers to a β-hairpin membrane-bound form (Tilley and Saibil, 2006).

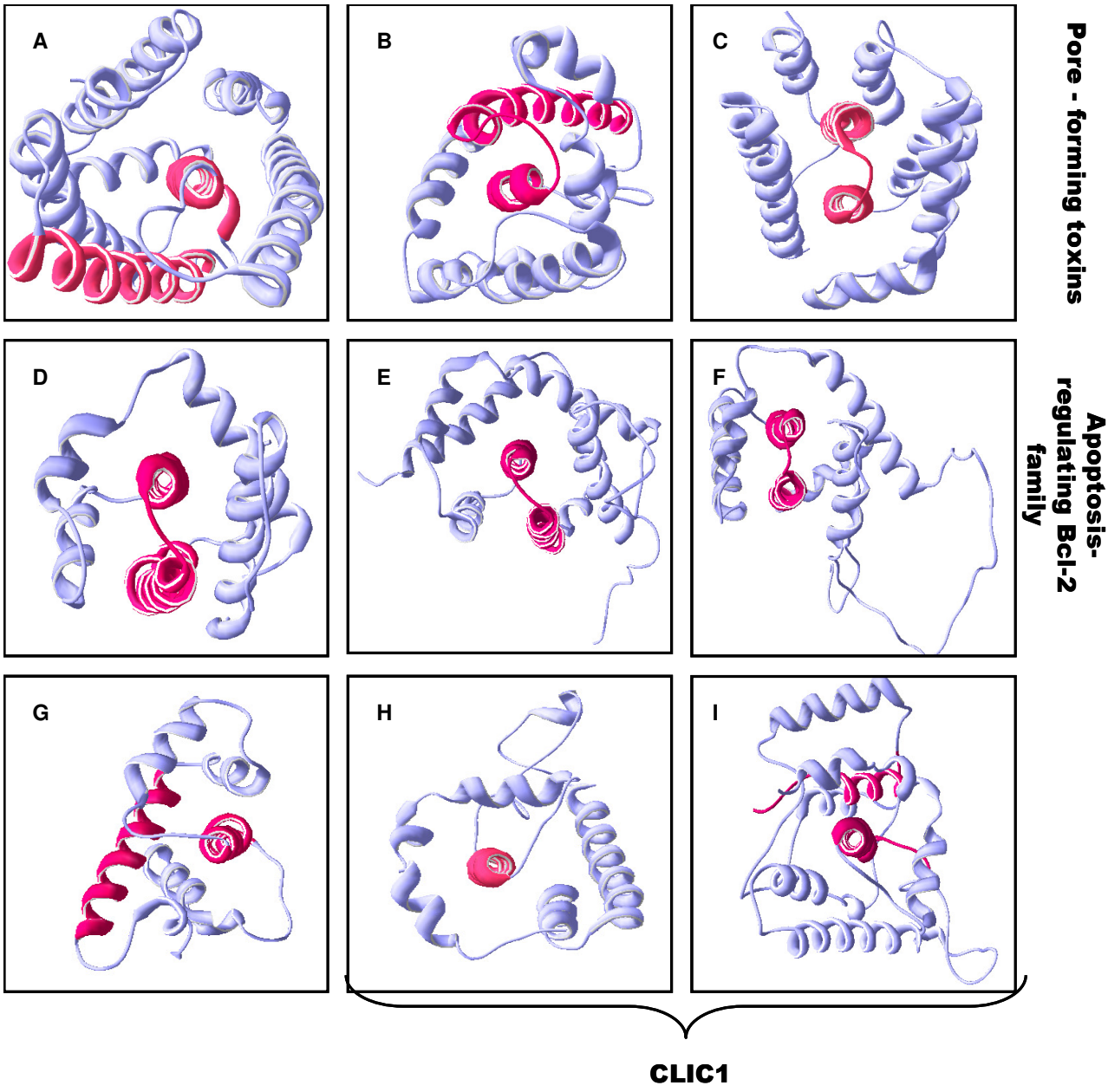


Figure 14: Comparison of CLIC1 topology with that of pore-forming proteins

Representations of the membrane translocation helices in four bacterial protein toxins (**A-C** and **G**), three apoptosis-regulating proteins (**D-F**) and the hypothesised membrane spanning helices in reduced and oxidised CLIC1 (**H** and **I** respectively). Highlighted helices indicate the proposed membrane spanning helices, in many cases predicted by hydropathy analysis. In all the proteins indicated except for exotoxin A and CLIC1 the two helices are concurrent in the protein sequence. **(A)** The N-terminal pore-forming domain of insecticidal δ-endotoxin (Grochulski *et al.*, 1995) PDB code 1ciy. **(B)** The

membrane spanning domain of diphtheria toxin (Bennett *et al.,* 1994) PDB code 1ddt. **(C)** Pore-forming domain of colicin A (Parker *et al.*, 1992) PDB code 1col. **(D)** Water-soluble anti-apoptotic human Bcl-x_L (Muchmore *et al.*, 1996) PDB code 1maz. **(E)** Water-soluble pro-apoptotic human Bax (Suzuki *et al.,* 2000) PDB code 1f16. **(F)** Water-soluble pro-apoptotic human Bid (Chou *et al.,* 1999) PDB code 2bid. **(G)** Catalytic domain of exotoxin A (Wedekind *et al.*, 2001) PDB code 1ikq. **(H)** The C-terminal all-helical domain of reduced CLIC1 (Harrop *et al.*, 2001) PDB code 1k0m. **(I)** The all-helical oxidised CLIC1 monomer (Littler *et al.,* 2004) PDB code 1rk4. The images were generated with Swiss PDB viewer (Guex and Peitsch, 1997). The figure was adapted from Cromer *et al.* (2001).

Proteins of the Bcl-2 family are involved in the release of apoptotic factors from the mitochondria to the cytoplasm probably by the formation of ion and/or protein transport channels (Gross *et al.*, 1999; Garcia-Saez *et al.,* 2004). Members of this family have been shown experimentally to possess channel-forming activity; especially at low pH and in the presence of acidic lipid membranes although *in vivo* they exist in the cytoplasm and are not typical channel-forming proteins (Minn *et al.,* 1997; Schendel *et al.,* 1997). These proteins demonstrate a striking similarity in structure to diphtheria toxin and the colicins, containing a pair of central hydrophobic helices surrounded by five to eight amphipathic helices (Muchmore *et al.*, 1996; Chou *et al.,* 1999; Suzuki *et al.,* 2000; Garcia-Saez *et al.,* 2004) (Figure 14). Furthermore these proteins are highly negatively charged with p*I* values in the vicinity of 4 to 5 (Thuduppathy *et al*., 2006). These proteins can be divided into three types depending on whether they have a pro- or anti- apoptotic effect (Garcia-Saez *et al.,* 2004). The type I proteins such as Bcl-x_L contain a stretch of hydrophobic residues at their C-terminal end that aids in anchoring the protein to intracellular membranes, primarily the outer mitochondrial membrane but also the nuclear envelope and parts of the endoplasmic reticulum (Janiak *et al.*, 1994; Schendel *et al.,* 1997). Type II and III proteins of the Bcl-2 family (like Bax and Bid) are soluble in the cytoplasm but migrate to the outer mitochondrial membrane on the onset of apoptosis where they promote the release of apoptogenic factors such as cytochrome *c* from the mitochondrion (Hsu *et al.,* 1997; Wolter *et al.,* 1997). The mitochondrial membrane has a large proton gradient and thus pH may act as a channel modulator in these proceedings. These proteins undergo major structural alterations which facilitate membrane insertion, for example Bax oligomerises to form transmembrane pores in a pH-dependent fashion in anionic lipid vesicles and although the protein exists as a monomer in the cytoplasm, this oligomerisation is a prerequisite for the pro-apoptotic activity of this protein (Schendel *et al.,* 1997; Antonsson *et al.,* 2001; Yethon *et al.,* 2003).

Interestingly, pH has been shown not to affect the structure or stability of soluble Bcl-$_{XL}$ *in vitro* and, unlike the pore forming toxins, this protein does not unfold via a molten globule-like intermediate (Thuduppathy and Hill, 2005). Thus any changes in the structure of this protein may only occur in the presence of lipid or perhaps in the presence of additional environmental conditions at the membrane surface such as reduced polarity or a strong negative potential. When in the presence of acidic lipid, however, both acidic pH (Xie *et al.,* 1998) and increased temperature (Pagliari *et al.,* 2005) have been seen to promote oligomerisation in some members of the Bcl-2 family. This conformational change in the solution to membrane form is therefore regulated by electrostatic interactions (Thuduppathy *et al.,* 2006).

The membrane locations of the members of the Bcl-2 family, as well as their role in the cell cycle show a remarkable similarity to the CLIC proteins- in particular CLIC4- which has been shown to participate in a stress-induced cell death pathway similar to that of Bax (Fernandez-Salas *et al.,* 2002). Furthermore both proteins are present in the cytosol and, whereas Bax localises to the outer mitochondrial membrane early in apoptosis, CLIC4 localises to the inner mitochondrial membrane. Thus these two proteins must cooperate with each other, exhibiting complementary action on the inner and outer membrane of the mitochondrion so as to promote the apoptotic response. CLIC1, CLIC3 and CLIC6 are also involved in cell processes such as cell division and cell growth and proliferation (Tonini *et al.,* 2000; Qian *et al.,* 1999; Griffon *et al.,* 2003). Thus the CLICs and the members of the Bcl-2 family of proteins are inextricably involved in processes concerning the regulation of cell life and death.

A structural feature common to these eukaryotic apoptosis-regulating proteins as well as to the bacterial α pore-forming toxins is that they contain a long antiparallel α-helical loop consisting of two consecutive hydrophobic helices that form a so called “helical hairpin” (Figure 14). These helices are shielded by the rest of the protein molecule. Thus, in order to insert into membranes,

these proteins need to undergo a degree of structural reorganisation so as to expose the hydrophobic helices and allow them to partition into the membrane interior. These soluble pore-forming proteins thus generally appear to undergo a structural rearrangement upon encountering the low pH and low dielectric constant at the membrane surface, where they essentially turn themselves inside out to expose the hydrophobic parts of the sequence that are more energetically favoured to membrane insertion.

How CLIC1 compares with the soluble pore-forming proteins

A striking observation with these soluble pore-forming proteins is that they do not necessarily share any sequence similarity (Cromer *et al.*, 2002) and yet they are able to adopt similar folds (Figure 14). This common fold therefore represents a way of packing hydrophobic helices into a soluble, globular structure and is a product of convergent evolution (Parker and Pattus, 1993). CLIC1 resembles these soluble pore-forming proteins in the following two ways: firstly the C-terminal domain is similar in topology to the α-helix bundles found in these proteins and the hydrophobic α6 helix of CLIC1 is 30 Å long and is thus sufficiently long to span the membrane (Figure 14); Secondly, like diphtheria toxin, CLIC1 too possesses a molecular dipole across its surface and contains regions of significant negative charge that could assist in the partitioning of the membrane at low pH (Figure 9).

Since a requirement of the membrane-inserting domains of the pore-forming proteins is that they be hydrophobic, it is likely that hydrophobic regions in CLIC1 would be responsible for membrane insertion. CLIC1 has two regions of significant hydrophobicity in its sequence (Valenzuela *et al.*, 1997; Tulk *et al.,* 2002; Nathaniel PHD thesis, in preparation) as determined by Kyte-Doolittle hydropathy plots (Kyte and Doolittle, 1982). Both these regions are sufficiently long to represent transmembrane domains. The first is the α1 helix and β2 strand in the N-terminal domain (amino acids 21 – 39) (Figure 7 and Figure 8). The second hydrophobic region is the α6 helix in addition to part of

the preceding loop in the C-terminal domain (amino acids 170 – 190) (Figure 7 and Figure 14). These hydrophobic regions are highly conserved and are found at a similar relative position in all members of the CLIC family (Valenzuela *et al.,* 1997; Tulk and Edwards, 1998; Tulk *et al.*, 2002; Nathaniel PHD thesis, in preparation). The only problem is that these two regions are not consecutive and are separated in CLIC1 by 130 amino acids, many of which are hydrophilic and would be energetically unfavoured to traverse the membrane. Therefore it is likely that only one of the two hydrophobic stretches in the CLIC1 sequence forms the transmembrane domain. Seeing as though the topology of the C-terminal domain is similar to that of the above mentioned pore-forming toxins, it was considered possible that the α6 helix could form the transmembrane helix. Thus there have been two proposed regions of membrane insertion in the CLIC1 structure:

1. A portion of the C-terminus (residues 170-233), with its similarity in structure to the pore-forming toxins and no known evolutionary origin was initially suggested to be involved in pore-forming function (Cromer *et al.*, 2002). Furthermore, the α-helices in this region show amphipathic character with three positive residues clustered at the end of α6 and five negative residues grouped at the end of α9. This could contribute to the ion-selectivity of a channel formed by these helices.
2. Recent evidence suggests, however, that it is the N-terminus that traverses the membrane with α1 and β2 forming the transmembrane region (blue section in Figure 8). The fact that the C-terminal domain remains on the cytoplasmic (or nucleoplasmic) side and the N-terminus spans the membrane and forms a small extracellular portion of only approximately 22 amino acids has been proved by selectively tagging a FLAG-epitope to either the N- or C- terminus and varying the side of the membrane from which chloride channel activity was recorded (Tonini *et al.*, 2000). Here CLIC1 was proven to be an integral membrane protein that crosses the membrane an

odd number of times. This result is complemented by similar experiments conducted in rat brain p64H1 and CLIC4 (Duncan *et al.,* 1997) and is further confirmed in CLIC1 using N-terminal directed antibodies (Singh and Ashley, 2006).

Further evidence against the C-terminus and supporting the N-terminus as the membrane inserting region is that truncation of EXC-4 (a worm member of the CLIC family) in the middle of the α6 helix does not affect the localisation of this protein to the luminal membrane whereas deleting β2 or disrupting α1 minimises membrane localisation of EXC-4 (Berry *et al.*, 2003). This seems to imply that, at least in the case of EXC-4, the N-terminus rather than the C-terminus is the part of the protein involved in membrane translocation. However, one cannot disregard the effect that the changes to α1 or β2 would have on the structure of the protein. It is likely that these mutations are highly disruptive, as were attempts to isolate a fully functional N-terminal domain in Grx2 (Xia *et al.,* 2001). If this is the case, then it is not surprising that the structurally interrupted mutant did not localise to the membrane and it does not necessarily imply that this is the membrane-forming domain. Berry and Hobert (2006) have recently proved that the C-terminal region is functionally equivalent, not only in the CLICs but also in their more remote relatives, the GSTs (specifically the Omega and Sigma classes). This finding implies that the N-terminal domain has evolved specific membrane targeting and inserting properties, particularly due to the strategic positioning of charged residues in the CLIC proteins' sequences (Berry and Hobert, 2006).

Model for CLIC1 membrane insertion

Conditions at the membrane surface appear to be sufficient to unfold proteins, at least partially. The negative charge at the membrane surface has been shown to denature proteins (Endo and Schatz, 1988). However, the pH at the membrane surface of at least 5 (McLaughlin, 1989; Menestrina *et al.,* 1989; Van der Goot *et al.*, 1991) is generally not low enough to induce complete

denaturation of the protein alone. Nevertheless, when the acidic pH is coupled with the low dielectric constant, the electrostatic repulsion of the negatively charged groups will become enhanced and this may encourage the unfolding of the protein under these conditions (Bychkova *et al.,* 1996). The protein probably will not unfold completely and it may form a molten globule-like intermediate state before inserting into the membrane.

Based on the fact that water can exist inside the molten globule state and hence a greater number of charged residues may be buried in the molten globule compared to in the native state, Bychkova *et al* (1988) were the first to propose that the molten globule state may be more accommodating of non-polar environments and thus could be involved in protein translocation across membranes. Van der Goot *et al.*, (1991) were the first to prove this hypothesis with the pore-forming domain of colicin A and it has since been observed in a number of pore-forming proteins (Table 2). Furthermore, the molten globule state has been detected in cytochrome *c*, which is not a pore-forming protein, when it is exposed to conditions that simulate the membrane surface, *i.e.,* moderately low pH and moderately low dielectric constant (Bychkova *et al.*, 1996). When α-lactalbumin, another protein whose physiological role is not pore formation, is in the vicinity of negatively charged membranes, it also undergoes a conformational change to a flexible molten globule-like state, that "is not a single conformation but rather a family of more or less ordered conformers" (Baňuelos and Muga, 1995).

The latest model for CLIC1 membrane insertion and channel conductance is offered by Singh and Ashley, 2006. They state that CLIC1 inserts a short portion of the N-terminal domain into the membrane resulting in Cys24 being on the *trans* side of the membrane and hence being exposed to a potentially oxidising extracellular or luminal environment. This causes the protein to form disulphide bonds with neighbouring subunits causing the channel to be "blocked". If the environment becomes reducing, the disulphide bonds will be broken and the channel will be "opened" and hence functional. It is proposed

that the conserved Pro25 may function as a type of “hinge” that opens and closes the channel. Thus the functionality of the channel is redox-sensitive. This model provides a clear interpretation for why far better conductance is detected when DTT is present in the protein’s microenvironment compared to GSH.

CLIC1 channels are likely to be oligomeric (Tonini *et al.,* 2000). In 2002 Tulk *et al.* proved (due to the linear relationship between protein concentration and channel activity) that CLIC1 may either insert into membranes in monomeric form or else it already exisits in solution in a multimeric form that is required for insertion and activity. Furthermore, based on channel conductance, the CLIC1 channel will preferably be an arrangement of at least four subunits with a single transmembrane domain located near the N-terminal end of each subunit (Warton *et al.,* 2002; Singh and Ashley, 2006).

1.5. Objectives

CLIC1 is unusual among integral membrane proteins in that it can exist in both a soluble form and in a membrane-bound form. It is hypothesised that in order for the protein to convert from its soluble state to its integral membrane form it has to undergo a degree of unfolding and then refold into its new structure.

The objectives of this project can be divided into three main aims: The first is to characterise the protein in terms of its secondary, tertiary and quaternary structure, the second is to determine its thermodynamic stability using urea-induced equilibrium unfolding and the third to measure its unfolding kinetics. The latter two goals have not been previously established. Ultimately, the aim of this research is to mimic the conditions at the membrane surface in terms of pH, polarity, ionic strength, temperature and redox conditions in order to determine whether these conditions would have an effect on the structure or stability of CLIC1 *in vitro* so as to provide an interpretation of the mechanism of membrane insertion and to offer an explanation for CLIC1's pore-forming function *in vivo.*

Chapter 2. Experimental

2.1. Materials

The GST-CLIC1 fusion protein has been cloned into the *Escherichia coli* plasmid pGEX-4T-1 (Valenzuela *et al.*, 1997) and was a gift from S. N. Breit, Centre for Immunology, St. Vincent's Hospital and University of New South Wales, Sydney Australia. Thrombin from human plasma (20 units) and the restriction enzymes *BamH1* and *Not1* were supplied by Roche Diagnostics (Basel, Switzerland). Isopropyl-β-D-thiogalactosidase (IPTG) and Dithiothretol (DTT) were acquired from Inqaba Biotech (Pretoria, South Africa). DTT was also obtained from Whitehead Scientific (Cape Town, South Africa). Reduced glutathione (GSH) was acquired from ICN Biomedicals (Aurora, Ohio, USA). SDS-PAGE molecular weight markers were purchased from Amersham® Biosciences (Buckinghamshire, UK). Ultrapure urea was purchased from Merck laboratory supplies, (Darmstadt, Germany). 8-Anilino-1-naphthalene sulphonate (ANS), Trifluoroethanol (TFE) (>99% grade) and bovine thrombin (1000 units) were obtained from Sigma-Aldrich (St. Louis, MO, USA). All other chemicals used were of standard analytical grade. All solutions were filtered before spectroscopic studies using a 0.22 μm acetate filter (Osmonics).

2.2. Methods

2.2.1. Plasmid Verification

Escherichia coli BL21 cells were transformed with the pGEX-4T-1 plasmid (Valenzuela *et al.*, 1997). The DNA was extracted and a restriction digest of this DNA was conducted using the enzymes *BamH1* and *Not1*. The DNA was

incubated with the enzymes for four hours at 37°C prior to the loading of the single and double digest of the plasmid onto a 1% agarose gel. The DNA of the CLIC1 insert was sequenced by Inqaba Biotech (Pretoria, South Africa) using the 5' pGEX primer that binds the nucleotides 869-891 and the 3' pGEX primer that binds nucleotides 1041-1019. The sequence translated to the correct CLIC1 sequence. The thrombin cleavage site present between the CLIC1 and GST protein sequences results in two additional residues (Gly-Ser) to the amino terminus of CLIC1 (Harrop *et al.*, 2001).

2.2.2. CLIC1 Expression and Purification

CLIC1 was purified every month from a four litre batch culture of BL21 *Escherichia coli* cells transformed with the pGEX-4T-1 plasmid. 100 µl of a glycerol stock of cells (glycerol : cells = 1:1) was added to 100 ml 2 x YT media (1.6 g yeast, 1 g tryptone and 0.5 g NaCl in 100 ml) containing 100 µg/ml ampicillin. These cells were left growing for 16 hours at 37°C in a rotating incubator at 250 r.p.m. A 50-fold dilution of this overnight grow was inoculated into fresh 2 x YT media containing 100 µg/ml ampicillin and left growing at 37°C at 250 r.p.m to late log phase (OD_{600} ~ 1.1). This took six hours on average. Thereafter, the over-expression of the fusion protein was induced by the addition of isopropyl-β-D-thiogalactosidase (IPTG) to a final concentration of 1 mM. The cells were left to grow for four to five hours so as to achieve optimal expression. The cells were then harvested by centrifugation at 5000 x g for ten minutes at 4 – 12°C. The pellet was resuspended in 15 ml resuspension buffer (10 mM Tris-HCl; 200 mM NaCl; 1 mM EDTA; 1 mM DTT, pH 7.5) and left overnight at -20°C.

The following morning the cells were defrosted and 10 µg/ml lysozyme; 10 mM $MgCl_2$ and 10 µl/ml DNase were added. The cells were lysed at 4°C by sonication. The lysed cells were then centrifuged at 16 000 x g for 30 minutes at 4°C. The supernatant was loaded onto a glutathione-Sepharose column that

was pre-equilibrated in 10 mM Tris-HCl, 150 mM NaCl, 1 mM EDTA buffer pH 8.0. 1 mM DTT was added fresh on the day. In the glutathione-Sepharose column, the glutathione is bound to the Sepharose matrix via its sulphyldryl group. The CLIC1-GST fusion protein binds to the glutathione on the column via the GST and the remaining proteins are removed in the flow through. Three units of human thrombin or 80 units of bovine thrombin per litre growth were added to 10 ml thrombin cleavage buffer, (200 mM Tris-HCl; 1.5 M NaCl; 25 mM $CaCl_2$, pH 8.4). This solution was added to the glutathione-Sepharose resin to which the fusion protein was bound (approximately 25 ml resin). The resin was gently mixed and 0.3 mM DTT was added to this mixture. The amount of DTT to add had to be optimised since although it is required to keep the protein in the reduced form, the reducing conditions deactivate the thrombin, so a compromise had to be made. The fusion protein and the thrombin were incubated with agitation for 16 hours at 20^{o}C.

The CLIC1-thrombin mixture was easily recoverable from the glutathione-Sepharose column since CLIC1 was no longer fused to the GST and therefore no longer bound to the column matrix. The GST and any uncleaved fusion protein were eluted off the column using 10 mM reduced glutathione in 50 mM Tris-HCl, pH 8.0. The CLIC1 and thrombin were separated using DEAE anion exchange chromatography. The column was attached to the Äktaprime purification system (Amersham® Biosciences) and equilibrated in 20 mM Tris-HCl; 0.02% NaN_3, pH 6.0. This pH was used because the p*I* of thrombin is around 8 while that of CLIC1 is 4.85. Therefore at pH 6.0 the thrombin will be positively charged and will not bind to the column matrix. CLIC1 binds the column at this pH but there was trouble with eluting CLIC1 by dropping the pH, even when the pH was dropped to 4.0, which is below its p*I*. Therefore, CLIC1 was eluted from the DEAE Sepharose column using a buffer with a high salt concentration (20 mM Tris-HCl; *300 mM NaCl*; 0.02% NaN_3, pH 7.0). Once the protein was recovered, 1 mM DTT was added and the protein was stored overnight.

The protein samples were electrophoresed on a 15% polyacrylamide SDS-PAGE gel (Laemmli, 1970). Once purity was established, the CLIC1 sample was concentrated if necessary, at 4^{o}C using a PM-10 membrane to a concentration of no more than 120 μM so as to prevent aggregation of the protein. The purified protein was then exchanged into storage buffer (50 mM Na_2HPO_4; 0.02% NaN_3; 1 mM DTT, pH 7.0) using a G25 size exclusion column attached to the Äktaprime system or by extensive dialysis. This protein was used for all subsequent experiments and was extensively dialysed against storage buffer containing 1 mM fresh DTT every week.

2.2.3. SDS-PAGE

All SDS-PAGE gels were constructed using a 15% separating gel (Laemmli, 1970): (30% acrylamide, 1% bisacrylamide; 10% sodium dodecyl-sulphate (SDS); 10% ammonium persulphate and 1.5 M Tris-HCl pH 8.8), and a 4% stacking gel: (30% acrylamide; 1% bisacrylamide; 10% SDS; 10% ammonium persulphate and 0.5 M Tris-HCl pH 6.8). Most samples were diluted two-fold with a 5 x sample buffer: (100 mM β-mercaptoethanol; 20% (v/v) glycerol, 10% (w/v) SDS; 0.05% (w/v) bromophenol blue and 0.5 M Tris-HCl, pH 6.8). The gels were stained with Coomassie Brilliant blue. The molecular weight markers from Amersham® Biosciences were: phosphorylase b (97 kDa), albumin (66 kDa), ovalbumin (45 kDa), carbonic anhydrase (30 kDa), trypsin inhibitor (20.1 kDa) and α-lactalbumin (14.4 kDa).

2.2.4. Protein Concentration Determination

The concentration of the protein was determined using the Beer Lambert law:

$$A = \varepsilon_{\lambda} cl \qquad \textbf{5}$$

where A is absorbance at 280 nm, ε_{λ} is the extinction coefficient of the protein at wavelength, λ calculated as ε_{280} = 17 170 M^{-1} cm^{-1} for CLIC1 (see equation 7), c is the concentration of the protein in M and l is the pathlength of the cuvette measured in cm. The determination of protein concentration was corrected for any absorbance by aggregates at 340 nm by using the following calculation:

$$A_{280(corrected)} = A_{280(protein)} - A_{280(buffer)} - \left(A_{340(protein)} - A_{340(buffer)}\right)\left(\frac{A_{280(buffer)}}{A_{340(buffer)}}\right) \qquad \textbf{6}$$

The concentration of protein was determined by fitting a linear regression to a series of 5 serial dilutions. Protein concentration was determined before each experiment.

The molar extinction coefficient of CLIC1 at 280 nm was determined using the extinction coefficients of tryptophan, tyrosine and cysteine residues (Perkins, 1986):

$$\varepsilon_{(280)}\left(M^{-1}cm^{-1}\right) = 5550\sum Trp + 1340\sum Tyr + 150\sum Cys \qquad \textbf{7}$$

$$= 5550(1) + 1340(8) + 150(6)$$

$$= 17170\ M^{-1}\ cm^{-1}$$

All absorbance measurements were made at 20°C using either a Hewlett Packard model 8452A diode array spectrophotometer or a Jasco V-550 UV-VIS spectrophotometer.

2.2.5. SEC-HPLC

Size exclusion HPLC was performed using a LKB 2150 pump (Pharmacia). The column used was a TSK G2000 SW_{XL} size exclusion column with resolution of 5 – 150 kDa (TOSOHAAS). The column was connected to a Spectroseries UV100 absorbance detector from SP Thermoseparation products.

For each experiment 5 μM protein was loaded onto the column. The absorbance at 280 nm was recorded using a flow rate of 0.5 ml/min and a chart speed of 30 cm/hr. The HPLC buffer used was 0.1 M Na_2HPO_4; 0.05% NaN_3. The concentration of Na_2SO_4 added to these buffers varied from 0 M to 0.5 M and the pH used was either 6.7 or 5.5 depending on the experiment. The standard curve was constructed using an HPLC buffer of 0.1 M Na_2HPO_4; 0.1 M Na_2SO_4 and 0.05% NaN_3, pH 6.7. The proteins used to construct the standard curve were: thyroglobulin (670 kDa); gammaglobulin (158 kDa); ovalbumin (44 kDa) and myoglobin (17 kDa).

2.2.6. Dynamic Light Scattering

The hydrodynamic diameter of the protein was measured at different pH, temperature and salt concentrations using a Zetasizer Nano-S light scattering device with the laser set at 523 nm (Malvern, UK). Dispersion Technology Software v4 was used. The solutions were filtered to 0.1 μm before measurement to eliminate dust contaminants. The concentration of protein used was at least 2 μM, although higher concentrations gave a better signal to noise ratio. The results are an average of five readings.

2.2.7. Changing pH, Polarity, Ionic Strength, Temperature and Redox Conditions

The protein was stored in 50 mM Na_2HPO_4, 0.02% NaN_3 buffer at all times. Experiments in which the pH, polarity, ionic strength, temperature or redox conditions of the protein solution had to be altered were conducted immediately after the protein was exchanged into the new buffer. Any left over protein was discarded. When reducing conditions were required, the protein was always preincubated in DTT at pH 7.0 before dropping the pH so as to avoid the slow reduction rate at low pH due to the S^{2-} ions being inhibited by low pH (Torchinsky, 1981).

CLIC1 was exchanged into a buffer of different pH and/or polarity and/or ionic strength from the storage buffer in the following way: the pH and/or polarity and/or ionic strength of the 50 mM Na_2HPO_4 buffer with fresh 1 mM DTT, pH 7.0 against which the protein was dialysed that week was altered with orthophosphoric acid or NaOH (to alter pH) and/or addition of 2,2,2-trifluoroethanol (TFE) (to alter polarity) and/or addition of NaCl/NaF/Na_2SO_4/KSCN to increase ionic strength. The protein was exchanged into the new buffer using size exclusion chromatography on a G25 matrix. The fractions that contained the eluted protein at the correct pH/polarity/salt concentration were determined using a calorimetric assay. Protein Assay Dye Reagent Concentrate (BioRad) binds to proteins and in so doing, the colour of the dye turns from brown to blue. 8 µl from each eluted fraction were added to a five-fold dilution of this dye so as to determine which fractions contained protein. The protein was recovered, filtered and its concentration was determined. All the above steps were performed on ice so as to prevent aggregation. This method was preferential to dialysis against the new buffer (although dialysis was also used) because it was quicker and dialysis often resulted in aggregation, especially when reducing the pH of the protein solution near to or beyond its p*I*. The salt effects were found to be immediate and the amount of time the protein was exposed to the different salts

before performing the measurement is negligible. The pH of the protein once it had been exchanged into the correct buffer was confirmed to be at the correct level before further experiments were administered. All pH measurements were conducted using a Crison micropH 2000 electrode.

Generally the protein was prepared in a reducing buffer containing 1mM DTT. For the experiments conducted under non-reducing conditions, the protein was purified in the absence of DTT and all experiments were conducted within the first week after purification so as to minimise erroneous results due to oligomerisation because of disulphide bonds forming between monomers. In some cases an oxidising environment was created by adding 2 mM oxidised glutathione (GSSG) to the protein solution (8.7 μM protein was incubated in the presence of 8.5 mM GSSG for one hour before adding urea, diluting to 2 μM protein plus 2 mM GSSG and unfolding for a further two hours). In order to quantify the amount of free sulphyldryls present, Ellman reagent (DTNB: 5, 5'-dithiobis-2-nitrobenzoic acid) was used. 20 mM DTNB was prepared in methanol and stored at 4^{o}C. A final concentration of 1 mM DTNB was added to 2 μM protein and the absorbance was measured at 412 nm. The extinction coefficient of 13 600 M^{-1} cm^{-1} was used to calculate the concentration of DTNB bound to exposed thiols. This was divided by the protein concentration so as to determine the number of exposed cysteine residues present in the solution.

The unfolding curves conducted at 37^{o}C were done so by heating the urea and buffer solution to 37^{o}C before adding the protein. The protein was then left to unfold at 37^{o}C for at least two hours before the readings were measured. Although a Peltier-type thermal-control system was only available for the circular dichroism measurements, equilibrium measurements were also performed using fluorescence as a probe by simply maintaining the solutions at 37^{o}C up until the moment that the reading had to be taken.

2.2.8. Circular Dichroism Measurements

Circular dichroism spectroscopy can be used to study proteins because the principle of circular dichroism relies on the asymmetry of the proteins in solution when they interact with polarised light (Reviewed by Greenfield, 1996). Far-UV circular dichroism spectroscopy is recorded over the wavelength range of 190 to 250 nm and measures the difference in absorbance of left and right handed circularly polarised light by chiral molecules, predominantly the peptide bonds in the protein backbone. Far-UV circular dichroism is therefore a technique that gives a good indication of the secondary structural content of a protein (Woody, 1995). A protein with a high α-helical secondary structural content displays a characteristic spectrum with two troughs of comparable magnitude, one at 208 nm which corresponds to the $\pi\pi^*$ transition and one at 222 nm which represents the $n\pi^*$ electronic transition of the amide bond, while the ellipticity becomes strongly positive at 195 nm representing the peptide bond $\pi\pi^*$ transition, the polarization of which is perpendicular to the helical axis (Woody, 1995). Therefore, measurement of the ellipticity of a protein solution at 222 nm will give a good indication of the α-helical content of the protein structure. Since CLIC1 is a predominantly α-helical protein, ellipticity at 222 nm was therefore used as a probe for secondary structural changes throughout this project.

All circular dichroism measurements were performed using a Jasco J-810 spectropolarimeter and the software Spectra Manager for windows v1.5.00 was used. A quartz cuvette with a pathlength of 2 mm was used in all far-UV circular dichroism measurements. The spectra were recorded as an average of ten scans at a scan speed of 100 nm/min and were measured over the far-UV wavelength range (190 – 250 nm). The bandwidth used was 1 nm and the data pitch was 0.2 nm for spectra and 0.2 seconds for time-course measurements. The protein concentration used varied from 1 μM to 5 μM. For the near-UV circular dichroism measurements a 5 mm pathlength was used and measurements were taken over the wavelength range of 250 – 340 nm. Here

the bandwidth used was 0.5 nm. The protein concentration used for the near-UV circular dichroism spectra was 40 μM.

The spectra were measured in protein storage buffer: 50 mM Na_2HPO_4; 0.02% NaN_3, 1 mM DTT at the desired environmental condition. In some cases the presence of high concentrations of chloride ions or urea prevented the achievement of reasonable spectra below 210 nm as the signal to noise ratio was too high. To eliminate this problem in some cases, the protein storage buffer was diluted ten fold to 5 mM Na_2HPO_4.

All temperature-dependent studies made use of a Jasco PTC-423S Peltier-type temperature control system to maintain the required temperature.

Spectra were corrected for the solvent and plotted using the software SigmaPlot® v8.0. The mean residue ellipticity [Θ] (deg.cm^2.dmol^{-1}.residue^{-1}) was calculated using the following equation:

$$[\Theta] = \frac{100\theta}{C n l} \qquad \textbf{8}$$

Where θ is the ellipticity (mdeg), an angular measure related to the change in absorbance of left and right circularly polarised light, C is the protein concentration (mM), n is the number of residues in the protein and l is the path length (cm) (Woody, 1995).

In the cases where the spectra were smoothed, the negative exponential smoothing technique (SigmaPlot® v8.0) was used. This methodology smoothes the data using polynomial regression and weights computed from the Gaussian density function with a sampling proportion of 0.1.

2.2.9. Fluorescence Measurements

When a molecule absorbs light of a specific wavelength, it may have the ability to emit this radiation at a lower energy. This phenomenon is known as fluorescence and is due to the excitation of electrons upon the absorption of light. These electrons then drop to lower energy levels (the ground state) and in so doing emit photons at a longer wavelength than the incident light (Lakowicz, 1999). The intrinsic fluorescence of a protein's aromatic amino acid residues, most specifically its tryptophan residues, is exquisitely sensitive to structural alterations within the protein molecule. There are two major fluorescence parameters that can be used to monitor the tertiary structure of a protein. These are the intensity of the emission and the wavelength of the emission peak (Royer, 1995). The wavelength at which a molecule emits, which is clearly the energy of emission, depends on the exposure of that molecule to the polar solvent. Thus as the solvent surrounds the excited state dipole of the tryptophan molecule, it lowers the energy of the excited state and results in a red shifted emission wavelength (Royer, 1995).

Intrinsic Fluorescence due to tryptophan and tyrosine

All fluorescence measurements were conducted on a Perkin-Elmer Luminescence Spectrometer LS50B at either 20^{o}C or 37^{o}C. The software, FLwinlab v4.00.0 was used. Excitation and emission slit widths were kept to 5 nm for 2 μM protein. A quartz cuvette with a pathlength of 1 cm was used in all experiments. The concentration of protein used ranged from 1 μM to 5 μM. The protein was excited at 280 nm for most experiments, including all equilibrium and kinetic unfolding studies, although, for comparison purposes, some spectra have been recorded where CLIC1 was excited at 295 nm. All spectra were measured as an average of five accumulations at a scan speed of 150 nm/minute. The spectra were plotted using the Sigmaplot® software, v8.0.

Extrinsic Fluorescence: binding of ANS

8-Anilino-1-naphthalene sulphonate (ANS) is an amphipathic dye that is able to bind to exposed hydrophobic clusters on a protein molecule. This probe is thus standard for diagnosing molten globule species present in protein unfolding and folding reactions (Engelhard and Evans, 1995). When excited at a wavelength of 390 nm, ANS will emit at 540 nm but when the ANS molecule binds to the exposed non-polar patches on a protein, this emission wavelength is usually shifted to lower wavelengths around 460 nm, depending on the hydrophobicity of the ANS binding site on the protein, and the fluorescence quantum yield increases significantly as a consequence.

ANS stock was made to a concentration of 2 mM. The concentration was confirmed using an extinction coefficient: $\varepsilon_{350} = 4\ 950\ M^{-1}cm^{-1}$. ANS stock was prepared in 50 mM Na_2HPO_4 buffer containing 0.02% NaN_3. Separate stocks were made at pH 7.0 and at pH 5.5 and in the presence and absence of salt or DTT.

Equilibrium unfolding in the presence of ANS was performed in the following way: the dilutions of the protein with urea were set up as in section 2.2.11 and incubated at 20°C or 37°C for one to two hours to reach equilibrium. ANS was then added to a final concentration of 200 μM and the protein dilutions were left for a further one to two hours to allow for the binding of the ANS to any exposed hydrophobic patches.

Each sample was excited at 390 nm at 20°C or 37°C using a 1 cm cuvette and the emission spectra were recorded over a 390 – 600 nm wavelength range. The spectra were an average of three accumulations at a scan speed of 400 nm/min. Both excitation and emission slit widths were kept at 5 nm in the absence of salt while they were dropped to 4 nm in the presence of salt. Spectra were corrected for free ANS and the emission at 460 nm was plotted as a function of urea concentration.

2.2.10. Reversibility Studies

In order for denaturation curves to be analysed, the reversibility of the unfolding reaction has to be established so as to ensure the reaction is at equilibrium (Pace, 1986a; Pace and Scholtz, 1997).

pH 7.0

The reversibility of unfolding was established at pH 7.0 by unfolding the protein at 10 μM in 6.8 M urea for two hours and then diluting this unfolded protein ten times to refold at 1 μM for one hour. A control of 1 μM protein in 0.68 M urea was prepared for comparison. The circular dichroism and fluorescence spectra of native and refolded protein were compared. The reversibility of all points along the unfolding curve was established by unfolding 10 μM CLIC1 in increasing concentrations of urea (0 M - 6.8 M) and then diluting to 1 μM protein in buffer. A refolding curve was also constructed using both circular dichroism and fluorescence as probes. The protein was unfolded in 6.8 M urea and refolded into decreasing concentrations of urea (6.8 M - 0 M).

pH 5.5

The reversibility of unfolding was established at pH 5.5 by unfolding the protein at 5 μM in 8 M urea for 30 minutes and then diluting this unfolded protein ten times to refold at 0.5 μM for 30 minutes. A control of 0.5 μM protein in 0.8 M urea was prepared for comparison. The circular dichroism and fluorescence spectra of native and refolded protein were compared. A refolding curve was also constructed using both circular dichroism and fluorescence as probes. Here the protein was unfolded in 8 M urea and then refolded as 0.5 μM into decreasing concentrations of urea (8 M - 0 M).

2.2.11. Urea - Induced Equilibrium Unfolding

Urea solution

The urea used for these experiments was prepared in the 50 mM sodium phosphate storage buffer that was dialysed against fresh 1 mM DTT that week. In the case of unfolding curves at a pH other than 7.0 or in the presence of salt, the dialysis buffer was first altered to the desired pH with orthophosphoric acid or to the desired ionic strength before the urea was prepared. Urea stocks were stored at -20^{o}C but were not kept for longer than a week since the urea solutions will slowly decompose to form ammonium and cyanate ions that will chemically modify amino groups. Furthermore, any unused urea was discarded after it had been defrosted once. The urea concentration was confirmed using the refractive index of urea:

$$[Urea] = 117.66\Delta n + 29.753\Delta n^2 + 185.56\Delta n^3 \qquad \textbf{9}$$

where Δn is the difference between the refractive index of urea and buffer. (Pace, 1986b)

Equilibrium unfolding

Denaturation curves are a convenient way of estimating the stability of a protein. Urea or guanidine hydrochloride can be used as a chemical denaturant and will shift the equilibrium between the native and unfolded states towards the unfolded state at higher concentrations of denaturant. This enables the accurate measurement of the equilibrium constant and hence the thermodynamic parameters defining the stability of a protein (discussed in Shirley, 1995).

The unfolding of CLIC1 at equilibrium was followed using both circular dichroism and fluorescence as probes. The unfolding curves were constructed at a protein concentration of 2 μM. CLIC1 was added to solutions of various

urea concentrations ranging from 0 M to 8 M, generally at 0.1 or 0.2 M increments. Once the protein was added, all dilutions were mixed by manually inverting the tubes gently five times. The solutions were left for one to two hours at 20^{o}C or 37^{o}C to reach equilibrium.

The fluorescence data were recorded as an average of three full spectra from 280 nm to 450 nm. The scan speed used was 200 nm/min and the excitation and emission slit widths were set to 5 nm. The protein was excited at 280 nm. The emission at 280 nm (Raleigh scatter) was recorded and plotted versus urea concentration to give an indication of scatter of light caused by aggregation.

The circular dichroism data were recorded at each urea concentration as an average of the ellipticity readings at 222 nm measured over 30 seconds. The scan speed used was 100 nm/min.

Data Analysis

Two criteria need to be met before the unfolding data can be analysed in terms of its thermodynamic parameters (Pace, 1986a). The first is that the reaction must be at *equilibrium* before the measurements are made and the second is that the *reversibility* of the unfolding reaction must be established.

The data obtained from circular dichroism and fluorescence studies at pH above 5.7 were fit to a two-state model while at pH below 5.7 the data were fitted to a three-state model.

The fluorescence data were first smoothed and then analysed in the following two ways:

1. The maximum emission of the protein (F_{max}) was recorded and plotted against urea concentration;
2. The wavelength at which the spectra peaked (λ_{max}) was plotted against urea concentration. This way proved to be the most effectual and most of the data presented in this thesis uses this method.

The circular dichroism data were analysed by plotting the average value of the ellipticity recorded at 222 nm as a function of urea concentration.

Typically the equilibrium unfolding data presented in this thesis are an average of three experiments (although the range is from two to six depending on the experiment). The data were first overlaid to detect outliers, the outliers were removed and then the data were averaged. The final product was normalised to fit between 0 and 1 for comparison purposes (F_D, see equation 12).

Two-state monomer unfolding mechanism:

The equilibrium unfolding curves that follow a two-state mechanism can be divided into three regions:

i) The *pre-transition region* in which the protein is still predominantly in the native state

ii) The *transition region* in which cooperative unfolding of the protein occurs

iii) The *post-transition region* in which the protein is predominantly in the denatured state

According to the two-state mechanism for a monomeric protein (native (N) ⇔ denatured (D)), the protein will either be in the *native state* or in the *denatured state*. Therefore the sum of the fraction of native (F_N) and fraction of denatured (F_D) protein present in the solution is equal to 1:

$$F_N + F_D = 1$$

$$\therefore F_N = 1 - F_D \qquad \textbf{10}$$

The physically recorded value of the unfolding curve using circular dichroism or fluorescence as probes will be referred to as y in the following discussion. Thus, using equation 10, the observed value of y at any point along the unfolding transition will be:

$$y = Y_N F_N + Y_D F_D \qquad \textbf{11}$$

where Y_N and Y_D represent the values of y typical of the folded and unfolded protein respectively.

A combination of equation 10 and equation 11 yields:

$$\therefore y = Y_N (1 - F_D) + Y_D F_D$$

$$\therefore y = Y_N - Y_N F_D + Y_D F_D$$

$$\therefore y - Y_N = F_D (Y_D - Y_N)$$

$$\therefore F_D = \frac{Y_N - y}{Y_N - Y_D} \qquad \textbf{12}$$

The principal measure of the stability of a protein as obtained from denaturational studies is ΔG, the free energy change upon unfolding. The values of the equilibrium constant, K_D and of ΔG can be calculated using the above equations as follows:

$$K_D = \frac{F_D}{F_N}$$

$$= \frac{F_D}{1 - F_D}$$

$$= \frac{Y_N - y}{y - Y_D} \qquad \textbf{13}$$

Thus using equation 13

$$\Delta G = -RT \ln K_D$$

$$= -RT \ln\left(\frac{Y_N - y}{y - Y_D}\right) \qquad \textbf{14}$$

where R is the universal gas constant (1.987 cal. mol^{-1}. K^{-1}) and T is temperature measured in Kelvin.

The generation of the equilibrium parameters ($\Delta G(H_2O)$ and m-value) obtained from the curves was performed using the *linear extrapolation method* first described by Greene and Pace (1973). This method assumes that the ΔG values from the transition region depend on the denaturant concentration in a linear manner. They are therefore extrapolated back to zero urea concentration so as to obtain the ΔG value in the absence of urea ($\Delta G(H_2O)$), according to the following calculation:

$$\Delta G = \Delta G(H_2O) - m[denaturant] \qquad \textbf{15}$$

The *m*-value obtained from equation 15 gives a measure of the dependence of the free energy on denaturant concentration (Shirley, 1995), and is related to the amount of surface area exposed to the solvent upon denaturation, assuming the urea-binding sites are equally distributed on the surface of the unfolded protein (Myers *et al.*, 1995).

The measurement of ΔG is based on a number of assumptions (Bolen and Santoro, 1988; Yao and Bolen, 1995). These assumptions include the number of states in the transition region, the reversibility of unfolding, the validity of the linear extrapolation method, that ΔG is only a measure of the protein structure and that the denaturant does not influence the ΔG value and finally, that ΔG is a thermodynamic function of state, in other words it has the properties of additivity and predictability. There are two alternate methods that could be used to estimate the $\Delta G(H_2O)$ values and they are Tanford's model and the denaturant binding model (reviewed in Pace, 1986a). The three models are in good agreement although the linear extrapolation model always gives the lowest values. However the linear extrapolation model was used in this thesis because it is the only method that is believed to give $\Delta G(H_2O)$ values that are a property of the protein and are independent of the denaturant (Greene and Pace, 1973; Santoro and Bolen, 1992).

The two-state assumption is not necessarily valid because it fails to include the presence of intermediate species. The above data analysis can therefore only be applied to data that appears to follow the two-state hypothesis. Thus in order for this model to be applied, the equilibrium unfolding curve should be an abrupt single step and there should be no inflection, shoulder or plateau evident in the curve. Furthermore, measurement of the unfolding of the protein by different techniques should yield unfolding curves that are superimposable with each other. Unfolding processes are not always this simple, and often intermediate states can be discernable at equilibrium. Thus more complex

multi-state models, such as the *three-state model* have been constructed in order to incorporate the intermediate species into the equation.

Three-state monomer unfolding mechanism:

A three-state model for a monomeric protein (N ⇔ I ⇔ D) was used for the data where native, intermediate and denatured species were detected at equilibrium (Pace, 1986a).

In a *multi-state* unfolding model, the stable intermediate species are defined as X_i where the subscript "*i*" denotes the number of intermediates present. The physically recorded property of X_i is denoted y_i and the concentration of X_i is denoted F_i.

In the *three-state model*, the presence of intermediate species at equilibrium means that the observed extent of unfolding at any point along the unfolding transition, denoted F_{obs} differs from the two-state fraction unfolded value (F_D) (equation 12) by an amount that depends on the concentration of the intermediates.

Hence

$$F_{obs} = F_D + \sum_i F_i Z_i \qquad \textbf{16}$$

where Z_i represents a fractional change in *y* as the protein goes from the native to the intermediate state and is represented by:

$$Z_i = \frac{y_i - Y_N}{Y_D - Y_N} \qquad \textbf{17}$$

For the reaction $N \underset{K_{app}}{\Leftrightarrow} I \underset{K_D}{\Leftrightarrow} D$, the apparent rate constant K_{app} is given by

$$K_{app} = \frac{F_{obs}}{1 - F_{obs}} \qquad \textbf{18}$$

Incorporating equation 13 and equation 16 into equation 18 and defining K_i as F_i / F_N gives

$$K_{app} = K_D \left(\frac{1 + \sum_i Z_i \left(\frac{K_i}{K_D} \right)}{1 + \sum_i K_i (1 + Z_i)} \right) \qquad \textbf{19}$$

The $\Delta G(H_2O)_I$ and $\Delta G(H_2O)_{II}$, can thus be obtained using equation 14 as

$$\Delta G(H_2O)_1 = -RT \ln\left(\frac{y - y_N}{y_i - y_N} \right) \text{ and } \Delta G(H_2O)_{II} = -RT \ln\left(\frac{y - y_i}{y_D - y} \right)$$

and the m_I and m_{II}- values can be obtained using equation 15 as

$$m_1[denaturant] = \frac{\Delta G}{\Delta G(H_2O)_I} \text{ and } m_{II}[denaturant] = \frac{\Delta G}{\Delta G(H_2O)_{II}}$$

where the subscript "1" denotes the N ⇔ I transition and the subscript "II" denotes the I ⇔ D transition. K_D is less than K_{app} below the midpoint of the transition region, while above the midpoint K_D is greater than K_{app}. Therefore if a three-state transition is fit to a two-state model, the $\Delta G(H_2O)$ and m-values will be underestimated from their true value (Pace, 1986a; Soulages, 1998).

Protein concentration dependence study

The dependence of the equilibrium unfolding transition on the concentration of CLIC1 was studied by determining the signal generated at the midpoint of the unfolding transition as a function of CLIC1 concentration. The study was conducted using both fluorescence (excitation at 280 nm) and circular dichroism (ellipticity at 222 nm) as probes. The protein was in a 50 mM Na_2HPO_4 buffer containing 0.02% NaN_3 and 1 mM DTT. The protein concentration dependence was determined at both pH 7.0 and at pH 5.5.

At pH 7.0, CLIC1 was denatured in 4.8 M urea for two hours prior to spectroscopic measurement. This concentration of urea corresponds to the midpoint of the unfolding transition at pH 7.0. At pH 5.5, the protein was denatured in 3.5 M urea for one hour prior to spectroscopic measurement.

All experiments were conducted at 20^{o}C and protein concentrations ranging from 1 μM to 10 μM were used. Fluorescence excitation and emission slit widths used were 3.5 nm. Both the ratio of the fluorescence emission at 356 nm to the emission at 345 nm and the ratio of the ellipticity at 222 nm to the concentration of protein were plotted as a function of CLIC1 concentration.

2.2.12. Unfolding Kinetics

While the equilibrium unfolding of a protein can give an indication of its stability and cooperativity, it is the kinetics studies that give information on the presence of transient on- or off- pathway intermediates along the unfolding/folding pathway. This information can be used to construct a specific folding pathway for the protein.

The unfolding kinetics of CLIC1 was recorded using manual mixing methods. The dead-time was 1 – 10 s. Both circular dichroism and fluorescence were used as probes. Unfolding kinetics studies were performed on 2 μM protein. The studies were conducted at various pH levels, temperatures, redox conditions and in the presence of different salts.

The circular dichroism trace was collected as the ellipticity at 222 nm over, at most two hours at 20^{o}C or 37^{o}C and the data interval was set to 1 second.

The fluorescence data interval was set to 0.001 minutes and the traces were recorded as the fluorescence emission intensity at 345 nm when the protein was excited at 280 nm over, at most two hours at 20^{o}C.

The unfolding kinetics trace was recorded by manual mixing of CLIC1 to a final concentration of 2 μM with buffer containing urea at final concentrations ranging from 5.5 M – 8 M urea for the denatured state or from 3 M – 4.2 M urea for the intermediate state. The native baseline was recorded by measuring the signal of native protein in buffer over 15 minutes. The denatured baseline was recorded by denaturing 2 μM CLIC1 in 5.5 M – 8 M urea or 3 M – 4.2 M urea (depending on the experiment) and leaving the solution to reach equilibrium for at least one hour before recording the fluorescence or circular dichroism signal over 15 minutes. All traces were recorded three times and the average of these traces was analysed using SigmaPlot® v8.0.

Data Analysis

The unfolding kinetics data were fit to the exponential decay model. Depending on the data, the unfolding trace was fit to either a single or double exponential model according to the equation:

$$A(t) = A(\infty) + \sum A_i e^{-K_i t} \qquad \textbf{20}$$

where $A(t)$ is the observed value of the circular dichroism or fluorescence intensity at a given time, t, $A(\infty)$ is the amplitude value when no further change is observed, K_i is the apparent rate constant of the i^{th} kinetic phase and A_i is the amplitude of the i^{th} phase.

The residuals for each plot show the error between the experimental points and the theoretical curves analysed according to either a single or double exponential model. They were computed and used to illustrate which model fit the data best.

To determine the unfolding rate in the absence of denaturant, the following equation was used:

$$\log(k_u) = \log(k_u(H_2O)) + m_u[denaturant] \qquad \textbf{21}$$

where k_u is the apparent rate constant for unfolding at different urea concentrations, $k_u(H_2O)$ is the apparent rate of unfolding in the absence of denaturant and m_u represents the change in the accessibility of the unfolded state to solvent.

Chapter 3. Results

3.1. CLIC1 Purification

3.1.1. Plasmid Verification

CLIC1 was expressed as a GST fusion protein cloned into the plasmid pGEX-4T-1. The restriction sites flanking the fusion protein are those for *BamH1* and *Not1* (Figure 15). The plasmid was transformed into *Escherichia coli* BL21 cells.

3.1.2. CLIC1 Expression and Purification

The purification of CLIC1 followed the basic protocol devised by Tulk *et al.*, (2000) (also see section 2.2.2).

Cells grown in the absence of IPTG produced a much lower yield of the fusion protein than the cells grown in 1 mM IPTG (Figure 16A lanes B and C respectively). The subunit of the *Sj*26GST that was fused to CLIC1 has a theoretical molecular mass of 25.5 kDa, and CLIC1 has a theoretical molecular mass of 26.9 kDa. Therefore the theoretical size of CLIC1-GST excluding the thrombin cleavage site is 52.4 kDa. The over-expressed band analogous to the fusion protein migrates a distance corresponding to 55.7 kDa on the SDS-PAGE gel (Figure 16A lane C). This is the correct approximate size for CLIC1-GST. It was determined as 54 kDa by Tulk *et al.* (2002).

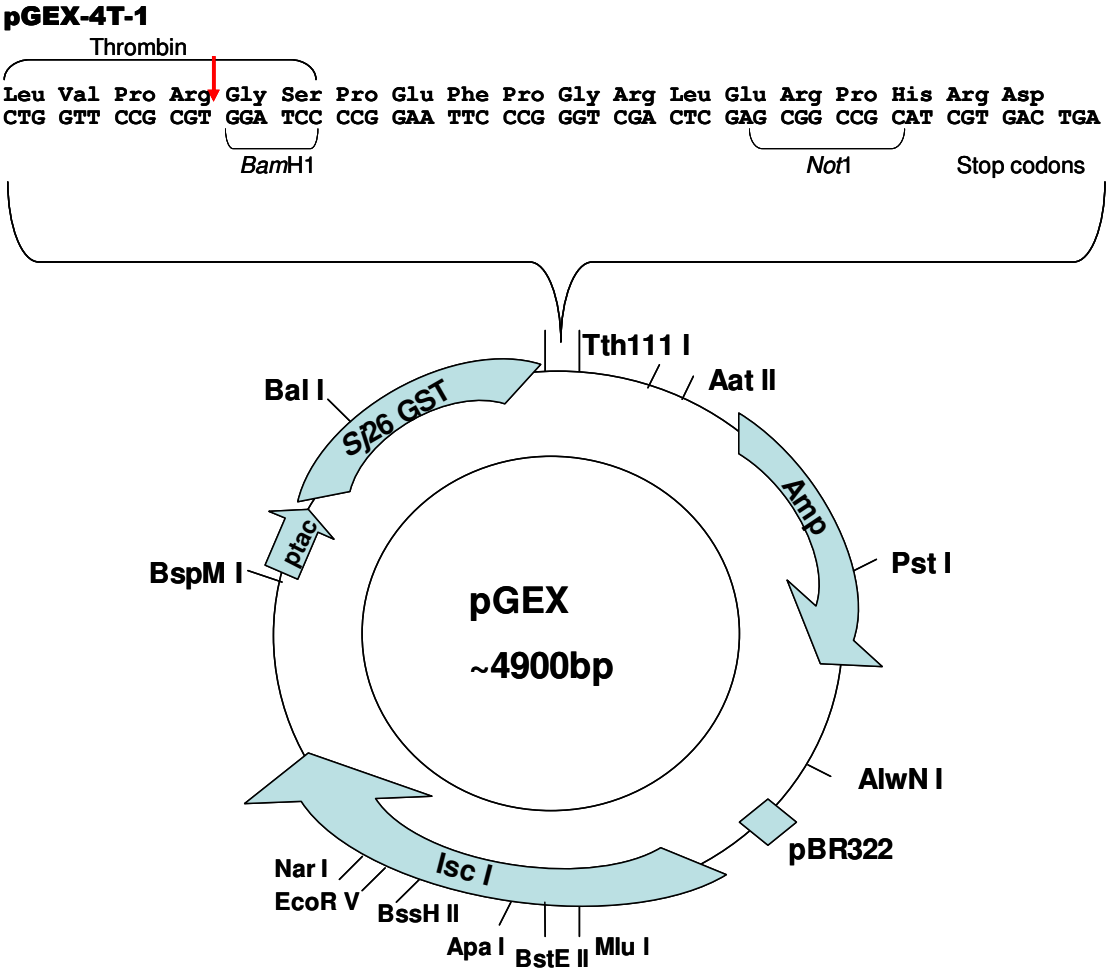


Figure 15: Restriction map of pGEX-4T-1

A schematic of the pGEX plasmid showing the pGEX-4T-1 insert (adapted from Valenzuela *et al.*, 1997). This plasmid contains a lac operon and will confer ampicillin resistance to cells transformed with pGEX-4T-1. The plasmid encodes GST fused to CLIC1 via a thrombin-cleavage site. This site, as well as the restriction sites flanking the CLIC1 cDNA is shown in the insert above the plasmid.

Soluble CLIC1 was found to be present in the supernatant, while a small fraction of insoluble protein appeared in the pellet (Figure 16A lanes E and D, respectively). Most of the protein was soluble, as seen by the prominent 56 kDa band in lane E of Figure 16A. The lack of the over-expressed band in lane F of Figure 16A indicates that most of the fusion protein had successfully bound to the column.

The fusion protein was efficiently cleaved with thrombin. This is shown in lane G of Figure 16A. The 26.5 kDa band is that of *Sj*26GST (determined as 27 kDa by Tulk *et al.* (2002)). There is a band at 56 kDa representing a small percentage of fusion protein. Since this is only a very faint band, the cleavage was efficient. The CLIC1-thrombin mixture (lane I of Figure 16A) was successfully separated using DEAE-Sepharose chromatography. The theoretical molecular weight of thrombin is 29.7 kDa. This protein migrated a distance on the SDS-PAGE gel that corresponded to a size of 29.5 kDa.

Elution of CLIC1 from the DEAE-Sepharose column with reduced pH proved to be ineffectual, since the protein remained bound to the column at pH levels as low as 4.0. This observation can be explained by realising that the true p*I* of a protein may be lower than the theoretical value. This is because the pK_a values of residues within a folded protein can be different to those in the isolated peptide, or even to that of the denatured protein. For example, the pK_a of aspartate observed in model compounds is 4.1 but the average value found in proteins is 3.4. Therefore the calculated p*I* is usually an overestimate of the true value, especially for acidic proteins (Shaw *et al.,* 2001) and it is likely that the true p*I* of CLIC1 is lower than the calculated value of 4.85. This could explain why the protein would not be eluted off the DEAE-Sepharose column, even when the pH was dropped below 4.85. Dropping the pH too low results in a degree of acid denaturation whereby the structural properties of CLIC1 are altered. Therefore, pure CLIC1 was rather eluted off the-DEAE Sepharose column (Figure 17A) using a buffer with an elevated salt concentration (20 mM Tris-HCl; *300 mM NaCl*; 0.02% NaN_3, pH 7.0).

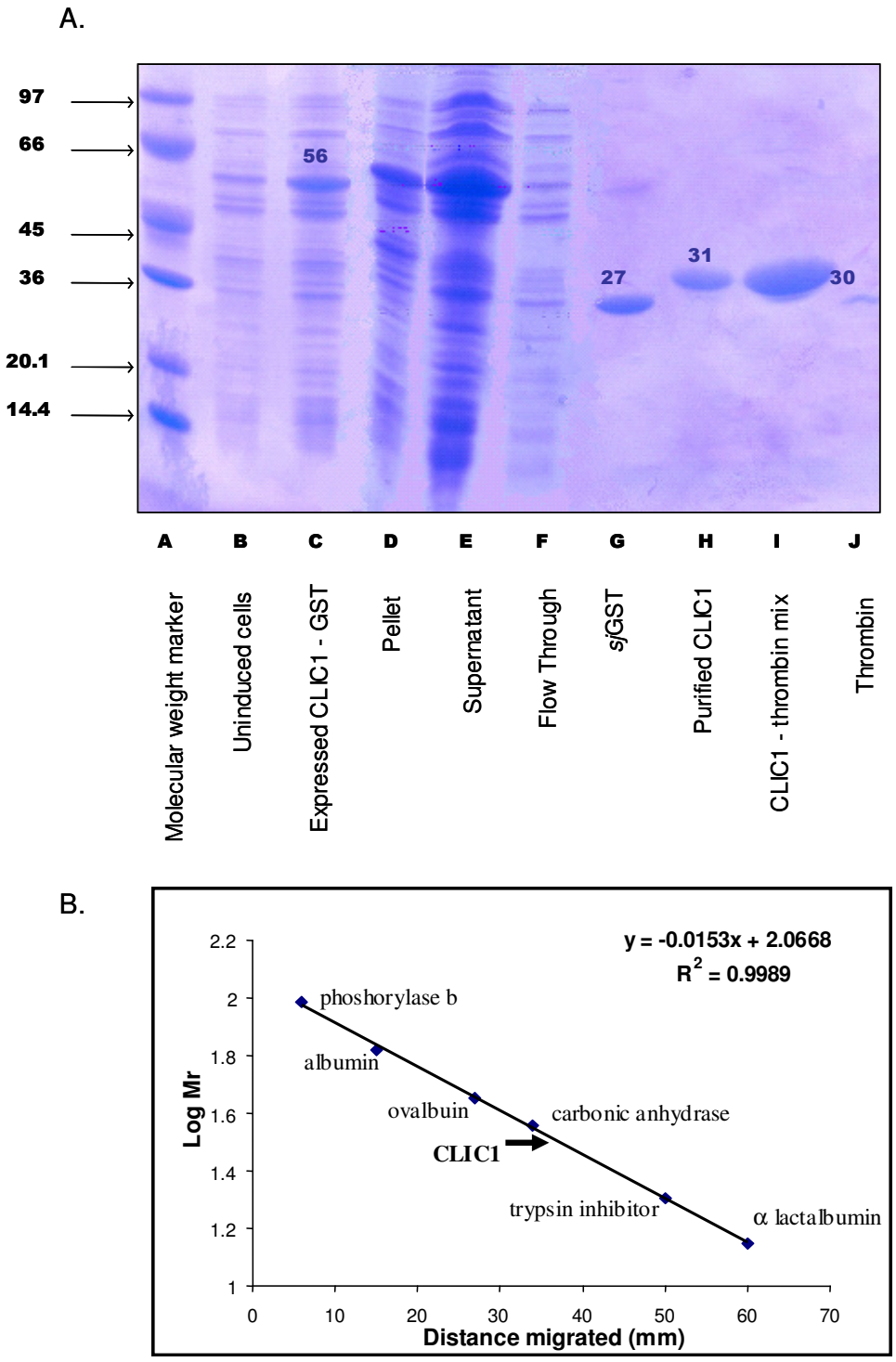


Figure 16: SDS-PAGE gel showing a representative CLIC1 purification

(A) A 15% polyacrylamide SDS-PAGE gel stained with Coomassie brilliant blue illustrating a representative purification of CLIC1. Lane A contains molecular weight markers; lanes B and C contain the protein complement of

Escherichia coli cells pre and post induction respectively; lanes D and E contain, respectively, the pellet and supernatant of the lysed cells. Lane F shows material off the glutathione-Sepharose column once the fusion protein had bound to the matrix. The cleaved *Sj*26GST and a negligible amount of uncleaved fusion protein are separated in lane G. Lane H reveals the band of successfully purified CLIC1, with an apparent molecular mass of 30.6 kDa. The mixture of CLIC1 and thrombin before complete purification is shown in lane I and the successfully removed thrombin is shown in lane J. All samples (except for that of thrombin) were diluted two-fold with 5 x sample buffer before loading onto the gel.

(B) The calibration curve for the SDS-PAGE gel shown in **A**. The molecular mass (in kDa) and distances migrated by the standard proteins in lane A of the gel were used to construct this curve.

The band of purified CLIC1 can be seen in lane H of Figure 16A. The migration of CLIC1 in the polyacrylamide gel is slightly impeded, giving an apparent molecular weight of 30.6 kDa instead of the theoretical value of 26.9 kDa. The reason for this discrepancy is unknown but slow migration in SDS-PAGE gels seems to be characteristic of members of the CLIC family and could be attributed to their low p*I* values and highly acidic nature relative to other proteins which will reduce the SDS: protein ratio (Tulk and Edwards, 1998; Edwards, 1999; Berryman and Bretscher, 2000; Nishizawa *et al.,* 2000; Tulk *et al.*, 2000; Board *et al.,* 2004). However, the size of 30.6 kDa corresponds well with the size of 31 kDa determined for CLIC1 by Berryman and Bretscher (2000) using SDS-PAGE and the band in lane H of Figure 16A represents purified CLIC1. Generally 20 mg of CLIC1 was purified per litre of culture. This is a 75% higher yield than the 5 mg of CLIC1 per litre of growth obtained by Tulk *et al.* (2000) using a similar purification method.

The absorbance spectrum of this protein is shown in Figure 17C. The A_{280} / A_{260} ratio was always close to 1.8 indicating low DNA contamination (Maniatis and Fristsch, 1982).

3.2. Structural Characterisation of CLIC1

3.2.1. Effect of pH on CLIC1 Structure

Secondary Structure

The secondary structure of CLIC1 was studied using circular dichroism spectroscopy. The far-UV circular dichroism spectra of CLIC1 at pH levels ranging from 4.5 to 8.2 were recorded over the wavelength range of 190 – 250 nm (Figure 18). The spectra are typical of an alpha helical protein and display the characteristic minima at 222 nm and 208 nm (Woody, 1995).

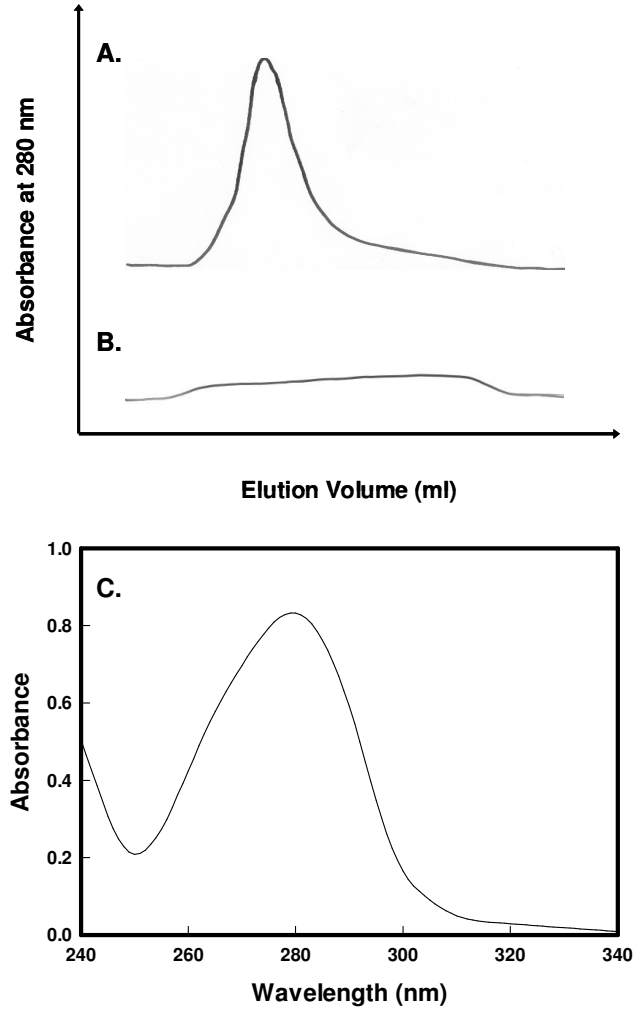


Figure 17: Elution off the DEAE-Sepharose anion exchange column

(A) The elution profile of CLIC1 off the DEAE-Sepharose column recorded using absorbance at 280 nm on the Äktaprime system. CLIC1 was eluted in 20 mM Tris-HCl; 300 mM NaCl, pH 7.0. CLIC1 was recovered from the column within 20 ml as a single symmetrical peak.

(B) Thrombin did not bind to the DEAE-Sepharose column at pH 6.5, the elution profile is constant and rather flat since it shows the thrombin being washed off the column. This procedure successfully separated CLIC1 from the contaminating thrombin.

(C) The absorbance spectrum of purified CLIC1. The absorbance at 280 nm is 0.85 which corresponds to a protein concentration of 50 μM. The purified protein does not have significant DNA contamination since the ratio of the absorbance at 280 nm to 260 nm is 1.8 and no aggregation is evident since the absorbance value at 340 nm is negligible.

Figure 18 indicates that the secondary structural content of the native state of CLIC1 is marginally affected by pH. Below pH 6.0 the negative ellipticity decreases. The protein displays the most secondary structure between pH 6.0 and pH 7.0.

In this work CLIC1 has been studied extensively at two pH values, namely pH 7.0 and pH 5.5 since this is the approximate pH of the cytoplasm and at the membrane surface respectively (Menestrina *et al.,* 1989; van der Goot *et al.,* 1991; Bortoleto and Ward, 1999; Chenal *et al.,* 2002). The circular dichroism spectra at pH 7.0 and pH 5.5 are compared in Figure 19. It is clear that the spectra are not superimposable at these two pH values, with the protein at pH 5.5 exhibiting an approximately 16% reduction in secondary structure compared to at pH 7.0. The spectra of the denatured state show that the predominantly α-helical secondary structure no longer exists when CLIC1 is in the presence of 8 M urea at either pH 7.0 or pH 5.5 and the protein essentially exists as a random coil under these conditions. This pH dependence of secondary structure is fairly unusual in that it has not been observed in other soluble membrane proteins for example α-toxin (Vecsey-Semjen *et al.,* 1996); diphtheria toxin (Chenal *et al.,* 2002) or Bcl-$_{XL}$ (Thuduppathy *et al.,* 2005). Thus the question remains as to the significance of the decline in CLIC1 secondary structure at low pH.

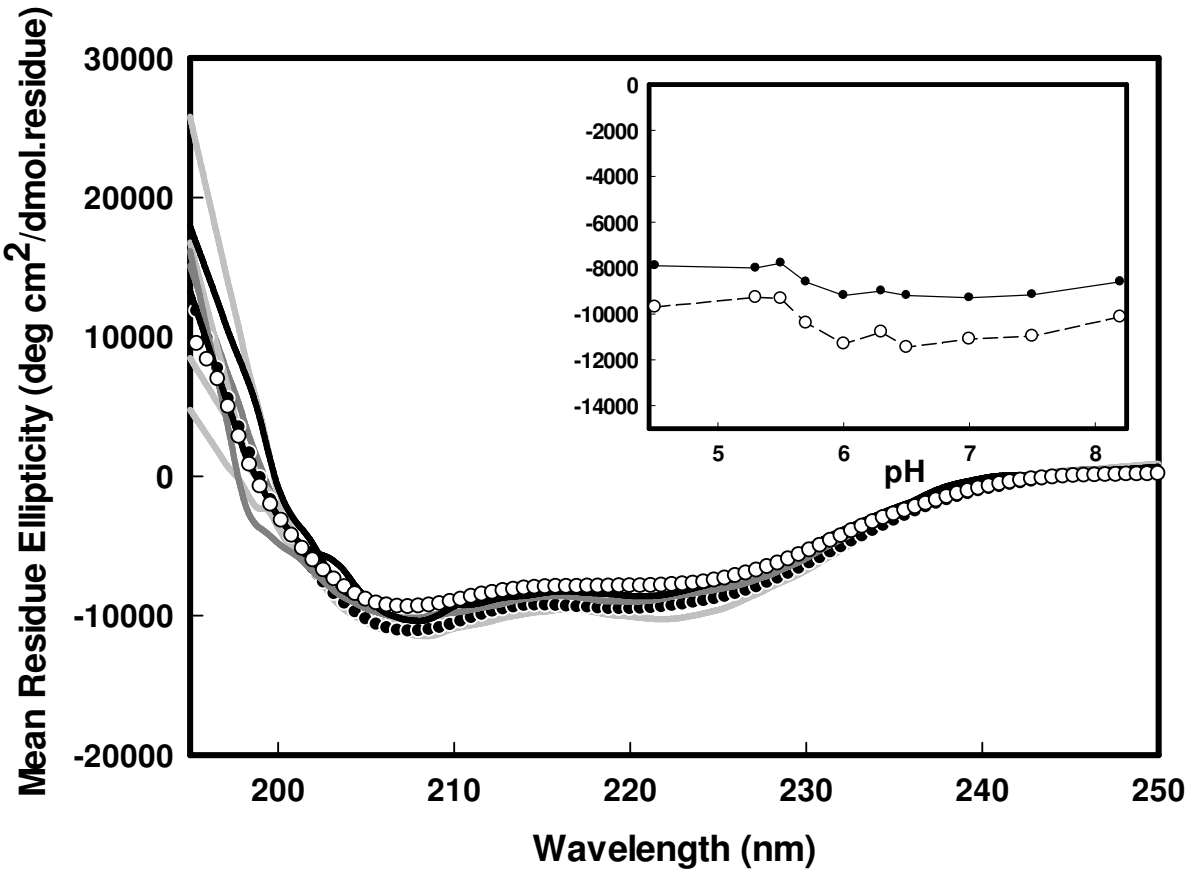


Figure 18: pH dependence of the far-UV circular dichroism spectra of CLIC1

Far-UV circular dichroism spectra of 5 μM CLIC1 (5 mM Na_2HPO_4; 0.1 mM DTT, pH 4.5 to 8.2). The spectra of CLIC1 are specially indicated at pH 7.0 (●) and at pH 5.5 (○). The spectra are all characteristic of an α-helical protein, displaying two minima: one at 222 nm and one at 208 nm. Spectra were corrected for the buffer blank and show an average of ten accumulations at 100 nm/min at 20°C. The data were smoothed using a negative exponential methodology. **The insert** shows the mean residue ellipticity at 208 nm (○) and at 222 nm (●) as a function of pH. There is a slight decrease in the negativity of the ellipticity below pH 6.0.

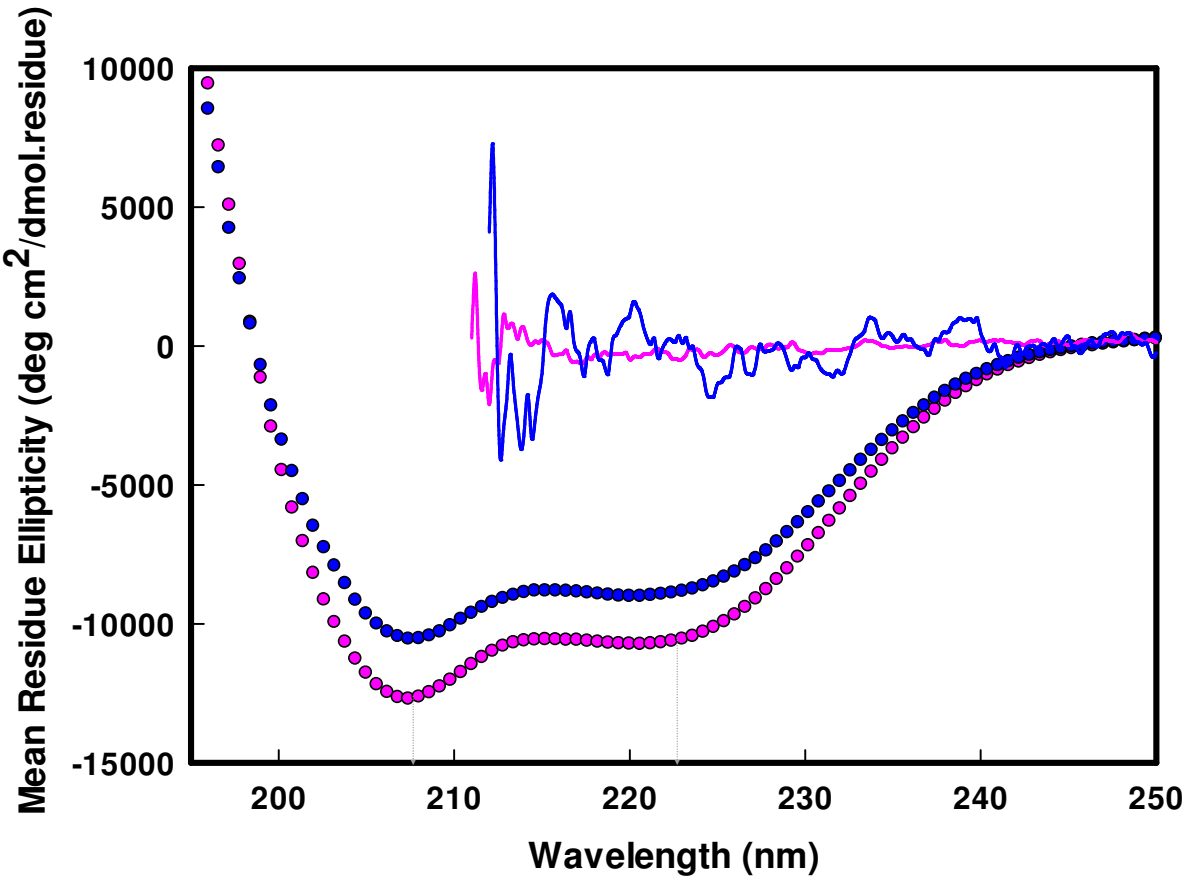


Figure 19: Comparison of the circular dichroism spectra at pH 7.0 and pH 5.5

Circular dichroism spectra of 5 µM CLIC1 (5 mM Na_2HPO_4; 0.1 mM DTT) recorded at pH 7.0 (pink) and pH 5.5 (blue) in the native state (●) and denatured in 8 M urea (solid line). The native spectra show minima at 208 nm and 222 nm (indicated by arrows) which is characteristic of an α-helical protein. CLIC1 has 16% more secondary structure when at pH 7.0 compared to at pH 5.5. The denatured spectra show a complete loss of secondary structure at either pH. Spectra were recorded at 20°C. The data were smoothed using the negative exponential methodology.

Tertiary Structure

The tertiary structure of CLIC1 was investigated using fluorescence spectroscopy. This technique provides information about the environment of most specifically, the tryptophan residues in a protein. CLIC1 has a single tryptophan residue, Trp35, which is located at the C-terminal end of the α1 helix in the N-terminal domain (see Figure 8). This helix has been proposed to traverse the membrane (Harrop *et al.,* 2001; Berry and Hobert, 2006; Singh and Ashley, 2006). Excitation of CLIC1 at 295 nm produces a rather weak signal (Figure 20). Since there is such a low quantum yield produced by selectively exciting the single tryptophan residue, all studies were conducted by exciting the protein at 280 nm, thereby exciting the eight tyrosine residues in addition to the tryptophan residue. Even so, the emission spectrum will reflect the environment of the tryptophan, especially in the native state of the protein where many tyrosines are in close enough proximity to the tryptophan for fluorescence resonance energy transfer to occur from the tyrosines to the tryptophan (Lakowicz, 1999). Nevertheless, excitation at 280 nm will give a more global depiction of the tertiary structure of CLIC1 than excitation at 295 nm.

The fluorescence emission maximum wavelength of CLIC1 is ~345 nm when excited at either 280 nm or 295 nm (Figure 21). Therefore, since the signal is much greater and the peak is sharper when exciting at 280 nm, all further experiments were conducted using 280 nm as the excitation wavelength. The emission maximum at ~345 nm is consistent with the crystal structure in that Trp35 is fairly exposed to the solvent in the native state of this protein.

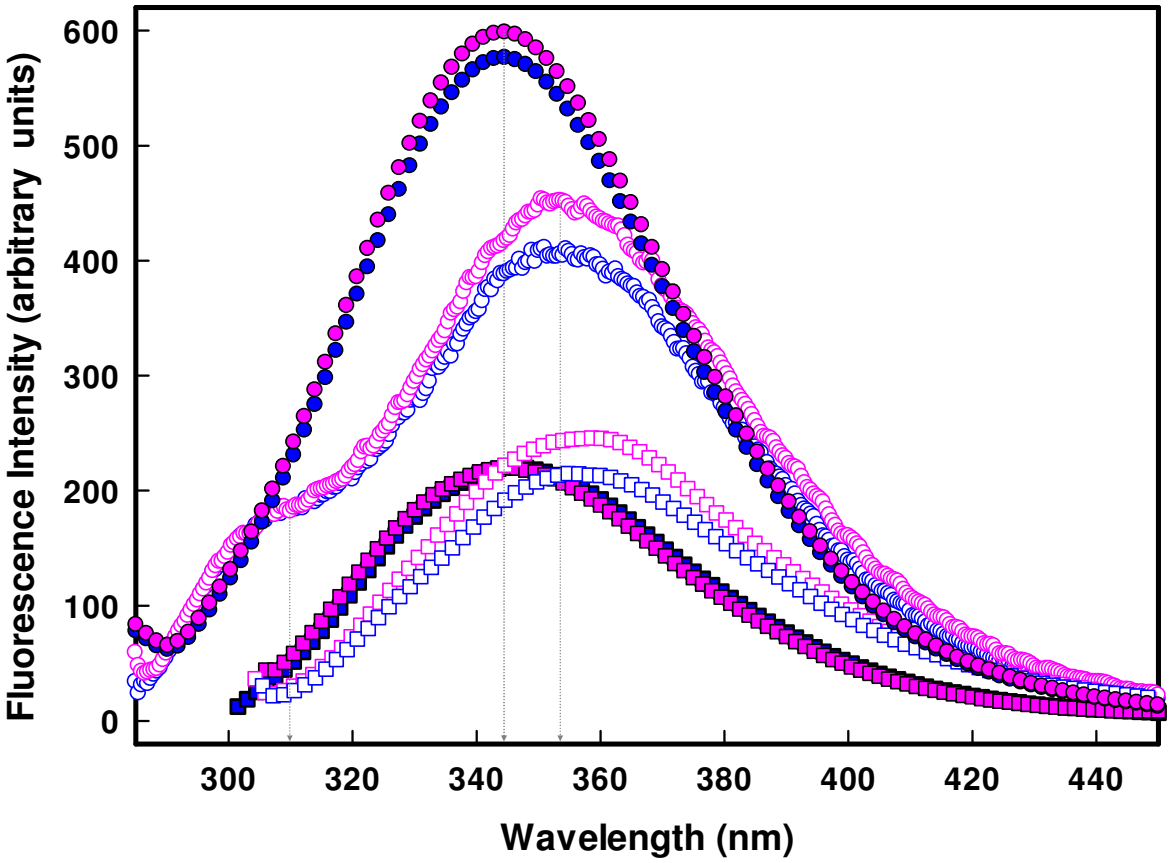


Figure 20: Comparison of the fluorescence spectra at pH 7.0 and pH 5.5

Fluorescence emission spectra of 5 µM CLIC1 (50 mM Na_2HPO_4; 0.02% NaN_3; 1 mM DTT) when excited at 280 nm (●/○) or at 295 nm (■/□). The native state is represented by closed symbols and the spectra peak at ~345 nm (indicated by arrow) regardless of whether the protein is excited at 280 nm or 295 nm. Emission at pH 7.0 is shown in pink and the pH 5.5 emission spectrum is blue. The denatured state (in 8 M urea) is represented by open symbols. CLIC1 displays red shifted emission upon denaturation and peaks at ~356 nm when excited at 280 nm (indicated by arrow) and at ~360 nm when excited at 295 nm. When the protein is excited at 280 nm there is a quenching of emission intensity by approximately 30% upon denaturation and a peak appears at ~310 nm (indicated by arrow). All spectra were recorded at 20°C and were smoothed using the negative exponential methodology.

When CLIC1 is denatured in 8 M urea, the spectrum shows a red shift in the emission maximum to ~356 nm as the tryptophan becomes more exposed to the polar solvent. Furthermore, when the denatured state is excited at 280 nm, emission due to the tyrosines can be seen by the presence of a peak at 310 nm (Edelhoch, 1967). This is because the energy transfer from tyrosine to tryptophan is uncoupled as the distance between these residues is increased upon unfolding. The intensity of the fluorescence signal also decreases by approximately 30% upon denaturation of the protein at both pH 7.0 and pH 5.5 (Figure 20 and Figure 21). This quenching of the fluorescence signal could be due to charged residues such as arginine or lysine in the denatured state being in closer proximity to the tryptophan than in the native, folded state or it could be due to solvent quenching in the denatured state.

The fluorescence spectra of CLIC1 were recorded at pH levels ranging from 4.5 to 8.2 in order to determine whether a change in the concentration of H^+ ions has any effect on the tertiary structure of this protein. Figure 21 shows that at pH levels at the far ends of the pH spectrum (*i.e.* pH 8.2 and pH 4.5) the protein displays slight alteration in tertiary structure, seen by quenching of the emission signal. The tertiary structure of CLIC1 is similar at pH values between pH 5.3 and 7.5, however.

The fluorescence intensity is not a very good indicator of changes in tertiary structure because slight fluctuations in the intensity could occur due to small changes in protein concentration. Therefore to avoid these errors, one can study the wavelength at which the spectrum peaks (λ_{max}) since this is independent of protein concentration and rather gives an indication of the polarity of the environment of the tryptophan residue. Both the λ_{max} and the emission intensity when excited at 280 nm are constant within the pH range of 5.3 to 7.5. Thus at the physiologically relevant pH 7.0 and pH 5.5 there is no difference in the tertiary structure of the protein, at least within the vicinity of the tryptophan residue (Figure 20).

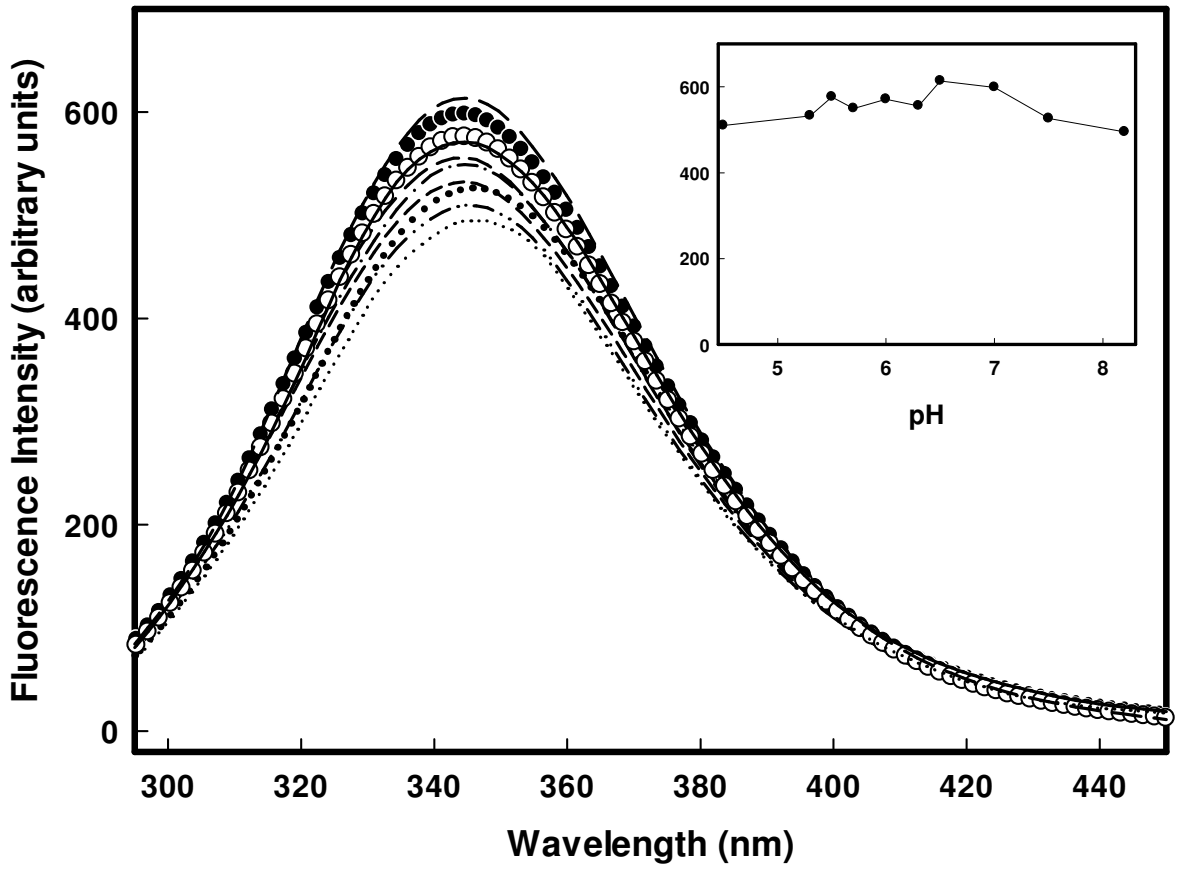


Figure 21: pH dependence of the fluorescence spectra of CLIC1

Fluorescence spectra of 5 μM CLIC1 (50 mM Na_2HPO_4; 0.02% NaN_3; 1 mM DTT, pH 4.5 to 8.2). The spectra of CLIC1 are highlighted at pH 7.0 (●) and at pH 5.5 (○). The protein was excited at 280 nm. Regardless of the pH, the protein emits at ~345 nm. Spectra were recorded at 20°C and were smoothed using the negative exponential methodology. **The insert** shows the fluorescence intensity at 345 nm as a function of pH.

Quaternary Structure

The quaternary structure of CLIC1 was investigated using SEC-HPLC (Figure 22) and dynamic light scattering (DLS) (Figure 23). The single peak obtained from loading 5 μM CLIC1 pH 7.0 and pH 5.5 onto the size exclusion column confirmed that the purified protein was not contaminated and exists as a single species in solution in its native state. However the hydrodynamic volume occupied by CLIC1 under these conditions appears to be much larger than that of a typical 27 kDa protein. The retention time taken to elute CLIC1 off the size exclusion column at pH 7.0 in the presence of 0.1 M Na_2SO_4 astonishingly corresponds to that of a protein of 70 kDa! This grossly exaggerated value is two and a half times the predicted molecular size of CLIC1 (Figure 22)! pH also has an effect on the retention time of the protein from the column. CLIC1 elutes quicker at pH 7.0 compared to at pH 5.5.

The hydrodynamic volumes occupied by CLIC1 obtained from the SEC-HPLC study seem improbable and the protein's premature elution from the column can be ascribed to anomalous behaviour of the protein on this column. However in order to confirm this assumption a dynamic light scattering technique was applied. In this technique a laser is shone onto the protein solution and the speed at which the molecules change their position is used to calculate the hydrodynamic diameter of the molecules present in the solution. The idea is that the smaller molecules will move faster than the larger molecules. DLS is thus a not a static technique since constant movement of the molecules is required for the calculations. Therefore a fair number of measurements have to be performed in order to obtain an accurate average of the hydrodynamic size of the protein. A drawback to this technique is its low sensitivity and high concentrations of the protein are often required for an accurate measurement which may lead to aggregation.

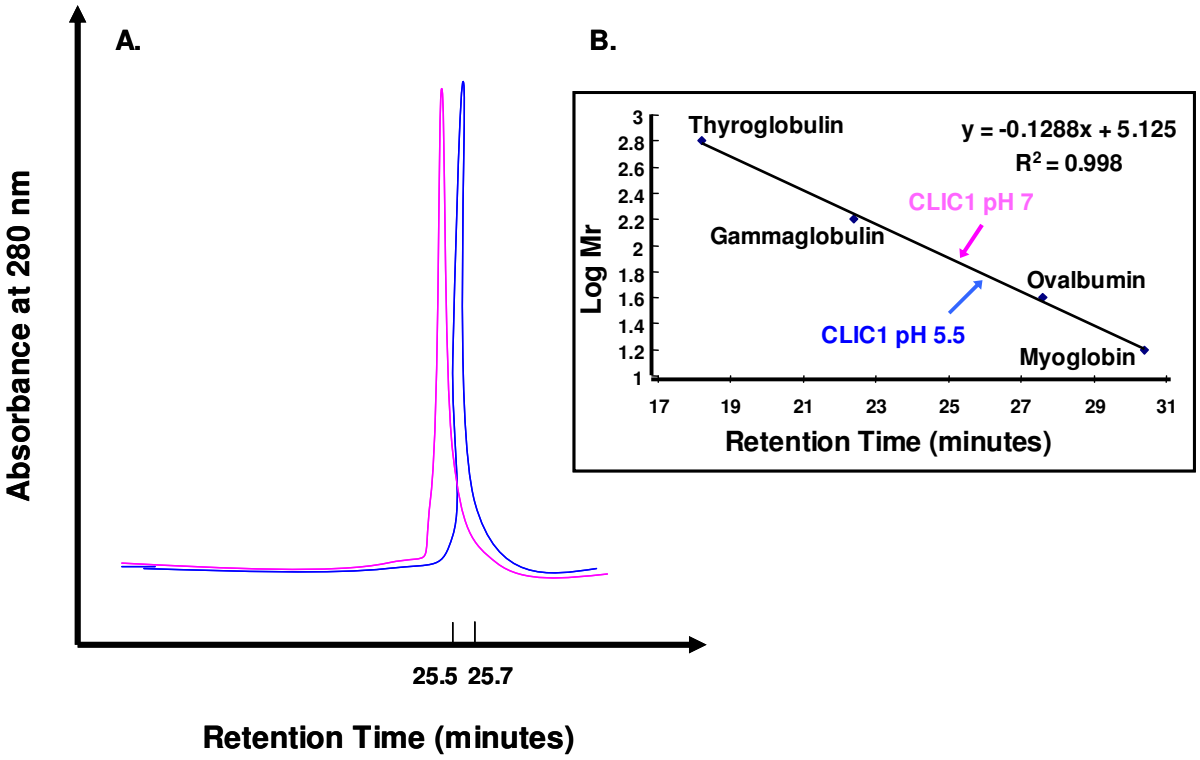


Figure 22: Comparison of the SEC-HPLC elution profiles at pH 7.0 and pH 5.5

(A) SEC-HPLC elution profile of 5 µM CLIC1 at pH 7.0 (pink) and pH 5.5 (blue) using an HPLC buffer containing 0.1 M Na_2HPO_4; 0.1 M Na_2SO_4; 0.05% NaN_3. The absorbance at 280 nm was recorded. The protein sample was pure as detected by SEC-HPLC and CLIC1 was eluted after 25.5 minutes at pH 7.0 and after 25.7 minutes at pH 5.5 at a flow rate of 0.5 ml/min (chart speed was 30 cm/hr).

(B) The calibration curve created using the standard proteins: thyroglobulin (670 kDa); gammaglobulin (158 kDa); ovalbumin (44 kDa) and myoglobin (17 kDa). The elution of these proteins was measured using absorbance at 280 nm. The buffer used was 0.1 M Na_2HPO_4; 0.1 M Na_2SO_4; 0.05% NaN_3 pH 6.7. The hydrodynamic volume occupied by CLIC1 at pH 7.0 and pH 5.5 is calculated as 70.0 kDa and 65.3 kDa respectively!

Nevertheless, taking all this into consideration, the pH dependence of the hydrodynamic size of 20 μM CLIC1 was measured using DLS (Figure 23). At low pH (4.5) the protein aggregates. This is due to the effect of both the pH and the high protein concentrations necessary for the technique. At a pH below 6.0 the protein exists as a monomeric species with a predicted size of approximately 27 kDa. At pH 7.0 the predicted size obtained from the hydrodynamic diameter is closer to that of a 40 kDa protein but CLIC1 is most likely still monomeric since 40 kDa is conceivably not large enough to represent a dimeric species. Therefore the protein probably exists as an "extended monomer" in solution that exhibits anomalous behaviour on the HPLC column possibly as a result of aggregation. However the comparison of the relative sizes at pH 7.0 and pH 5.5 could still be used and it is interesting to note that when using both SEC-HPLC and DLS, the hydrodynamic volume occupied by the protein at pH 7.0 is slightly larger than at pH 5.5.

3.2.2. Effect of Salt on CLIC1 Structure

Secondary structure

Circular dichroism spectra were recorded at both pH 7.0 and pH 5.5 in the presence of increasing concentrations of various salts (0 – 1 M NaCl, NaF and Na_2SO_4, (Figure 24)). At all salt concentrations the dynode voltage at 222 nm and 208 nm is well below 600 mV so the error due to light scattering at high salt concentrations is marginal. At pH 7.0, NaCl and Na_2SO_4 have little effect on the secondary structure, while a maximum of 0.2 M NaF increases the secondary structure by ~17%. At pH 5.5 the salts have a greater impact on the secondary structure of CLIC1. 0.2 M NaCl increases the secondary structure by ~23%, 0.5 M NaF increases the secondary structure by up to 33% and concentrations of up to 1 M Na_2SO_4 affect the secondary structure of CLIC1 at pH 5.5 with an increase of up to ~31% being recorded.

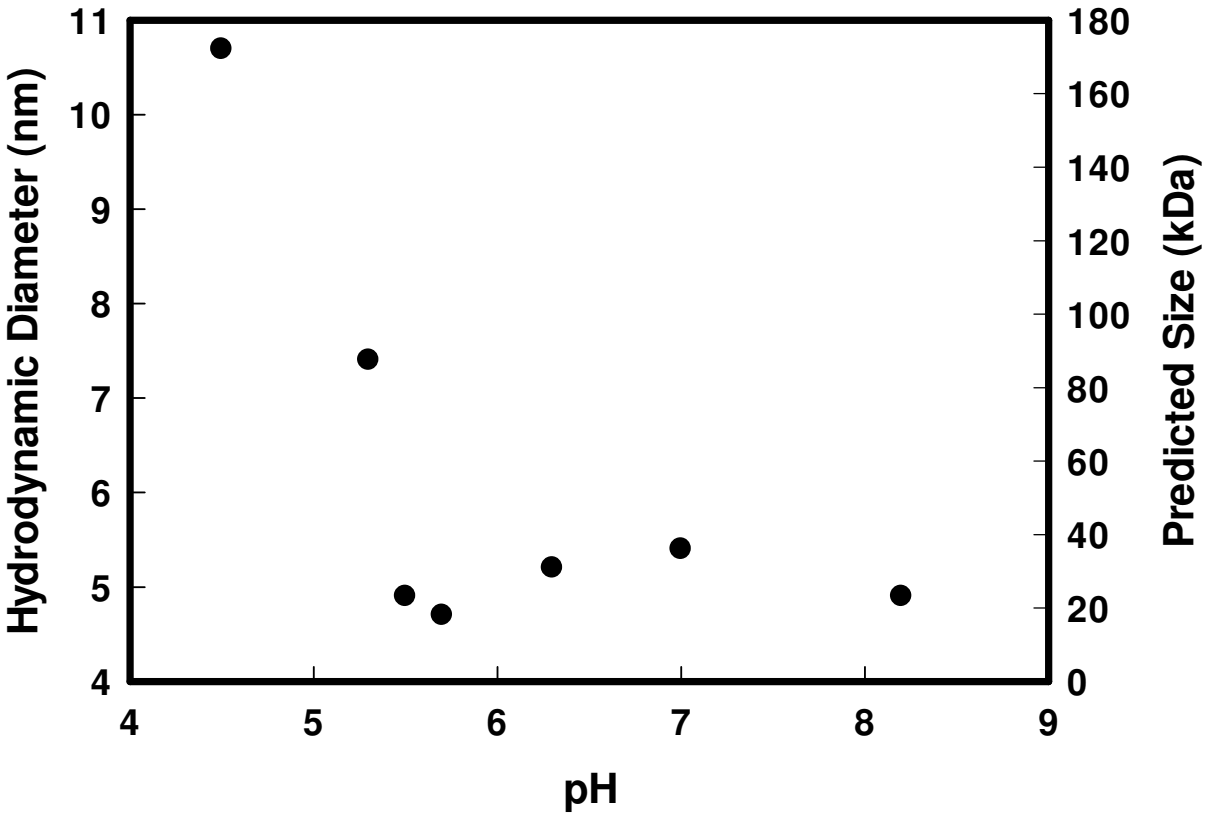


Figure 23: pH dependence of the hydrodynamic diameter of CLIC1

The hydrodynamic diameter of 20 µM CLIC1 (50 mM Na_2HPO_4; 0.02% NaN_3; 1 mM DTT) was determined at pH 4.5 to 8.2 using dynamic light scattering. The predicted size of the protein in kDa based on the hydrodynamic diameter is given on the right axis. Besides where aggregation is concerned, pH does not appear to have a marked effect on the size of the protein. All measurements are an average of 10 accumulations at 25°C.

In the absence of salt the secondary structure is reduced at pH 5.5 compared to at pH 7.0 (Figure 19). However, as soon as any salt is added, the negative ellipticity at pH 5.5 is increased to the same as or in some cases even more than at pH 7.0. NaF has the greatest effect on the negative ellipticity of CLIC1 and at 1 M NaF there is no difference in the secondary structure of CLIC1 at pH 7.0 or pH 5.5 (Figure 24). It is interesting that high concentrations of both NaCl and Na_2SO_4 result in a greater increase in the proportion of secondary structure at pH 5.5 than at pH 7.0. This indicates that salt in general has a greater effect on the native state of this protein when at pH 5.5. Na_2SO_4 is the only salt where very high concentrations (1 M) actually result in decreased secondary structure and this only at pH 7.0.

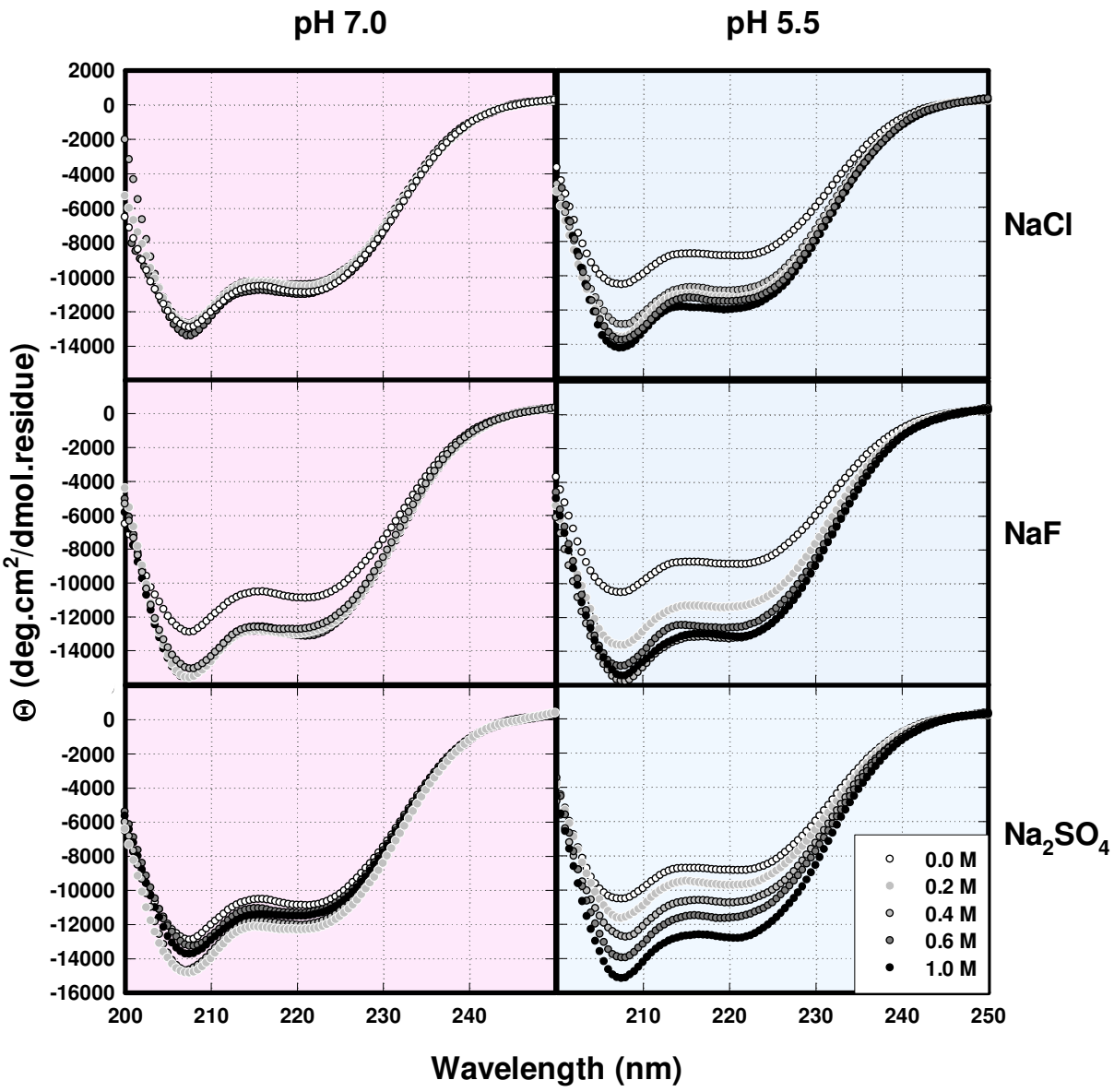


Figure 24: Effect of salts on the circular dichroism spectra of CLIC1 at pH 7.0 and pH 5.5

Far-UV circular dichroism spectra of CLIC1 at pH 7.0 (pink) and pH 5.5 (blue) in the presence of 0 M to 1 M NaCl (top panel), NaF (middle panel) and Na_2SO_4 (bottom panel). Colours range from light to dark shades of grey as the salt concentration is increased. In general, salt has more of an effect on CLIC1 structure at pH 5.5. All measurements were performed on 5 µM protein at 20°C. The buffer used in all cases was 5 mM Na_2HPO_4; 0.1 mM DTT in the presence of various concentrations of salts. All spectra were smoothed using the negative exponential method.

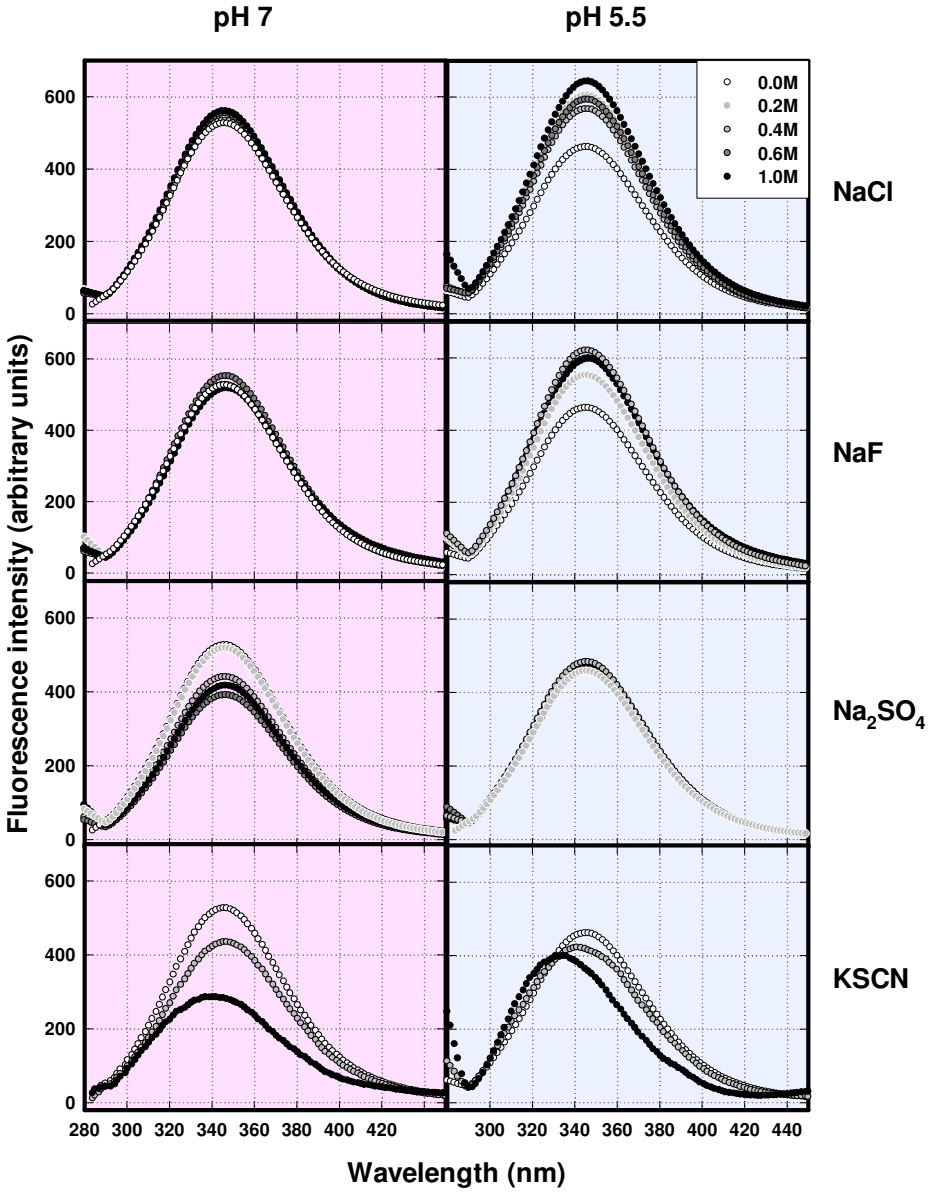


Figure 25: Effect of salts on the fluorescence spectra of CLIC1 at pH 7.0 and pH 5.5

Fluorescence spectra of CLIC1 at pH 7.0 (pink) and pH 5.5 (blue) in the presence of 0 - 1 M NaCl (top panel), NaF (second panel), Na_2SO_4 (third panel) and KSCN (bottom panel). Colours range from light to dark shades of grey as the salt concentration is increased. NaF and Na_2SO_4 result in quenching of the fluorescence intensity at pH 7.0 while NaCl and NaF cause enhanced fluorescence intensity at pH 5.5. 1 M KSCN causes a blue shift in the λ_{max} which is more pronounced at pH 5.5. All measurements were performed on 5 μM protein at 20°C. The buffer used in all cases was 5 mM Na_2HPO_4; 0.1 mM DTT in the presence of various concentrations of salts. All spectra were smoothed using the negative exponential method.

Tertiary structure

As with the circular dichroism spectra, the fluorescence spectra were recorded at pH 7.0 and pH 5.5 in the presence of 0 – 1 M NaCl, NaF and Na_2SO_4. In addition, the effect of the chaotropic salt KSCN on the tertiary structure was studied. KSCN produces very noisy circular dichroism spectra and therefore only the fluorescence spectra were recorded in the presence of this salt (Figure 25).

CLIC1 is sensitive to salt effects and at different pH values it responds differently to different salts. NaCl and NaF do not affect the tryptophan fluorescence of CLIC1 at pH 7.0 but at pH 5.5 both salts cause an enhancement of the emission intensity by approximately 25%. Furthermore, in the presence of salt, the emission of CLIC1 at pH 5.5 is enhanced compared to at pH 7.0 under the same conditions despite the fact that in the absence of salt there is no significant difference in the fluorescence intensity at pH 5.5 and pH 7.0 (Figure 20). Na_2SO_4 has no effect on the fluorescence spectra at pH 5.5 but quenches the signal fairly significantly at pH 7.0. KSCN is a known chaotropic salt. It is interesting that at a 1 M concentration of this salt the fluorescence spectra no longer peak at ~345 nm but are blue shifted at both pH 7.0 and pH 5.5 although the blue shift in the λ_{max} is far more pronounced at pH 5.5 (Figure 25). In contrast to NaCl, NaF and Na_2SO_4, KSCN causes major tertiary structural alterations to the protein.

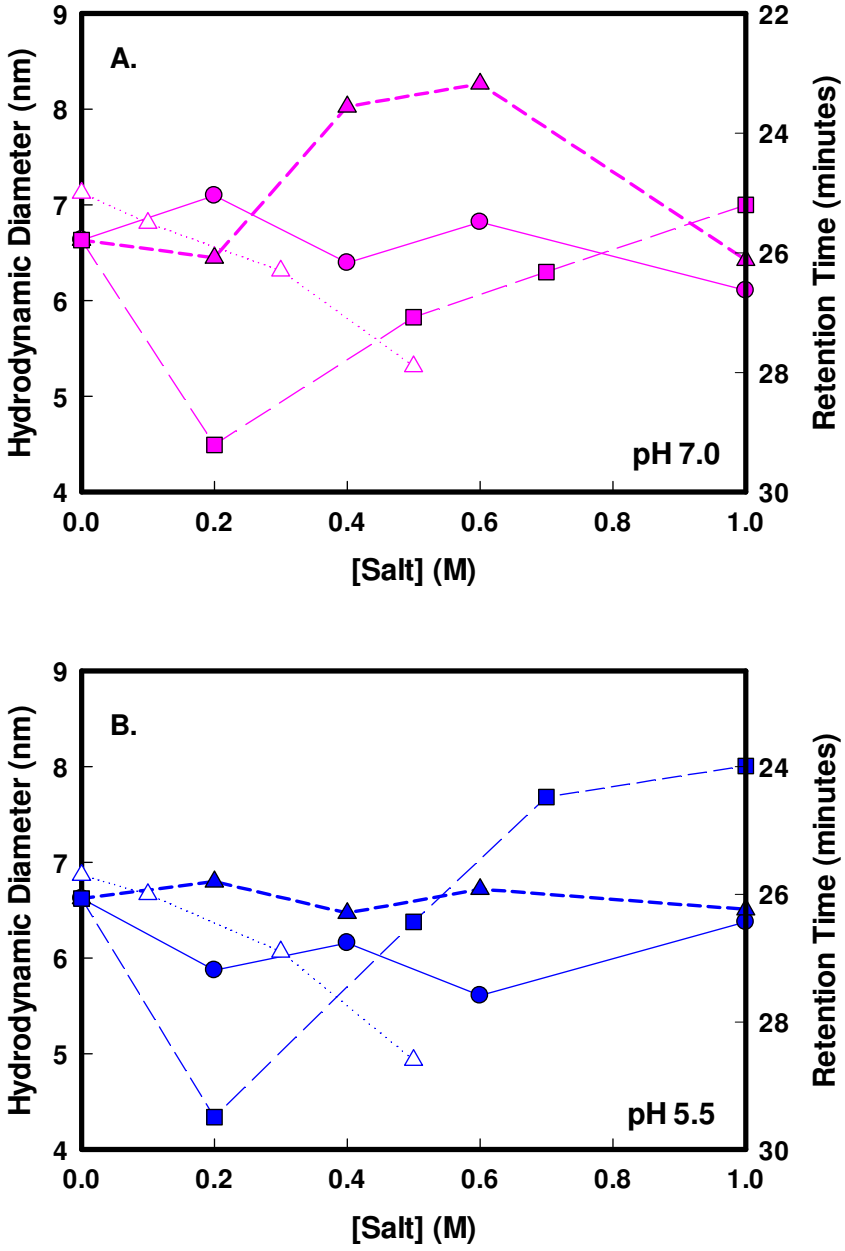


Figure 26: Salt dependence of the hydrodynamic volume occupied by CLIC1 using SEC-HPLC and DLS as probes

The effect of salt on the size of CLIC1 at pH 7.0 (pink) **(A)** and pH 5.5 (blue) **(B)**. The retention time taken to elute 5 µM CLIC1 off the size exclusion column (△) is shown as a function of sodium sulphate concentration. The HPLC buffer used in all cases was 0.1 M Na_2HPO_4; 0.05% NaN_3 containing various amounts of Na_2SO_4 (0 M – 0.5 M). The signal was measured by evaluating the absorbance at 280 nm. The DLS measurements were performed on 5 µM CLIC1 in the presence of 0 – 1 M NaCl (●), NaF (■) and Na_2SO_4 (▲) at 20°C

Quaternary structure

The elution of CLIC1 off the size exclusion column was recorded at both pH 7.0 and pH 5.5 in the presence of HPLC buffers containing increasing concentrations of Na_2SO_4 (0 M - 0.5 M). The results were compared with the hydrodynamic size of the protein obtained from DLS measurements. Here 0 - 1 M NaCl, NaF and Na_2SO_4 were used (Figure 26).

The results from SEC-HPLC and DLS do not complement each other. The protein takes longer to elute off the size exclusion column the higher the concentration of sodium sulphate in the solution. The protein thus appears to be unusually large in the absence of the salt and it only seems to be the correct size when in the presence of 0.5 M Na_2SO_4.

DLS, on the other hand, reports the opposite effect where in the absence of salt the hydrodynamic diameter of CLIC1 is closest to that of a 27 kDa protein and when in the presence of increasing concentrations of Na_2SO_4 the hydrodynamic diameter of CLIC1 at pH 7.0 actually increases. A similar effect was observed with DLS when the protein was in the presence of increasing concentrations of NaF at both pH 7.0 and pH 5.5. NaCl however, did not appear to have any effect on the hydrodynamic diameter of CLIC1. Na_2SO_4 also did not affect the hydrodynamic diameter of the protein when at pH 5.5 and the change observed at pH 7.0 is on a smaller scale than the HPLC results. The HPLC results are therefore likely erroneous due to the anomalous behaviour of the protein on this the column, thus explaining the discrepancy in the results obtained from these two techniques.

3.2.3. Effect of Temperature on CLIC1 Structure

Melting curve

The thermal unfolding of CLIC1 at pH 7.0 and pH 5.5 was monitored using circular dichroism ellipticity at 222 nm (E_{222}) and the hydrodynamic diameter

of the protein as probes (Figure 27). At pH 7.0 CLIC1 still retains a high proportion of secondary structure at temperatures as high as 100°C! This secondary structure is considerably altered from the structure at 20°C, however (Figure 28). Furthermore, this alteration to the structure induced by high temperatures is irreversible upon cooling. The T_m for the thermal unfolding of the secondary structure of CLIC1 at pH 7.0 is 57°C while at pH 5.5 it is 51.5°C. At pH 5.5 the protein loses all its negative ellipticity at 58°C. These high temperatures cause CLIC1 to precipitate at pH 5.5 however, and insoluble aggregates were often visible in the cuvette after the protein was exposed to temperatures above 60°C. It is not surprising, therefore, that the thermal unfolding of CLIC1 at pH 5.5 is also irreversible upon cooling.

The thermal unfolding curve of CLIC1 monitored with DLS at pH 7.0 is superimposable with the circular dichroism-monitored unfolding curve (Figure 27). This implies that the secondary structure of this protein unfolds simultaneously with its hydrodynamic volume when exposed to high temperatures at this pH. Unlike the E_{222}-monitored curve, the DLS-monitored curve has no plateau up to 65°C. This is because the high protein concentrations required for adequate light scattering data cause aggregation in the already unstable thermally unfolded state of the protein which causes the measured hydrodynamic diameter to increase incessantly.

At pH 5.5, the light scattering technique is even less successful in monitoring the thermal unfolding of CLIC1. The protein is already destabilised by the low pH and the introduction of high temperatures causes the protein to aggregate under the high protein concentrations required for the DLS technique. It can be seen in Figure 27 that at pH 5.5 CLIC1 remains in its native state up to 27°C. Thereafter its quaternary structure changes and eventually it simply forms larger and larger aggregated structures that do not follow the same unfolding trend as the circular dichroism-monitored unfolding curve at this pH.

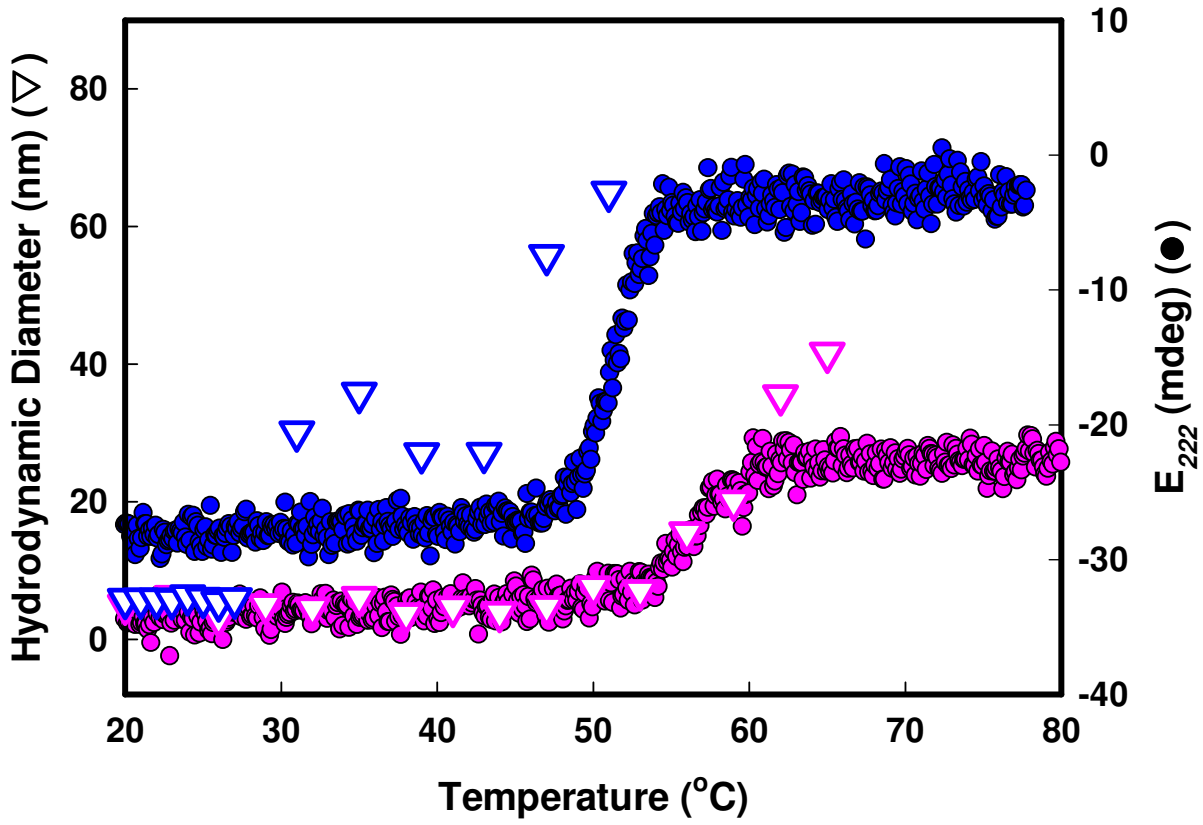


Figure 27: Melting curve of CLIC1 at pH 7.0 and pH 5.5 using circular dichroism and dynamic light scattering as probes

Thermal unfolding of CLIC1 at pH 7.0 (pink) and pH 5.5 (blue) using ellipticity at 222 nm (●) and hydrodynamic diameter (▽) as probes. The T_m for unfolding of the secondary structure at pH 5.5 is 51.5°C while at pH 7.0 it is 57°C. Temperatures as high as 80°C do not cause the protein to form a complete random coil at pH 7.0 and it still retains a high degree of secondary structure at this temperature. The thermal unfolding transition of CLIC1 at pH 7.0 as monitored by DLS overlays well with the CD-monitored unfolding transition. At pH 5.5 the protein aggregates when above 30°C as measured by DLS. All data were collected on 5 µM CLIC1 (circular dichroism) or on 10 µM CLIC1 (DLS) in the presence of 50 mM Na_2HPO_4; 1 mM DTT and 0.02% NaN_3.

Secondary structure

Far-UV circular dichroism spectra were recorded and compared at 20^{o}C, the physiologically relevant 37^{o}C and at 80^{o}C (Figure 28). At pH 7.0 an increase in the temperature from 20^{o}C to 37^{o}C results in a decrease in the α-helical nature of the secondary structure of CLIC1 by ~13% and the secondary structure of the native state at pH 7.0 / 37^{o}C bears a resemblance to that at pH 5.5 / 20^{o}C.

At pH 5.5, an increase in the temperature to physiological body temperature causes a further reduction in the α-helical secondary structure by 12% from that present at pH 5.5 / 20^{o}C. The shape of the spectrum is not significantly altered, however.

Interestingly, exposing the protein to temperatures as high as 80^{o}C did not destroy all the secondary structure present at pH 7.0 and, although the spectrum no longer displays the characteristic minimum at 222 nm, there is certainly a trough at 206 nm indicating that a degree of secondary structure still remains in this protein, even when exposed to disruptive high temperatures. This spectrum is not as a result of light scattering masking the true circular dichroism spectrum because the dynode voltage reading is below 600 mV at 206 nm and furthermore the ellipticity at 195 nm is approximately double the value at 208 nm which is correct. At pH 5.5, temperatures above 60^{o}C cause excessive aggregation. The insoluble aggregates thus formed have no secondary structure as observed by far-UV circular dichroism (Figure 28).

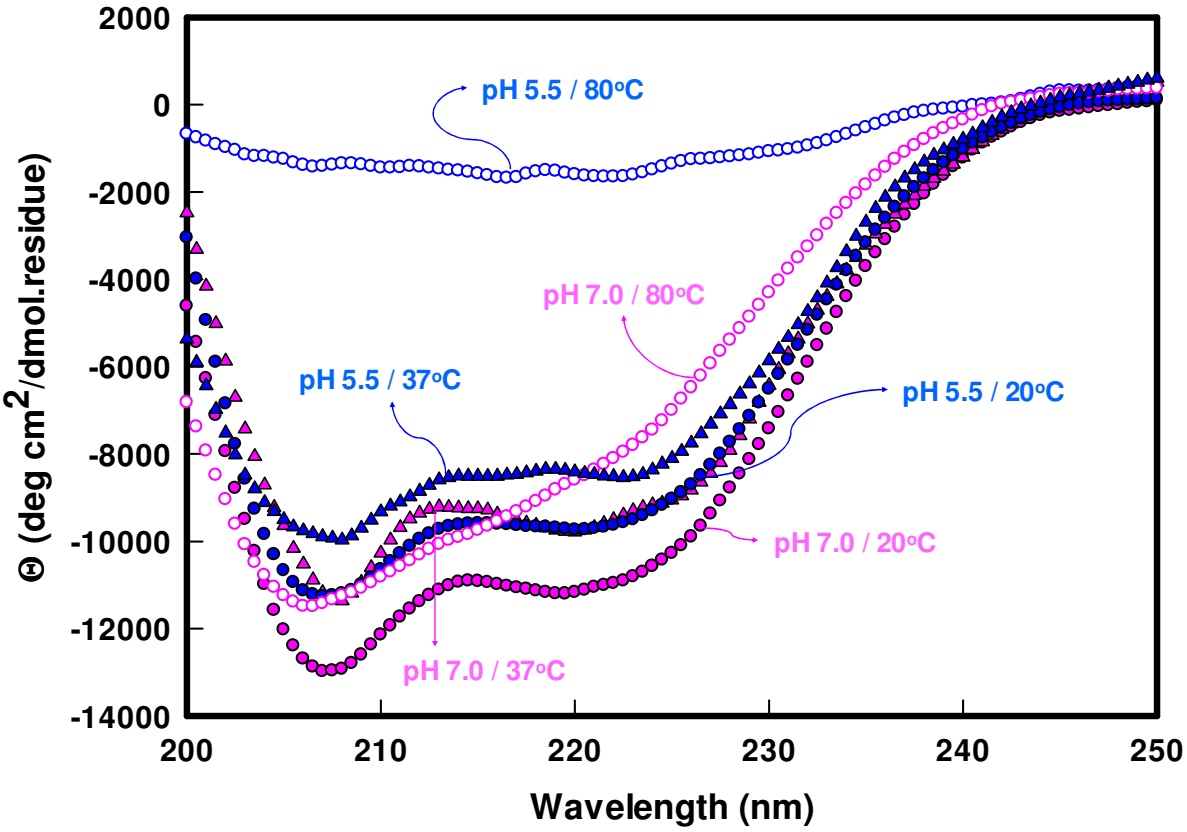


Figure 28: The effect of temperature on the circular dichroism spectra at pH 7.0 and pH 5.5

Far-UV circular dichroism spectra of 5 µM CLIC1 (5 mM Na_2HPO_4; 0.1 mM DTT) at pH 7.0 (pink) and pH 5.5 (blue). Spectra were recorded at 20°C (●); at 37°C (▲) and at 80°C (○). At pH 7.0 / 37°C the secondary structure is similar to that of the protein at pH 5.5 / 20°C. High temperatures result in reduced secondary structure at both pHs. There is a huge difference between the circular dichroism spectra recorded at pH 7.0 / 80°C and at pH 5.5 / 80°C. Spectra were smoothed using the negative exponential method.

Tertiary structure

The fluorescence spectra display reduced emission intensity upon increasing the temperature from 20°C to 37°C at both pH 7.0 and pH 5.5 (Figure 29). This is a normal occurrence upon increasing the temperature because the mobility of the chromophores and fast quenching processes of certain molecules is increased leading to relaxation of the excited state (Lakowicz, 1999; Mauring *et al.*, 2005). What is far more interesting is that there is a slight blue shift in the λ_{max} from ~345 nm at pH 5.5 / 20°C to ~343 nm at pH 5.5 / 37°C. This is not observed at pH 7.0 at either 20°C or 37°C.

3.2.4. Effect of Non - Reducing Conditions on CLIC1 Structure

Secondary structure

Since CLIC1 is affected differently by oxidising and reducing conditions (Singh and Ashley, 2006) and is known to form a dimer when oxidised with hydrogen peroxide (Littler *et al.* 2004), the protein was studied in the presence and absence of 1 mM DTT to see whether there is a difference in the structure of CLIC1 under reducing and non-reducing conditions. pH does not appear to have an effect on the secondary structure of the protein when under non-reducing conditions (Figure 30). The lack of reducing conditions does result in a decrease in the secondary structure of the native state from that at pH 7.0 and pH 5.5 when in the presence of reducing agent, however.

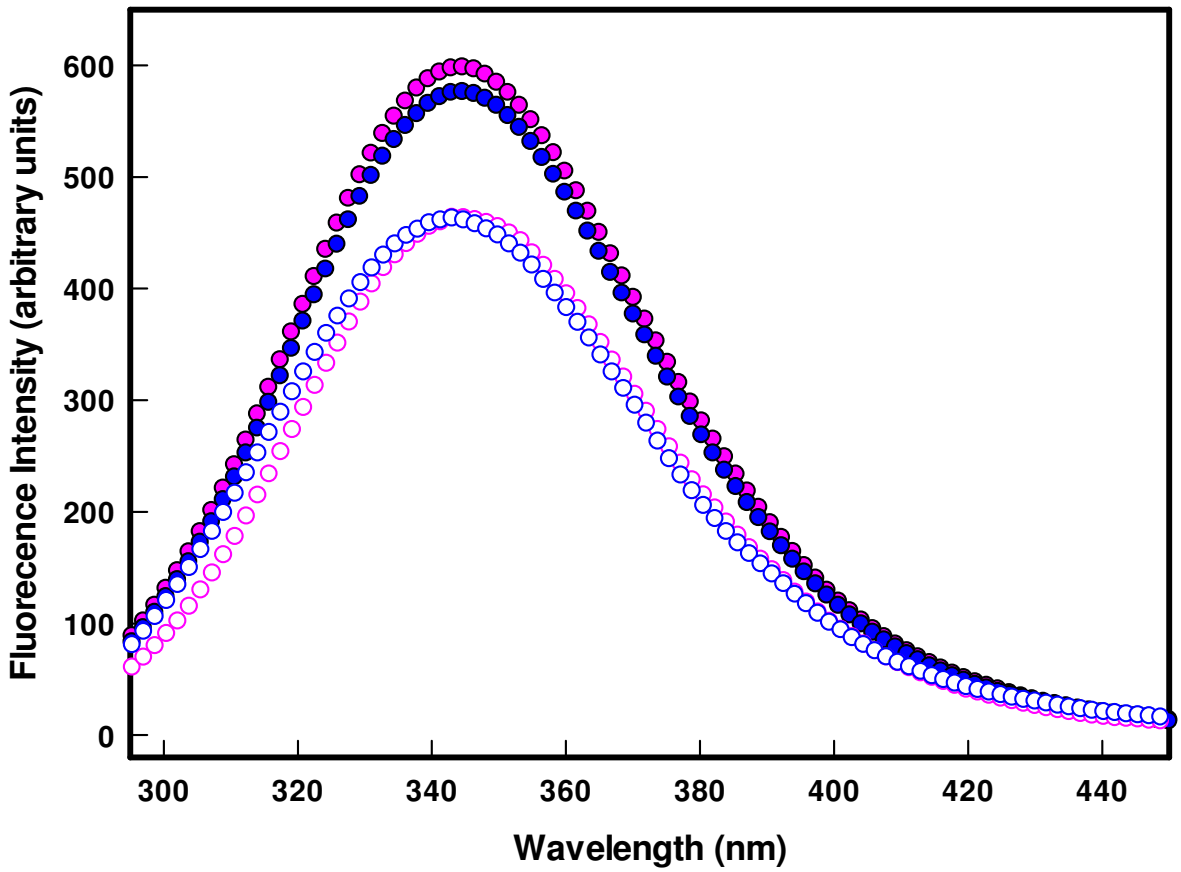


Figure 29: Fluorescence spectra at 20°C and 37°C at pH 7.0 and pH 5.5

Fluorescence spectra of 5 µM CLIC1 (5 mM Na_2HPO_4; 0.1 mM DTT) at pH 7.0 (pink) and pH 5.5 (blue) recorded at 20°C (●) and at 37°C (○). The increase in temperature results in a decrease in the fluorescence emission. Note that the spectrum at pH 5.5 / 37°C has a blue shifted emission peak compared to the other spectra.

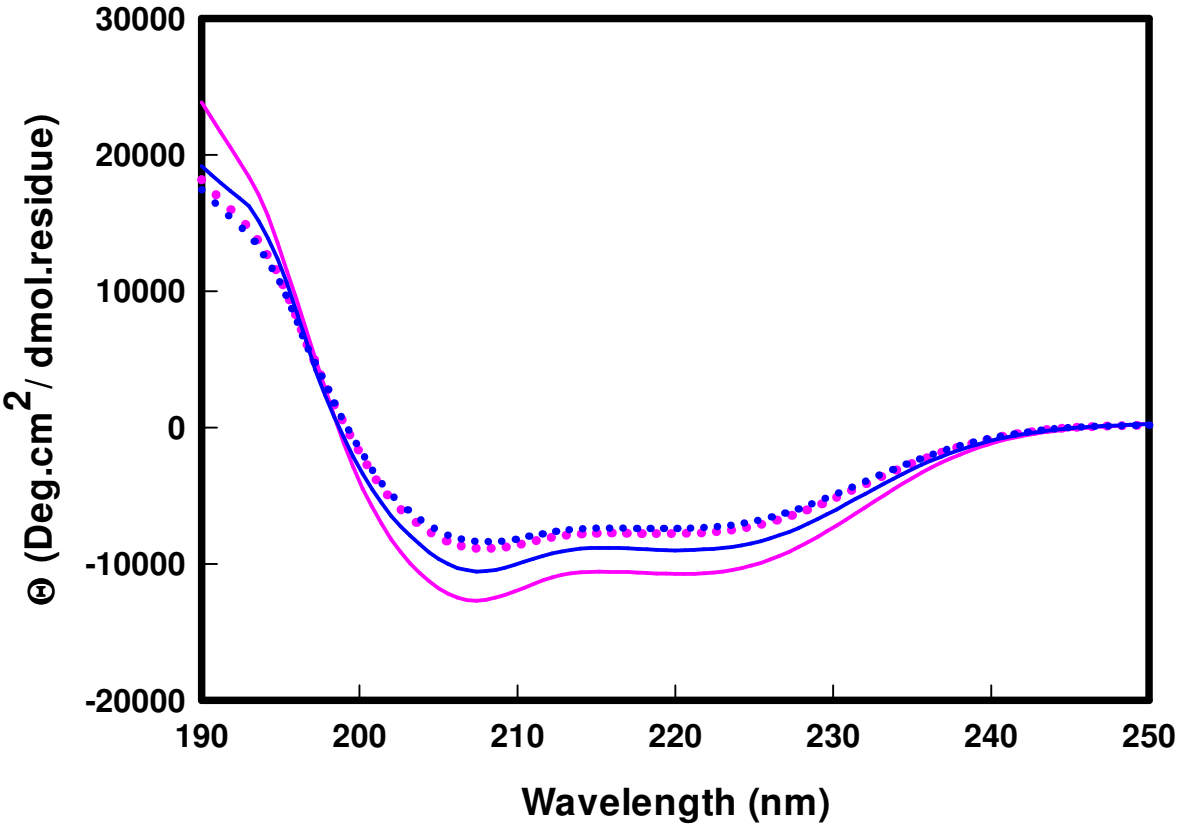


Figure 30: Effect of non-reducing conditions on circular dichroism spectra at pH 7.0 and pH 5.5

Circular dichroism spectra of 5 µM CLIC1 under reducing conditions (1 mM DTT) (solid line) and under non-reducing conditions (no DTT) (dotted line) at pH 7.0 (pink) and pH 5.5 (blue). Non-reducing conditions result in a decrease in the secondary structure at both pH 7.0 and pH 5.5. The spectra were recorded at 20°C and smoothed using the negative exponential method.

Tertiary structure

When under non-reducing conditions the emission intensity is quenched at pH 7.0 and pH 5.5 compared to when the protein is in the presence of 1 mM DTT (Figure 31). This is likely due to the formation of at least one disulphide bond since the disulphide bond is known quencher of tryptophan fluorescence (Sakai *et al.,* 2000). The signal is even further quenched when 2 mM GSSG is added to the protein under non-reducing conditions. This quenching of Trp35 suggests that it might be in close proximity to the disulphide bond. Could Cys24 be involved? A more likely explanation for the drop in fluorescence intensity is quenching due to solvent, however. There is no pH dependence of the fluorescence spectra under non-reducing conditions. Nevertheless, it is interesting to note that when under non-reducing conditions the λ_{max} of the native state is blue shifted and the spectra peak at ~341 nm compared to at ~345 nm when under reducing conditions (Figure 20). This implies burial of the single tryptophan residue in a non-polar environment. Therefore the tertiary structure of CLIC1 is, indeed, affected by the absence of reducing agent.

Quaternary structure

Study of the hydrodynamic diameter of 50 μM CLIC1 under reducing and non-reducing conditions at pH 7.0 and pH 5.5 using DLS reveals that the protein is more compact when under reducing conditions (~6 nm *vs.* ~8 nm). Furthermore the polydispersity index is increased under non-reducing conditions, which implies an increase in the number of species present in the solution (Figure 32). This could be because a number of different disulphide-bonded species may be present in the solution. Is this sufficient evidence to support the observation by Littler *et al.,* (2004) that CLIC1 forms a dimer under oxidising conditions despite the fact that in this instance the protein was only exposed to non-reducing conditions and not to oxidising conditions?

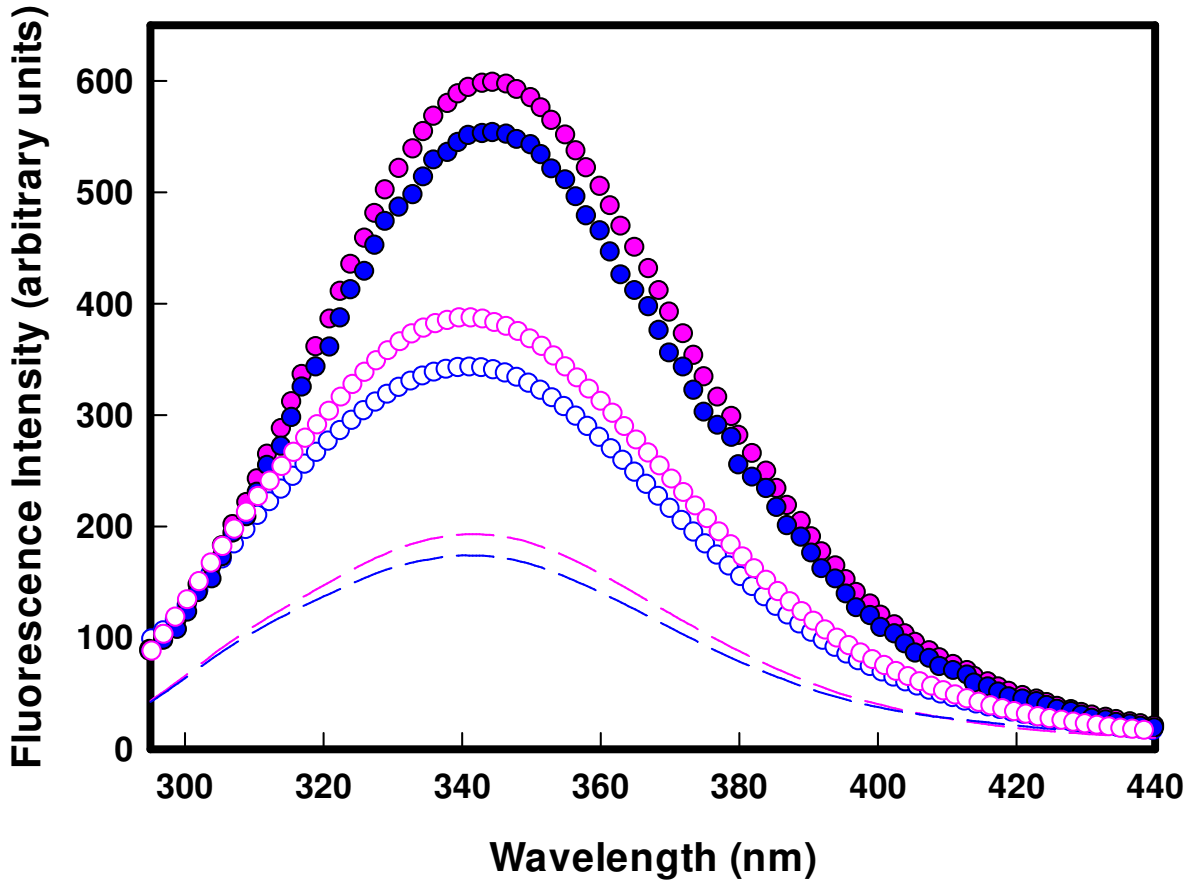


Figure 31: Effect of non-reducing conditions on the fluorescence spectra of CLIC1 at pH 7.0 and pH 5.5

Fluorescence emission spectra of 5 µM CLIC1 when under reducing (1 mM DTT) (●) and non-reducing (no DTT) (○) conditions. Spectra were also recorded in the presence of 2 mM GSSG (dashed lines). Spectra were recorded at pH 7.0 (pink) and pH 5.5 (blue) by exciting the protein at 280 nm at 20°C. The λ_{max} is blue shifted under non-reducing conditions compared to under reducing conditions.

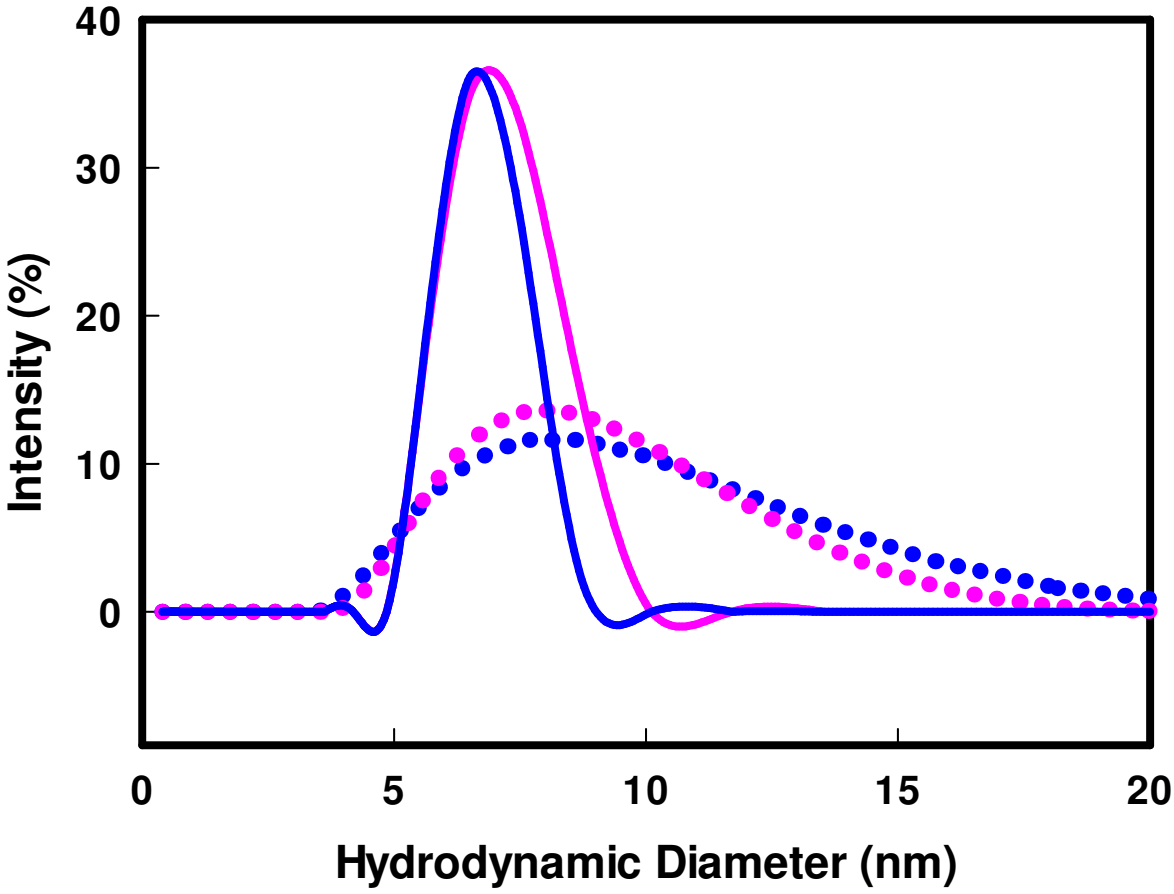


Figure 32: Effect of redox conditions on the hydrodynamic size of CLIC1

DLS measurements of 50 µM CLIC1 at pH 7.0 (pink) and pH 5.5 (blue) in the presence (solid) and absence (dotted) of 1 mM DTT. The hydrodynamic diameter increases from ~6 nm in the presence of reducing conditions to ~8 nm in the absence of reducing conditions and the polydispersity index increases from 25% in the presence of DTT to 45% in the absence of reducing conditions. Experiments were conducted at 15^{o}C.

Exposed cysteines

DTNB was used in order to determine the number of cysteines that are exposed to the solvent (and hence will bind the DTNB) at pH 7.0. In the denatured state, 12 μM DTNB bound to the protein which corresponds to six exposed thiols per monomer which is the number of cysteines in the CLIC1 sequence. Therefore when in the denatured state the protein is unfolded and all the cysteines are exposed to the solvent. In the native state four cysteines are exposed when under reducing conditions which is consistent with the crystal structure. When in the presence of GSSG only three cysteines are exposed in both the native and the denatured state implying the presence of disulphide bonds when the protein is not under reducing conditions. These disulphide bonds could be a result of two situations: 1. CLIC1 could be oligomerising by forming inter- or intra-molecular disulphide bonds when in the presence of this oxidising agent. 2. The disulphide bonds that were detected could simply be mixed disulphides formed between the protein and the GSSG.

3.2.5. Effect of Change in Polarity of Solvent on the Structure of CLIC1

Secondary structure

The dielectric constant at the membrane surface is considerably lower than that of water. In order to establish whether a lower polarity of the solvent will have an effect on the protein structure, CLIC1 was incubated in the presence of 0% to 25% (v/v) of the fluorinated alcohol, trifluoroethanol (TFE). TFE results in an increase in the α-helical secondary structure of the protein by at most 21% at pH 7.0 when in the presence of 10% TFE and by at most 28% at pH 5.5 when in the presence of 6% TFE (Figure 33). Higher concentrations of TFE caused the protein to aggregate. At pH 7.0 CLIC1 seems to get trapped in a possibly aggregated state that retains a degree of secondary structure. Increasing the concentration of TFE from 14% to 25% does not alter the structure of this "aggregated" state of the protein. At pH 5.5 the protein adopts

this same "aggregated" conformation at 10% TFE but higher concentrations (12 – 25%) result in complete destruction of the secondary structure and insoluble aggregates are certainly present. At moderately low pH, low concentrations of alcohol (below 25%) will mimic the membrane environment (Bychkova *et al.,* 1996) and it is interesting that particularly at pH 5.5, CLIC1 undergoes an increase in α-helical secondary structure when under these conditions.

Tertiary structure

The fluorescence spectra in the presence of TFE (Figure 34) show that when the protein is in the presence of 6% TFE and shows enhanced secondary structure there is not a significant change in the microenvironment of the tryptophan residue at either pH 7.0 or pH 5.5. However, the aggregated structures in the presence of 12% TFE show quenched fluorescence emission and show a blue shifted λ_{max} to ~340 nm. The Raleigh scatter at 280 nm is high under these conditions due to the scatter of light caused by the aggregates.

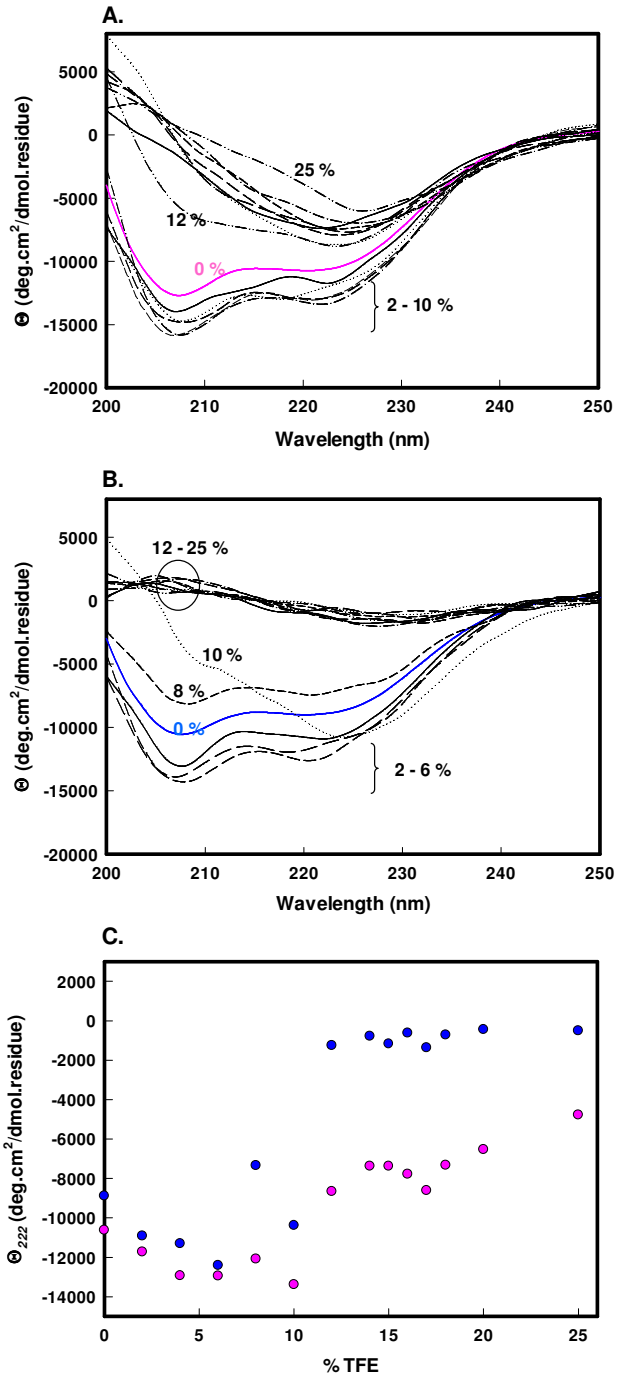


Figure 33: Circular dichroism spectra of CLIC1 at pH 7.0 and pH 5.5 in the presence of increasing concentrations of TFE

Circular dichroism spectra of 5 µM CLIC1 at pH 7.0 **(A)** and pH 5.5 **(B)** recorded in the presence of 0 to 25% (v/v) TFE. Spectra were recorded at 20°C and are smoothed using the negative exponential method. The mean residue ellipticity at 222 nm as a function of TFE concentration is shown in **(C)** for CLIC1 at pH 7.0 (pink) and at pH 5.5 (blue).

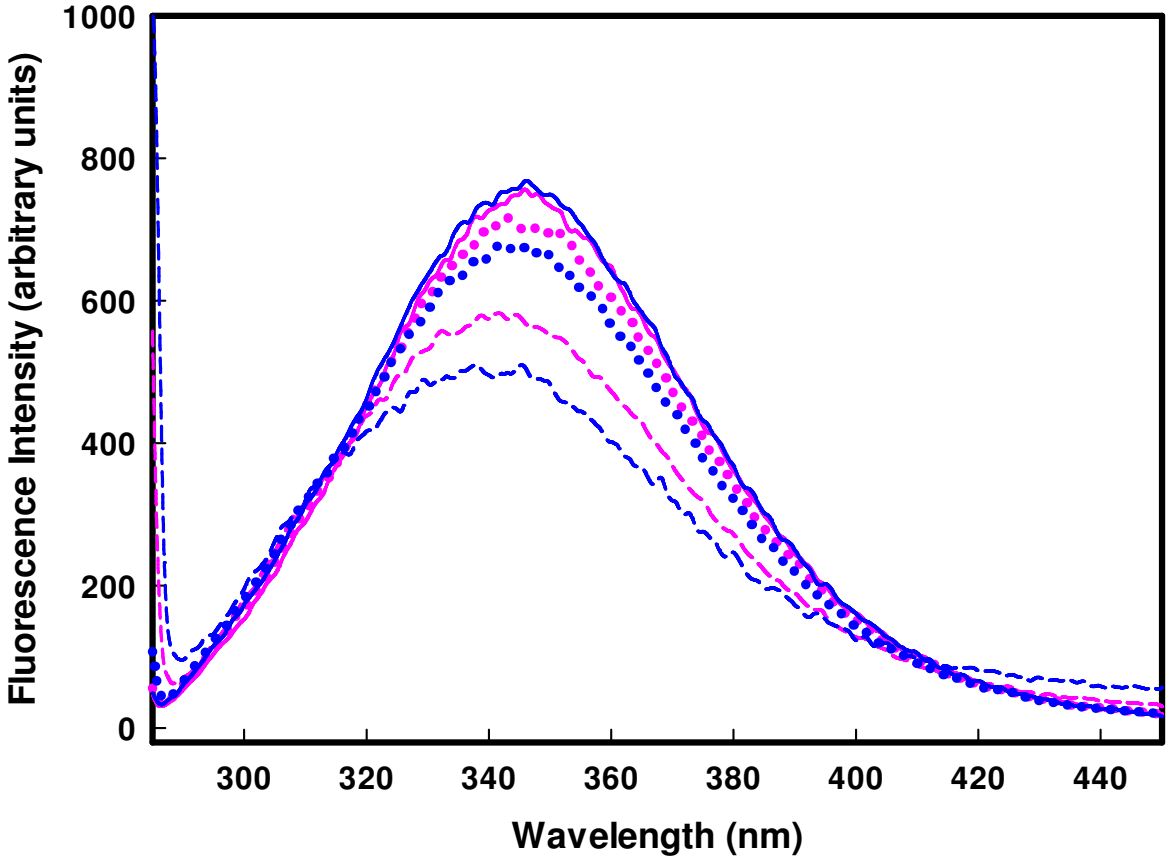


Figure 34: Fluorescence spectra of CLIC1 in the presence of TFE

Fluorescence of 5 μM CLIC1 at pH 7.0 (pink) and pH 5.5 (blue) in the presence of 0% (solid line); 6% (dotted line) and 12% (dashed line) (v/v) TFE. Spectra were recorded by exciting the protein at 280 nm at 20^{o}C.

3.3. Urea – Induced Equilibrium Unfolding of CLIC1

3.3.1. Reversibility Studies

In order for the unfolding transitions to be analysed in terms of their thermodynamic parameters, the reversibility of unfolding of the protein has to be established (Pace, 1986a). The protein was shown to exhibit 90% - 105% recovery of secondary and tertiary structure over the pH range of 4.0 to 8.2 (Figure 35 A and B).

The recovery of the secondary and tertiary structure of the protein after denaturation in 8 M urea was monitored at a urea concentration ranging from 0 M to 8 M (Figure 35 C). The native structure of CLIC1 is approximately 100% recoverable at both pH 7.0 and pH 5.5 using both circular dichroism and fluorescence as probes except for at pH 5.5 in the presence of 3 M urea where there is only a 70% recovery of secondary structure. The refolding curves are superimposable with the unfolding curves at both pH 7.0 and pH 5.5 when using both circular dichroism and fluorescence as probes (Figure 35 D). There is no evidence of hysteresis in the unfolding/refolding transitions of CLIC1.

At pH 5.5, the conditions governing the reversibility of the reaction were found to be more stringent than at pH 7.0. The extent of reversibility of the protein decreased with the time the protein was exposed to denaturant before refolding. Thus although the process was found to be completely reversible when the unfolded sample was diluted after 30 minutes, if the protein was exposed to denaturant for longer than two hours, the recovery of tertiary and secondary structure was only 70%. Furthermore, if the protein was left in the refolding buffer for longer than 90 minutes, regardless of the length of time to which it was exposed to denaturant, the reversibility was also found to be less than optimal. This result was not observed at pH 7.0. However, a similar effect has been shown with β-lactoglobulin at pH 3.0 (Pace and Tanford, 1968).

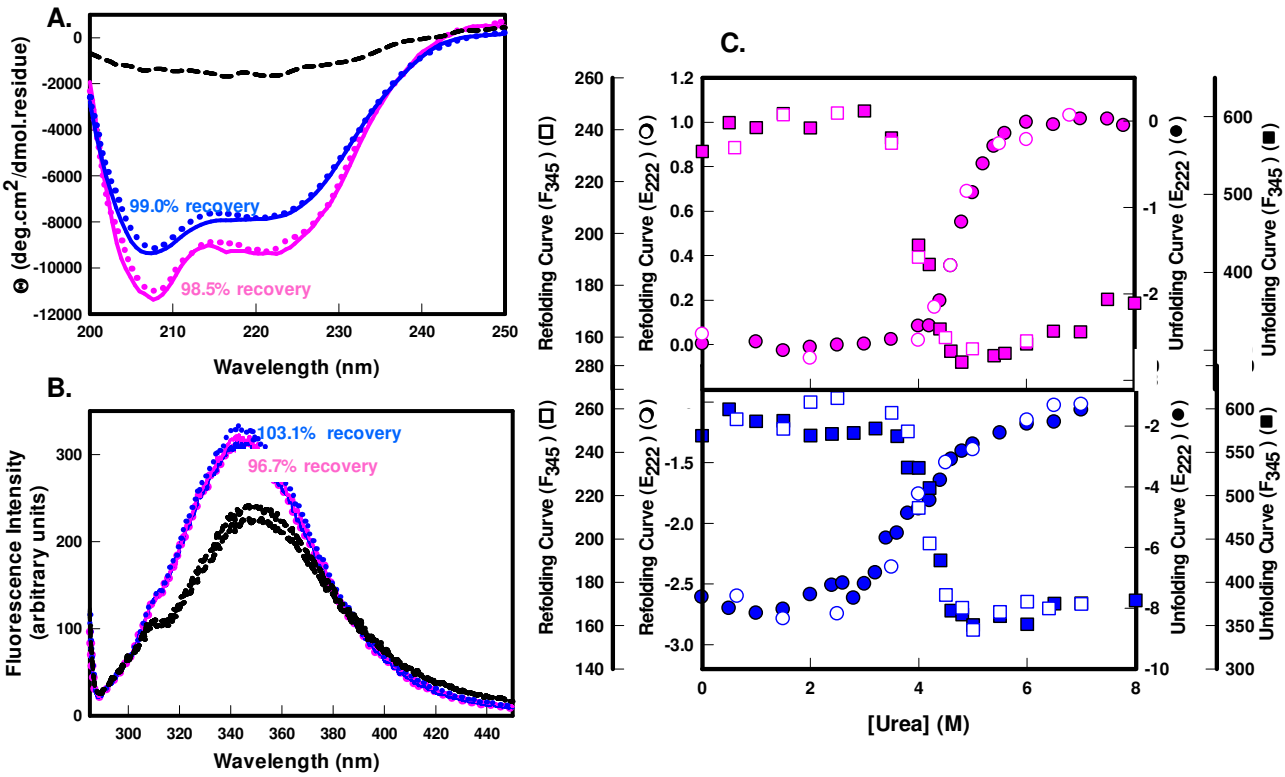


Figure 35: Recovery of secondary and tertiary structure of CLIC1

Recovery of secondary structure **(A)** and tertiary structure **(B)** of CLIC1 at pH 7.0 (pink) and pH 5.5 (blue). Native spectra are shown with a solid line, refolded spectra with a dotted line and denatured spectra are given by a black dashed line. The recovery of the E_{222} value (●) and F_{345} value (□) when CLIC1 is unfolded in the presence of increasing concentrations of urea is shown in **(C)**. The curves at both pH values and using both probes overlay and show no evidence of hysteresis. For the unfolding curves 2 µM CLIC1 was used in all cases.

Since the reversibility of unfolding was confirmed at pH 7.0 and the conditions under which CLIC1 unfolds reversibly were established at pH 5.5, the unfolding curves of CLIC1 at these pH values can be analysed and thermodynamic parameters such as the free energy of unfolding in the absence of denaturant ($\Delta G(H_2O)$) and the *m*-value of unfolding can be obtained from these curves and will give an indication of the stability of CLIC1.

Furthermore all pH-dependent changes were found to be reversible and the protein exhibits the same behaviour (including structure and thermodynamic stability) when returned to pH 7.0 after it has been exposed to a pH of 5.5 as if it had never been exposed to the low pH.

3.3.2. Concentration Dependence Studies

The quaternary structure of CLIC1 is a matter of contention since both SEC-HPLC and light scattering show the hydrodynamic volume occupied by the protein to be larger than expected (Figure 22 and Figure 23). Therefore in order to confirm the monomeric nature of the native state of the protein, the circular dichroism and fluorescence properties measured at the mid-point of the equilibrium unfolding transition were monitored at increasing protein concentrations. It is known that due to the law of mass action, the equilibrium unfolding of dimers and oligomers is concentration-dependent and a shift in the unfolding transition is observed with increasing protein concentration (Stevens *et al.,* 1998; Wallace *et al.,* 1998ab; Perrett *et al.,* 1999; Stevens *et al.,* 2000). Therefore, since monomers show no protein concentration dependence, a comparison of the equilibrium unfolding transitions at increasing concentrations of protein will give an indication as to whether or not the protein is a monomer.

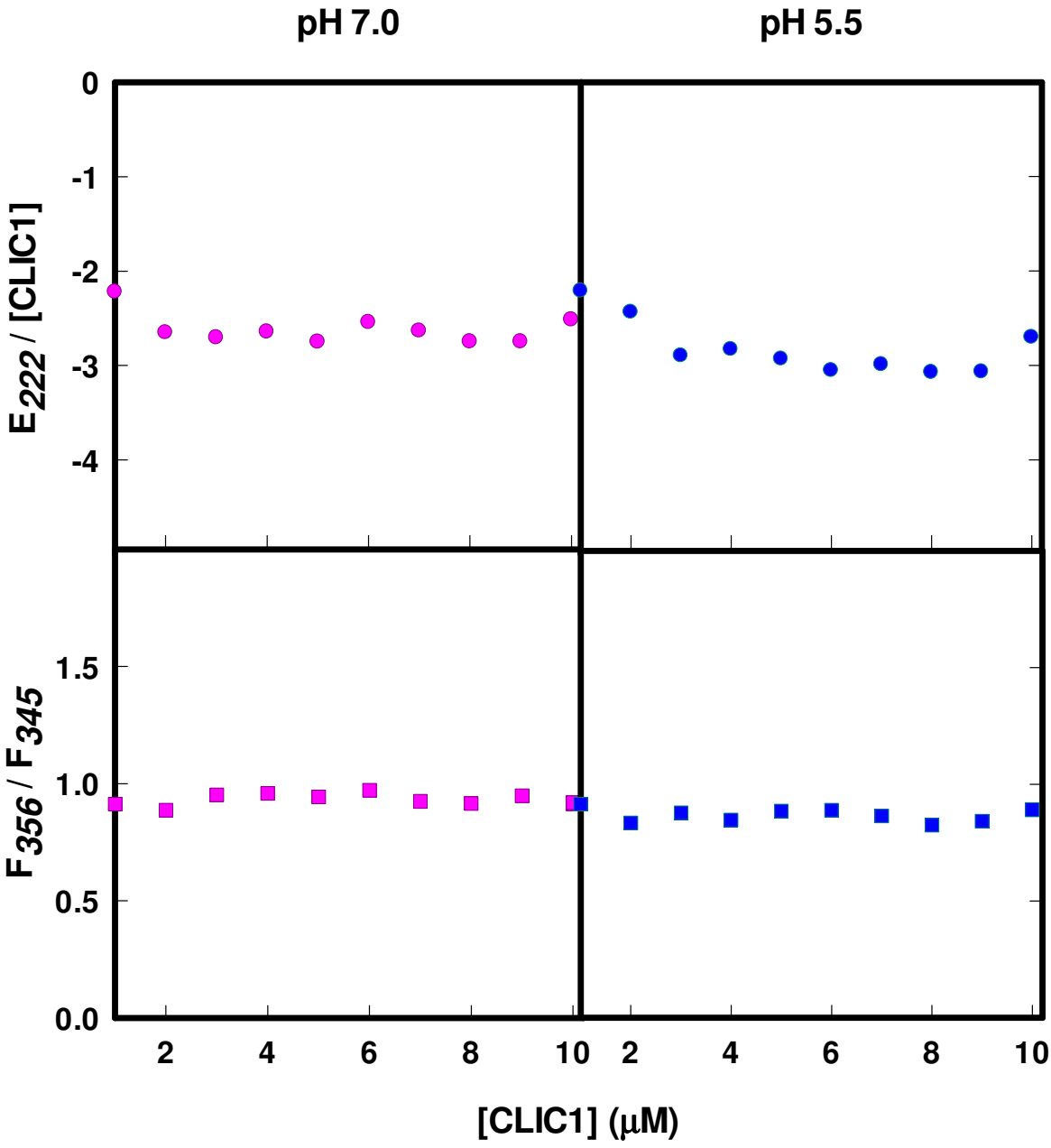


Figure 36: Protein concentration dependence study

The CLIC1 concentration dependence of the midpoint of the equilibrium unfolding transition at both pH 7.0 (pink) and pH 5.5 (blue). The study was conducted at 20°C using both E_{222} (●) and the ratio F_{356} / F_{345} (■) as probes. The concentration of CLIC1 ranged from 1 μM to 10 μM. The buffer used was a 50 mM Na_2HPO_4 containing 0.02% NaN_3; 1 mM DTT and 4.8 M urea at pH 7.0 or 3.5 M urea at pH 5.5.

Under the conditions studied the E_{222} recorded at the mid point of the unfolding and the ratio of the fluorescence emission at the λ_{max} of the denatured state (356 nm) to the λ_{max} of the native state (345 nm) (F_{356} / F_{345}) do not change with increasing protein concentration. CLIC1 is thus monomeric at a 2 μM concentration.

3.3.3. Effect of pH on Stability

Unfolding of secondary structure

Far-UV circular dichroism was used as a probe to monitor the urea-induced equilibrium unfolding of 2 μM CLIC1 at a pH ranging from 4.5 to 8.2 (Figure 37). Although the hydrodynamic volume occupied by CLIC1 is deceptively large for a monomeric globular protein, there are a number of factors that demonstrate that it is monomeric in its native state (see discussion). Therefore monomeric models were used to fit the data (see section 2.2.11). The change in the E_{222} was monitored with increasing urea concentration. At all pH greater than 5.3, the curves were fit to a two-state monomer model (N ⇔ D where N and D represent the native monomer and denatured state respectively) because they show a single transition indicating a highly cooperative loss of secondary structure and no inflection is present to imply a three-state fit. Furthermore, the fits to the two-state model are good; the dependencies of the variables are low and the R^2 values are above 0.98 in all instances. At pH 5.3 and pH 4.5 a small inflection present in the unfolding transition at approximately 4 M urea warrants further attention.

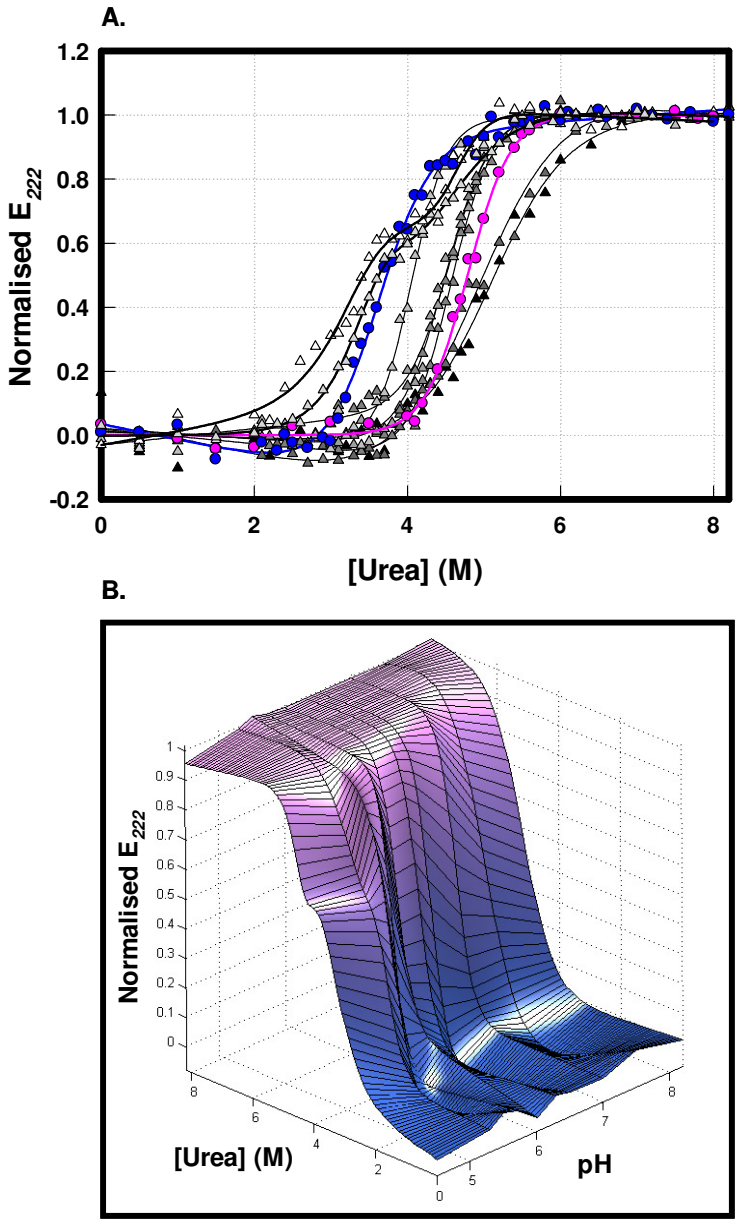


Figure 37: pH dependence of CLIC1 unfolding at equilibrium using circular dichroism as a probe

(A) Equilibrium unfolding curves of 2 µM CLIC1 in the presence of 0 M - 8 M urea at 20°C. Colours range from black to white as the pH drops from 8.2 to 4.5 respectively. For clarity the unfolding curve at pH 7.0 is shown in pink and at pH 5.5 in blue. For comparison purposes the curves have been normalised between 0 and 1 and the solid lines represent the fit to a two- or three-state model using the method described in section 2.2.11. Curves were fitted using the programme Sigmaplot® v8.0. All fits had an R^2 value over 0.98. The buffer used was 50 mM Na_2HPO_4; 0.02% NaN_3 containing 1 mM DTT. **(B)** Surface showing the urea and pH dependence of the ellipticity of CLIC1 at 222 nm. The surface was created using MATLAB v7

The equilibrium unfolding curves in Figure 37 show that the unfolding of the secondary structure of CLIC1 at equilibrium is certainly pH-dependent. The general trend is that the mid-point of the unfolding transition (C_m) shifts to lower urea concentrations as the pH drops. A similar effect was observed with α-toxin (Bortoleto and ward, 1999). The slope of the unfolding curves is steepest at pH 6.0 to pH 7.0 and the unfolding becomes far less cooperative at the extremes of the pH range studied. This is illustrated clearly in Figure 37 B.

Unfolding of tertiary structure

The fluorescence data were plotted in two ways:

1. by observing the change in the maximum fluorescence emission intensity (F_{max}) with increasing urea concentration (Figure 38).
2. by plotting the wavelength at which the spectra peak (λ_{max}) as a function of the urea concentration (Figure 39). This manner of representing the fluorescence data is independent of the absolute fluorescence intensity but cannot be used to quantify thermodynamic parameters because it is not dependent on the protein concentration. Therefore data plotted in this way is used for a qualitative rather than quantitative analysis.

All F_{max}-monitored curves show a single transition and appear to be two-state in nature even at low pH (Figure 38). The fits to the two-state model are good fits in terms of the R^2 and dependencies. However the curves plotted using λ_{max} show a radical change in the unfolding transition at pH 5.5 and below compared to at higher pH (Figure 39 B)! There is a dip in the unfolding curve that starts to manifest at ~3 M urea and is at its maximum at ~3.8 M urea at pH 5.5. This dip is as a result of a blue shift in the λ_{max} from ~345 nm in the native state to ~340 nm when under mild denaturing conditions. It is likely that this deviation from two-state behaviour is due to the presence of an *intermediate species* that is significantly populated along the equilibrium unfolding transition of CLIC1 at low pH and under mild denaturing conditions (3 M – 5

M urea). It can be seen that although present at pH 5.5, the intermediate is far more populated at a pH below 5.5.

Like the secondary structure, unfolding of the tertiary structure of CLIC1 is pH-dependent and, once again the slope of the unfolding transitions is steepest between pH 6.0 and pH 7.0 (Figure 38 B and Figure 39 B). At high pH (above 7.0), the protein is destabilised. However no intermediate is detectable at high pH in the shape of the unfolding transition as is the case at low pH (below pH 5.7).

The Raleigh scatter was measured at 280 nm in order to detect the presence of aggregates that would scatter the light at the excitation wavelength (Figure 40). It is important to note that 280 nm is not ideal to measure Raleigh scatter because the protein absorbs light at this wavelength. Therefore, these experiments were also carried out by measuring the scatter at 390 nm at pH 8.2, pH 7.0 and pH 5.5 when in the presence of ANS (section 3.4). There was no significant difference in the results obtained and therefore the scatter at 280 nm is reported here for the entire pH range studied. There is no significant increase in the Raleigh scatter of the native state at any pH studied nor is any increase in scatter evident along the entire unfolding transition. Thus it can be concluded that light-scattering aggregates are not a concerning factor in this study. It deserves mention here however, that at pH ≤ 4.5 the native protein is, in fact, highly aggregate-prone and great care has to be taken to prevent aggregation at this pH. A similar effect is observed with diphtheria toxin (Blewitt *et al.,* 1985). It could be that under these conditions *in vivo* the protein multimerises and the hydrophobic aggregates that occur *in vitro* are due to the lack of membrane into which the protein could insert.

Unfolding using dynamic light scattering as a probe

The unfolding transitions monitored at pH 7.0 with circular dichroism, fluorescence and DLS as probes are all superimposable (Figure 41). This

implies the simultaneous unfolding of the secondary, tertiary and quaternary structure of CLIC1 at pH 7.0 in a *single, cooperative step* with no intermediates populated at equilibrium.

At pH 5.5, not only are the E_{222}- and F_{max}-monitored curves non-superimposable but the λ_{max} is blue shifted at 3 M – 5 M urea (Figure 39). Over this range of urea concentration, the hydrodynamic diameter of the protein as measured by DLS is fairly constant, indicating the presence of a relatively compact species that is not native-like or denatured-like in size (Figure 41). The DLS-monitored unfolding transition complements the λ_{max}-monitored transition at pH 5.5 and gives further evidence for a stable equilibrium intermediate species populated under these conditions.

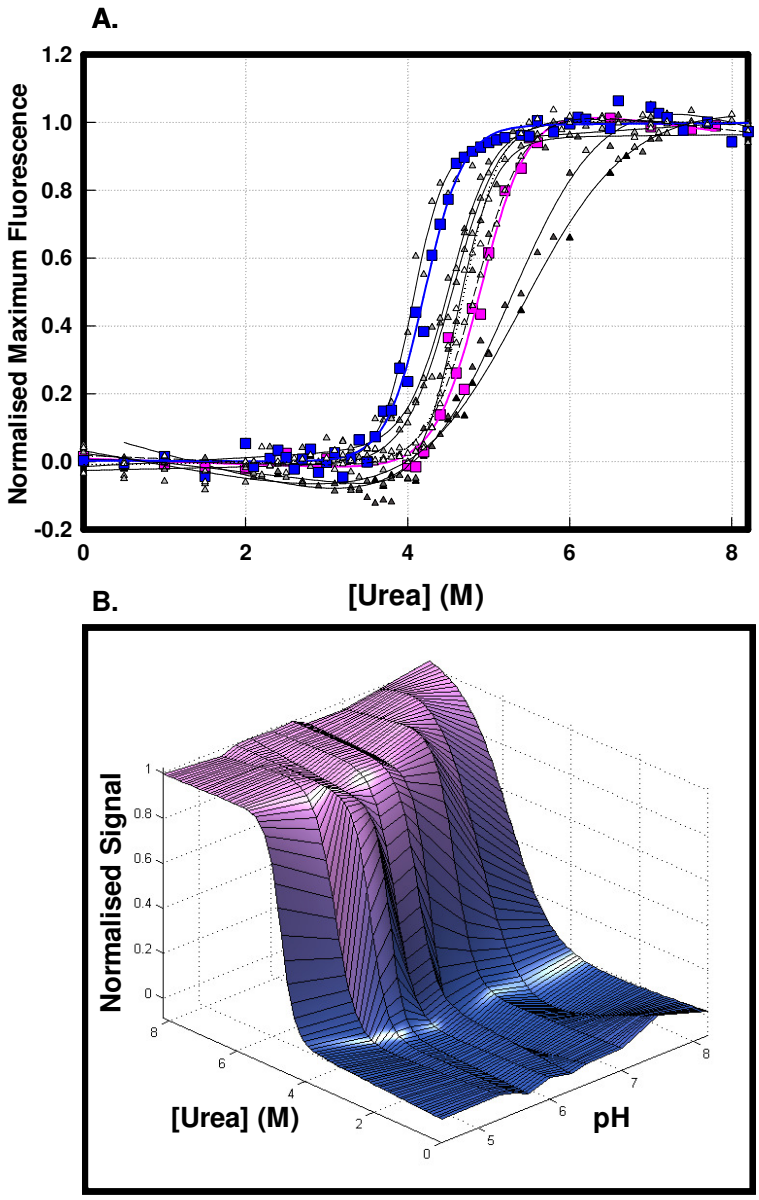


Figure 38: pH dependence of CLIC1 unfolding at equilibrium using the maximum fluorescence emission intensity as a probe

(A) Equilibrium unfolding curves of 2 µM CLIC1 in the presence of 0 M - 8 M urea at 20°C. Colours range from black to white as the pH drops from 8.2 to 4.5 respectively. For clarity the unfolding curve at pH 7.0 is shown in pink and at pH 5.5 in blue. For comparison purposes the curves have been normalised between 0 and 1 and the solid lines represent the fit to a two-state model using the method described in section 2.2.11. All fits have an R^2 value over 0.98. The buffer used was 50 mM Na_2HPO_4; 0.02% NaN_3 containing 1 mM DTT. **(B)** Surface showing the urea and pH dependence of the maximum fluorescence emission intensity (F_{max}) of CLIC1 when excited at 280 nm. The surface was created using MATLAB v7.

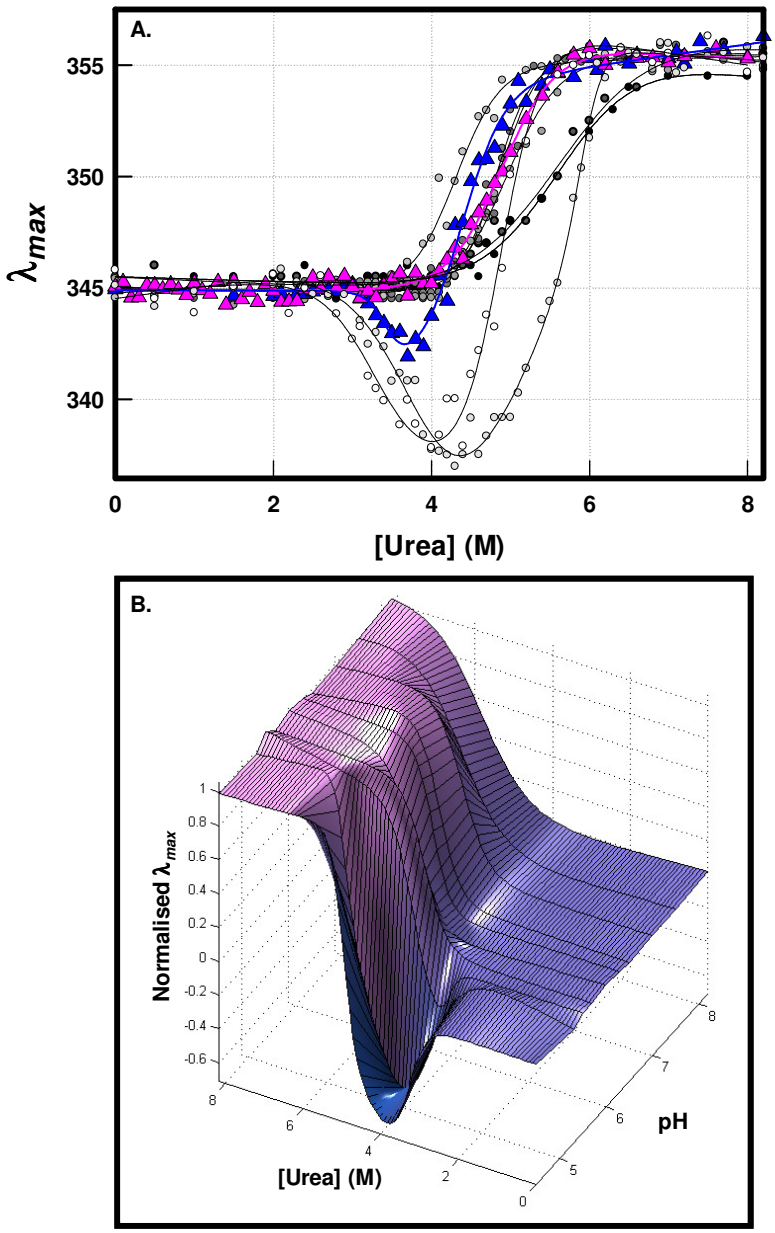


Figure 39: pH dependence of CLIC1 unfolding at equilibrium using the wavelength of maximum emission as a probe

(A) Equilibrium unfolding curves of 2 µM CLIC1 monitored by λ_{max} as a function of urea concentration at 20°C. Colours range from black to white as the pH drops from 8.2 to 4.5 respectively. For clarity the unfolding curve at pH 7.0 is shown in pink and at pH 5.5 in blue. The solid lines represent the fit to a two-state or three-state model using the method described in section 2.2.11. The buffer used was 50 mM Na_2HPO_4; 0.02% NaN_3 containing 1 mM DTT. **(B)** Surface showing the urea and pH dependence of the λ_{max} of CLIC1 when excited at 280 nm. A dip in the unfolding transition is clearly visible at pH below 5.7 at approximately 3 M – 5 M urea. The surface was created using MATLAB v7.

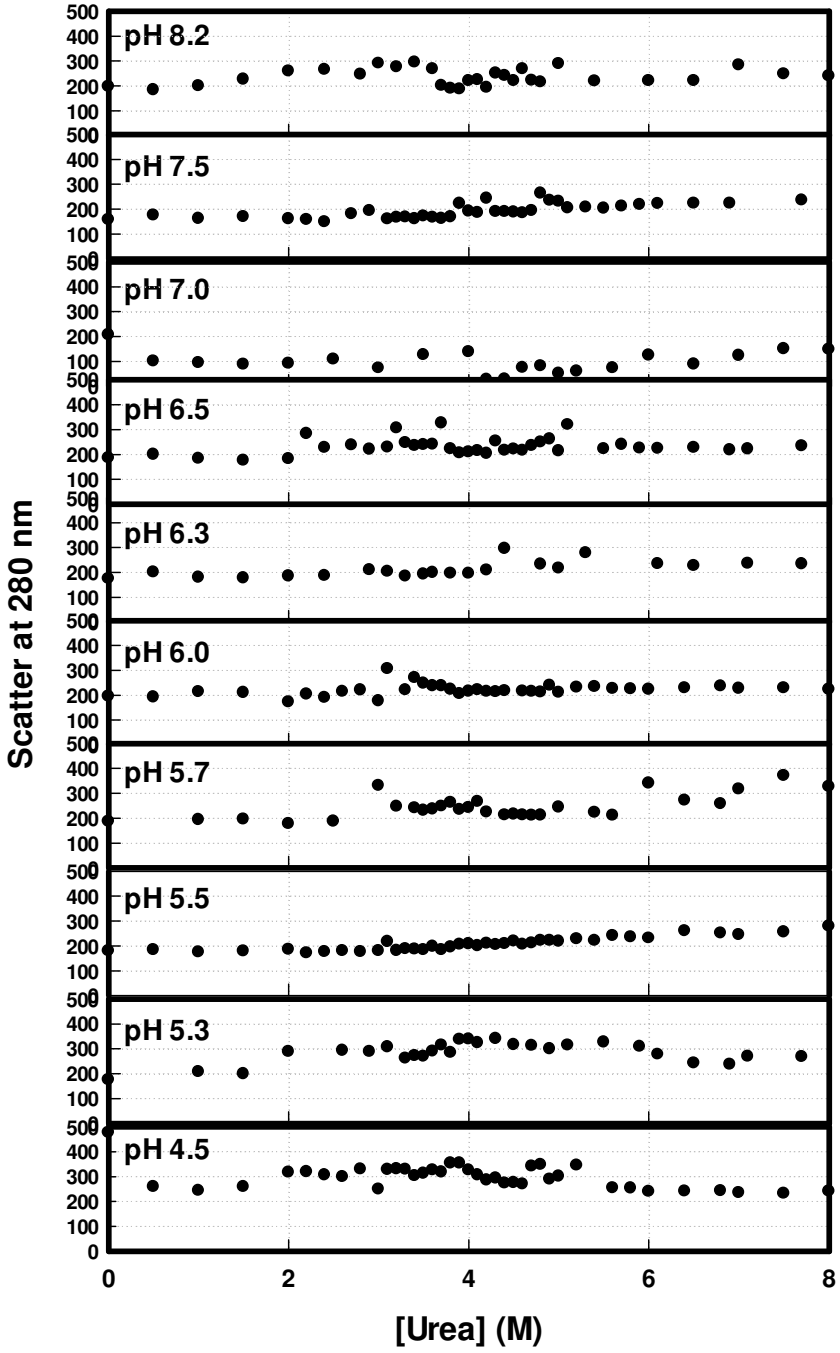


Figure 40: Raleigh scatter to detect aggregation

The scatter produced by 2 μM CLIC1 at 280 nm when excited at 280 nm at pH 8.2 to pH 4.5 in the presence of increasing concentrations of urea. The plots do not show an increase in scatter at any point along the unfolding transition, which implies the absence of aggregation in the pH range studied.

Detecting an intermediate: the three-state model

At pH below 5.7 the CLIC1 equilibrium unfolding transition is visibly no longer two-state. Whitten and Garcia-Moreno, 2000 have listed six criteria to use to check whether a transition follows the two-state model:

1. The ΔG value obtained from different probes and different denaturants must be identical (if this point does not hold, the process is not two-state although the occurrence of this point does not necessarily mean that the transition is two-state in nature).
2. The quality of the two-state fit to the data must be good. Statistical methods such as high R^2 values and low dependencies of the variables are used to confirm a high quality fit.
3. The transitions must be superimposable when monitored with different probes because changes in the different properties of the protein as monitored by the different probes occur simultaneously for a two-state transition.
4. The shape of the unfolding curve must be sigmoidal with no visible shoulder or inflection which would imply a multistate process.
5. Size-exclusion chromatography must not provide evidence for any compact species other than the native state populated during the denaturation process.
6. The ratio of the calorimetric to van't Hoff enthalpies must be close to one.

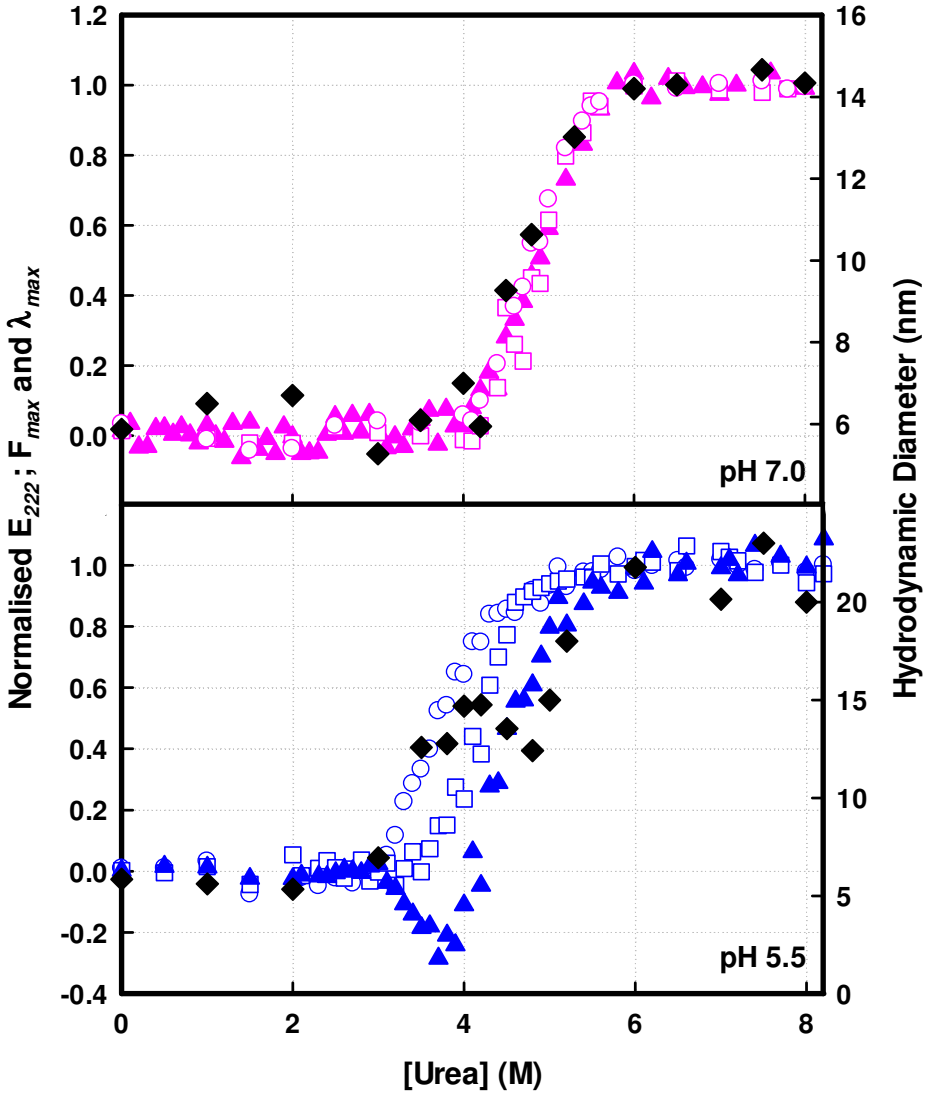


Figure 41: Comparison of equilibrium unfolding curves of CLIC1 at pH 7.0 and pH 5.5 using circular dichroism, fluorescence and light scattering as probes

Urea-induced equilibrium unfolding curves of CLIC1 at pH 7.0 (pink) and pH 5.5 (blue). The unfolding curves monitored with ellipticity at 222 nm (○), fluorescence maximum emission (□) and λ_{max} (▲) are compared with the unfolding curve monitored using dynamic light scattering (◆) as a probe. All curves are superimposable at pH 7.0, indicative of the two-state nature of the unfolding transition. At pH 5.5 the curves are not superimposable and the intermediate is detectable by the shift in the λ_{max} and by the change in hydrodynamic diameter with increasing urea concentrations. All measurements were performed at 20°C on 2 µM CLIC (50 mM Na_2HPO_4; 0.02% NaN_3; 1 mM DTT, pH 7.0 and pH 5.5).

At pH > 5.7 points 1 to 5 above are valid and there is therefore little dispute that CLIC1 follows a two-state denaturation process under these conditions. This is not the case at pH ≤ 5.5, however. Here only point number 2 seems to apply. Although size exclusion chromatography was not used to verify point number 5, dynamic light scattering was used to probe the change in the hydrodynamic diameter of CLIC1 with increasing urea concentrations at pH 7.0 and pH 5.5 (Figure 41). This technique indicates the presence of a compact intermediate species (relative to the denatured state) at pH 5.5 under mild denaturing conditions that is not detectable at pH 7.0. Calorimetric enthalpies (point 6) were not determined in this study. They can be established using a calorimetric profile of heat absorption upon denaturation and the van't Hoff equation:

$$\Delta H = 4RT\left(\frac{\Delta C_p}{Q}\right) \qquad \textbf{22}$$

where ΔC_p is the height of the heat absorption peak at the midpoint of the transition and Q is the area of the peak (Privalov, 1992).

Overview

The unfolding curves of CLIC1 at pH 8.2 to pH 4.5, as monitored with the different spectroscopic probes, are compared in Figure 42. They are divided into four groups based on the shape of the unfolding transition.

At pH 8.2 and pH 7.5 (Group A) the protein is *destabilised*. The $\Delta G(H_2O)$ and *m*-value are reduced (Table 3). There is no dramatic difference in the unfolding curves measured with the different spectroscopic probes (although the E_{222}-monitored curve has a slightly reduced C_m value). The curves are *monophasic* and there is no evidence from these curves of an intermediate present at high pH.

At pH 7.0 to pH 6.5 (Group B) the protein is at its *most stable* with a $\Delta G(H_2O)$ of ~10 kcal/mol and an *m*-value of ~2 kcal/mol/M urea (Table 3) which is in agreement with (albeit slightly lower than) the predicted value of 2.8 kcal/mol/M urea as calculated from the amino acid content of CLIC1 (Myers *et al.*, 1995). The transitions are *monophasic and superimposable* with a C_m of 4.8 M urea.

At pH 6.3 to pH 5.7 (Group C) the *stability has not changed* from that of Group B although there is greater variance depending on the probe used. Also the curve measured using λ_{max} as a probe is *no longer superimposable* with the other curves (slightly higher C_m).

At pH 5.5 to pH 4.5 (Group D) the curves measured by the different probes are *no longer superimposable* and an *intermediate species is clearly detectable* under mild denaturing conditions. This intermediate is more highly populated at pH 5.3 and pH 4.5 hence it is even detectable using circular dichroism at these low pH values whereas at pH 5.5 it is not. The unfolding curves are fit to a three-state model; N ⇔ I ⇔ D (where "I" represents the intermediate state). The N → I transition is more stable and the unfolding is more cooperative than that of the I → D transition.

The thermodynamic parameters obtained from unfolding CLIC1 at different pH are compared in Figure 43. The $\Delta G(H_2O)$ and *m*-values follow a similar trend with decreasing pH. They are both low at high pH and then increase at pH 7.0 and remain constant until the unfolding of the protein follows a three-state transition below pH 5.7. Here the parameters measured from F_{max} continue to increase because the transition has been fit to a two-state model and is capturing the N → D conversion rather than distinguishing the intermediate in a three-state model.

The thermodynamic parameters obtained from the three-state fit below pH 5.7 show lower stability and cooperativity since they represent the N → I and I → D transitions which theoretically should add up to the value for the N → D transition. The C_m values decrease proportionally with decreasing pH. This implies that the protein is less stable at lower pH although the high C_m value at pH 8.2 is accompanied by a very low *m*-value and $\Delta G(H_2O)$ and since the C_m value is not always correlated with the structural integrity of the protein (Nishii *et al.,* 1995), CLIC1 is likely destabilised at high pH despite the high C_m value.

The thermodynamic parameters obtained from the unfolding curve of CLIC1 at pH 7.0 (Table 3) are lower than that of Grx2 (215 amino acids), the only other known monomeric member of the GST superfamily. This protein has a $\Delta G(H_2O)$ value of 12.7 ± 1.5 kcal/mol which is 22% greater than that of CLIC1 and a *m*-value of 2.7 ± 0.2 kcal/mol/M urea which is 26% greater than the *m*-value obtained for CLIC1 (Gildenhuys PHD thesis, 2006). This means that the CLIC1 native state is less compact than that of Grx2.

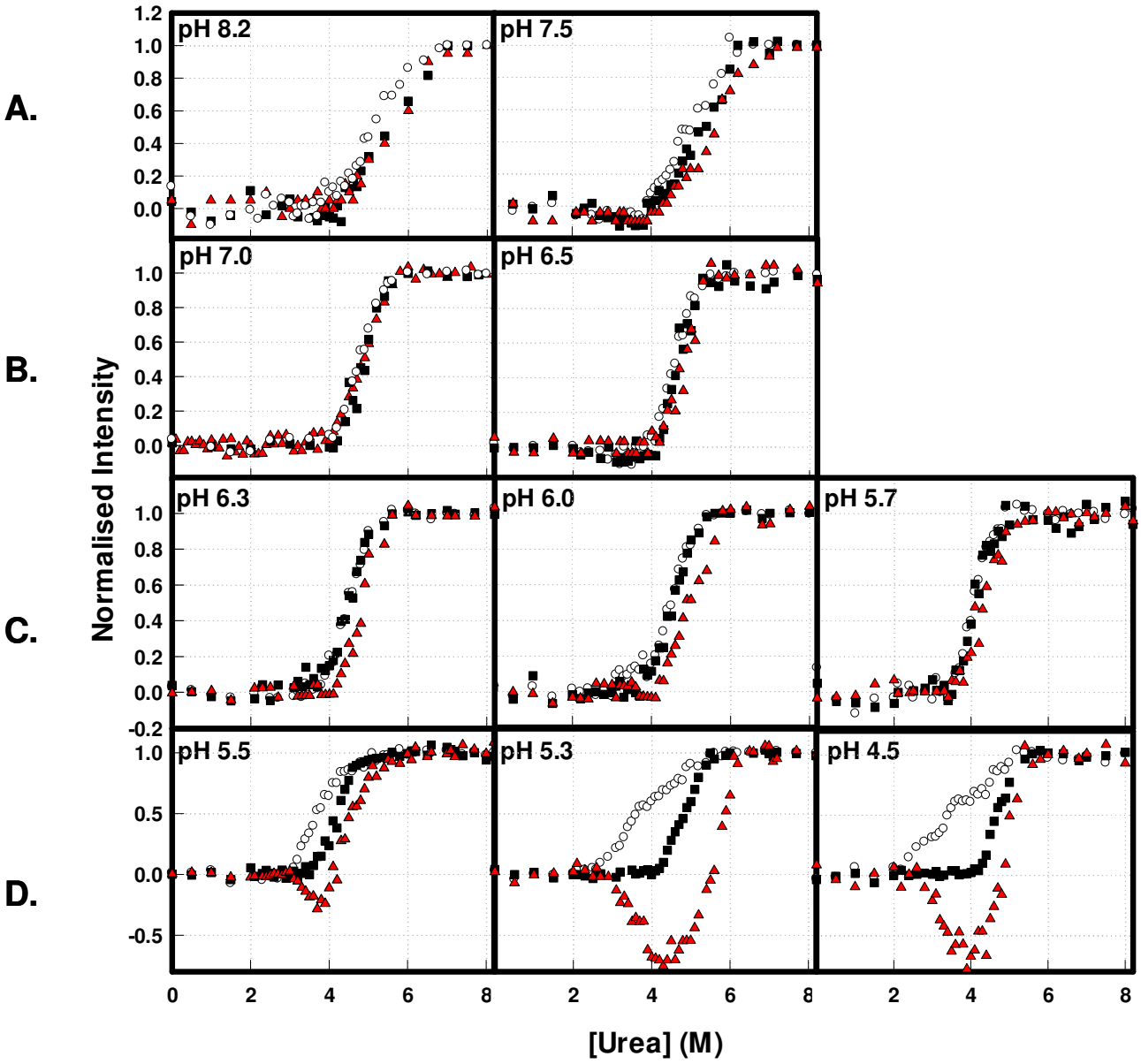


Figure 42: Equilibrium unfolding of CLIC1 at pH 8.2 to pH 4.5 using circular dichroism and fluorescence as probes

The unfolding of CLIC1 was monitored using E_{222} (○); F_{max} (■) and λ_{max} (▲) as probes. All transitions were normalised between 0 and 1 for comparison purposes. The unfolding curves at different pH can be divided into four groups (A to D) depending on the shapes of the transitions. All experiments were conducted at 20°C on 2 μM CLIC1.

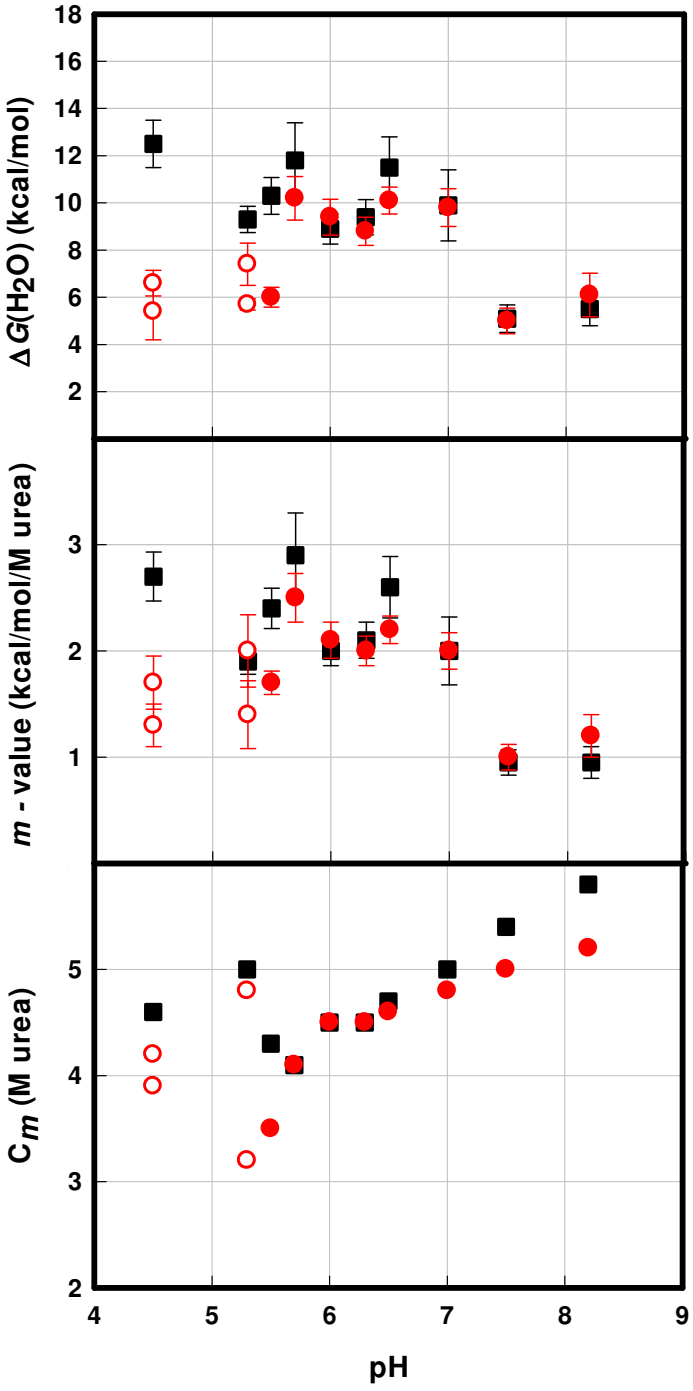


Figure 43: pH dependence of thermodynamic parameters

The dependence of the $\Delta G(H_2O)$ **(A)**, *m*-value **(B)** and C_m **(C)** on pH. The parameters obtained from E_{222} are red circles and those obtained from F_{max} are black squares. Closed symbols represent parameters obtained from a fit to a two-state model while open symbols represent parameters obtained from a fit to a three-state model. The error bars represent the standard error on each point.

Table 3: Comparison of the thermodynamic parameters obtained from equilibrium unfolding curves of CLIC1 at different pH

	E_{222}			F_{max}		
pH	$\Delta G(H_2O)$ (kcal/mol)	***m*-value** (kcal/mol/M urea)	C_m (M urea)	$\Delta G(H_2O)$ (kcal/mol)	***m*-value** (kcal/mol/M urea)	C_m (M urea)
8.2	6.1 ± 0.92	1.2 ± 0.20	5.2	5.5 ± 0.70	0.95 ± 0.15	5.8
7.5	5.0 ± 0.54	1.0 ± 0.12	5.0	5.1 ± 0.58	0.95 ± 0.12	5.4
7	9.8 ± 0.80	2.0 ± 0.17	4.8	9.9 ± 1.50	2.0 ± 0.32	5.0
6.5	10 ± 0.57	2.2 ± 0.13	4.6	11 ± 1.3	2.6 ± 0.29	4.7
6.3	8.8 ± 0.60	2.0 ± 0.14	4.5	9.4 ± 0.75	2.1 ± 0.17	4.5
6	9.4 ± 0.76	2.1 ± 0.17	4.5	8.9 ± 0.64	2.0 ± 0.14	4.5
5.7	10 ± 0.92	2.5 ± 0.23	4.1	11 ± 1.6	2.9 ± 0.40	4.1
5.5	6.0 ± 0.42	1.7 ± 0.11	3.5	10 ± 0.78	2.4 ± 0.19	4.3
5.3	7.4 ± 0.90 5.7 ± 0.24	2.0 ± 0.34 1.4 ± 0.32	3.7 4.0	9.3 ± 0.56	1.9 ± 0.12	5.0
4.5	6.6 ± 0.54 5.4 ± 1.2	1.7 ± 0.25 1.3 ± 0.20	3.9 4.2	12 ± 1.0	2.7 ± 0.23	4.6

E_{222} represents the ellipticity measured at 222 nm and F_{max} represents the maximum fluorescence intensity.

A mutant form of CLIC1 has been created where Met32 is replaced by an alanine (Stoychev PHD thesis, in preparation). It is interesting that when this mutant is at pH 7.0 it has the same properties as the wild type at pH 5.5 (C_m of E_{222}-monitored curve is ~3.5 M urea) and the wavelength of maximum fluorescence emission is also blue shifted so that the λ_{max}-monitored curve also shows three-state behaviour. The stability and cooperativity of the M32A mutant CLIC1 at pH 7.0 is similar to wild type at pH 5.5. Thus the M32A mutation that uncouples interactions at the domain interface has the same effect on the protein secondary structure and stability as a drop in pH does. The intermediate that accumulates at equilibrium as a result of the decrease in cooperative folding of the mutant protein is comparable to the stable intermediate species detected in the wild type protein at low pH in terms of structure and stability although they may not be the identical species.

3.3.4. Effect of Salts on Stability

Since pH has a pronounced effect on the stability of CLIC1, and hence the stability of this protein is closely related to electrostatics, the next logical question to answer would be whether a change in the ionic strength of the solution would have any effect on the stability of the protein. Four different salts were used: NaCl lies in the neutral region of the Hofmeister series (Figure 2) and thus this salt will give an indication as to the effect of an increase in the ionic strength of the solution on the stability of the protein. NaF also lies in the neutral region of the Hofmeister series. Initially this salt was used simply because the fluoride ions would produce a cleaner circular dichroism spectrum than the chloride ions in NaCl. NaF has since been found to have a *specific effect* on the structure and stability of CLIC1. The effect of the kosmotrope, Na_2SO_4 and the chaotrope, KSCN on the stability of CLIC1 were also investigated.

NaCl

At pH 7.0 / 20^{o}C the unfolding curves monitored using circular dichroism and fluorescence as probes are *superimposable* whether in the presence or absence of NaCl (Figure 44). The unfolding is *cooperative* and no intermediates are detectable at equilibrium. Furthermore, the unfolding transitions are superimposable with those monitored in the absence of NaCl.

Alternatively, at pH 5.5 / 20^{o}C, the native state of CLIC1 appears to be *stabilised* by the presence of NaCl as seen by an increase in the C_m (Figure 44, Table 4). The fact that the *m*-value is unaffected means that the increase in $\Delta G(H_2O)$ can be interpreted as an increase in stability of CLIC1. The presence of NaCl has no effect on the blue shift in the λ_{max} that represents the intermediate state populated in the pre-transition region of the unfolding curve at pH 5.5 (Figure 44). Thus NaCl can be said to stabilise both the native and intermediate states of CLIC1 at pH 5.5 although it has no effect on the structures of these states.

NaF

0.5 M NaF has a pronounced effect on the unfolding transition of CLIC1 at both pH 7.0 and pH 5.5 (Figure 44).

At pH 7.0 / 20^{o}C the stability of CLIC1 is reduced by 40% upon addition of 0.5 M NaF! The cooperativity of unfolding is also reduced by approximately 50% (Table 4). To contradict these results, the C_m is substantially higher which implies a stabilised native state (Myers *et al.*, 1995). It is therefore possible that the transition is no longer two-state in nature at pH 7.0 when in the presence of 0.5 M NaF. However any intermediates that may be present are not sufficiently populated to be detected with the spectroscopic methods used.

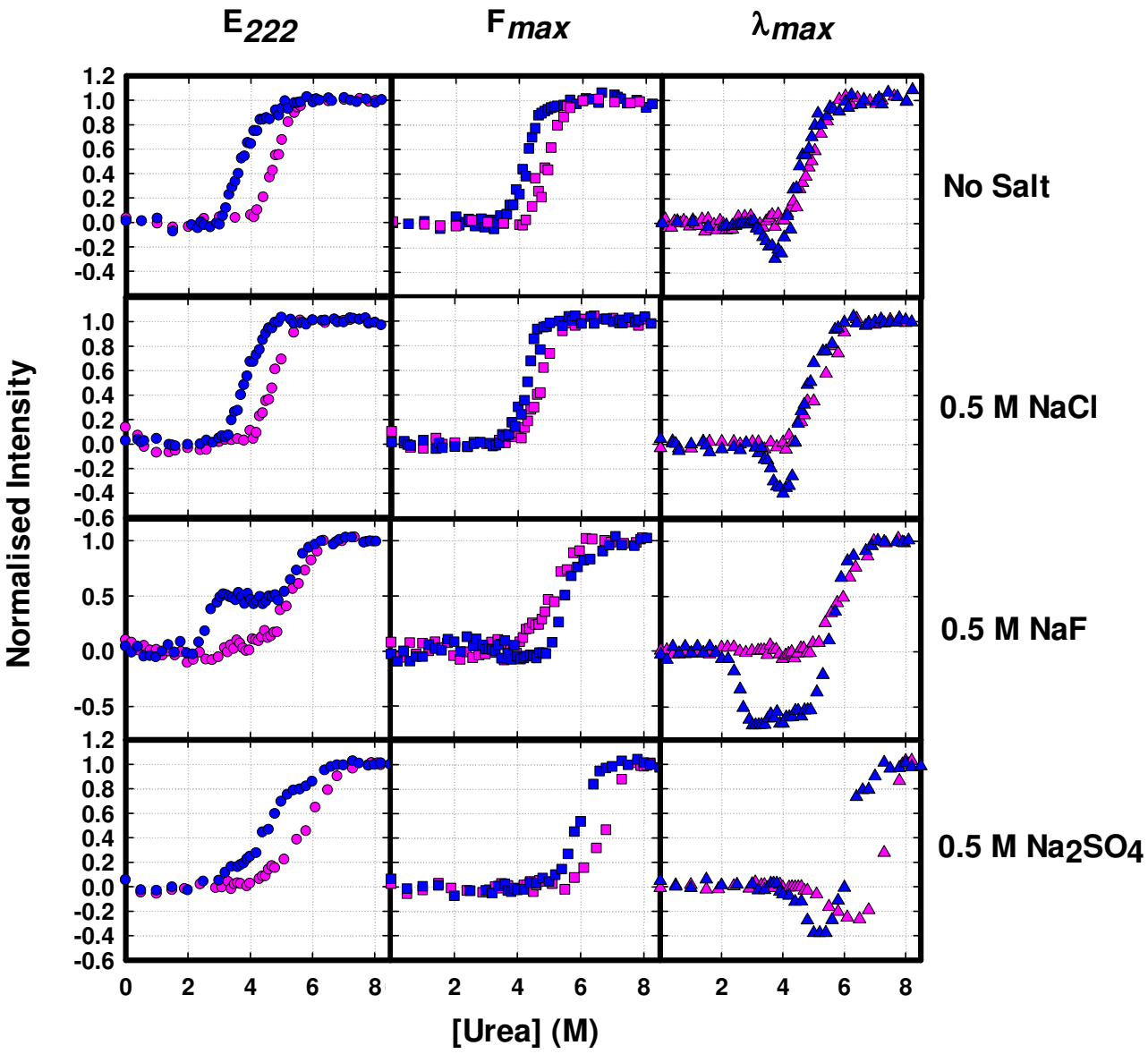


Figure 44: Equilibrium unfolding of CLIC1 at pH 7.0 and pH 5.5 in the presence of NaCl, NaF and Na_2SO_4

Equilibrium unfolding of 2 μM CLIC1 at pH 7.0 (pink) and pH 5.5 (blue). Transitions were monitored using E_{222} (●), F_{max} (■) and λ_{max} (▲). The unfolding curves were measured in the absence of salt (top panel), and in the presence of 0.5 M NaCl (second panel); 0.5 M NaF (third panel) or 0.5 M Na_2SO_4 (bottom panel). All experiments were conducted at 20°C.

At pH 5.5 / 20°C there is an impressive difference in the unfolding transitions when monitored in the presence of 0.5 M NaF. The most noticeable difference is the explicit three-state nature of the circular dichroism-monitored unfolding transition (Figure 44). The intermediate species appears to be considerably stabilised by the presence of NaF. The F_{max}-monitored curve still appears to be two-state but both the stability and the *m*-value are increased (Table 4). The thermodynamic parameters obtained from this curve greatly surpass the values obtained at pH 7.0 in the presence of 0.5 M NaF! *This is the only instance where the protein appears more stable at pH 5.5 than at pH 7.0*. The C_m is also increased at pH 5.5 to higher urea concentrations than at pH 7.0 under the same conditions. The λ_{max}-monitored curve once again shows how the intermediate state is stabilised by the presence of 0.5 M NaF. The intermediate is observed at lower concentrations of urea than in the absence of NaF and causes a greater blue shift in the fluorescence wavelength of maximum emission. The intermediate state is also present over a greater range of urea than in the absence of NaF.

Na_2SO_4

Sodium sulphate is a known kosmotrope. Interestingly, when CLIC1 is unfolded in the presence of 0.5 M Na_2SO_4, the unfolding transitions as monitored by circular dichroism and fluorescence do not superimpose at either pH 7.0 or pH 5.5 (Figure 44). Furthermore, the λ_{max}-monitored transition confirms the presence of a pre-transition intermediate state at both pH 7.0 and pH 5.5! Na_2SO_4 therefore stabilises the intermediate to such an extent that it is even detectable at pH 7.0 / 20°C, albeit at higher urea concentrations. Higher concentrations of urea are required to denature the protein when in the presence of Na_2SO_4 and the C_m is increased by the presence of this salt. Nevertheless, the native state of CLIC1 is not necessarily stabilised by Na_2SO_4 as may have been expected by the kosmotropic nature of the salt. According to the values obtained using E_{222}, the $\Delta G(H_2O)$ is reduced by 46% upon addition of 0.5 M Na_2SO_4 at pH 7.0, while according to the F_{max} data the $\Delta G(H_2O)$ is in fact, increased by 12% under these conditions (Table 4). These discrepancies in the

estimate of the $\Delta G(H_2O)$ measured at pH 7.0 using a two-state model are due to the stabilisation of the equilibrium intermediate as evidenced by the λ_{max} data (Soulages, 1998). The cooperativity of the N → D transition is much reduced upon addition of Na_2SO_4. This is once again due to the stable intermediate present under these conditions.

At pH 5.5 the intermediate is detectable in both the E_{222}-monitored and λ_{max}-monitored transitions when in the presence of 0.5 M Na_2SO_4. The three-state fit implies an increase in the stability of the intermediate species compared to when in the absence of salt although NaF stabilises the intermediate to an even greater extent than Na_2SO_4. Thus it can be concluded that the kosmotropic salt, sodium sulphate does not stabilise the native state of CLIC1 at pH 7.0 / 20°C or pH 5.5 / 20°C but instead *stabilises the intermediate state*.

KSCN

Potassium thiocyanate is a known chaotropic salt. SCN^- along with the other denaturing ions of the Hofmeister series (Figure 2) denatures proteins by interacting more strongly with the denatured state than the native state (Baldwin, 1996). Therefore this salt was used in place of urea to denature CLIC1 at pH 7.0 / 20°C and pH 5.5 / 20°C (Figure 45). Concentrations of KSCN higher than 4.6 M urea caused aggregation of CLIC1 when at pH 5.5 and had no further effect on results at pH 7.0 therefore only results of 0 M to 4.6 M KSCN are displayed. It is interesting that 1 M KSCN causes the λ_{max} to shift from ~345 nm to ~343 nm at pH 7.0 and to ~338 nm at pH 5.5! Further increases in the concentration of KSCN do not result in further blue shifts of the λ_{max} at pH 5.5, but at pH 7.0 the λ_{max} is shifted to as low as 334 nm when in the presence of 3 M KSCN. Is this wavelength shift representative of the formation of the intermediate state and therefore does KSCN stabilise the intermediate state relative to both the native and denatured states of CLIC1?

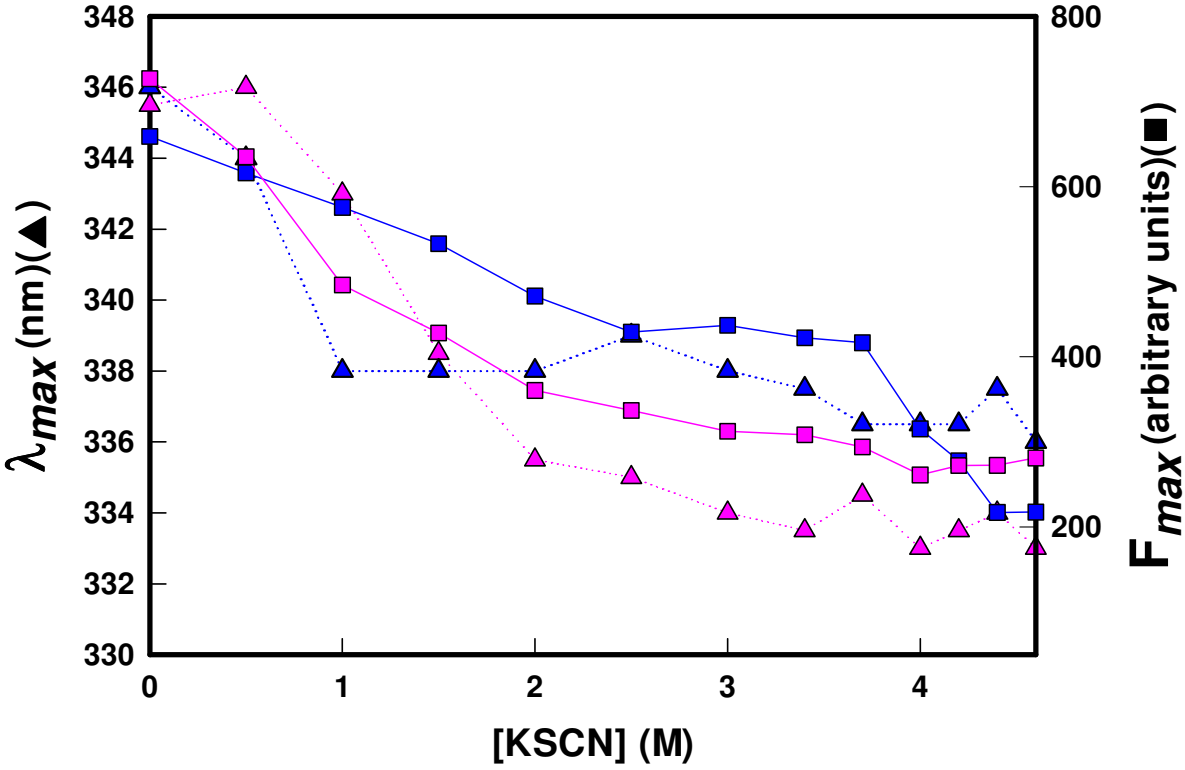


Figure 45: KSCN-induced unfolding of CLIC1 at pH 7.0 and pH 5.5

2 µM CLIC1 at pH 7.0 (pink) and pH 5.5 (blue) in the presence of increasing concentrations of KSCN monitored with fluorescence F_{max} (■) and λ_{max} (▲). Lines simply join the recorded points. All spectra were recorded using an excitation wavelength of 280 nm at 20°C.

Table 4: Comparison of the equilibrium thermodynamic parameters obtained under different environmental conditions

	E_{222}			F_{max}		
	$\Delta G(H_2O)$ (kcal/mol)	*m*-value (kcal/mol/M *urea)*	C_m (M urea)	$\Delta G(H_2O)$ (kcal/mol)	*m*-value (kcal/mol/M *urea)*	C_m (M urea)
No Salt	9.8 ± 0.8	2.0 ± 0.17	4.9	9.9 ± 1.5	2.0 ± 0.32	5.0
	6.0 ± 0.42	1.6 ± 0.11	3.5	10 ± 0.78	2.4 ± 0.19	4.2
Non-reducing	0.26 ± 0.80	0.65 ± 0.13	2.3	5.6 ± 2.4	1.4 ± 0.59	4.7
	0.43 ± 1.7	0.60 ± 0.11	2.2	3.1 ± 0.95	0.74 ± 0.2	4.7
At 37°C	4.3 ± 0.33	1.2 ± 0.09	3.7	11 ± 0.98	2.9 ± 0.24	4.1
	-	-	-	-	-	-
0.2 M NaCl	9.6 ± 1.2	2.0 ± 0.26	4.8	10 ± 1.2	2.1 ± 0.25	4.8
	5.9 ± 0.32	1.3 ± 0.08	3.8	13 ± 1.3	3.1 ± 0.31	4.3
0.5 M NaCl	8.3 ± 0.96	1.8 ± 0.21	4.6	9.3 ± 0.8	2.0 ± 0.17	4.7
	7.0 ± 0.36	1.8 ± 0.09	3.9	12 ± 1.1	2.8 ± 0.26	4.3
0.5 M NaF	5.5 ± 0.56	0.99 ± 0.12.	5.3	6.3 ± 0.82	1.2 ± 0.17	5.1
	14 ± 3.4 17 ± 3.3	5.3 ± 1.3 3.1 ± 0.61	2.6 5.5	20 ± 4.7	3.8 ± 0.87	5.5
0.5 M Na_2S0_4	5.3 ± 0.42	0.86 ± 0.09	5.8	11 ± 1.2	1.6 ± 0.19	6.8
	5.4 ± 0.72 30 ± 49	1.2 ± 0.16 4.7 ± 0.77	4.4 6.4	9.5 ± 0.75	1.6 ± 0.13	5.9

E_{222} represents the ellipticity at 222 nm and F_{max} represents the maximum fluorescence intensity

Key

pH 7
pH 5.5

Equilibrium unfolding at 37^{o}C

CLIC1 was unfolded in the presence of urea at 37^{o}C at pH 7.0 and pH 5.5 and the results were compared with the unfolding of the protein at 20^{o}C (Figure 46). At pH 7.0, an increase in temperature to 37^{o}C results in CLIC1 no longer following the highly cooperative two-state unfolding transition that occurs at 20^{o}C. The transitions monitored with circular dichroism and fluorescence are no longer superimposable at pH 7.0 / 37^{o}C. Furthermore, a dip is evident in the λ_{max}-monitored transition that is similar to the situation at pH 5.5 / 20^{o}C. In fact, the unfolding of CLIC1 at pH 7.0 / 37^{o}C bears a striking resemblance to the unfolding at pH 5.5 / 20^{o}C (Figure 46)! The most insinuating similitude is the blue shift in the λ_{max} of the fluorescence spectra at pH 7.0 / 37^{o}C at the same concentrations of urea as at pH 5.5 / 20^{o}C! In addition, the E_{222}-monitored and F_{max}-monitored transitions are similar at pH 7.0 / 37^{o}C and at pH 5.5 / 20^{o}C. Thus an increase in temperature has a similar effect on CLIC1 stability as a drop in pH. At pH 7.0 the native structure of denatured CLIC1 is 100% recoverable at 37^{o}C and therefore the thermodynamic parameters may be analysed under these conditions.

Unfolding at pH 5.5 / 37^{o}C is plagued by aggregation and introduction of even small concentrations of denaturant simply causes the already destabilised CLIC1 to aggregate. This is proved by the high Raleigh scatter along the unfolding transition from 0.3 M to 4.2 M urea (Figure 46). Although these transitions at pH 5.5 are replicable, the unfolding of the protein at pH 5.5 / 37^{o}C is not reversible due to the aggregation and therefore the transitions cannot be investigated further in terms of their thermodynamic parameters.

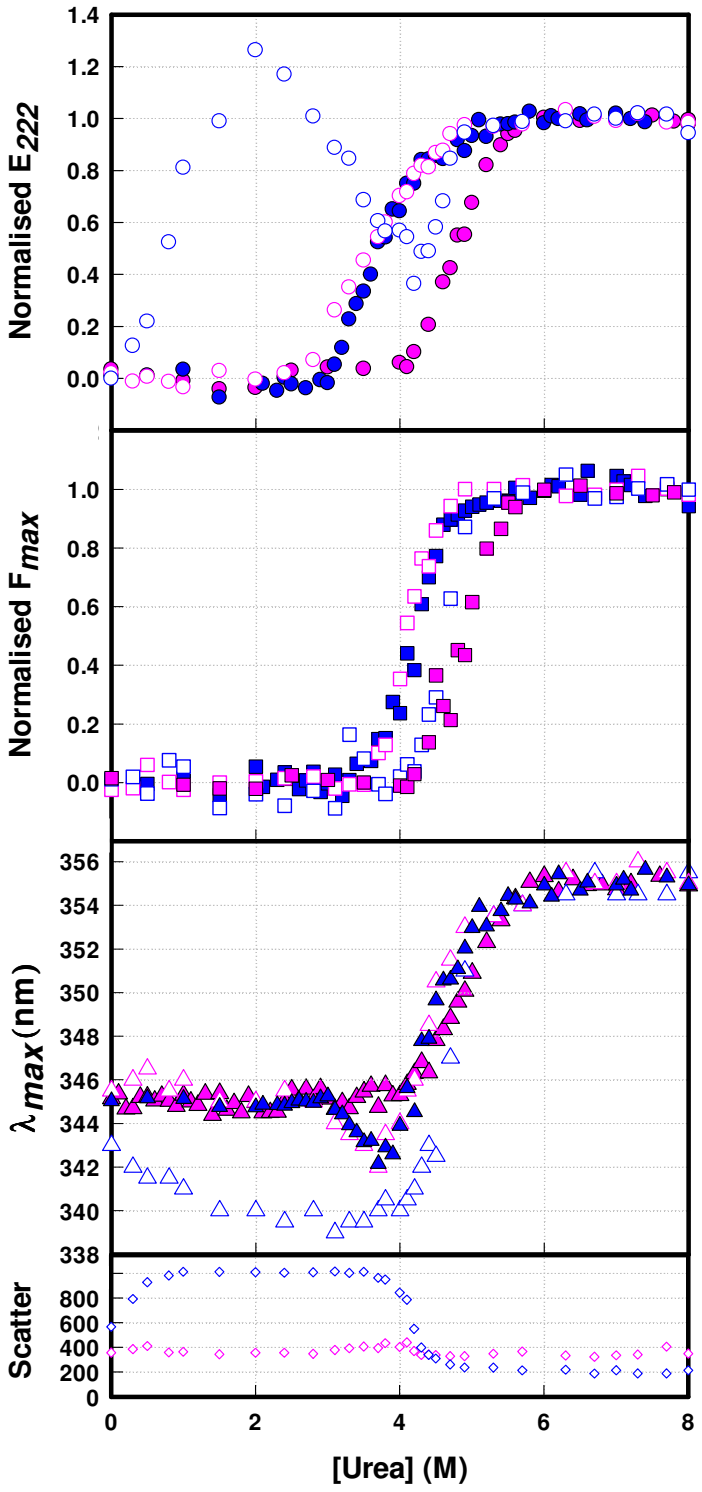


Figure 46: Comparison of unfolding at 37°C and 20°C

Comparison of the urea-induced equilibrium unfolding of 2 µM CLIC1 at pH 7.0 (pink) and pH 5.5 (blue) at 20°C (closed) and at 37°C (open). The unfolding was monitored using E_{222} (●/○), F_{max} (■/□) and λ_{max} (▲/△) as probes. The Raleigh scatter at 280 nm / 37°C (◇) proves the presence of aggregates at pH 5.5 from 0.3 M to 4.2 M urea.

The stability of the native state of CLIC1 at pH 7.0 / 37°C as measured with circular dichroism is reduced by 59% to that at pH 7.0 / 20°C and is reduced by 33% compared to that at pH 5.5 / 20°C (Table 4)! The high $\Delta G(H_2O)$ and *m*-value recorded using F_{max} as a probe mimics the situation at pH 5.5 / 20°C. The intermediate state formed at pH 7.0 / 37°C is on a whole less stable than the intermediate formed at pH 5.5 / 20°C.

3.3.6. Effect of Non - Reducing Conditions on Stability

CLIC1 is believed to be a redox-regulated protein and changes in the oxidising and reducing nature of its environment are believed to have an impact on the way this protein behaves (Littler *et al.,* 2004; Singh and Ashley, 2006). It is for this reason that CLIC1 was unfolded under non-reducing conditions and the results compared with those obtained under reducing conditions (Figure 47). The unfolding of CLIC1 at pH 7.0 / 20°C and pH 5.5 / 20°C in the absence of DTT is reversible and the scatter at 280 nm remains low and constant at both pH 7.0 and pH 5.5 negating the option of aggregation along the unfolding transition under non-reducing conditions. Furthermore, if DTT is added to the protein when under non-reducing conditions, the structure and stability of the protein will return to that typical for when under reducing conditions. Unfolding transitions were monitored in the absence of DTT and in the presence of 2 mM GSSG. There is not a significant difference between the two unfolding curves and therefore only the curves in the absence of DTT are reported here (Figure 47).

There is no doubt that the reducing nature of the environment of CLIC1 is important and when the protein is unfolded under non-reducing conditions the curves differ in shape to those obtained under reducing conditions and they lack the sigmoidal form which is typical of a two-state transition. Furthermore, in contrast to when under reducing conditions, the F_{max} increases with increasing urea concentration in the pre-transition region and is a maximum at

~4 M urea (Figure 47). It is interesting that there is no longer a difference in the nature of the transitions monitored at pH 7.0 and pH 5.5. *The pH dependence of the stability of CLIC1 is therefore inextricably linked to the reducing nature of the environment of the protein*. The λ_{max}-monitored transition in the absence of DTT is identical at pH 7.0 and pH 5.5 but is not superimposable with either of the curves created in the presence of DTT. Furthermore, the three-state nature of the curve as detected by the inflection is not evident under non-reducing conditions. However, the λ_{max} in the pre-transition region *including that of the native state* is shifted to ~341 nm from ~345 nm when under reducing conditions. This is the wavelength at which the spectra peak in the urea-induced intermediate state detected under reducing conditions. The stability of CLIC1 plummets when under non-reducing conditions no matter what probe is used (Table 4). Therefore *reducing conditions are essentially a requirement for CLIC1 to retain its native folded structure*.

3.4. Binding of ANS

ANS is an amphipathic dye (Figure 48) that binds to exposed hydrophobic patches on proteins and in so doing exhibits enhanced fluorescence when excited at 390 nm. Since a property of a molten globule-like intermediate state is that it binds to ANS (Semisotnov *et al.*, 1991), CLIC1 was incubated in the presence of 200 μM ANS under different conditions and its spectroscopic properties analysed in order to further characterise the native, denatured and intermediate states of this protein.

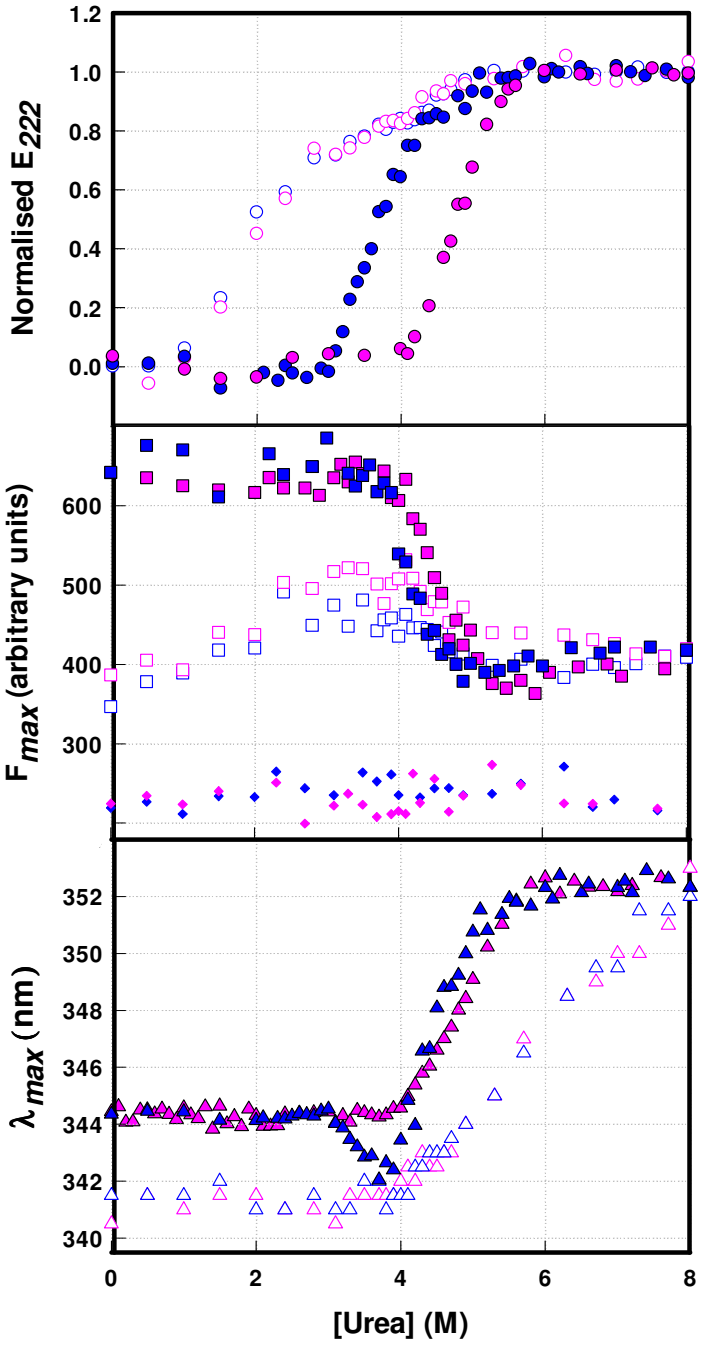


Figure 47: Equilibrium unfolding of CLIC1 in the presence and absence of 1 mM DTT at pH 7.0 and pH 5.5

Urea-induced equilibrium unfolding of 2 µM CLIC1 at pH 7.0 (pink) and pH 5.5 (blue) in the presence (closed) and absence (open) of 1 mM DTT. The unfolding was monitored using E_{222} (●/○), F_{max} (■/□) and λ_{max} (▲/△) as probes. The Raleigh scatter at 280 nm under non-reducing conditions is also given (◆).

3.4.1. Effect of pH on ANS Binding

CLIC1 was incubated in the presence of 200 μM ANS at pH 8.2, pH 7.0 and pH 5.5 in the presence of increasing concentrations of urea in order to determine whether pH has any effect on ANS binding to the protein at any point along the unfolding transition (Figure 49).

The emission spectrum of free ANS in the absence of protein peaks at 540 nm when excited at 390 nm and the spectra are identical at pH 8.2, pH 7.0 or pH 5.5 (Figure 49 A). Thus any increases in ANS fluorescence intensity when in the presence of CLIC1 are not due to changes in pH but are due to increased binding of ANS to the protein which is as a result of exposed hydrophobic surfaces on the protein. Although ANS binds near to the subunit interface of dimeric GSTs (Sayed *et al.,* 2002, Dirr *et al.,* 2005), it does not bind to the native state of Grx2, the only other monomeric member of the GST superfamily (Gildenhuys PHD thesis, 2006). Conceivably therefore, since CLIC1 is also monomeric, ANS does not bind to native CLIC1 at any pH studied. In fact, ANS does not bind to CLIC1 over the entire unfolding transition at pH 8.2 and at pH 7.0 (Figure 49 B).

At pH 5.5, however, there is considerable fluorescence due to ANS binding to the protein at 3 M to 5 M urea (Figure 49 A and B). This is the same urea concentration range over which the intermediate species is detected at pH 5.5 (Figure 41). The intensity of the emission is enhanced compared to that of free ANS in solution. A representative spectrum of ANS binding to CLIC1 at pH 5.5 in the presence of 3.8 M urea is shown in Figure 49 A.

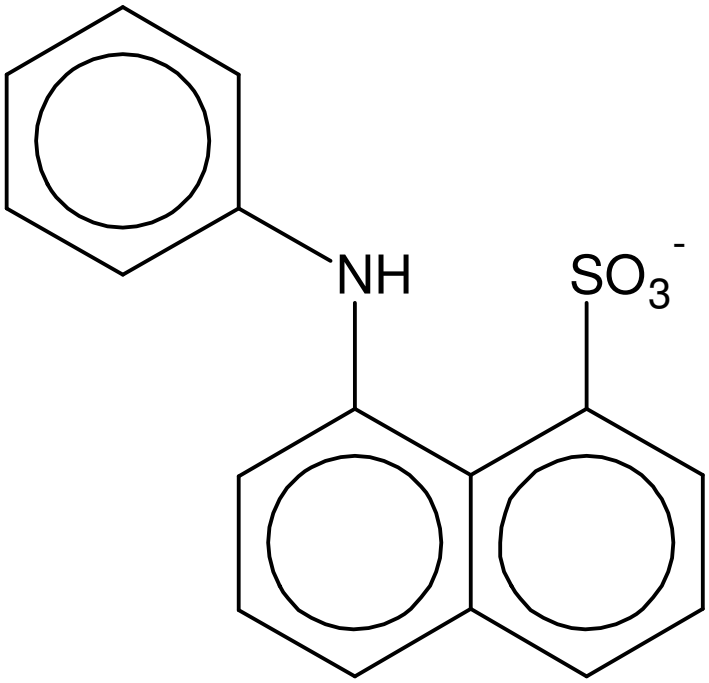


Figure 48: The structure of ANS

ANS is a charged hydrophobic fluorescent molecule with a molecular mass of 673 Da. It is minimally fluorescent in polar environments but its fluorescence increases dramatically when in non-polar environments

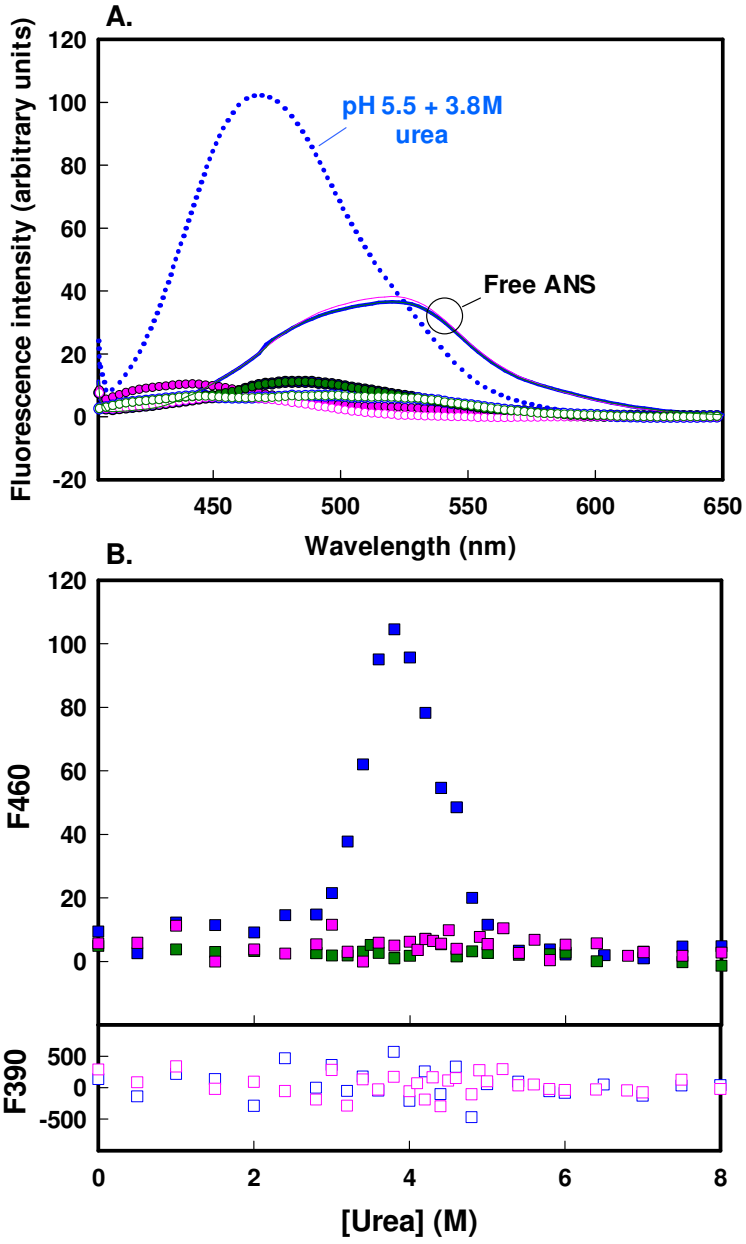


Figure 49: Binding of ANS to CLIC1 at pH 8.2, pH 7.0 and pH 5.5 along the equilibrium unfolding transition

(A) Fluorescence emission spectra of native CLIC1 (closed circles) and that of the protein denatured in 8 M urea (open circles) when in the presence of 200 µM ANS at pH 8.2 (green), pH 7.0 (pink) and pH 5.5 (blue). The spectrum of the protein at pH 5.5 in the presence of 3.8 M urea is given by a blue dotted line. The spectra were corrected for free ANS. The emission spectrum of free ANS is shown with a solid line and is identical at different pH. The urea dependence of ANS binding at pH 8.2 (green), pH 7.0 (pink) and pH 5.5 (blue) is indicated in **(B)** Emission of each sample at 460 nm (■) and scatter at 390 nm (□) are shown. The protein was at a concentration of 2 µM at 20°C. The samples were excited at 390 nm and spectra were smoothed using the negative exponential smoothing method.

The plot of Raleigh scatter (F_{390}) as a function of urea concentration (Figure 49 B) does not indicate increased scatter at any point along the unfolding transition at any pH studied. Therefore, the binding of ANS to CLIC1 at pH 5.5 is not due to the presence of hydrophobic aggregates at 3 M to 5 M urea, but rather it is due to the formation of some alternate state of the protein that is different in exposed hydrophobic surface to both the native and denatured state.

3.4.2. Effect of Salt on ANS Binding

Since ANS has a negatively charged sulphonate anion (Figure 48) and hence could potentially bind in an electrostatic manner to cationic groups on a protein (Matulis and Lovrein, 1998) and even induce the formation of a partially compact molten globule state from an acid-unfolded protein (Ali *et al.,* 1999), an increase in ionic strength would reduce the binding of this ligand to CLIC1. This mode of ANS binding is pH dependent, however, and ANS fluorescence has been shown to be altered due to electrostatic interactions with bovine serum albumin when the pH is below 3.0 or above 11.0 (Matulis and Lovrein, 1998). At a pH within the range of 3.0 to 11.0, any detected fluorescence should thus not be due to electrostatic effects. Nevertheless ANS binding studies were conducted at elevated salt concentrations in order to confirm that the observed binding of ANS to CLIC1 at pH 5.5 was mainly due to hydrophobic and not electrostatic interactions.

ANS binding studies were performed in the presence of 0.5 M NaCl; 0.5 M NaF and 0.5 M Na_2SO_4 at pH 7.0 / 20^{o}C and pH 5.5 / 20^{o}C and compared with the results obtained in the absence of salt (Figure 50). At pH 7.0 ANS does not bind to CLIC1 in the native state nor along the entire unfolding transition in the presence of any of the salts used except for 0.5 M Na_2SO_4. Sodium sulphate causes a relatively small amount of fluorescence due to ANS binding to CLIC1 at high urea concentrations (the same concentrations that result in the dip in the λ_{max}-monitored unfolding transition under these conditions (Figure 44)).

At pH 5.5 / 20°C CLIC1 does not bind ANS in its native state in the presence of NaCl, or Na_2SO_4. The equilibrium unfolding transitions at pH 5.5 in the presence of ANS (Figure 50 B) show that NaCl has no effect on the binding of ANS to the intermediate state. The intensity of the fluorescence emission is identical in both cases. Thus, since the intensity did not decrease, this implies that the binding of ANS is to hydrophobic patches on the protein surface and is not due to electrostatic interactions involving the sulphonate ion. There are no significant differences in the binding of ANS when CLIC1 is in the presence of 0.5 M Na_2SO_4 to when the protein is in the presence of 0.5 M NaCl or in the absence of salt.

However when CLIC1 is in the presence of 0.5 M NaF at pH 5.5 / 20°C, the unfolding transition is extremely different. Firstly, ANS binds to CLIC1 in the absence of urea under these conditions and the emission is enhanced by almost 500% (Figure 50 A)! Secondly, as the urea concentration is increased, so the emission intensity decreases until at 4 M urea it reaches the same intensity as the maximum emission in the absence of salt. These remarkable results are not observed to any extent at pH 7.0 in the presence of NaF and therefore it can be concluded that a NaF-induced specific change is occurring in CLIC1 at pH 5.5. NaF interacts specifically with the native state and all urea-induced states up to ~5.8 M urea. It must be noted here that a similar effect has been observed with the M32A mutant CLIC1 at pH 7.0 (Stoychev PHD thesis, in preparation).

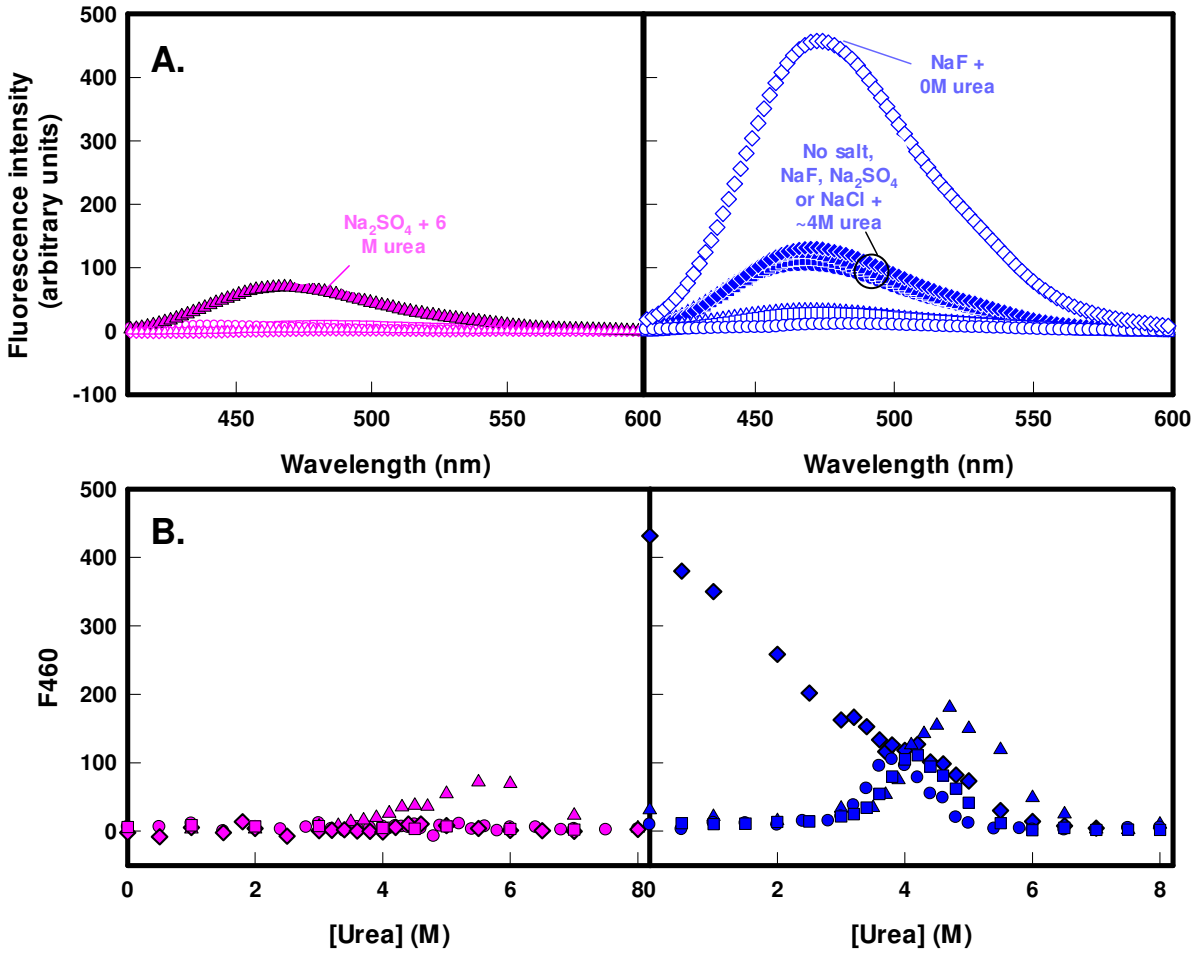


Figure 50: ANS binding to CLIC1 in the presence of different salts and increasing urea concentrations

2 µM CLIC1 was incubated in the presence of 200 µM ANS at pH 7.0 (pink) and pH 5.5 (blue) in the presence of 0.5 M NaCl (■/□); 0.5 M NaF (◆/◇); 0.5 M Na_2SO_4 (▲/△) and in the absence of salt (●/○). The top panel **(A)** shows the fluorescence emission when the solution was excited at 390 nm. All spectra were corrected for free ANS. Open symbols represent the protein in the absence of urea while closed symbols represent the protein in the presence of the concentration of urea at which the spectra show maximum fluorescence. The bottom panel **(B)** shows the urea-induced equilibrium unfolding transitions of CLIC1 in the presence of the various salts and 200 µM ANS. The fluorescence emission was recorded at 460 nm.

3.4.3. Effect of Temperature on ANS Binding

The equilibrium unfolding curve of CLIC1 at pH 7.0 / 37°C bears a striking resemblance to that at pH 5.5 / 20°C to such an extent that the intermediate species is detectable along the unfolding transition (Figure 46). In order to establish whether this intermediate is similar if not identical to the one detected at pH 5.5 / 20°C, ANS binding studies were conducted at pH 7.0 / 37°C. The fluorescence spectra are compared in Figure 51 A. Free ANS in the absence of protein has the identical spectrum whether at 20°C or at 37°C. At pH 7.0 CLIC1 does not bind ANS in the native or denatured state at 37°C or at 20°C. However at pH 7.0 / 37°C, the protein shows enhanced fluorescence due to ANS binding between 2.5 M and 4.5 M urea (Figure 51 B). This is not the case at pH 7.0 / 20°C. This intermediate species has 30% enhanced ANS fluorescence intensity compared to the intermediate detected at pH 5.5 / 20°C. Furthermore, the intermediate species is detectable at slightly lower concentrations of urea at pH 7.0 / 37°C. This is due to the protein being destabilised by the higher temperature.

At pH 5.5, ANS does not bind the native or denatured state of CLIC1 at 20°C, nor does it bind the denatured state at 37°C. However the fluorescence emission spectrum of *native* CLIC1 at pH 5.5 / 37°C shows enhanced fluorescence due to ANS binding (Figure 51 A). The intensity of the emission is only 20% lower than that of the urea-induced intermediate species detected at 20°C. Does the native state of CLIC1 at pH 5.5 / 37°C resemble the intermediate state at pH 5.5 / 20°C? At 2 M urea there is substantial fluorescence due to ANS binding to the protein at pH 5.5 / 37°C. This is likely to be due to aggregation, however, as can be seen by the increased Raleigh scatter at 390 nm compared to at pH 7.0. Also the pattern of the increase in ANS fluorescence with increasing urea concentration (Figure 51 B) is different to that of the other ANS-binding unfolding curves implying aggregation.

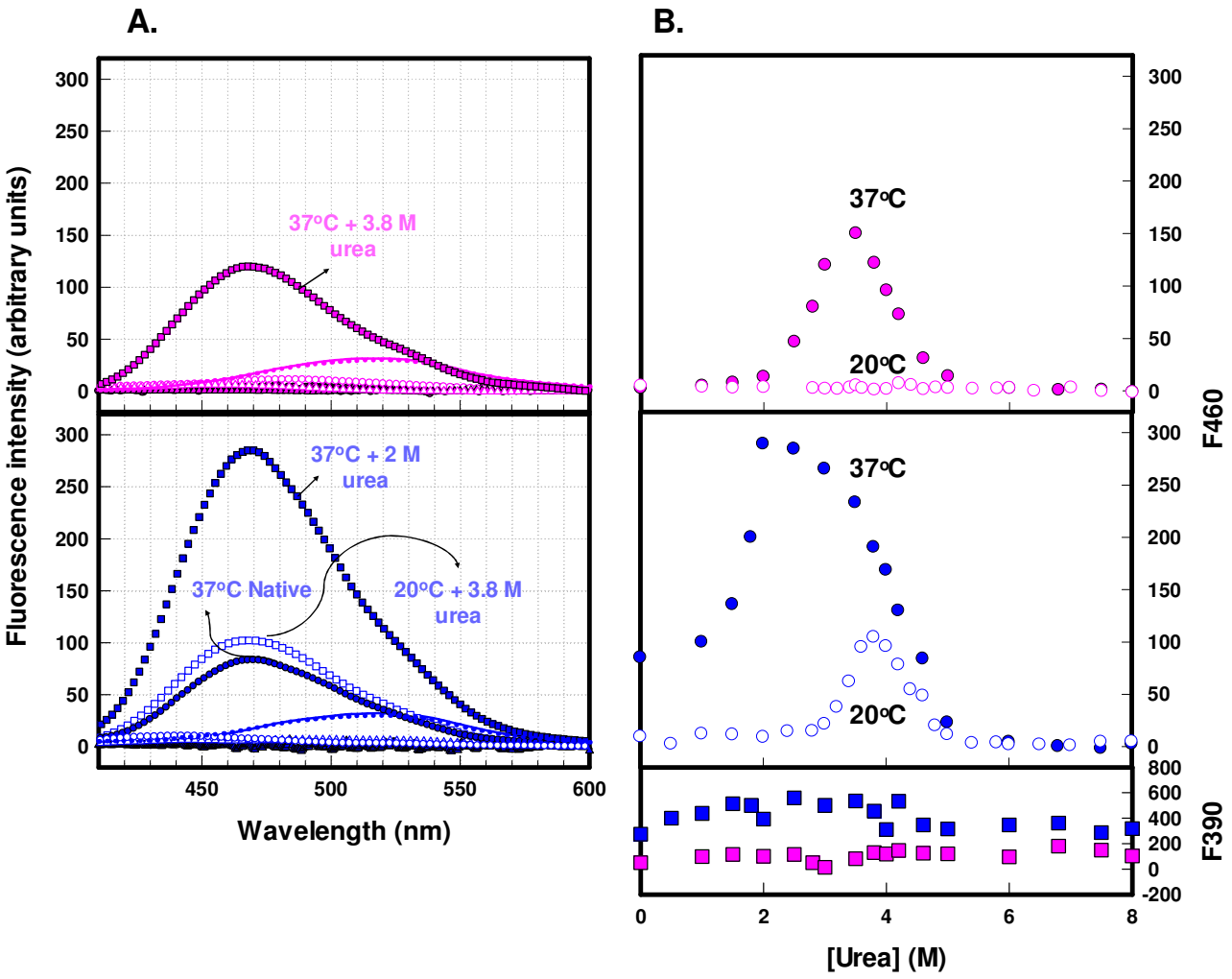


Figure 51: Effect of temperature on ANS binding to CLIC1

(A) Emission spectra showing binding of 200 µM ANS to 2 µM CLIC1 at pH 7.0 (pink) and pH 5.5 (blue) at 37°C (closed symbols) and 20°C (open symbols). Spectra were corrected for free ANS. The spectrum of free ANS is shown by a solid line at 37°C and a dotted line at 20°C. Spectra of the native state (●/○), the denatured state (▲/△) and urea concentrations at which the spectra show maximum emission (■/□) are represented. All spectra were smoothed using the negative exponential method. **(B)** Urea-induced equilibrium unfolding curves of 2 µM CLIC1 in the presence of 200 µM ANS at pH 7.0 (pink) and pH 5.5 (blue) at 37°C (closed symbols) and at 20°C (open symbols). The protein was excited at 390 nm and its emission at 460 nm was recorded (●/○). The Raleigh scatter at 390 nm at 37°C (■) is given.

3.4.4. Effect of Non - Reducing Conditions on ANS Binding

The most significant aspect of the ANS-binding study under non-reducing conditions is that the "*native state"* (i.e. the state in the absence of urea) *binds ANS at both pH 7.0 / 20^{o}C and pH 5.5 / 20^{o}C* (Figure 52). Thus the absence of DTT has caused structural alterations to the native state and the question remains as to whether or not this ANS-binding state of the protein resembles the ANS-binding urea-induced intermediate species. The denatured state does not bind ANS at either pH. When under non-reducing conditions there is not a significant difference in the binding of ANS to the unfolding transition whether CLIC1 is at pH 7.0 or at pH 5.5 except that the emission intensity is higher at pH 5.5.

3.5. Unfolding Kinetics of CLIC1

3.5.1. Effect of pH on Unfolding Kinetics

The N → D transition

CLIC1 was unfolded from the native state to the denatured state (final urea concentrations ranging from 5.5 M to 8.5 M urea which are representative of the post transition region of the equilibrium unfolding curves) at pH 5.3, pH 5.5, pH 7.0 and pH 8.2 in order to determine whether pH has an effect on the rate at which the native state of the protein unfolds. A representative unfolding trace of CLIC1 at pH 7.0 and pH 5.5 at a final denaturant concentration of 7.5 M urea is given in Figure 53. Both circular dichroism ellipticity at 222 nm (E_{222}) and fluorescence emission intensity at 345 nm (F_{345}) were used to probe the rate of unfolding of the secondary and tertiary structure respectively of the protein.

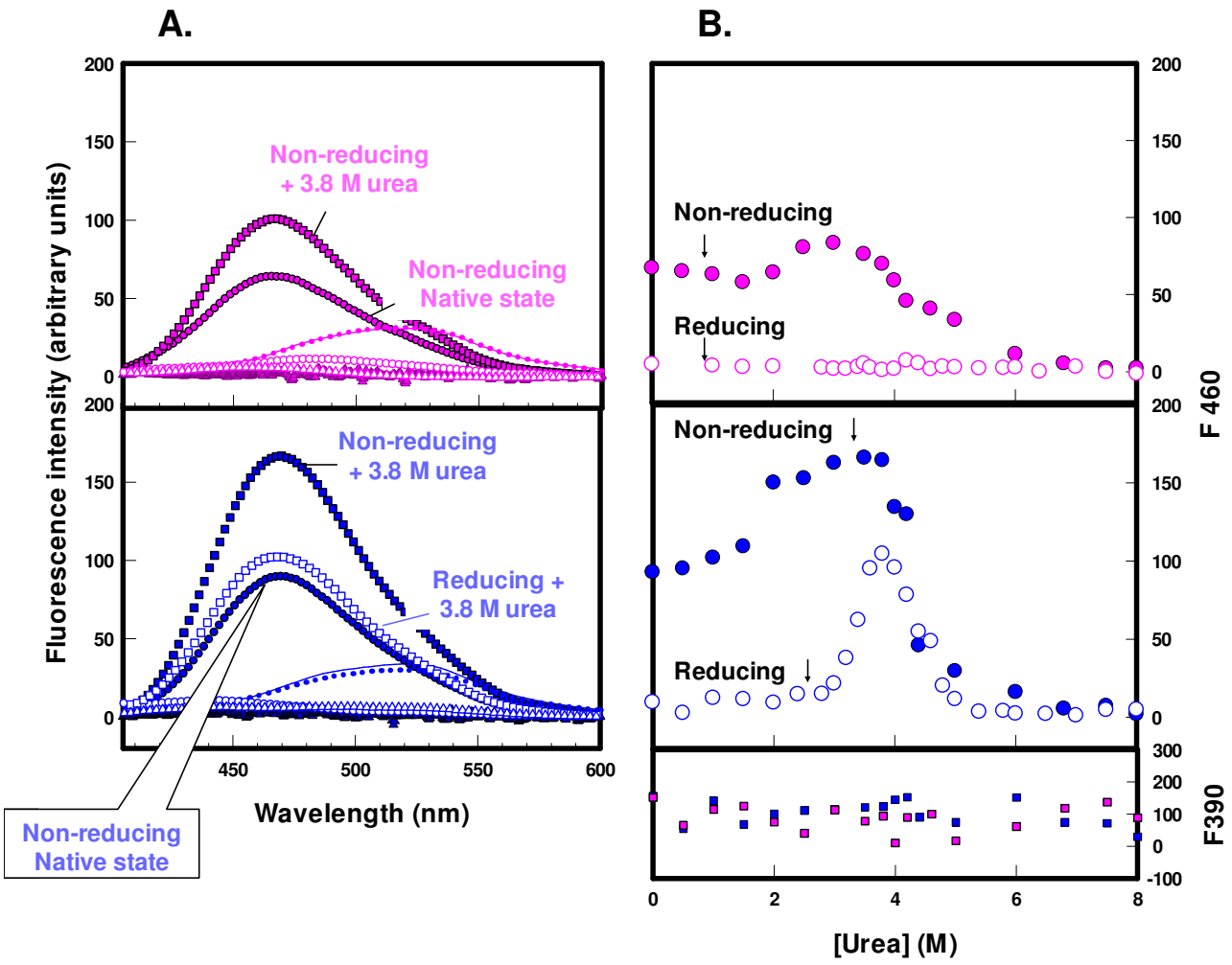


Figure 52: ANS binding to CLIC1 under non-reducing conditions

(A) Emission spectra showing binding of 200 µM ANS to 2 µM CLIC1 at pH 7.0 (pink) and pH 5.5 (blue) under non-reducing conditions (closed symbols) and in the presence of 1 mM DTT (open symbols). Spectra were corrected for free ANS. The spectrum of free ANS under non-reducing conditions is shown by a solid line and a dotted line is given for the free ANS under reducing conditions. Spectra of the native state (●/○), the denatured state (▲/△) and at urea concentrations at which the spectra show maximum emission (■/□) are shown. All spectra were recorded at 20°C and smoothed using the negative exponential method**. (B)** Urea-induced equilibrium unfolding curves of 2 µM CLIC1 in the presence of 200 µM ANS at pH 7.0 (pink) and pH 5.5 (blue) under non-reducing conditions (closed symbols) and under reducing conditions (open symbols). The protein was excited at 390 nm and its emission at 460 nm was recorded (●/○). The Raleigh scatter at 390 nm of CLIC1 under non-reducing conditions (■) is shown in the bottom panel. The term "native state" refers to the state in the absence of urea.

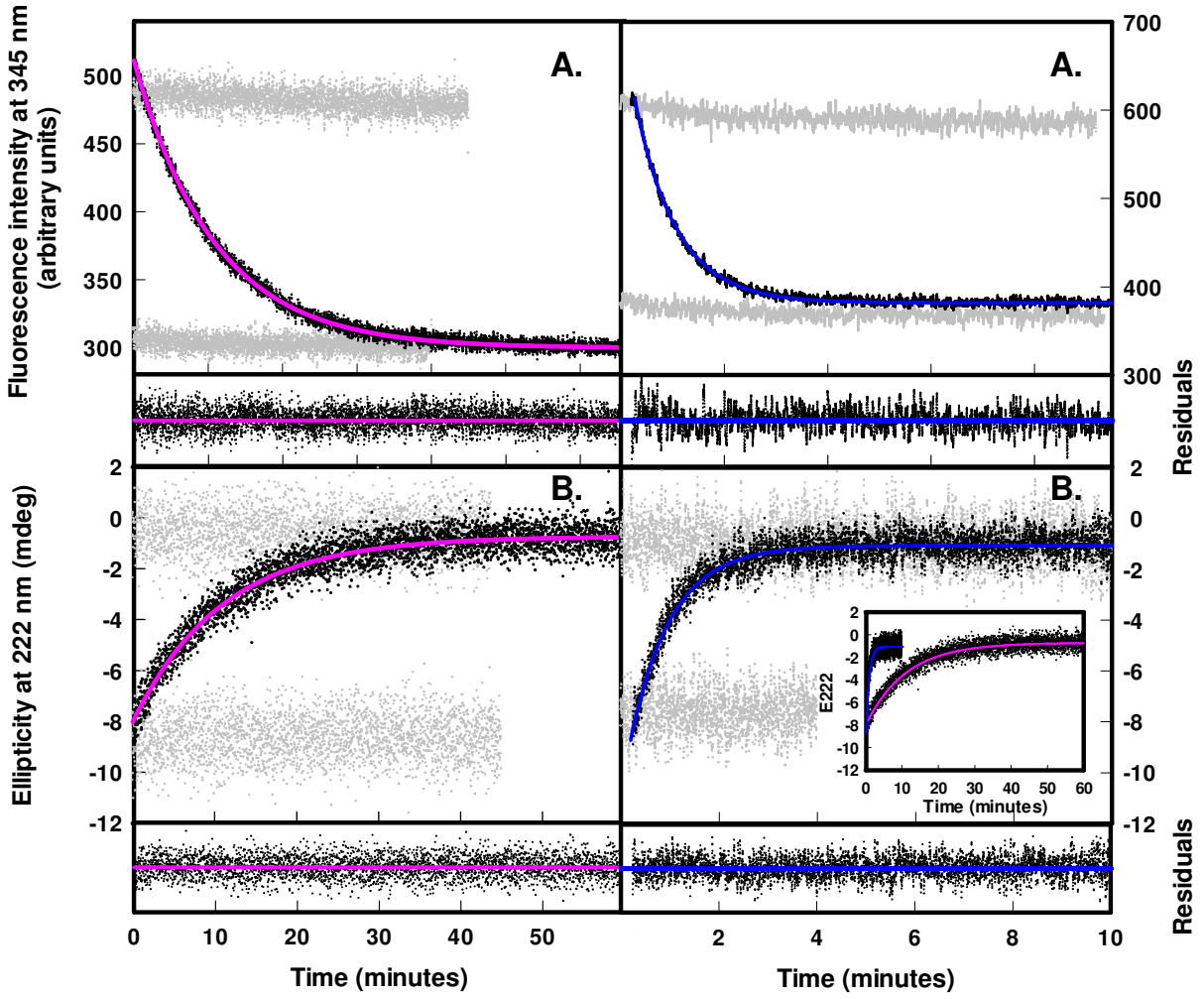


Figure 53: Unfolding kinetics using fluorescence and circular dichroism as probes

Unfolding kinetics of 2 µM CLIC1 pH 7.0 (pink) and pH 5.5 (blue) in the presence of a final concentration of 7.5 M urea using both fluorescence emission at 345 nm **(A)** and circular dichroism ellipticity at 222 nm **(B)** as probes. Baselines of the native state and CLIC1 denatured in 7.5 M urea are shown in grey. The unfolding traces were recorded at 20°C using manual mixing methods. The traces were fit to a single exponential model using SigmaPlot® v8.0. The R^2 value for each fit was > 0.97. The residuals are plotted in the panel below each figure. **The insert** shows a comparison of the E_{222}-monitored unfolding trace at pH 7.0 and pH 5.5.

Unfolding of CLIC1 at pH 7.0 / 20^{o}C occurs at similar rates when using either circular dichroism or fluorescence as probes. The traces fit a single exponential model at all final urea concentrations measured and there is no burst phase detected. The unfolding of CLIC1 at pH 7.0 is fairly slow, much slower than the unfolding of other members of the GST superfamily including the monomeric Grx2 (Wallace *et al.,* 1998b; Gildenhuys PHD thesis, 2006).

As at pH 7.0, the unfolding reaction at pH 5.5 / 20^{o}C is first order and fits a single exponential model with no detectable burst phase. The secondary and tertiary structures of CLIC1 at pH 5.5 also unfold at essentially the same rate. However there is a major difference in the unfolding rates monitored at pH 7.0 and pH 5.5. At pH 5.5 CLIC1 unfolds ~40 times faster than at pH 7.0! The circular dichroism-monitored traces at pH 7.0 and pH 5.5 are compared in the insert in Figure 53.

The dependence of the unfolding rate constants on urea was compared at pH 5.3, pH 5.5, pH 7.0 and pH 8.2 (Figure 54). The rate at which CLIC1 unfolds is proportional to the pH, the higher the pH, the longer the protein takes to unfold. The M_u value is defined as the change of the rate constant with urea concentration as the protein unfolds. It is represented by the apparent m_u value multiplied by the temperature and the universal gas constant.

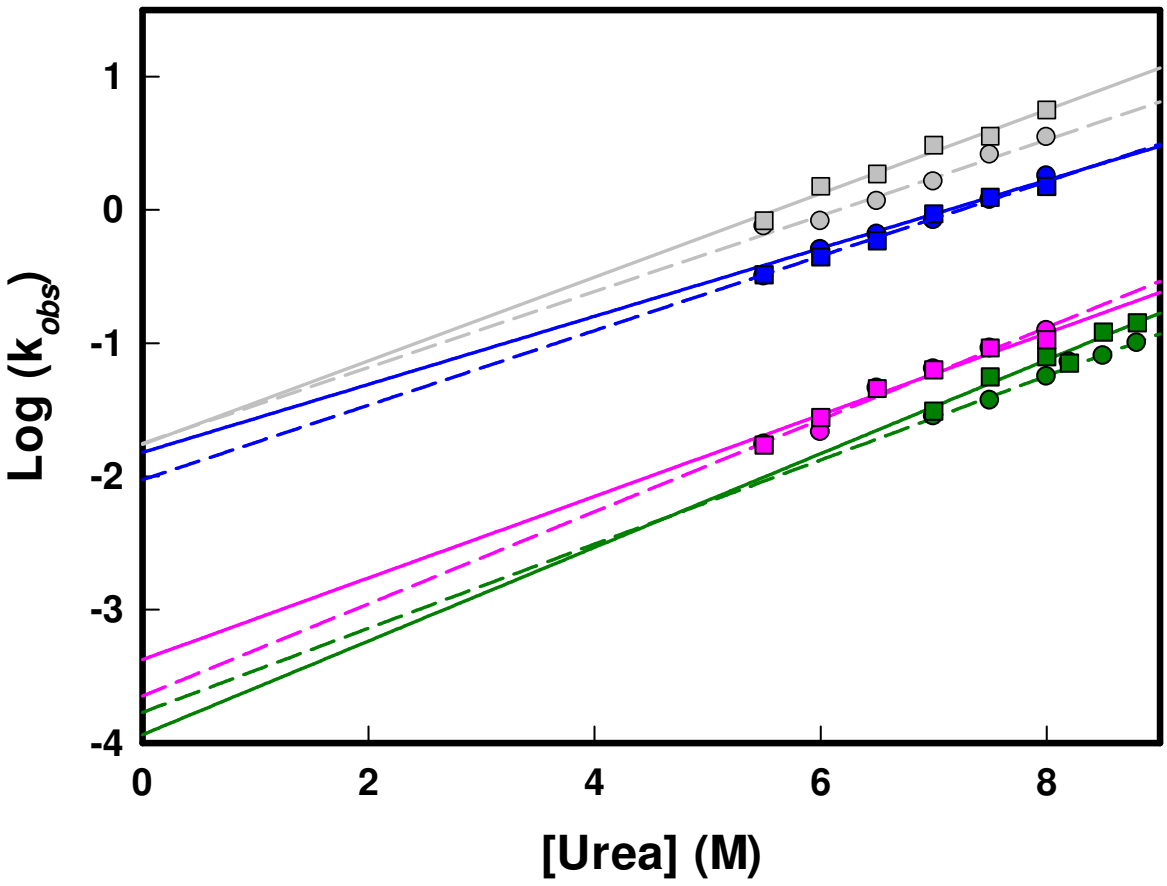


Figure 54: Urea dependence of the unfolding rates of CLIC1 at pH 8.2, 7.0, 5.5 and 5.3

Urea dependence of the single exponential unfolding rate constant (k_{obs}) for 2 µM CLIC1 at pH 8.2 (green), pH 7.0 (pink), pH 5.5 (blue) and pH 5.3 (grey). Unfolding experiments were conducted in 50 mM Na_2HPO_4 buffer, 0.02% NaN_3 and 1 mM DTT at 20°C using circular dichroism ellipticity at 222 nm (E_{222}) (●) and fluorescence emission at 345 nm (F_{345}) (■) as probes. Manual mixing methods were employed. The linear fit to the circular dichroism data is given by a dashed line while the fit to the fluorescence data is given by a solid line. The slopes of the linear fits to the data are used for the M_u values represented in Table 5. The slopes are parallel and the M_u values are therefore similar despite the different pH.

The I → D transition

Is the rate at which the intermediate species unfolds identical to the rate at which the native state unfolds? In order to answer this question CLIC1 was incubated at equilibrium in the presence of 3.8 M urea at pH 5.5 / 20^{o}C so as to obtain the stable intermediate species. This species was then unfolded in the presence of a final concentration of 5.5 M to 8 M urea. As a control, the same experiment was conducted at pH 7.0 / 20^{o}C despite the fact that the intermediate is not detectable under these conditions. Representative unfolding traces are shown in Figure 55. At pH 7.0 there is not much difference in the spectroscopic signals whether the protein is in its native state or in the presence of 3.8 M urea. The unfolding trace is monoexponential and no burst phase is detectable. At pH 5.5 there is a large difference between the native and intermediate baselines especially when E_{222} is used as a probe. The unfolding trace still fits to a single exponential model but a burst phase can be detected in the circular dichroism-monitored transitions at high urea concentrations (> 7 M).

Interestingly, *the rate of unfolding of the intermediate species is equivalent to that of the native state* (Figure 56). Since at pH 7.0 the protein is still in the pre transition region when in the presence of 3.8 M urea and there is no detectable intermediate under these conditions (Figure 42) it is not surprising that the protein unfolds at the same rate as the native state when in the presence of 3.8 M urea. At pH 5.5 / 20^{o}C the equilibrium intermediate species that is stable in 3.8 M urea also appears to unfold at the same rate as the native state, however. Furthermore the secondary and tertiary structures of this species unfold at the same rate. The percentage surface area exposed in the transition state when the intermediate state is unfolded is comparable with the amount of surface area exposed upon unfolding of the native state (Table 5) which implies that the intermediate species is relatively compact in nature.

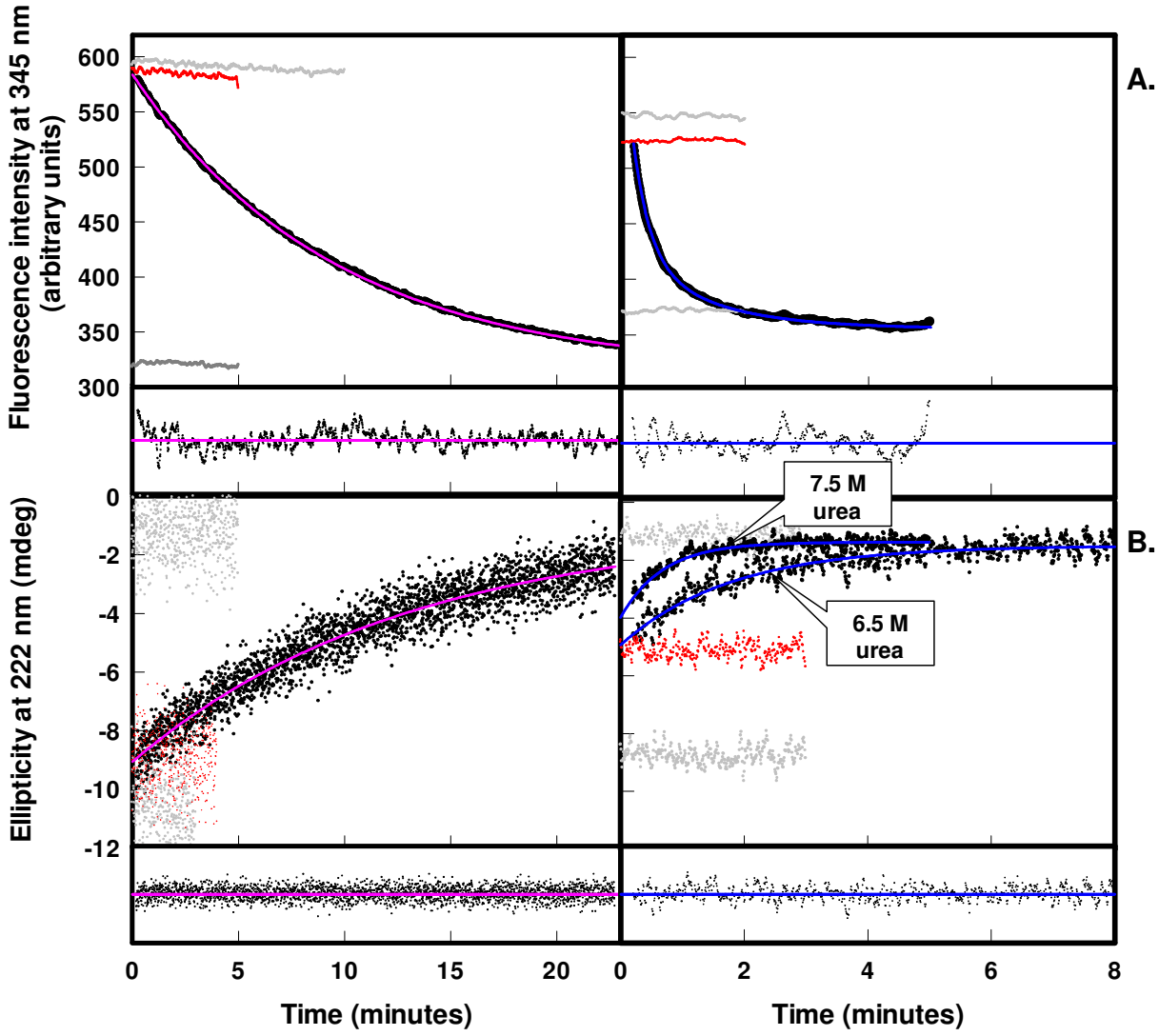


Figure 55: Unfolding kinetics of the CLIC1 equilibrium intermediate

Representative unfolding kinetics traces of 2 µM CLIC1 at 20°C in the presence of 3.8 M urea at pH 7.0 (pink) and pH 5.5 (blue). Unfolding was conducted using manual mixing methods and both F_{345} **(A)** and E_{222} **(B)** were used as probes. The solid lines represent the fit to a single exponential function and the residuals are plotted in the panels beneath each figure. The R^2 value for each fit was > 0.95. Native and denatured baselines are shown in grey while the baseline representing the intermediate species (CLIC1 in 3.8 M urea) is red. All traces are representative of CLIC1 in a final concentration of 7.5 M urea except for the trace at pH 5.5 using circular dichroism as a probe where two traces (final urea concentration of 7.5 M and 6.5 M) are represented.

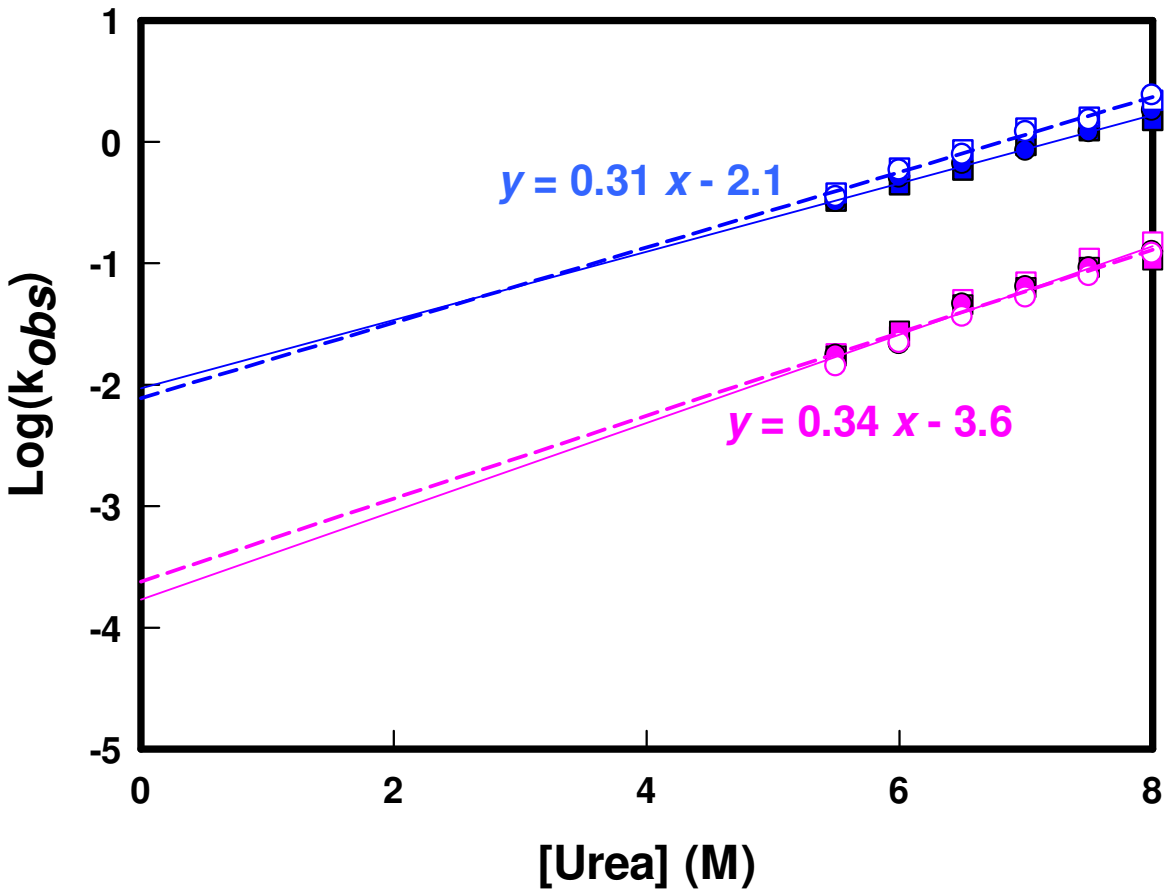


Figure 56: Urea dependence of the unfolding rate constants of CLIC1 - comparison of the N → D and I → D transitions

The urea dependence of the single exponential rate constants for the unfolding of 2 µM CLIC1 from 3.8 M urea to the denatured state. The unfolding was conducted at pH 7.0 (pink) and pH 5.5 (blue) using E_{222} (●/○) and F_{345} (■/□) as probes. Both the N → D (closed) and I → D (open) transitions are represented. The equations for the fits to the I → D transitions (dashed lines) are shown. For comparison the equation for the N → D transition at pH 7.0 is $y = 0.36\ x - 3.8$ and at pH 5.5 is $y = 0.28\ x - 2.0$.

The N → I transition

Since there is not much difference in the rate of the N → D and I → D transitions it is likely that there is a difference in the rate of the N → I transition and that this transition actually forms the rate limiting step in the unfolding process of CLIC1. Therefore, at pH 5.5 / 20^{o}C CLIC1 was unfolded from the native state to urea concentrations at which the intermediate species is populated at equilibrium (2.8 M – 4.5 M urea). A representative unfolding trace in the presence of a final denaturant concentration of 4 M urea is shown in Figure 57. Both circular dichroism (E_{222}) and fluorescence (F_{345}) were used to probe the rate of intermediate formation.

The F_{345}-monitored trace is most intriguing because the unfolding of the native state to the intermediate state as monitored by fluorescence of Trp35 is no longer monophasic but clearly exists in two exponential transitions. The fluorescence intensity initially drops with a relatively large change in amplitude as happens in the N → D transition, but then the intensity becomes enhanced (small amplitude change) before finally reaching the baseline. The E_{222}-monitored transition cannot distinguish between the two phases and the unfolding kinetics trace as monitored by circular dichroism still fits well to a single exponential model.

The dependence of the unfolding rate constants on urea (Figure 58) clearly indicates the two distinct phases in the fluorescence-monitored N → I transition as opposed to the single phase in the N → D or I → D transitions. The two phases detected by fluorescence are marked by distinct differences in their M_u values. One phase has the same urea-dependence on the rate constant as the N → D and I → D transitions (M_u ~0.17 kcal/mol/M urea) (Table 5). The other phase has a much greater slope (M_u ~0.63 kcal/mol/M urea) which implies that at the higher urea concentrations required to produce the denatured state this phase would occur so fast that it would not be detected.

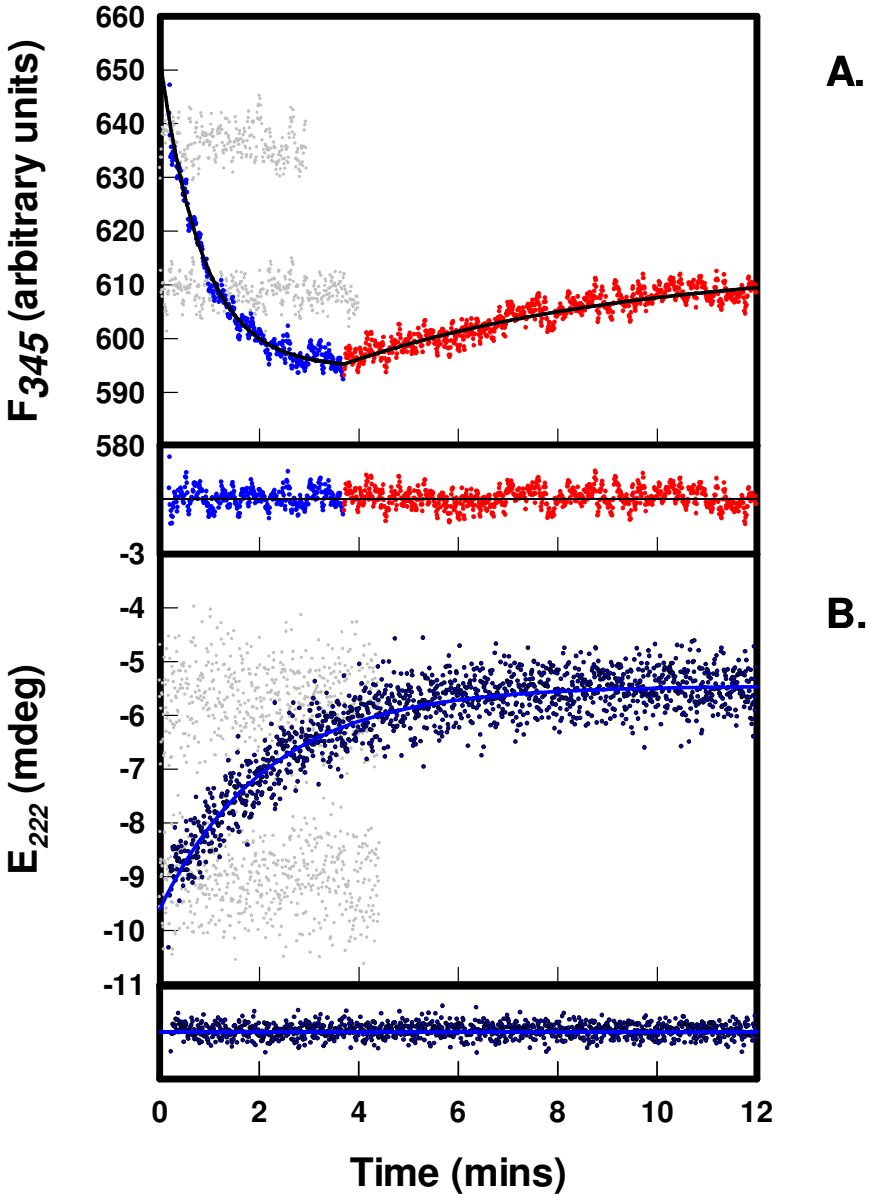


Figure 57: Kinetics of formation of the equilibrium intermediate

Representative unfolding kinetics traces of 2 µM native CLIC1 at pH 5.5 / 20°C. Unfolding was conducted using manual mixing methods and both F_{345} **(A)** and E_{222} **(B)** were used as probes. The solid lines represent the fit to a single exponential function and the residuals are plotted in the panels beneath each figure. The R^2 value for each fit was > 0.95. The F_{345}-moitored transition occurs in two phases which are represented in blue and red for clarity. Native and denatured baselines are shown in grey. All traces are representative of CLIC1 in a final concentration of 4.0 M urea, which is characteristic of the equilibrium intermediate.

This could account for the burst phase observed at high urea concentrations in the I → D transition (Figure 55). The two phases represent two species present as the protein unfolds, one that is either more compact to start with or that results in being far less compact than the other. Circular dichroism only identifies a single exponential reaction because it only detects the phase with the increased M_u (Table 5).

3.5.2. Effect of Salt on Unfolding Kinetics

NaCl

NaCl has the least effect of the salts studied on the structure or stability of CLIC1. The effect of 0.5 M NaCl on the kinetics of the N → D transition was studied at pH 7.0 / 20°C and pH 5.5 / 20°C using E_{222} and F_{345} as probes (Figure 59). The unfolding rate has a greater dependence on urea at both pH when in the presence of 0.5 M NaCl than when in the absence of salt and the apparent m_u value is increased at both pH. This means that the native state is more compact when in the presence of NaCl. Confirming this conclusion, the percentage buried surface area exposed in the transition state upon unfolding is greater when in the presence of NaCl at both pH (Table 5). The time constant increases 12.6 times at pH 5.5 and 2.9 times at pH 7.0 (Table 5) and therefore the presence of NaCl can be said to have a stabilising effect on the native state and far more so at pH 5.5.

NaF

Since NaF has a pronounced effect on the structure of the protein and was shown to stabilise the equilibrium intermediate, its effect on the unfolding kinetics was studied (Figure 60). Both the N → D and N → I transitions were considered.

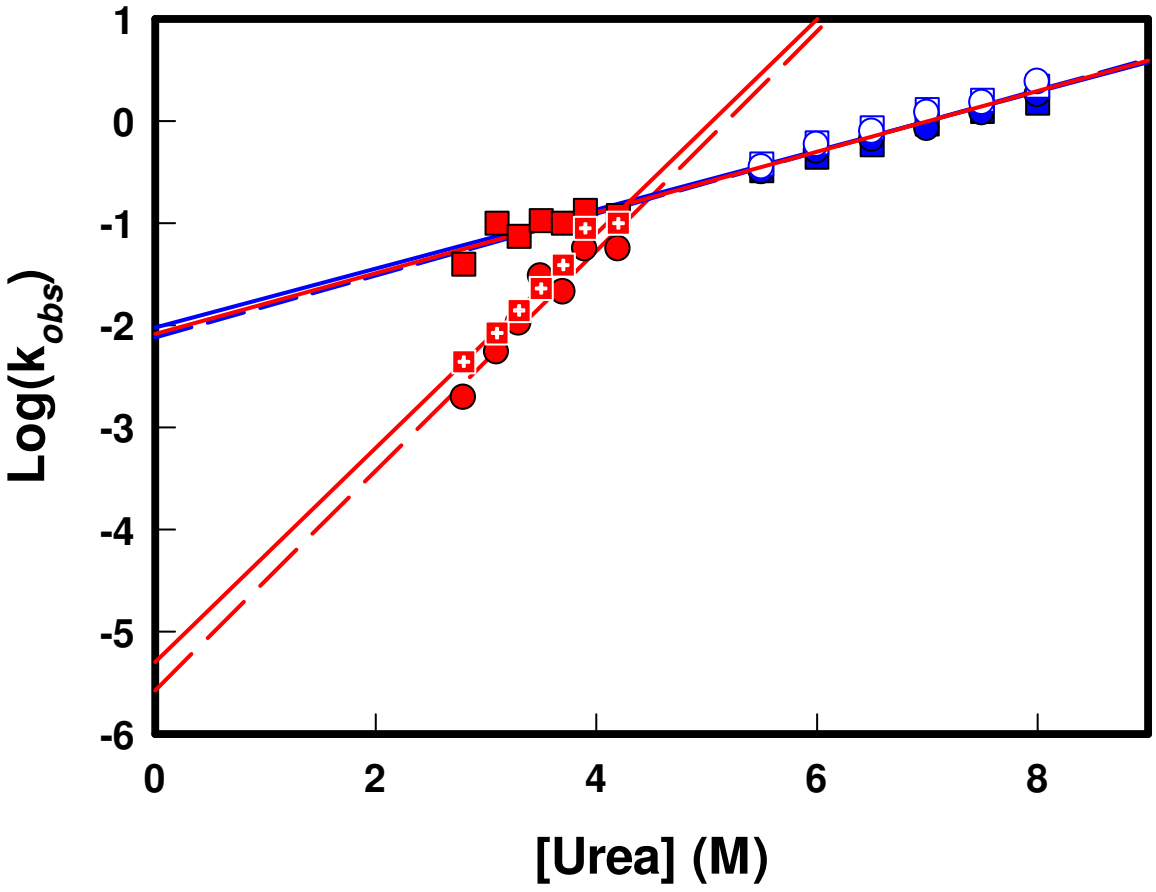


Figure 58: Urea dependence of the rate constants for the N → I transition

2 µ M CLIC1 was unfolded at pH 5.5 / 20°C from the native state (0 M urea) to the intermediate state (2.8 M to 4.5 M urea). The unfolding was conducted using E_{222} (●/○) and F_{345} (■/□/⊠) as probes. The N → D (closed blue symbols and solid blue line); I → D (open blue symbols and dashed blue line) and N → I (red) transitions are represented. The N → I transition consists of the single E_{222}-monitored phase (red circles and dashed red line) and the two F_{345}-monitored phases (red squares and solid red lines).

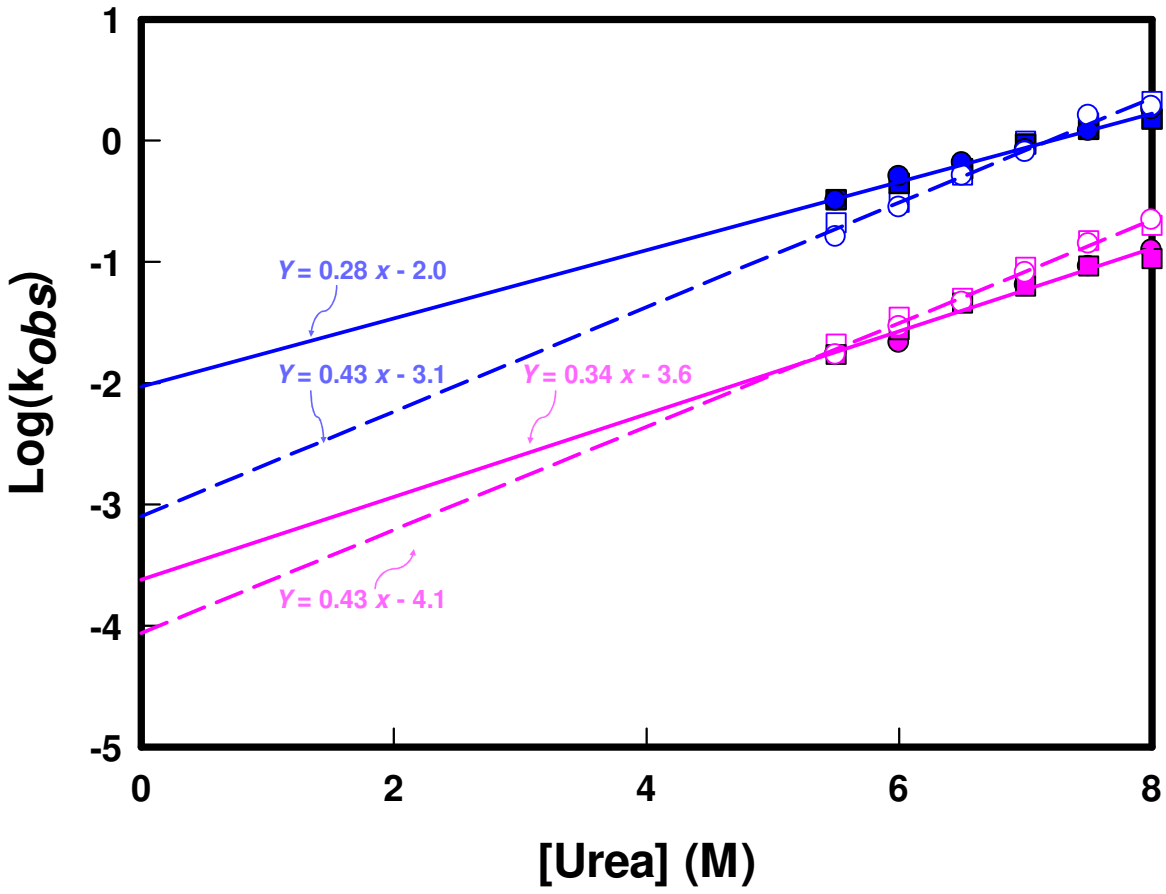


Figure 59: Comparison of unfolding kinetics of CLIC1 in the presence and absence of NaCl

Urea dependence of the unfolding rate of 2 µM CLIC1 at pH 7.0 (pink) and pH 5.5 (blue) when in the presence (open symbols and dashed lines) and absence (closed symbols and solid lines) of 0.5 M NaCl. E_{222} (●/○) and F_{345} (■/□) were used to probe the unfolding rate of the N → D transition at 20°C. The equations for the linear fit to the points (a combination of the circular dichroism and fluorescence data) are represented next to each curve.

At pH 7.0 / 20°C, 0.5 M NaF *slows down* the unfolding rate by about 5 times the rate in the absence of salt (Table 5). At pH 5.5 / 20°C however, the rate at which the protein unfolds is actually *increased* 15.4 times by NaF, so much so that the F_{345}-monitored transitions were too quick to capture using manual methods and only the E_{222}-monitored transitions are reported here. This increase in the rate constant is not observed at pH 7.0 in the presence of NaF and nor is it observed at pH 7.0 or pH 5.5 in the presence of NaCl. Furthermore NaF causes a decrease in the percentage buried surface area exposed in the transition state upon unfolding. This is the opposite effect to when in the presence of NaCl at pH 7.0 or pH 5.5 or to when in the presence of NaF at pH 7.0. This means that either NaF reduces the compactness of the native state or it increases the compactness of the denatured state at pH 5.5. Nevertheless it is certain that NaF interacts specifically with CLIC1 at pH 5.5 in a way that is different to when in the presence of any other salts or to the situation at pH 7.0. The apparent m_u value is increased in 0.5 M NaF at pH 7.0 (Table 5) which is the same effect as when CLIC1 is in the presence of 0.5 M NaCl (Figure 59). At pH 5.5, the apparent m_u value remains unchanged whether in the presence or absence of NaF.

The N → I transition was monitored in the presence of 0.5 M NaF at pH 5.5 / 20°C only. As in the absence of NaF, the F_{345}-monitored transitions are visibly biexponential and follow the same trend as in the absence of salt (Figure 57). Once again, the E_{222}-monitored transition only distinguishes one phase. The only difference is that the intermediate is formed faster when in the presence of NaF than when in the absence of salt. This could be because this salt stabilises the intermediate state relative to the native state. The same situation is observed with the slow fluorescence phase when in the presence and absence of NaF. The fast fluorescence phase is not dependent on the NaF however, and is identical whether in the presence or absence of NaF. This phase (which corresponds to the phase of the most change in amplitude) does not represent intermediate formation and the formation of the intermediate is a much slower, NaF-affected, process.

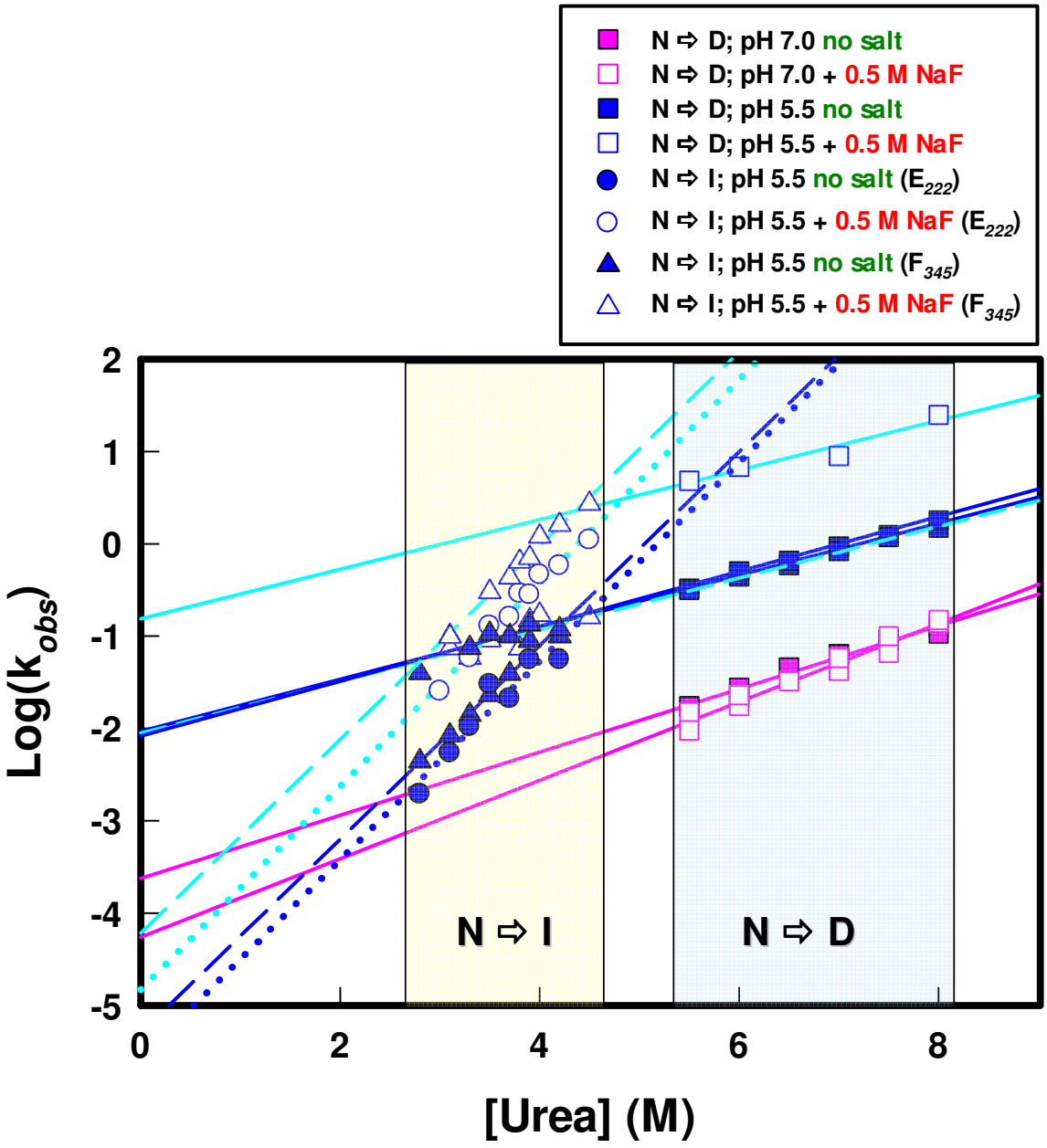


Figure 60: Unfolding kinetics in the presence of NaF

Urea dependence of the unfolding rate constants of 2 µM CLIC1 at pH 7.0 (pink) and pH 5.5 (blue) in the presence (open symbols) and absence (closed symbols) of 0.5 M NaF at 20°C. The N → D transition was monitored by both circular dichroism and fluorescence and is represented by squares (■/□) and solid lines. The N → I transition was only determined at pH 5.5. Circles (○/●) and dotted lines represent the E_{222}-monitored transition and triangles (▲/△) and dashed lines represent the F_{345}-monitored transitions. Cyan lines represent the fit to data in the presence of 0.5 M NaF while blue lines represent the fit to the data in the absence of salt.

3.5.3. Effect of Temperature on Unfolding Kinetics

Since the equilibrium properties of CLIC1 at pH 7.0 / 37^{o}C imitate those at pH 5.5 / 20^{o}C, the rate of unfolding at pH 7.0 / 37^{o}C was compared with events at 20^{o}C. Unfortunately only circular dichroism could be used to probe the unfolding kinetics at 37^{o}C due to the absence of a thermal regulator for fluorescence experiments. CLIC1 is prone to aggregate at pH 5.5 / 37^{o}C in the presence of even mild concentrations of urea (Figure 46) so the experiments were only conducted at pH 7.0 / 37^{o}C (Figure 61).

Once again the properties of CLIC1 at pH 7.0 / 37^{o}C resemble those of the protein at pH 5.5 / 20^{o}C. The rate of unfolding at pH 7.0 is increased at 37^{o}C from the slow rate at 20^{o}C to the same rate as at pH 5.5 / 20^{o}C (Table 5). This is true for both the N → D and the I → D transitions. Both these transitions are monophasic as monitored by circular dichroism and a slight burst phase is only noticeable in the I → D transition at high urea concentrations. An increase in the temperature to 37^{o}C at pH 7.0 greatly increases both the rate of unfolding of the native state and the percentage surface area exposed upon unfolding due to the destabilising nature of the higher temperature.

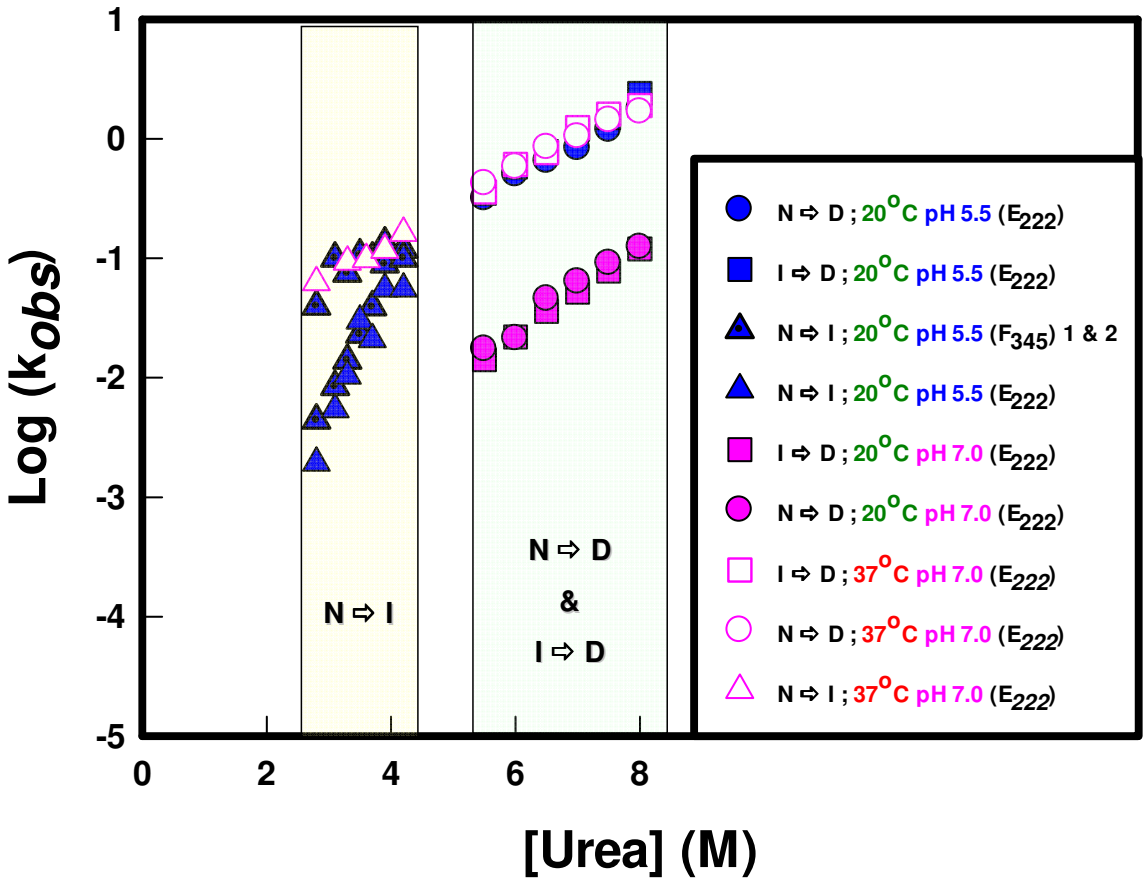


Figure 61: Unfolding kinetics of CLIC1 at pH 7.0 / 37°C

Urea dependence of the unfolding rate constants of 2 µM CLIC1 at pH 7.0 (pink) and pH 5.5 (blue) at 20°C (closed symbols) and at 37°C (open symbols). Only circular dichroism data is represented for the N → D (●/○) and I → D (■/□) transitions. In the N → I transition (▲/△) the dotted triangles represent F_{345}-monitored transitions. All other transitions are monitored by E_{222}.

The N → I transition is interesting in that, similar to when at pH 5.5 / 20°C, E_{222} can only detect one unfolding phase. However, unlike when at pH 5.5 / 20°C, this phase corresponds with the fast unfolding kinetics phase and has the same rate of unfolding and apparent m_u value as the I → D and N → D transitions. The slow kinetics phase that is detected by E_{222} at pH 5.5 / 20°C is not to be seen at pH 7.0 / 37°C! This gives rise to several questions: Does this mean that E_{222} is not detecting the formation of the intermediate at pH 7.0 / 37°C? Does this, in turn, imply that the intermediate at pH 7.0 / 37°C is different to the pH 5.5 intermediate, or at least that the rate of formation of this intermediate is different? Unfolding of the native state to the intermediate state at pH 7.0 / 37°C occurs relatively quickly (time constant of 1.1 hours) and a much lower percentage of buried surface area is exposed in the transition state between the native and intermediate states compared to at pH 5.5 / 20°C which suggests that either the intermediate state is more compact or the native state is less compact when at the high temperature.

3.5.4. Effect of Non - Reducing Conditions on Unfolding Kinetics

The unfolding of CLIC1 under non-reducing conditions occurs in a single phase (Figure 62); however a large burst phase is detected at both pH 7.0 / 20°C and pH 5.5 / 20°C at all final urea concentrations studied. This burst phase is present in both the circular dichroism and fluorescence-monitored transitions although it is more pronounced in the circular dichroism monitored transitions (Figure 62 A).

The urea dependence of the unfolding transitions is similar whether in the presence or absence of DTT. The unfolding is slightly faster when under non-reducing conditions at pH 7.0 but the apparent m_u values are analogous. Despite the fact that the equilibrium unfolding transitions and the structure of CLIC1 show little to no pH dependence when under non-reducing conditions,

it is interesting that there is still a difference in the rate of unfolding of CLIC1 at pH 7.0 and pH 5.5 when under non-reducing conditions. This difference is smaller than when under reducing conditions, however.

3.5.5. Summary of Kinetic Parameters

The kinetic parameters for the unfolding of CLIC1 under different conditions are compared in Table 5. There is no significant difference in the M_u value obtained using circular dichroism or fluorescence as probes for the N → D and I → D transitions. This means that the secondary and tertiary structure of the protein unfold simultaneously. This is not the case for the N → I transition. The general trend is that CLIC1 unfolds faster the lower the pH, possibly due to acid destabilisation of the native state. The M_u value is also lower at lower pH which implies the native state becomes less compact as the pH is dropped. This is substantiated by the fact that the percentage buried surface area exposed in the transition state upon unfolding is lower at lower pH.

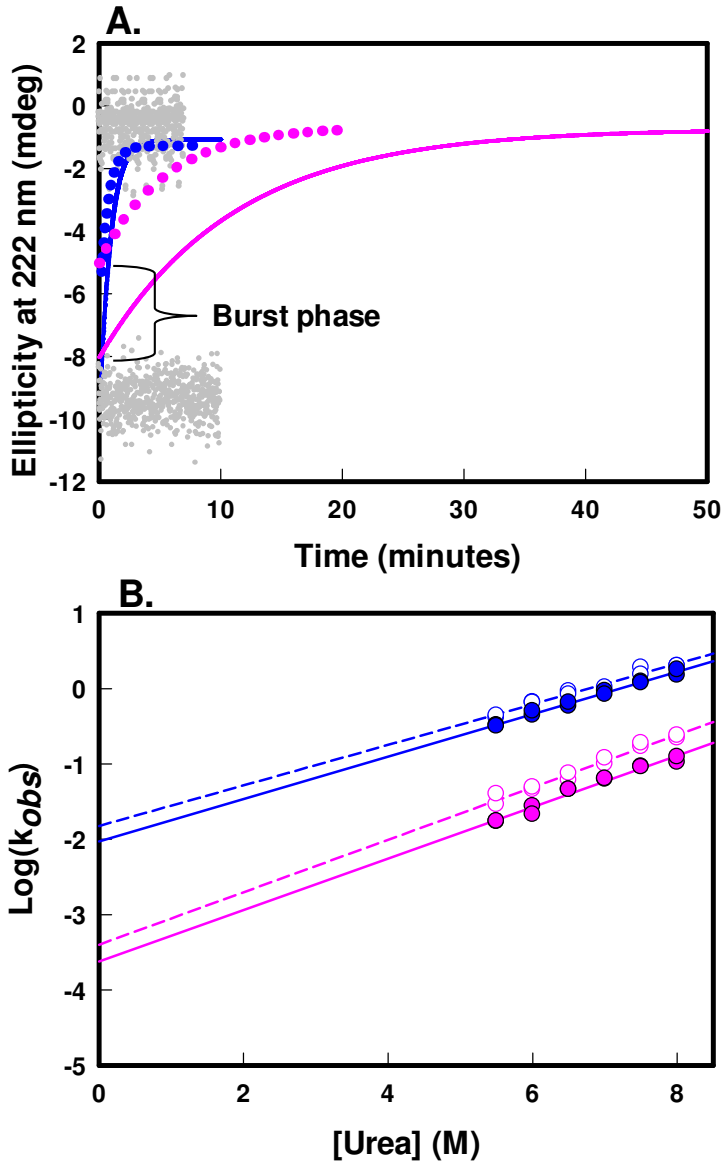


Figure 62: Unfolding kinetics when under reducing and non-reducing conditions

(A) Unfolding kinetics of 2 µM CLIC1 at 20°C in a final concentration of 7.5 M urea as monitored by circular dichroism at pH 7.0 (pink) and pH 5.5 (blue) in the presence (solid lines) and absence (dotted lines) of 1 mM DTT. Curves represent the single exponential fit to the data. Native and denatured baselines are grey. The burst phase detected under non-reducing conditions is indicated. **(B)** Urea dependence of the unfolding of CLIC1 at pH 7.0 (pink) and pH 5.5 (blue) from the native state (0 M urea) to the denatured state (5.5 M to 8 M urea). The experiment was conducted in the presence (●) and absence (○) of 1 mM DTT. Circular dichroism and fluorescence were used to probe the unfolding.

Table 5: Parameters for the unfolding kinetics of CLIC1 under different environmental conditions

		Mu (kcal/mol/M)		Time Constant in the Absence of Denaturant (hours)		Mu / *m*-value (% buried surface area exposed in transition state)	
		CD	Fluorescence	CD	Fluorescence	CD	Fluorescence
pH 8.2	N → D (20°C)	0.19 ± 0.05	0.2 ± 0.05	105	132	16	21
pH 7.0	N → I (37°C)	0.15 ± 0.56	-	1.1	-	6.5	-
	"I" → D (20°C)	0.21 ± 0.05	0.19 ± 0.04	105	105	-	-
	I → D (37°C)	0.18 ± 0.08	-	1.7	-	12	-
	N → D (37°C)	0.15 ± 0.06	-	0.84	-	15	-
	N → D (20°C)	0.21 ± 0.03	0.19 ± 0.03	84	53	11	9.5
	N → D + 0.5 M NaF (20°C)	0.22 ± 0.37	0.27 ± 0.39	167	527	22	18
	N → D + 0.5 M NaCl (20°C)	0.26 ± 0.03	0.23 ± 0.03	264	132	14	12
	N → D (20°C) non-reducing	0.19 ± 0.27	0.21 ± 0.29	33	53	29	15
pH5.5	N → I (20°C)	0.63 ± 0.81	(1) 0.61 ± 0.70 (2) 0.17 ± 0.48	1162	(1) 1332 (2) 2.1	20	(1) 20 (2) 5.5
	N → I + 0.5 M NaF (20°C)	0.64 ± 0.18	(1) 0.61 ± 0.24 (2) 0.16 ± 0.46	1127	(1) 270 (2) 1.9	12	(1) 13 (2) 3.3
	I → D (20°C)	0.19 ± 0.08	0.17 ± 0.03	2.6	1.7	-	11
	N → D (20°C)	0.17 ± 0.06	0.16 ± 0.07	1.7	1.7	10	6.7
	N → D + 0.5 M NaF (20°C)	0.16 ± 0.31	-	0.11	-	4.2	-
	N → D + 0.5 M NaCl (20°C)	0.26 ± 0.11	0.24 ± 0.1	26	17	14	8.6
	N → D (20°C) non-reducing	0.15 ± 0.06	0.16 ± 0.06	1.3	1.1	25	22
pH 5.3	N → D (20°C)	0.18 ± 0.09	0.16 ± 0.1	0.96	0.96	9.5	8.4

3.6. Properties of the Intermediate

CLIC1 appears to form a stable intermediate species at equilibrium under different conditions. These conditions include: at pH 5.5 / 20°C under mild *denaturing conditions*; at pH 7.0 / 37°C under mild *denaturing conditions*; in the presence of *mild concentrations of KSCN* at either pH 7.0 / 20°C or pH 5.5 / 20°C; in the *native state* at pH 5.5 / 37°C or in the *absence of urea* when under non-reducing conditions at 20°C. Furthermore, the urea-induced intermediate species is stabilised by the presence of NaF and Na_2SO_4. It is important to characterise these detected intermediate states in terms of their structure in order to determine whether they are all the same species or whether there are differences in the structure and stability of the intermediate when formed under these different conditions.

3.6.1. Secondary Structure of the Intermediate

The far-UV circular dichroism spectra of CLIC1 were compared under different conditions when in the native state as well as when in the presence of 3.8 M urea (Figure 63).

At pH 5.5 / 20°C and at pH 7.0 / 37°C, the native states appear to have similar secondary structures. Furthermore, the secondary structures of the intermediate species (in the presence of 3.8 M urea) are comparable, both showing a loss of secondary structure of about 25% from that of the native state. Therefore an increase in temperature or a decrease in pH appears to have a similar effect on the secondary structure of the native state as well as of the urea-induced intermediate state of the protein. At pH 7.0 / 20°C, native CLIC1 has enhanced secondary structure compared to at pH 7.0 / 37°C or at pH 5.5 / 20°C. When the protein is exposed to 3.8 M urea at pH 7.0 / 20°C, the secondary structure does not change which is consistent with the fact that the urea-induced intermediate species is not detectable under these conditions.

The native state at pH 5.5 / 37°C exhibits a ~12% drop in secondary structure compared to at 20°C. This state is not identical to the intermediate species formed under mild denaturing conditions because it contains a higher degree of secondary structure and the negative peak at 222 nm is more pronounced (Figure 63). Nevertheless, the increase in temperature to 37°C as well as the drop in pH to 5.5 has caused changes to the native structure of the protein that do resemble the urea-induced intermediate state to some extent.

When under non-reducing conditions, both at pH 7.0 / 20°C and at pH 5.5 / 20°C, the state that CLIC1 assumes in the absence of denaturant resembles the urea-induced intermediate species in terms of secondary structure (Figure 63).

3.6.2. Tertiary Structure of the Intermediate State

The intermediate species of CLIC1 was first detected with fluorescence at pH 5.5 / 20°C when the protein was under mild denaturing conditions. While the intensity is quenched in the denatured state, the fluorescence emission of the intermediate state is native-like in terms of intensity (Figure 64). Intriguingly the wavelength of the fluorescence peak shifts from approximately 345 nm in the native state to approximately 340 nm when under mild denaturing conditions. This blue shift is most apparent at 3.8 M urea and is not evident at pH 7.0 / 20°C (Figure 64 and Figure 20). The shift in the λ_{max} can be seen at pH 7.0 / 37°C when CLIC1 is in the presence of 3.8 M urea, however. Here the fluorescence emission is decreased from at 20°C due to the increase in temperature but the shapes of the spectra are identical and they peak at the same wavelength (~340 nm). Thus it is plausible that the tertiary structures of the pH- and temperature-induced species are similar.

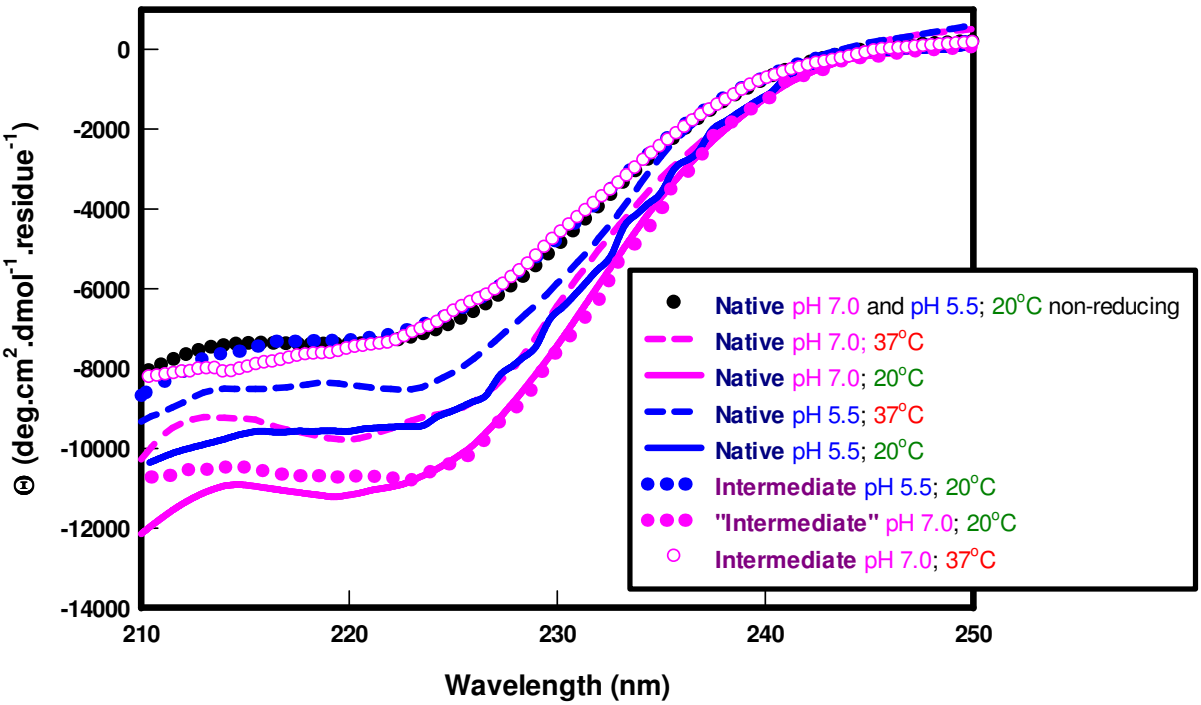


Figure 63: Far-UV circular dichroism spectra of the CLIC1 native state and intermediate species

Far-UV circular dichroism spectra of 5 µM CLIC1 (5 mM Na_2HPO_4, 0.1 mM DTT) at pH 7.0 (pink) and pH 5.5 (blue) in the presence of 3.8 M urea (dotted) and in the native state at 20°C (solid), at 37°C (dashed) and when under non-reducing conditions at 20°C (●).

At pH 5.5 the native state at 37°C also shows a blue shift in the λ_{max}; however it is not shifted as much (to ~343 nm). Presumably the native state at pH 5.5 / 37°C is a state that has a structure that is in between that of the native state at 20°C and that of the intermediate state formed under mild denaturing conditions.

The tertiary structure and packing of the protein molecule was studied further using near-UV circular dichroism at 20°C (Figure 65). The near-UV circular dichroism spectra measured at pH 7.0 in the presence and absence of 3.8 M urea have a sharp negative peak at ~285 nm due to the fixed packing of the aromatic side chains, a relatively small peak at ~278 nm and a large peak at ~267 nm. The tertiary structure of the native state at pH 5.5 is less rigid than at pH 7.0, evidenced by the far broader negative band at ~285 nm. Furthermore, the peak at ~278 nm is not pronounced at pH 5.5, although the large peak at ~267 nm remains, confirming that there is certainly a degree of tertiary structure present at this pH. When the protein is in its intermediate state (pH 5.5 + 3.8 M urea), the tertiary structure is far less defined and the protein is therefore more flexible which is typical of a molten globule state. The negative band at ~285 nm is still present although it is not well defined and the peaks at ~278 nm and ~267 nm are no longer present.

3.6.3. Hydrodynamic Diameter of the Intermediate State

The hydrodynamic diameter of the CLIC1 intermediate as detected by dynamic light scattering is larger and less compact than that of the native state although the protein is not as expanded as when in the denatured state (see Figure 41).

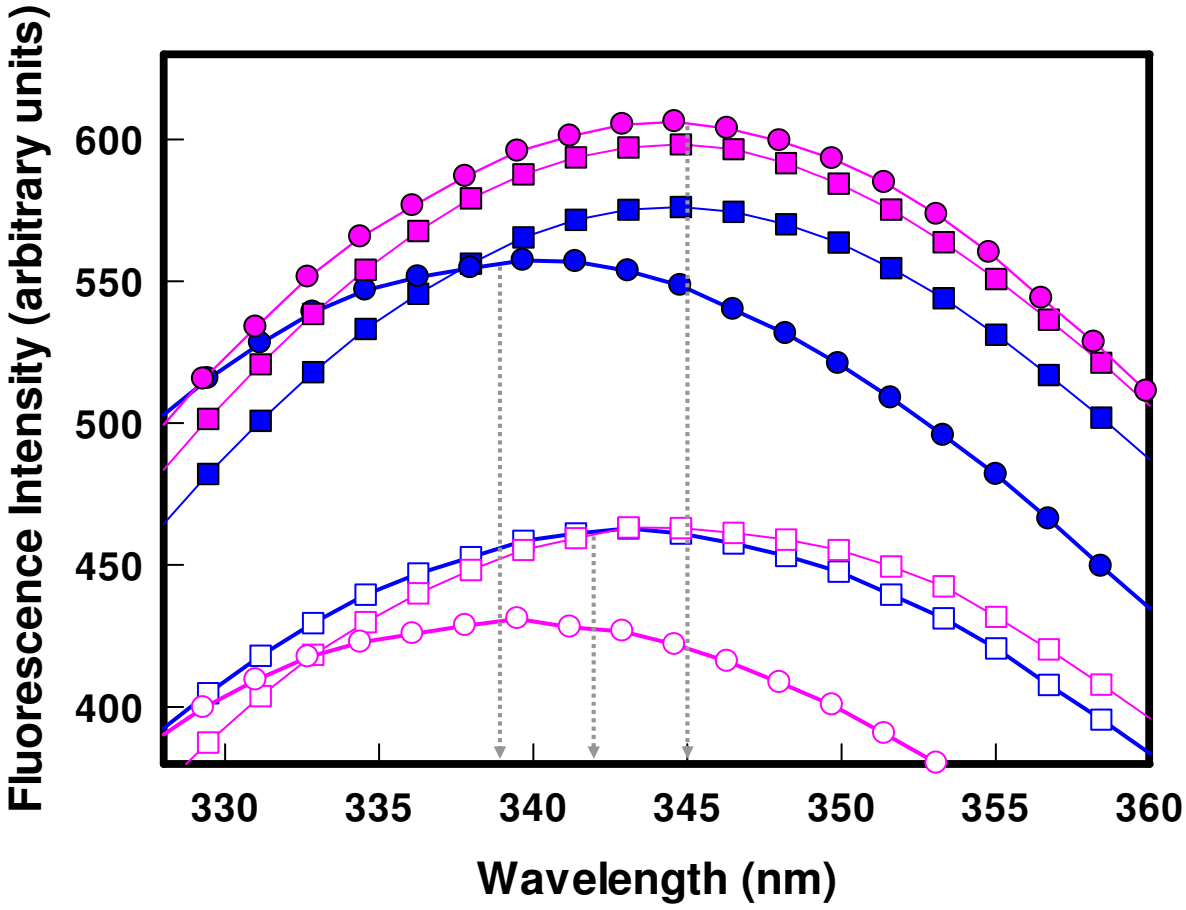


Figure 64: Fluorescence spectra of the CLIC1 native state and intermediate species

Fluorescence emission spectra of 2 µM CLIC1 (50 mM Na_2HPO_4; 0.02% NaN_3; 1 mM DTT) at pH 7.0 (pink) and pH 5.5 (blue) in the native state (■/□) and in the presence of 3.8 M urea (●/○). The protein was excited at 280 nm at 20°C (closed symbols) and at 37°C (open symbols).

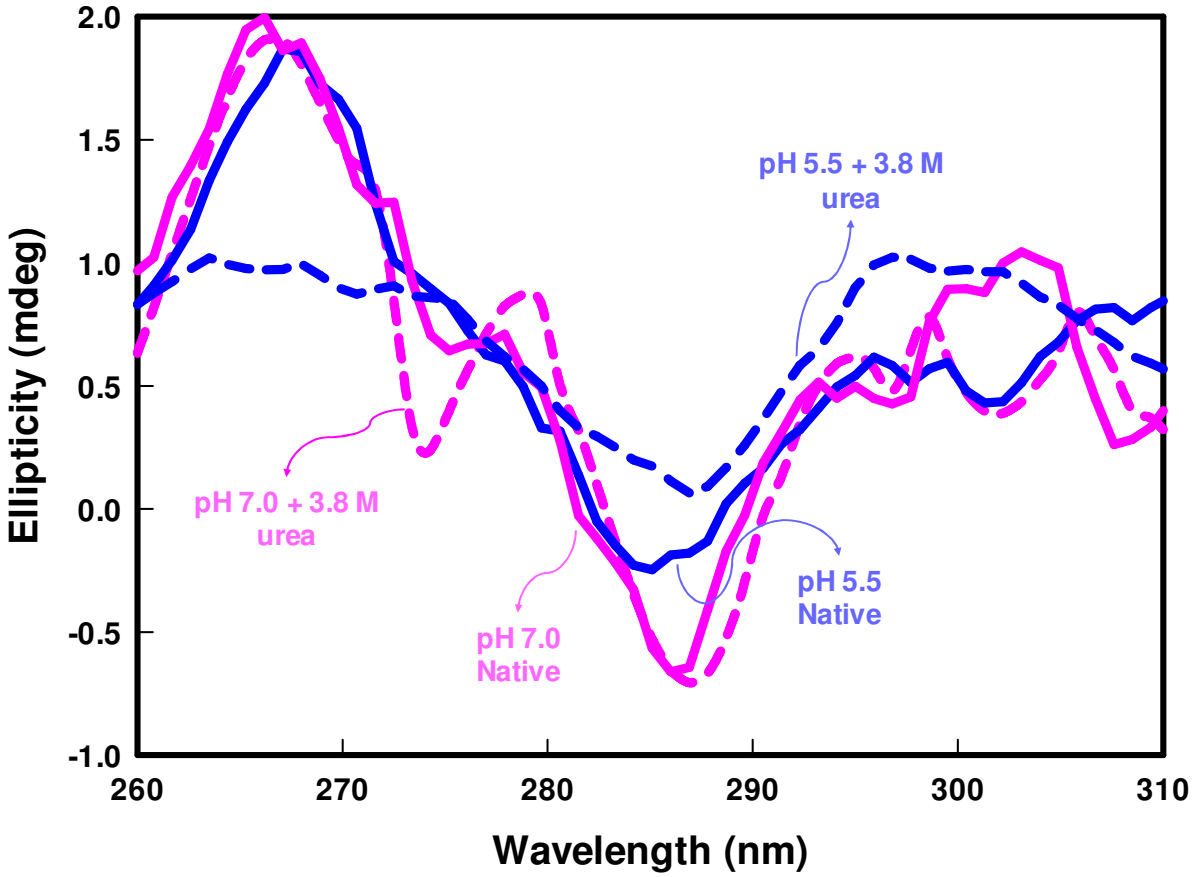


Figure 65: Near-UV circular dichroism spectra of CLIC1 at pH 7.0 and pH 5.5 in the presence and absence of 3.8 M urea

Near-UV circular dichroism spectra of 40 µM CLIC1 at 20°C at pH 7.0 (pink) and pH 5.5 (blue) in the native state (solid line) and in the presence of 3.8 M urea (dashed line). Spectra are smoothed using the negative exponential smoothing method.

3.6.4. ANS Binding to the Intermediate

The intermediate species has far more exposed hydrophobic surfaces than the native or denatured states. This is confirmed by the fact that the intermediate species binds ANS while the native and denatured states at 20°C do not (Figure 66). The unfolding curves at pH 7.0 / 37°C and pH 5.5 / 20°C are identical and superimposable whether circular dichroism or fluorescence are used as probes. The λ_{max}-monitored curve sports a dip at urea concentrations where the intermediate is populated due to the blue shifted λ_{max} of the intermediate species. ANS binds to CLIC1 at the same urea concentrations at which the dip is present, further confirming that it is the intermediate state that binds to ANS and that the intermediate has different properties to either the native or the denatured states.

At pH 5.5 / 37°C, the native state binds ANS by the same proportion as the intermediate state in the presence of mild concentrations of urea (shown by the ringed triangle in Figure 66). Furthermore, ANS binds to CLIC1 at pH 7.0 and pH 5.5 in the absence of urea when under *non-reducing conditions* at 20°C. Thus "native" CLIC1 resembles the denaturant-induced intermediate species when the temperature is increased, when the pH is dropped or when reducing conditions are removed.

3.6.5. Kinetics of Formation of the CLIC1 Intermediate

While unfolding of CLIC1 from the native to the denatured state is a single exponential reaction at both pH 7.0 and pH 5.5 under all conditions studied, the formation of the intermediate species from the native state occurs in two distinct kinetic phases as detected by fluorescence of Trp35. The fast phase resembles the unfolding rate from the N → D transition while the slow phase is unique to the N → I transition. The rate of formation of the intermediate species is increased by the presence of NaF, while an increase in temperature to 37°C at pH 7.0 results in a destabilised intermediate and native state.

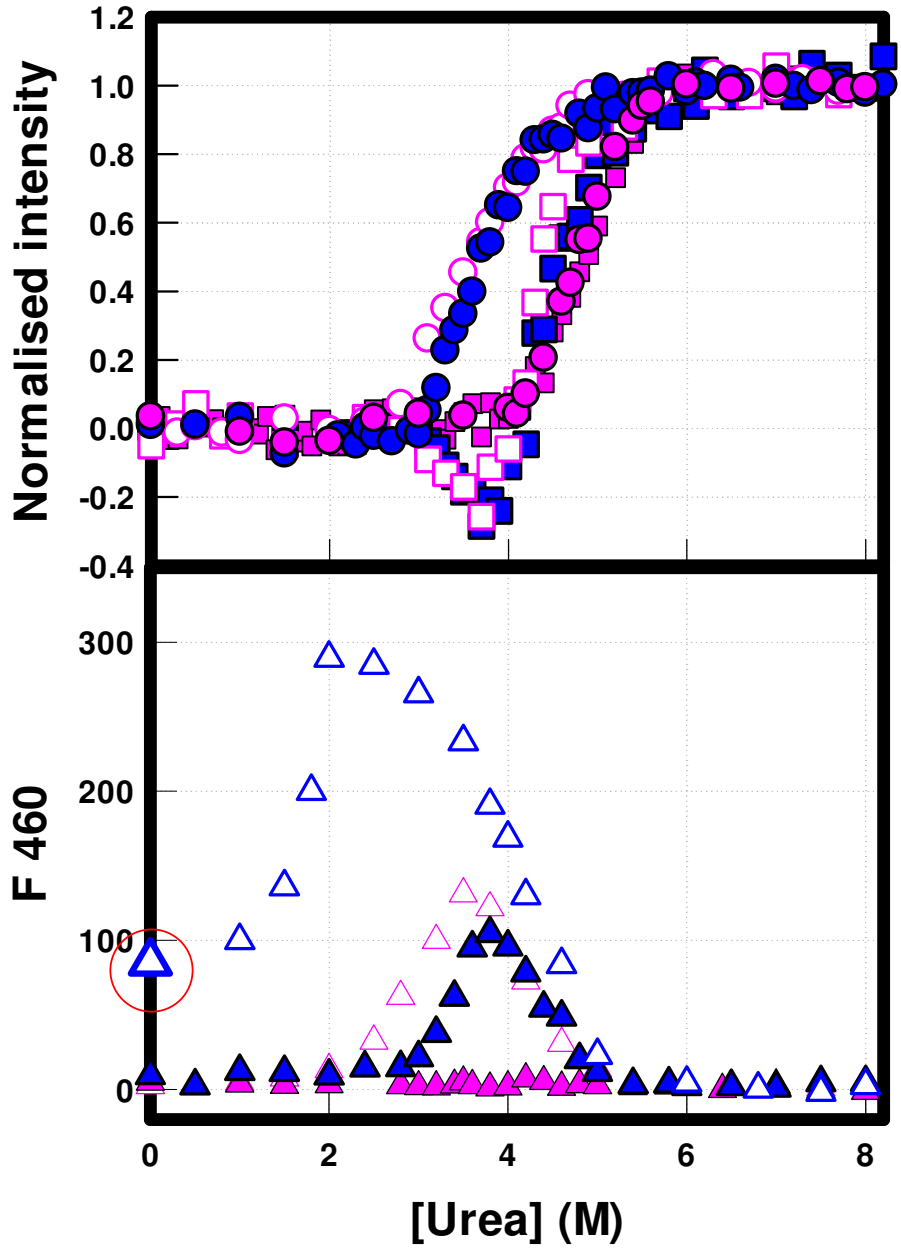


Figure 66: ANS binds to the equilibrium intermediate at 20°C and 37°C

Equilibrium unfolding of 2 µM CLIC1 at pH 7.0 (pink) and pH 5.5 (blue) at 20°C (closed symbols) and at 37°C (open symbols). Unfolding is monitored with E_{222} (●/○), λ_{max} (■/□) and fluorescence due to binding of 200 µM ANS to CLIC1 (▲/△). It can be seen that ANS binds to the intermediate species. The ringed triangle highlights the fact that ANS binds the native state at pH 5.5 / 37°C

Chapter 4. Discussion

CLIC1 is an unusual membrane protein in that it can exist in a *soluble state* in the cytoplasm as well as in a *membrane-bound* conformation. The principal question asked in this thesis is how does the protein convert between these two states? This necessarily leads to further probing questions: What properties of the environment are required for the conversion, when is it energetically most favourable, what structures are involved and how are they formed? In order to answer these questions the structure and stability of CLIC1 were investigated under environmental conditions typical of the cytoplasm and of the membrane surface.

4.1. Equilibrium Unfolding: Two-State *versus* Three-State

4.1.1. CLIC1 is Most Stable at pH 7.0 / 20°C

When CLIC1 is present in its soluble state in the cytoplasm/nucleoplasm of the cell, it exists in a highly reducing environment (Hwang *et al.,* 1992) at a pH of approximately 7.0. Therefore the structure and stability of the protein was studied under these conditions in order to give some indication as to the behaviour of soluble CLIC1 *in vivo*.

Structure of the native state at pH 7.0 / 20°C

pH certainly has an effect on the structure of CLIC1. The protein has the most pronounced α-helical secondary structure (Figure 18) and enhanced fluorescence (Figure 21) when in the pH range of 6.0 to 7.0 compared to at further extremes of the pH spectrum. These results complement those obtained by Warton *et al.* (2002). They compared the far-UV circular dichroism and fluorescence spectra of CLIC1 at pH 7.0 and pH 6.0 and did not find a significant difference in either of the spectra when compared at those two pHs.

When CLIC1 is in the native state at pH 7.0 / 20°C, it has the highest degree of α-helical secondary structure of any pH / temperature combination studied (Figure 19). The mainly helical nature of the protein as determined by far-UV circular dichroism is not surprising since according to the crystal structure, soluble CLIC1 is 45% α-helical in nature (Figure 8). The tertiary structure is relatively compact at pH 7.0 / 20°C with tightly packed side chains as demonstrated by near-UV circular dichroism (Figure 65) and the single tryptophan residue, Trp35 is relatively exposed to the polar solvent as evidenced by the wavelength of maximum emission of the fluorescence spectra being ~345 nm (Figure 20). This is expected since according to the crystal structure, Trp35 is ~25% solvent-exposed when CLIC1 is in its native state. The size of the protein is deceptively large according to HPLC (Figure 22) and DLS (Figure 23), while the independence of the equilibrium C_m value on protein concentration (Figure 36) implies- according to the law of mass action- that CLIC1 occurs as a monomer in solution.

It is likely that the protein exists as an "extended monomer" in solution, occupying a larger hydrodynamic volume than its more compact globular relatives such as Grx2. This can be explained in part by the highly charged nature of CLIC1 relative to Grx2 and other members of the GST superfamily. Thus CLIC1 is more hydrophilic than these proteins, and since the native state will therefore be able to interact more favourably with water, this results in a potentially more expanded native state of CLIC1, when compared to that of the other members of the family. In fact, the diameter of the crystal structure of monomeric CLIC1 can be as high as 62 Å, which is comparable with the diameter of the dimeric GSTs such as GST A1-1 (Figure 67). CLIC1 therefore has a hydrodynamic diameter closer to that of a dimer than of a monomer, which can explain the uncharacteristic results obtained from HPLC and DLS studies. The rather elongated oxidised CLIC1 dimer occupies an even greater volume, with its diameter being as high as 89 Å (Figure 67).

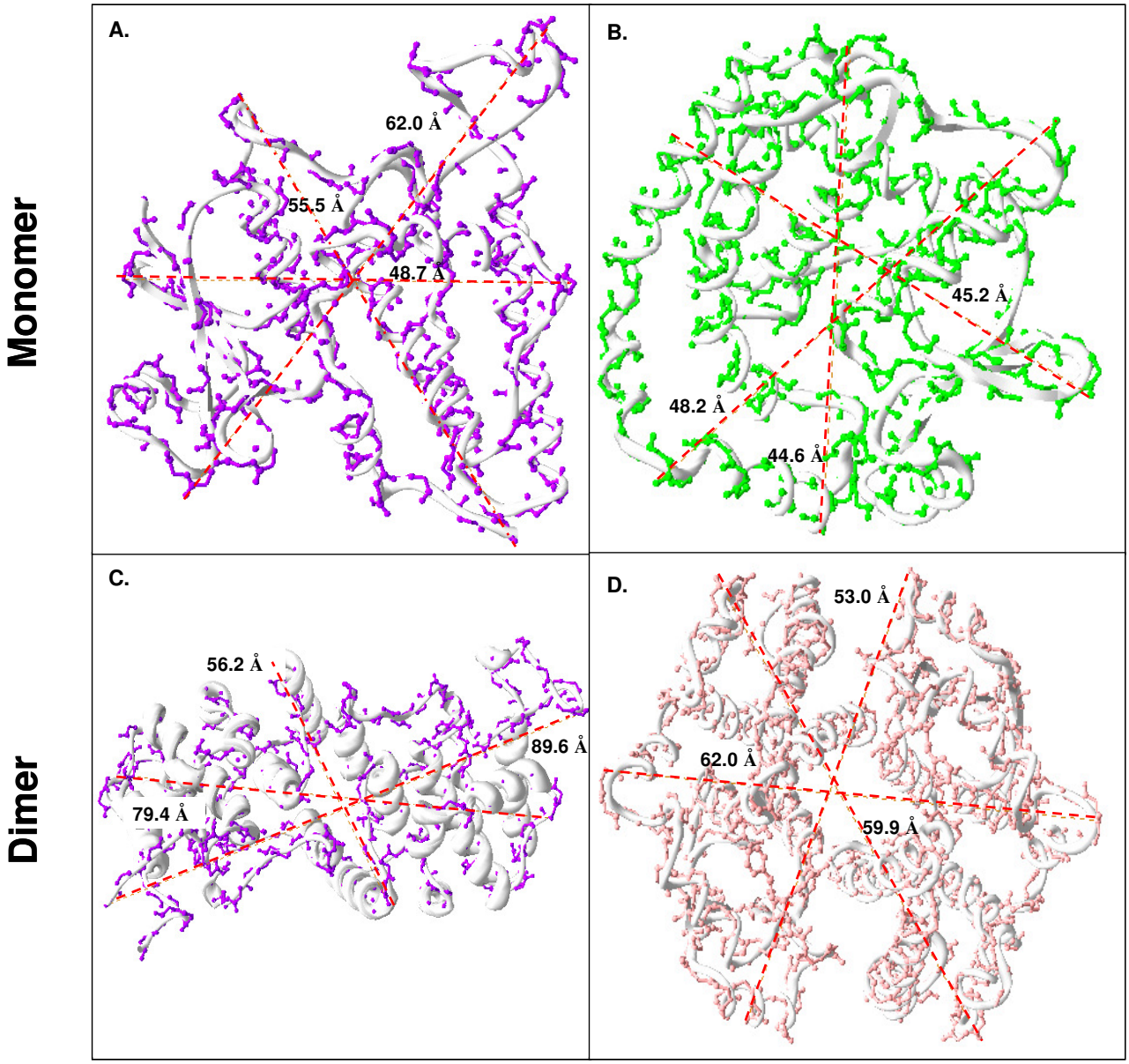


Figure 67: Dimensions of CLIC1, Grx2 and GST A1-1

Comparison of the diameter of monomeric CLIC1 **(A)** Grx2 **(B)** dimeric CLIC1 **(C)** and GST A1-1 **(D)** as obtained from the published structures 1k0m (Harrop *et al.,* 2001), 1g7o (Xia *et al.,* 2001); 1rk4 (Littler *et al.,*2004) and 1guh (Sinning *et al*, 1993) respectively. It can be seen that the hydrodynamic diameter of monomeric CLIC1 is closer to that of dimeric GST A1-1 rather than to monomeric Grx2 while dimeric CLIC1 would occupy the largest hydrodynamic radius of the four proteins.

Stability of the native state at pH 7.0

CLIC1 is at its most stable at pH 7.0 / 20°C with a $\Delta G(H_2O)$ of approximately 10 kcal/mol (Table 3). Nevertheless, this is less stable than the only other known monomeric member of the GST superfamily, Grx2. This protein has a $\Delta G(H_2O)$ value 22% greater than that of CLIC1 and a *m*-value 26% greater than the *m*-value obtained for CLIC1 (Gildenhuys PHD thesis, 2006). The difference in these values, which is fairly substantial considering Grx2 is the smaller of the two proteins, implies that the CLIC1 native state structure is not only *less stable* than the Grx2 structure but is also *less compact*, exposing a smaller proportion of surface area upon unfolding than Grx2 does. Further evidence for the CLIC1 native state being more flexible than perhaps is anticipated by its crystal structure lies in the fact that the *m*-value predicted from its amino acid constitution (Myers *et al.,* 1995) is 29% higher than the true value. Does this lower stability and decreased compactness mean that CLIC1 has a greater potential to undergo a degree of unfolding *in vivo* compared to Grx2?

The unfolding transitions of CLIC1 as monitored with circular dichroism and fluorescence are superimposable at pH 7.0 / 20°C and the protein essentially unfolds from the native state to the denatured state in a single cooperative step (Figure 42). The two-state nature of the unfolding transition negates the possibility of a stable intermediate species being populated at equilibrium at any point along the urea-induced unfolding transition of soluble "cytosolic" CLIC1. The protein therefore exists in a stable state at pH 7.0 / 20°C; however, since the stability is lower than that of other members of the family, the possibility that CLIC1 could unfold spontaneously should the conditions be optimal certainly exists. Therefore it is the aim of this work to expose the conditions under which soluble CLIC1 may unfold, at least partially, so that membrane insertion is energetically favoured.

4.1.2. CLIC1 Forms an Intermediate at pH 5.5 / 20°C

As the pH of the protein environment is lowered, protons are more likely to interact with the charges on the protein surface. This contact between hydrogen ions and surface residues will not alter the size of the residues and nor will it have significant effects on the solvent properties of water as is the case with denaturants such as urea (Kuhlman *et al.*, 1999). However, changing the pH of a protein solution will alter the charges of the residues and hence the net charge on the protein which can eventually lead to its denaturation. The addition of H^+ ions to a protein solution will have the effect of neutralizing the negatively charged residues while concurrently making the basic residues more positive. Thus, by decreasing the pH from 7.0 to 5.5, the net charge on CLIC1 will theoretically drop from -7 at pH 7.0 to -3 at pH 5.5. The intramolecular repulsive forces on the surface of CLIC1 will increase and the likely effect will be a drop in the stability of the protein at the lower pH.

Structure at low pH

A comparison of the structure of CLIC1 at pH 7.0 / 20°C and pH 5.5 / 20°C reveals that the secondary structure of this protein has reduced α-helical content at low pH compared to at pH 7.0 (Figure 19) while the tertiary structure is fairly similar as seen by the essentially equivalent fluorescence spectra (Figure 20).

The structure of the native state of CLIC1 is *more flexible at pH 5.5* and certain configurations that form rigid helices at pH 7.0 are less pronounced when at pH 5.5. This has been confirmed by hydrogen exchange mass spectrometry (Nathaniel PHD thesis, in preparation) where regions in the α1 helix and the α3 helix have been shown to become more flexible as the pH is dropped from 7.0 to 5.5. This is probably due to disruption at the low pH of the salt bridge that is formed at pH 7.0 between Arg29 in α1 and Glu81 in α3. The α8 helix in the C-terminal domain (which also forms contacts with α1) is also more flexible at pH 5.5 than at pH 7.0. The increase in the flexibility of the helices at

the low pH could explain the apparent loss of α-helical secondary structure at pH 5.5 (Figure 19). It is interesting that although Trp35 is present in the α1 helix that does become more flexible at pH 5.5, there is no significant difference in the fluorescence spectra at pH 7.0 and pH 5.5 (Figure 20). The reason for this could be that Trp35 is fairly exposed to the solvent when in the native state (Figure 8) so that even if α1 becomes more flexible it will not significantly alter the local environment and hence the degree of solvation of Trp35. Besides, it is unlikely that fluorescence will be able to detect changes in flexibility of the helices because the spectra obtained are of the protein at equilibrium which will represent an average of the small fluctuations induced by increased flexibility. Time resolved fluorescence spectroscopy would be more likely to detect increased motion of the tryptophan-containing helix.

The increased flexibility of CLIC1 at the low pH would imply a lower stability of the native state under these conditions. This improves the probability of at least a portion of CLIC1 unfolding spontaneously when at low pH. In fact this "portion" of the protein is likely to be none other than the proposed transmembrane domain including the residues of the α1 helix and β2 strand of the N-terminal domain that have a high propensity to form a helix according to AGADIR analysis (Nathaniel PHD thesis, in preparation). Exposure of these residues to the solvent will allow them to fulfil this predisposition to form a helix, which could then be driven into the membrane to form the transmembrane portion of the protein; causing the more stable C-terminal domain to remain behind.

Stability at low pH

The urea-induced equilibrium unfolding curves in Figure 41 and the data in Table 3 illustrate that CLIC1 is at its *most stable at pH 7.0 / 20^{o}C* and its stability decreases when the pH is increased or decreased from 7.0. The apparent greater stability of CLIC1 at pH 7.0 means that the protein requires more energy to unfold when at pH 7.0 and the interior packing forces of the

native state of the protein are also greater at this pH (Neet and Timm, 1994). The apparent drop in stability of CLIC1 with a drop in pH can be explained in the following way: The native and denatured states as well as any potential intermediate states of the protein may have different capacities for the binding of H^+ ions, the consequence of which will be a change in the stability of the different states of the protein as the pH is changed (Tan *et al.*, 1995). The dependence of a protein's stability on pH is controlled by the net charge on the protein as well as the pK_a of the ionisable residues in the native and denatured states (Shaw *et al.,* 2001). Thus, although Linderstrøm-Lang theorised in 1924 that a protein should be most stable at its p*I* because of a reduced number of unfavourable electrostatic interactions among charged residues, this is not necessarily the case. For example CLIC1 shows a reduced stability at pH 5.5 despite the fact that the p*I* of this protein is around 5. The reason for this can be ascribed to the burial of nontitratable ionic groups that causes the electrostatic contribution towards the stability of the protein to become asymmetrical (Stigter and Dill, 1990).

CLIC1 contains 12 aspartate and 21 glutamate residues (14% acidic character) most of which are on the surface of the protein, accessible to both water molecules and solvent ions and therefore highly sensitive to the external proton concentration. A number of these residues form salt bridges and hydrogen bonds on the surface of CLIC1. It is specifically these interacting residues that will have an effect on the stability of the protein as the pH is dropped. This is because these residues are more difficult to protonate since they are involved in interactions. The decreased pK_a of their carboxylate group means they will only become protonated at a lower pH than the non-interacting residues (Kuhlman *et al.*, 1999).

The thus likely depressed pK_a values of some of the acidic residues on the surface of CLIC1 and the fact that its stability appears to drop as the pH is lowered (Table 3) implies that the non-native states of CLIC1 have a higher binding affinity for protons than the native state and stabilising electrostatic

interactions are likely to occur between the acidic and basic residues on the surface of the non-native states when at low pH (Whitten and Garcia-Moreno, 2000). These non-native states are thus selectively stabilised as the pH is dropped. The stability of the native state of CLIC1 at pH above 7.0 is also decreased (Table 3) and this could be due to similar reasons involving the arginine and lysine residues. It is clearly no coincidence that CLIC1 is most stable at the pH at which it exists *in vivo* in its soluble globular state.

Three-state unfolding transition at low pH

Interestingly, unfolding of CLIC1 at equilibrium below pH 5.7 clearly follows a *three-state transition* (Figure 39). This is seen by the fact that the transitions monitored by different probes are no longer superimposable and a dip in the λ_{max}-monitored unfolding curve becomes apparent due to a blue shift in the wavelength of maximum fluorescence emission in the pre-transition region. Furthermore if a two-state transition is assumed, the stability of the protein at low pH is drastically reduced compared to at pH 7.0 (Table 3). This could mean one of two things; either the unfolding does, indeed, follow a two-state model but there is still a high percentage of residual structure present in the denatured state at low pH (Neet and Timm, 1994), or the unfolding transition does not fit well to the two-state model. This is the most likely explanation and a depressed $\Delta G(H_2O)$ value was proved to be a known result of a two-state fit to a three-state process by Soulages (1998). He simulated the chemical unfolding transition and studied the effects of analysing a three-state process as a two-state process. He found that in the presence of an intermediate, the two-state model would underestimate the $\Delta G(H_2O)$ by as much as 35%!

The apparent *m*-value of CLIC1 can be seen to drop with a drop in pH (Figure 43). This means that the exposed surface area of the denatured state relative to the native state decreases as the pH is dropped. In other words either the denatured state becomes more compact or the native state becomes less compact at low pH compared to at pH 7.0. The reduced *m*-value further

indicates that unfolding at low pH is less cooperative than at pH 7.0. These interpretations imply the *formation of an equilibrium intermediate at low pH* (Spudich and Marqusee, 2000; Whitten *et al.,* 2001). The technique of circular dichroism is unable to distinguish the potentially molten globule-like intermediate form from the native state at pH 5.5 which results in an overestimation of the concentration of protein present in the native state (Soulages, 1998).

An intermediate species is thus believed to be formed at equilibrium at pH 5.5 / 20^{o}C when in the presence of mild concentrations of urea (3 M to 5 M). The binding of the hydrophobic dye, ANS to the protein in this region (Figure 66) further confirms that CLIC1 is in a hydrophobic conformation that is neither native-like nor denatured-like in nature at these urea concentrations. A factor to consider at this stage is aggregation of the protein since aggregated structures often have an excess of exposed hydrophobic surface. Furthermore, at a pH close to the p*I* of a protein, its propensity to form aggregates is increased (Tanford, 1961; Shaw *et al*., 2001). In fact, CLIC1 is extremely aggregate-prone at pH 4.0. However, there has been no evidence of aggregation at pH 5.5 at any point along the unfolding transition since the solutions were clear, negating the possibility of insoluble aggregates. Furthermore the scattering of light at the excitation wavelength was low and constant (Figure 40) thus implying that no soluble aggregates have formed. This gives additional confirmation for the presence of a stable intermediate species at equilibrium.

The three-state nature of the unfolding curve observed for CLIC1 at low pH is not uncommon. A similar effect has been observed for recombinant human prion protein, PrP (Swietnicki *et al.,* 1997; Jackson *et al.,* 1999). Like CLIC1 this protein exhibits a high degree of structural plasticity and its stability is dependent on the redox potential, temperature and pH conditions of its environment. The protein follows a cooperative two-state transition at pH 7.0. At pH 5.0 the transition remains two-state but the free energy of unfolding drops. At pH 3.6 the transition becomes three-state with a stable hydrophobic

intermediate with enhanced β-structure being present at equilibrium. It is interesting that in a similar manner, the stability of CLIC1 at pH 5.7 is reduced but still follows a two-state transition and only at pH 5.5 or below is the three-state transition observed (Figure 42).

A drop in pH is therefore sufficient to destabilise the native state of CLIC1 to such an extent that the intermediate species becomes significantly populated when under mild denaturing conditions. However, if this intermediate species is to be significant *in vivo* it is necessary that it has the *potential to form spontaneously given the conditions within the cell*. Therefore CLIC1 has been exposed to different conditions present within the cellular environment: both in the cytoplasm and at the membrane surface, so as to define a clear role for the observed intermediate species.

4.1.3. At 37°C an Intermediate-Like Species is Detectable at pH 7.0 Under Mild Denaturing Conditions and at pH 5.5 in the Absence of Denaturant

The most critical question posed at this point is: is this detected equilibrium intermediate species physiologically significant? If so, is it involved in any way with the conversion of CLIC1 from the soluble state to its membrane-bound conformation? It would be convenient to assume that this highly flexible, partially denatured, molten globule-like state is the "membrane-competent" conformation adopted by CLIC1 before inserting into the membrane as is the case with many of the pore forming toxins (reviewed in Parker and Pattus, 1993; Gouaux, 1997; Parker and Feil, 2005; Tilley and Saibil, 2006). However this assumption requires proof and the first obstacle to be overcome is the fact that the intermediate state is not formed by the low pH at the membrane surface alone. Some other factors must be present *in vivo* that simulate the function of urea *in vitro* and cause the partial denaturation of the protein. These factors possibly include the negative potential at the membrane (Endo and Schatz,

1988), the low dielectric constant at the membrane surface (Bychkova *et al.,* 1996) or even the physiological body temperature of 37^{o}C. Zhao and London (1986) showed that at high temperature diphtheria toxin forms a molten globule state that is similar, although not identical to the molten globule state formed at low pH. They propose that similar behaviour may occur in other proteins that are known to undergo conformational changes at low pH and that a conformation made up of a combination of the pH- and temperature-induced molten globule states may be triggered by the conditions *in vivo*.

Structure at pH 7.0 at high temperatures

When CLIC1 was exposed to high temperatures at pH 7.0, the protein interestingly did not unfold to completion even when exposed to extremely disruptive temperatures as high as 100^{o}C (Figure 27)! Instead, CLIC1 becomes trapped in a high temperature-induced conformation that is different from the native state in that it has reduced α-helical secondary structure but is far from being completely denatured and still retains a fair degree of secondary structure (Figure 28). This result is not as bizarre as it first appears. There are, in fact, a number of mesophilic proteins that are structurally stable at elevated temperatures (Duy and Fitter, 2005). As with the thermophilic proteins this thermal stability can be attributed to one or a combination of: a high proportion of hydrogen bonds both on the surface of the protein and in the core (Vogt *et al.,* 1997; Scandurra *et al.,* 1998); charge clusters and salt bridges on the protein surface (Jaenicke and Bohm, 1998; Scandurra *et al.,* 1998; Sadeghi *et al.,* 2006); improved packing of the hydrophobic core (Jaenicke and Bohm, 1998; Scandurra *et al.,* 1998; Wei and Song, 2005); reduced flexibility at low temperatures (Scandurra *et al.,* 1998; Zavodszky *et al.,* 1998) or increased polar surface area (Jaenicke and Bohm, 1998). Indeed, 26.1% of the amino acid residues in the CLIC1 sequence are charged which is higher than the 24.1% quoted for mesophilic proteins by Jaenicke and Bohm, 1998 although it is not as high as the 29.8% quoted for thermophilic proteins.

These results imply that the structure of the native state of CLIC1, the state in which this protein exists in the cytoplasm, contains *a number of stabilising interactions*, both on the surface and in the core. This state would require a substantial amount of energy to unfold spontaneously under these conditions. Therefore there are certain thermodynamic barriers embedded within the structure of cytosolic CLIC1 that prevent it from unfolding. The question is: do these barriers remain at the low pH and low dielectric constant encountered at the membrane surface? Or are they removed to some extent so that CLIC1 is capable of unfolding spontaneously, at least partially, so that it can insert into the membrane?

Physiologically the relevant temperature is 37^{o}C since CLIC1 is a human protein and this is the approximate temperature that it is exposed to *in vivo* within the cell. The native structure of CLIC1 at pH 7.0 / 37^{o}C has reduced α-helical structure from that at 20^{o}C and resembles the structure of the protein at pH 5.5 / 20^{o}C (Figure 28). Therefore the increase in temperature has the same effect on the structure of the protein as a drop in pH. It is unlikely that the increase in temperature increases the stability of the non-native states of the protein as does the drop in pH. It is more likely that at 37^{o}C the native state is destabilised possibly because of the violation of stabilising interactions on the surface of the protein by the high temperature.

Stability at pH 7.0 / 37^{o}C

A particularly remarkable observation is that when CLIC1 is unfolded at equilibrium in the presence of urea at pH 7.0 / 37^{o}C, the unfolding transition resembles that of the protein at pH 5.5 / 20^{o}C (Figure 46 and Figure 66) and the intermediate species is clearly detectable under these conditions! Thus when CLIC1 is present in a soluble state *in vivo*, all that is required for it to transform from the native state to the possibly membrane-competent intermediate state is some condition that causes partial denaturation of the protein as does mild urea concentrations *in vitro*. The question remains as to whether this condition is simply the lower pH found at the membrane surface or whether other

conditions such as the lower polarity and dielectric constant or perhaps a change in the reducing nature of the environment play a role in the conversion of CLIC1 from its soluble cytosolic form to a "membrane-competent" conformation.

Structure at pH 5.5 / 37^{o}C

Unlike at pH 7.0, exposure of CLIC1 to high temperatures at pH 5.5 causes the protein to form insoluble aggregates (Figure 28) as observed by the turbidity of the solution. Furthermore, at pH 5.5 the melting transition is shifted to lower temperatures than at pH 7.0 (Figure 27). At body temperature of 37^{o}C, the protein does not aggregate when in its native state at pH 5.5. However its native structure is altered in a rather intriguing manner.

- Firstly the *secondary structure is reduced* from that of the native state at pH 5.5 / 20^{o}C or at pH 7.0 / 37^{o}C. However the protein still retains more secondary structure in the native state at pH 5.5 / 37^{o}C than the urea-induced intermediate state (Figure 63).
- Secondly the wavelength at which the fluorescence spectrum of CLIC1 at pH 5.5 / 37^{o}C peaks, is *blue shifted* to ~343 nm from ~345 nm at pH 5.5 / 20^{o}C (Figure 64). This λ_{max} lies between the λ_{max} of the native state at pH 5.5 / 20^{o}C and that of the urea-induced intermediate state.
- Thirdly the native state at pH 5.5 / 37^{o}C *is hydrophobic* and binds ANS (Figure 66) as does the equilibrium intermediate.

Is it possible that the native state of CLIC1 at pH 5.5 / 37^{o}C is similar although not identical to the molten globule-like intermediate species detected at pH 5.5 / 20^{o}C and at pH 7.0 / 37^{o}C under mild denaturing conditions? If so, this species could well be involved in the membrane insertion process of CLIC1 and perhaps all that is required for the transformation from the soluble to membrane-competent conformation is the low pH at physiological body

temperature. It is important to note, here, however, that the native state of CLIC1 at pH 5.5 / 37°C is extremely unstable and exceptionally prone to aggregate when exposed to any amount of urea (Figure 46). This could be due to its increased hydrophobic nature (Figure 51) and the lack of lipid membrane *in vitro* into which the protein can insert.

4.2. The CLIC1 Intermediate

There is no doubt from this study that CLIC1 is capable of forming a state that is unlike the native state or the denatured state in many ways. The questions that remain to be answered are: what are the conditions that are necessary for CLIC1 to form this intermediate species? How do these conditions compare with the situation *in vivo*? What is the mechanism of its formation? And what is the structural and functional significance of this intermediate species relative to the native state of CLIC1?

4.2.1. Conditions Required for the Intermediate to Form

The CLIC1 intermediate state is characterised by certain changes in its secondary, tertiary and quaternary structure as well as by a change in its hydrophobicity. All these effects will be discussed below. An intermediate-like species is detected under a variety of conditions. These conditions include:

- CLIC at low pH (below pH 5.7) / 20°C at equilibrium under mild denaturing conditions (3 M to 5 M urea)
- CLIC1 at pH 7.0 / 37°C at equilibrium under mild denaturing conditions (3 M to 5 M urea)
- a M32A mutation of CLIC1 at pH 7.0 / 20°C at equilibrium under mild denaturing conditions (Stoychev PHD thesis, in preparation)

- CLIC1 at either pH 7.0 / 20°C or pH 5.5 / 20°C at equilibrium in the presence of 1 M to 4 M KSCN
- CLIC1 in the absence of denaturant at pH 5.5 / 37°C
- CLIC1 in the absence of denaturant at either pH 7.0 / 20°C or pH 5.5 / 20°C when under non-reducing conditions

The "intermediate" states thus detected under the above mentioned conditions have similar properties but they may not be identical.

4.2.2. Structure of the Intermediate

Why is it that the intermediate form is detectable at 20°C at low pH but not at pH 7.0 unless the temperature is increased to 37°C or reducing conditions are removed? It is likely that at pH 7.0 / 20°C the intermediate state is far less stable than either the native state or the denatured state and therefore is not sufficiently populated at any stage along the unfolding transition to be identified. The native state loses stability as the pH is dropped from 7.0 to 5.5 or as the temperature is increased from 20°C to 37°C and this allows the intermediate form to be stabilised at low urea concentrations. When Met32 is mutated to an alanine (Stoychev PHD, in preparation), the intermediate state is formed in a similar manner at pH 7.0 / 20°C. Therefore an increase in temperature or a decrease in pH can be said to have a similar effect on the structure of CLIC1 as removal of the hydrophobic interactions involving Met32. Furthermore, an increase in the temperature at low pH or removal of the reducing conditions affects CLIC1 in a similar way to when the protein is in the presence of mild concentrations of urea. These conditions stabilise the flexible, expanded, and partially denatured "intermediate" conformation of the protein.

There are two questions that need to be answered regarding the structure of the intermediate state of CLIC1 and they are: firstly what is the secondary, tertiary

and quaternary structure of this intermediate species relative to that of the native and denatured states of the protein? And secondly is this intermediate species comparable with the molten globule intermediates that have been implicated in the membrane-inserting states of many pore forming toxins?

Is the intermediate a molten globule?

In order for an intermediate species to be defined as a molten globule it needs to satisfy four criteria (Fink, 1995). The first is that the molten globule intermediate has to have *a high degree of defined secondary structure*. The intermediate state of CLIC1 present at low pH / 20^{o}C or at pH 7.0 / 37^{o}C when under mild denaturing conditions has an altered secondary structure from the native state, exhibiting reduced α-helical content although a certain proportion of secondary structure still remains (75% native-like) and the protein is not a random coil or in its denatured state (Figure 63). This result is not consistent with the general definition of a molten globule state where native-like secondary structure is a definitive property. However, molten globule states have been reported where a loss in secondary structure was recorded. An example of this is the molten globule form of the α subunit of tryptophan synthase when in the presence of 3.1 M urea (Ogasahara *et al.*, 1993) and the intermediate state of sperm whale apomyoglobin produced at pH 4.0 and low temperature (Barrick and Baldwin, 1993b). Furthermore, the burst phase molten globule species detected in the refolding of β-lactoglobulin also possesses secondary structure that is not native-like in nature (Kuwajima *et al.,* 1996). The important fact is that in all these proteins the intermediate state still retains a degree of secondary structure, which is also the case with the CLIC1 intermediate.

The second property of a molten globule species is that it has *a poorly defined, less rigid tertiary structure*. The CLIC1 intermediate appears to have a well-defined tertiary structure, at least within the vicinity of the tryptophan residue. The tertiary structure is native-like in nature, displaying neither enhanced nor

quenched intrinsic fluorescence intensity to the native state, although the blue shift in the wavelength of maximum emission implies that the single tryptophan residue, Trp35 is even more buried in the intermediate state than in the native state (Figure 64). This means that the intermediate is liable to be compact and native-like in structure with a minimal difference in exposed surface area to that of the native state. This also suggests that the relative positions of the tyrosine and tryptophan residues in the intermediate state are similar to in the native state. This property of the CLIC1 intermediate species is unusual for a molten globule state as in most cases the wavelength of maximum emission of the molten globule intermediate species lies between that of the native and denatured species (Barrick and Baldwin, 1993b; Ogasahara *et al.,* 1993; Kuwajima *et al.*, 1996; Manceva *et al,* 2004). Could this be because the CLIC1 intermediate state forms an *oligomeric structure* in which the tryptophan becomes more buried upon oligomerisation then when in the native monomeric state? A similar effect is observed with the oligomeric "pre-pore" intermediate of Cry1Ab toxin (Rausell *et al.,* 2004). Here the λ_{max} of the soluble monomer is 336 nm while that of the oligomeric intermediate is blue shifted to 333 nm. The near-UV circular dichroism spectra of CLIC1 do show, however, that the tertiary structure of the intermediate species is less defined and hence more flexible than that of the native state at either pH 7.0 or pH 5.5 (Figure 65), which is true to the definition of the molten globule state.

The third requirement for a molten globule state is that it contains a *high proportion of exposed hydrophobic surface* which can be detected by the binding of the protein to the amphipathic dye ANS (Figure 48). ANS was first noticed by Semisotnov *et al*. (1991) to have a high affinity for the molten globule state compared to the native and denatured states of a protein. When ANS binds to hydrophobic patches on a protein, the fluorescence emission depends on the absence of fluorescence quenching due to water molecules and thus is due to the non-polar nature of the immediate surroundings of the ANS molecule (Matulis and Lovrein, 1998). The CLIC1 intermediate is certainly more hydrophobic than either the native or denatured states since only the

intermediate state binds ANS (Figure 66). The peak at 460 nm is a result of a relatively large blue shift which signifies an extremely hydrophobic binding site for the dye on the protein. For example, when ANS binds near to the dimer interface of class Alpha GST, the wavelength of the peak only shifts to 475 - 485 nm (Wallace and Dirr, 1999; Sayed *et al*., 2002) and when ANS binds to the extremely hydrophobic site in apomyoglobin, the blue shift is as far as to 454 nm (Stryler, 1965). The Raleigh scatter (F_{390}) does not indicate increased scatter at any point along the unfolding transition of CLIC1 (Figure 49). Therefore, the binding of ANS to CLIC1 is not due to the presence of hydrophobic aggregates at 3 M to 5 M urea, but rather it is due to the formation of some alternate state of the protein that is different to both the native and denatured states. It appears that at the physiological body temperature of 37^{o}C low pH alone can cause the protein to form an ANS-binding hydrophobic state that is similar to the intermediate species detected under mild denaturing conditions at pH 5.5 / 20^{o}C (Figure 66). Furthermore, when in the absence of reducing conditions CLIC1 forms a non-native state that binds to ANS when in the absence of urea at both pH 7.0 / 20^{o}C and pH 5.5 / 20^{o}C (Figure 52) The results show that ANS binds to the intermediate, non-native-like, species without doubt, and hence this property of a molten globule species is satisfied by the CLIC1 intermediate.

The last stipulation for a molten globule intermediate state is that it has a *compactness approaching that of the native state rather than the denatured state*. From the results obtained, it is difficult to define clearly the compactness of the intermediate state. DLS measurements of the native, intermediate and denatured state of CLIC1 show the intermediate to be 2.5 times larger than the native state and 1.4 times smaller than the denatured state (Figure 41). This implies that the intermediate state is more denatured-like in terms of the hydrodynamic volume that it occupies. Since the *m*-value decreases with decreasing pH (Figure 43) and hence the probability of the equilibrium intermediate being populated along the unfolding transition increases with decreasing pH, it is likely that the pK_a of the residues in the intermediate state

resembles that of the ionised residues of the denatured state rather than the native state and both the intermediate and denatured states are stabilised relative to the native state as the pH is dropped (Whitten *et al.*, 2001). The intermediate state thus has a similar affinity for proton binding to that of the denatured state. Thus it appears that the *intermediate state is more denatured-like in nature.* However the fact that the fluorescence emission data (Figure 64) implies that the intermediate is conceivably even more compact than the native state (since Trp35 is more buried in the intermediate state than in the native state) provides some, perhaps contradictory evidence for a compact, native-like intermediate state. Nonetheless, according to near-UV circular dichroism, the tertiary structure of the intermediate species is less tightly packed than in the native state (Figure 65). On a whole, the results therefore suggest that the intermediate species is more denatured-like in terms of its size, proton-binding properties and compactness. Therefore one cannot say conclusively that the intermediate is a molten globule in terms of the definition. However, if the intermediate is hypothetically assumed no longer to be monomeric, the possibility of a molten globule-like oligomeric intermediate species with a buried tryptophan residue and a greater hydrodynamic diameter than the native state certainly exists.

4.2.3. Stability of the Intermediate

The intermediate state is only marginally more stable than the denatured state despite having a degree of native-like secondary structure. An interesting interpretation of these results could be that the lower free energy required to form the intermediate state from the unfolded state may implicate the intermediate state as an early intermediate on the folding pathway which could make it important in the *in vivo* folding process. Proteins that have a molten globule intermediate state present at equilibrium have been proposed to possess a similar state as a major kinetic intermediate in the burst phase at the start of the folding pathway (Barrick and Baldwin, 1993a,b; Engelhard and Evans, 1995; Fujiwara *et al.*, 1999).

The results from this work indicate that the α-helical secondary structure and the side chain packing that are absent in the CLIC1 molten globule-like intermediate state (Figure 65) contribute towards the stability the native protein at low pH. It is clear that the conformational stability of the intermediate is less complicated than that of the native state since the intermediate is devoid of certain structures and packing interactions that characterise the native state. Being a molten globule-like state, it is likely that the intermediate is stabilised by the residues that are buried in the native state as well as by hydrophobic and native-like packing interactions in the core of the native protein (Kuwajima, 1996; Wu and Kim, 1998). Since the stability of the intermediate state is decreased by an increase in temperature (seen by an increase in the unfolding rate (Figure 61)), it is likely also to be stabilised by hydrogen-bonding interactions (Bhuyan and Udgaonkar, 1998).

4.3. Mechanism of CLIC1 Unfolding

4.3.1. Unfolding of the Native State

CLIC1 unfolds from the native state to the post-transition region in a single phase and no intermediates are detected along the unfolding pathway. The unfolding of the native state of CLIC1 at pH 7.0 / 20^{o}C and at higher pH is significantly slower than at pH 5.5 / 20^{o}C and at lower pH (Figure 53 and Figure 54). This is consistent with the equilibrium studies which showed the protein to be most stable at pH 7.0 / 20^{o}C (Table 3). The slower rate of unfolding of CLIC1 at pH 7.0 / 20^{o}C compared to at pH 5.5 / 20^{o}C means that at pH 7.0, CLIC1 has a greater percentage of local stabilising interactions than at pH 5.5 and thus at pH 5.5 the protein can be said to have less tertiary structure (Kuhlman *et al*., 1998). The enhanced unfolding rate at pH 5.5 implies that less energy is required to solvate the core of CLIC1 when the protein is at pH 5.5, possibly because of decreased residue hydrophobicity. The positive slope of the urea dependence of the unfolding rates at all pH (Figure

54) is consistent with the exposure of surface area as the protein unfolds and the M_u values are similar at pH 7.0 / 20°C and pH 5.5 / 20°C despite the fact that the protein unfolds approximately 40 times faster at pH 5.5 (Table 5).

The circular dichroism and fluorescence-monitored curves are superimposable at both pH values indicating that unfolding of the secondary and tertiary structure occurs at approximately the same rate, although the circular dichroism-monitored transition is slightly slower than the fluorescence-monitored transition and generally indicates a greater amount of buried surface area exposed in the transition state upon unfolding (Table 5). It is likely that the unfolding of the regions of the protein monitored with tyrosine and tryptophan fluorescence is quicker than the unfolding of the secondary structure of the protein in its entirety.

The M_u values are related to the solvent accessible surface area of the transition state and are calculated using equation 21 as $M_u = RT \log\left(\frac{K_u}{[urea]}\right)$. The ratio of M_u to the equilibrium *m*-value gives an indication of the surface area of the protein that is exposed to solvent in the transition state relative to the denatured state (Tanford, 1970; Doyle *et al.,* 1996). At pH 7.0 / 20°C the ratio M_u / *m*-value implies that the solvent accessible surface area of the transition state is ~10% denatured-like in nature while at pH 5.5 / 20°C, the ratio M_u / *m*-value indicates that the solvent exposed surface area of the transition state is only ~8.5% denatured-like (Table 5). Therefore the transition state is slightly more native-like at pH 5.5 than at pH 7.0 and this could be due to potential compact intermediate species being populated along the unfolding transition at pH 5.5. Grx2 exposes 12% of the hydrophobic surface buried in its native state in the transition state upon unfolding. These results imply that the transition state for unfolding of CLIC1 at either pH 7.0 or pH 5.5 is more native-like than that of its only monomeric cousin, Grx2. This result can be explained by the fact that the native state of CLIC1 is less compact than the native state of Grx2 (see section 4.1.1 and Figure 67). The dimeric class Pi GST only exposes 6% of its

buried surface area in the transition state (Wallace and Dirr, in preparation) and class Alpha GST unfolds in two phases, exposing 6.4% of buried hydrophobic surface in the slow unfolding phase, and only 2.8% in the fast phase (Wallace *et al.,* 1998b). The transition states for unfolding of these two dimers are therefore more compact than for CLIC1.

The unfolding rate constants (k_u) of mesophilic proteins range from 1808 min^{-1} to 0.007 min^{-1} (Wittung-Stafshede, 2004). Thus log(k_u) ranges from 3.3 to -2.2 for mesophilic proteins. Log(k_u) for CLIC1 at pH 5.5 / 20^{o}C is -1.9 which lies comfortably within this range. However, at pH 7.0 / 20^{o}C it is -3.5 which is slower than for most mesophilic proteins. Thermophilic proteins unfold far slower than mesophilic proteins, often in the order of weeks (Mukaiyama *et al.,* 2004; Duy and Fitter, 2005). It is interesting therefore, that at pH 7.0 when CLIC1 unfolds at its slowest rate (Figure 53 and Figure 54) it also shows the most resistance to thermal denaturation (Figure 27). It is also remarkable that Grx2 unfolds far quicker than CLIC1 at pH 7.0 despite being the more stable of the two proteins (Gildenhuys PHD thesis, 2006). This could be because CLIC1 has evolved certain specific interactions designed to prevent the protein from spontaneously unfolding within the cytoplasm and to direct the unfolding of CLIC1 to where it is necessary for its pore-forming function, which is the low pH environment at the membrane surface.

If the temperature is increased to the physiologically relevant 37^{o}C, the rate at which CLIC1 unfolds at pH 7.0 is increased to the same as the rate of unfolding at pH 5.5 / 20^{o}C (Figure 61). This means that the stability of the native state is decreased by the increase in temperature. This is because the flexibility of the native state is probably increased at 37^{o}C. A higher percentage of surface area (15%) is exposed in the transition state upon unfolding of the native state to the denatured state at this pH (Table 5), implying that the transition state is somewhat less compact and more denatured-like possibly due to the disruptive nature of the elevated temperature (Matouschek *et al.,* 1995).

4.3.2. Unfolding of the Intermediate State

Unfolding of the intermediate species to the denatured state occurs in a single phase at the same rate as the unfolding of the native state to the denatured state (Figure 56). However, a *burst phase* is detectable at high urea concentrations. It is likely that this burst phase represents an intermediate species that is inconsistent and possibly forms too quickly to be detected under the high denaturing conditions required. If the intermediate is assumed to be oligomeric it is unlikely that it will unfold in a single phase and it is far more probable that it will initially dissociate into monomeric form before unfolding to completion (Gonzalez-Mondragon *et al.,* 2006). Therefore it is possible that the unfolding of the intermediate to the denatured state does not occur in a single phase that is identical in rate to the unfolding of the native state as is observed but rather two or more phases are present, most of which being too fast and erratic to detect using manual mixing methods.

4.3.3. Slow Formation of the Intermediate State

By far the most interesting transition monitored by kinetics is the transition of the native state to the intermediate state. This transition was monitored under conditions where the intermediate is detectable. That is at pH 5.5 / 20^{o}C in the presence and absence of 0.5 M NaF and at pH 7.0 / 37^{o}C.

Unfolding of the native state to the intermediate state at pH 5.5 / 20^{o}C clearly occurs in two phases: a *fast phase* and a *slow phase* when monitored using fluorescence as a probe (Figure 57 and Figure 58). It is unclear from this data whether the two phases occur in sequence or in parallel. The *fast phase* occurs at the same rate as the N → D and I → D transition and thus probably does not represent the formation of the intermediate species. Most of the species present in this phase are present early in the unfolding transition. The *slow phase* is dominant later and this is the phase that likely corresponds to the formation of the intermediate species. It is characterised by a steep dependence of the

unfolding rate on urea and a large increase in the M_u value. Is it possible that this slow phase is detecting an oligomerisation step as a potentially oligomeric intermediate species forms? This assumption is consistent with the fact that oligomerisation is a relatively slow process compared to denaturation. Furthermore the surface area exposed in the transition state upon formation of the intermediate is large (Table 5) which supports the hypothesis that the intermediate state is oligomeric. Circular dichroism cannot distinguish between the fast and slow phase since it cannot detect the intermediate at pH 5.5. However the urea dependence of the circular dichroism-detected rate constants is high (Figure 58) which means that both the fast and slow phases have been incorporated into the circular dichroism results.

Unfolding kinetics at 37°C could only be studied using circular dichroism as a probe which is unfortunate considering fluorescence is the probe that detects both phases. The single phase detected by circular dichroism under these conditions has the same dependence on urea as the N → D and I → D transition (Figure 61). The slow phase is not detected at all at pH 7.0 / 37°C. This is probably because the increase in temperature further destabilises the native state. Moreover, perhaps the intermediate state is not oligomeric under these conditions and only the monomeric state is formed at pH 7.0 / 37°C.

4.3.4. Unfolding Pathway of CLIC1

The results do not provide clear evidence for whether the intermediate species that is detectable at equilibrium is an on- or off-pathway intermediate species as CLIC1 unfolds from its native state to the denatured state. For these purposes the assumption is that the equilibrium intermediate is on-pathway. A schematic representation of the unfolding process of CLIC1 is given in Figure 68.

The free energy required to achieve the transition state for the N → I transition is the highest point on the energy diagram for the unfolding of CLIC1 (Figure

68). Therefore creation of the intermediate species requires a relatively large amount of energy which is mandatory to the creation of a potentially oligomeric intermediate form of CLIC1 with increased exposure of hydrophobic surface and a reduced degree of secondary structure. Possibly two transition states are present in the N → I transition, one native-like transition state that represents the fast phase and possibly does not require as much energy to form and an oligomeric transition state that possibly creates the transition state energy barrier towards intermediate formation and therefore can only form under the conditions where the intermediate species is most highly populated.

The I → D transition occurs in a single phase and the energy barrier presented by the transition state is not as high as in the N → I transition (Figure 68). The transition state remains intermediate-like in terms of the amount of surface area exposed in the I → D transition. This transition state probably has less structure and is more flexible if not than the intermediate species then definitely than the native state. The presence of a burst phase in the unfolding transition implies that the I → D transition may also occur in two phases but the extremely denaturant-dependent slow phase representative of the intermediate species would occur too quickly to be detected at the high urea concentrations required.

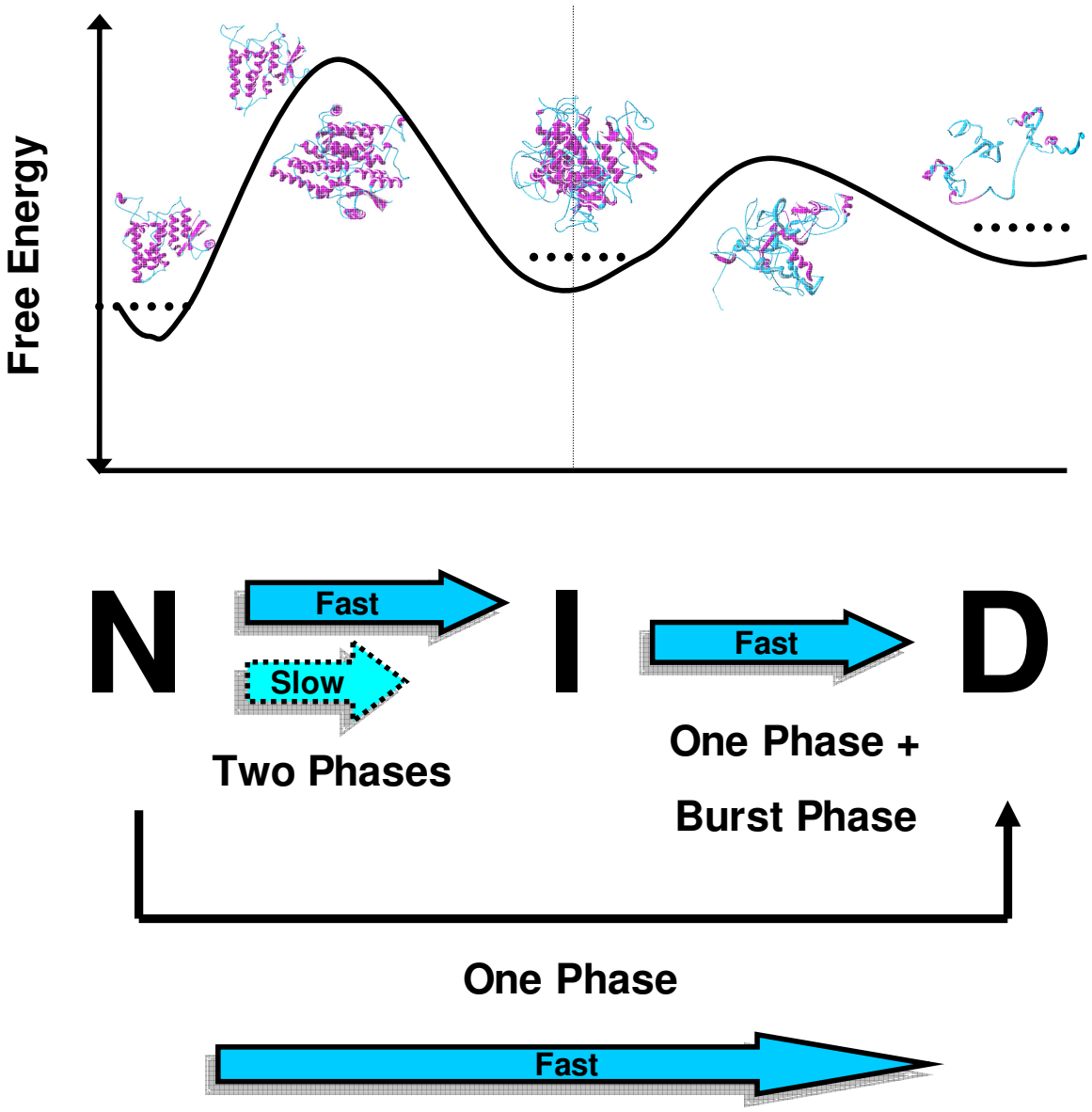


Figure 68: Proposed scheme for the unfolding pathway of CLIC1

Unfolding scheme to the first approximation for native CLIC1 at 20°C including an energy diagram illustrating the energies and possible structures for the native, intermediate, denatured and transition states. Secondary structure is shown in purple while non-specific, mostly hydrophobic, flexible structure is shown in blue. The protein unfolds from the native state to the equilibrium intermediate state in a fast and a slow phase which possibly represent two structures in the transition state. CLIC1 unfolds from the native state to the denatured state in a single relatively fast phase.

When CLIC1 is unfolded from the native state to urea concentrations at which the equilibrium intermediate species is populated (3 M to 5 M urea), the unfolding occurs in two distinct phases although it is not known whether these phases occur in sequence or whether they occur concurrently. The fast phase occurs at roughly the same rate as the N → D transition (rate constant of ~2 hours in the absence of urea). This phase is represented by the largest change in amplitude signifying that the majority of the species follow this pathway. The fast phase prevails early in the unfolding reaction. Only a small percentage of surface area buried in the native state is exposed in the transition state in this phase. The fast phase transition state is therefore native-like in nature and in compactness. The slow phase is distinguished from the fast phase by the tremendously slow rate constant in the absence of urea (approximately 1200 hours!!). This means that this phase would not occur spontaneously under any circumstances and would need some sort of denaturing stimulus in order to occur. The slow phase is characterised by a small increase in amplitude as monitored by fluorescence that is dominant in the late stages of the unfolding transition. The surface area exposed in the transition state in the slow unfolding phase is increased to as much as 20%! This implies that the slow unfolding step may represent a slow oligomerisation step in the intermediate-formation process whereby the surface area of the intermediate state is greater than that of the native state. It is unlikely that the protein would transit exclusively to this oligomeric intermediate form, however and a monomeric intermediate is likely to be the precursor to the oligomeric state. Perhaps the unfolding pathway shown in Figure 68 is better represented by the scheme in Figure 69? Here a monomeric intermediate state and a stable oligomeric intermediate state are proposed to interconvert in a slow process that is rate-limited by environmental factors such as temperature or salt concentration so that in some cases the conversion to the oligomeric form might be too slow to be detected and the intermediate remains in monomeric form. This may be what is occurring at pH 5.5 / 20^{o}C when in the presence of 0.5 M NaCl and at pH 7.0 / 37^{o}C.

4.4. Different Electrostatic Conditions Influence the Structure and Stability of CLIC1

When the soluble protein comes into the vicinity of the membrane surface, the negative potential of its immediate environment will increase thus changing the electrostatic nature of the protein's surroundings. Furthermore the dielectric constant and the polarity of the environment of the protein will drop. These diverse and electrostatically complex conditions present at the membrane surface were studied individually *in vitro* so as to establish the effect of each element separately on the structure and stability of the protein in an attempt to make an accurate hypothesis as to what causes CLIC1 to transform from its soluble state to a state that is able to insert into the membrane. It is essential to bear in mind that none of the conditions studied separately here occur individually within the cell but rather are amalgamated to create the environment to which the protein is exposed. Nevertheless, study of each situation independently will give an indication as to what effect, if any, each condition contributes to the structure and stability of the protein.

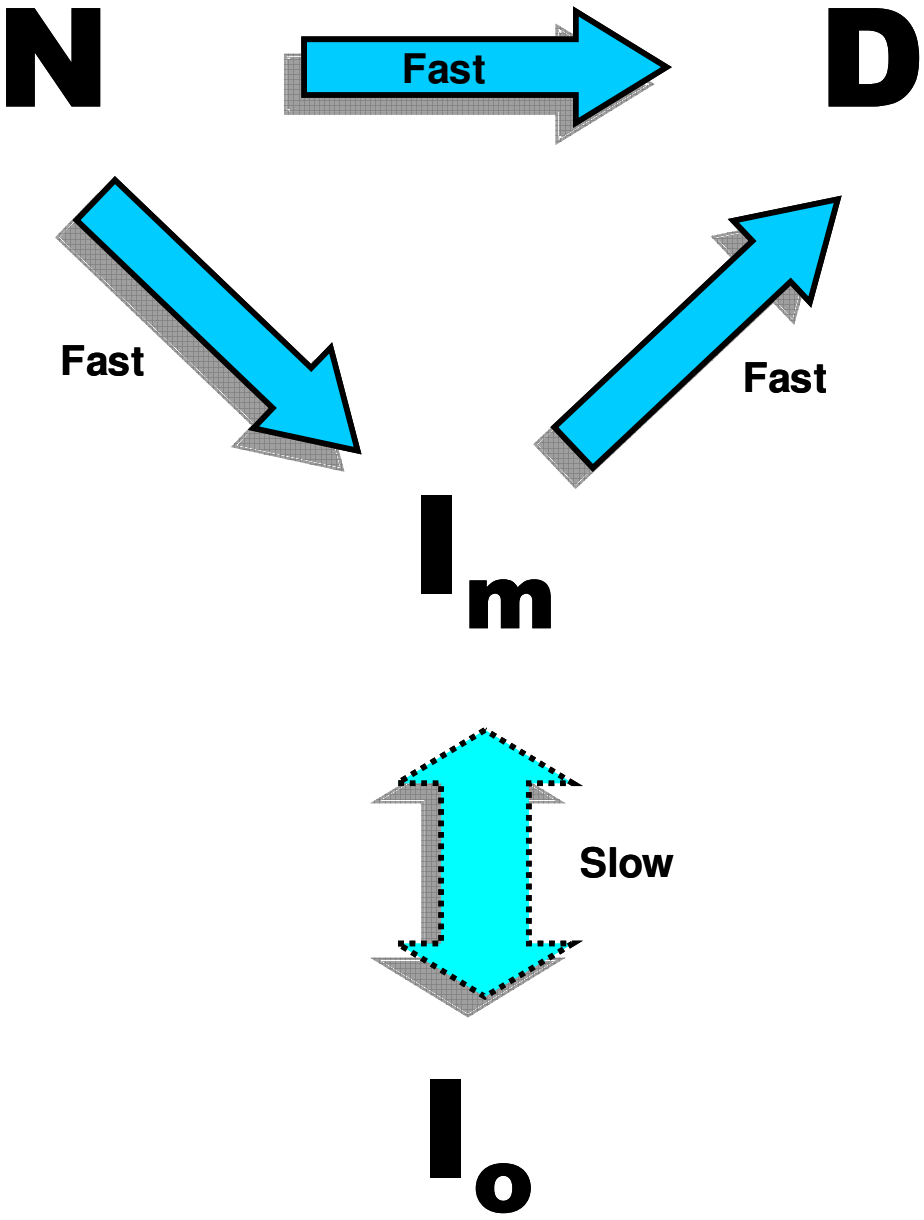


Figure 69: Alternative unfolding pathway for CLIC1

Unfolding scheme for native CLIC1 at 20°C. The protein unfolds from the native state to either the denatured state or a stable monomeric equilibrium intermediate state (I_m) in a fast phase. The monomeric intermediate state and a stable oligomeric intermediate species (I_o) interconvert in a slow phase where the population of the species is dependent on the environment. The intermediate unfolds relatively quickly from its monomeric state to the denatured state.

4.4.1. NaCl Stabilises the Native and Intermediate States of CLIC1

Effect of NaCl on the structure and stability of CLIC1

Since most of the charged residues of this negatively charged protein are exposed to the solvent (Figure 70 A), theoretically it is likely that salt will have an effect on the electrostatic interactions within the protein and on the protein surface. This effect could be enforced by three mechanisms: 1. *General* ionic strength effects where the electrostatic interactions between charged groups on the protein surface are screened by the salts. 2. *Specific* salt effects where there are direct chemical interactions between ions and protein. This preferential binding of counterions to charged sites occurs specifically at low salt concentrations. 3. *Chaotropic* effects caused by changes in the structure of water. These effects are most often observed in high salt concentrations. Here the high concentrations of ions in the solution influence the properties of water and perturb the specific salt effects. At high salt concentrations, the hydrophobic effect is more likely to come into play. The high ionic strength causes the structure of water to become more disordered and the dielectric constant of the solvent decreases. The like charges will pack more closely but at the same time ionic pairing could become destabilised resulting in the shrinking of the protein at high salt concentrations (Darwin *et al.*, 1991). The Na^+ and Cl^- concentration inside cells is 5 – 15 mM and the total concentration of salts within a cell is approximately 170 mM (Alberts *et al.,* 1994). Salt concentrations used in the *in vitro* studies in this project were as high as 500 mM, greatly exceeding physiological values.

NaCl does not affect the structure of the native state of soluble CLIC1 at pH 7.0 / 20^{o}C. At pH 5.5 / 20^{o}C, however, there is a pronounced increase in the secondary structure (Figure 24) along with an enhancement of the fluorescence emission intensity (Figure 25) and a decrease in the hydrodynamic diameter (Figure 26) of CLIC1 when in the presence of at least 0.2 M NaCl.

The unfolding transitions of CLIC1 at pH 7.0 / 20°C in the presence of 0.5 M NaCl are superimposable (Figure 44) as in the absence of salt. The $\Delta G(H_2O)$ value and the C_m decrease only slightly when in the presence of NaCl (Table 4). This minor decrease in the stability may be as a result of the weakening of favourable local interactions between acidic and basic residues in the native state due to the effect of increased concentrations of anions and cations in the solution. NaCl does not have a noteworthy effect on the stability of CLIC1 at pH 7.0 / 20°C.

The effect of salt on the stability of proteins is not constant throughout the entire pH range and depends on two aspects: one is the *distribution of charge on the native protein* and the other is the effect of salt on the *denatured state* (Tan *et al.*, 1995). At pH 5.5 / 20°C, NaCl has a *greater effect* on the stability of the protein than at pH 7.0 / 20°C. 0.5 M NaCl significantly increases the stability of the native state at pH 5.5 / 20°C while having little effect on the cooperativity of the unfolding transition (Table 4). When the pH is dropped to 5.5, the number of long-range electrostatic repulsions between like-charges on the surface of CLIC1 will increase due to the positively charged residues coming into contact with the higher concentrations of H^+ ions. Therefore the increase in NaCl concentration at low pH results in stabilisation of the native and intermediate states of the protein since the salt will screen and weaken the repulsions that drive unfolding (Tan *et al.*, 1995). The presence of NaCl in the solution does not influence the structure or ANS-binding properties of the intermediate state. Furthermore the intermediate state remains detectable at pH 5.5 / 20°C when in the presence of NaCl and mild concentrations of urea.

NaCl affects the *rate of unfolding* of the native state in the same way at both pH 7.0 / 20°C and at pH 5.5 / 20°C. The M_u value is increased 1.3 times at both pH by NaCl (Figure 59 and Table 5). This means that more surface area is exposed in the transition state as the protein unfolds when in the presence of NaCl then when in the absence of the salt, implying that this salt causes the native state to be *more compact* at both pH. This explains the drop in the

hydrodynamic diameter measured in the presence of increasing concentrations of NaCl (Figure 26). The time constants for unfolding are also increased (three times at pH 7.0 and ten times at pH 5.5) upon the addition of 0.5 M NaCl (Table 5). These results imply that NaCl has a *stabilising effect* on the native state of CLIC1 and more so at pH 5.5.

The greater effect that NaCl appears to have on CLIC1 structure and stability at pH 5.5 / 20^{o}C compared to at pH 7.0 / 20^{o}C could be because at pH 7.0 a greater number of the acidic residues will be ionised than at pH 5.5 and therefore there will be more stabilising salt bridges on the protein surface when at pH 7.0. Thus the presence of salt will compensate for the contribution of salt bridges towards stability at pH 5.5, hence increasing the stability (Takano *et al.,* 2000). According to Linderstrøm-Lang (1924), the salt-sensitivity of a protein with a *uniform distribution of charge* is related to the distance of the isoelectric pH of that protein from the pH of the solution. He stated that proteins at their isoelectric points would show lower sensitivity to changes in the salt concentration because their net charge would be 0 and all their attractive and repulsive interactions would be balanced. However, CLIC1 is *asymmetrically charged* and contains hotspots of both negatively and positively charged residues (see Figure 9 and Figure 70 A). Therefore, even at a pH of 5.5, which is closer to the p*I* of the protein, the charges on the protein surface will not be neutralised. This charge imbalance will thus lead to the significant salt sensitivity observed at this pH.

Salt effects have been studied on other members of the GST superfamily. The stability of *Sj*26GST has been shown to be insensitive both to the salt type and the salt concentration (Yassin *et al.,* 2003). The reason for this insensitivity to salt is believed to be due to the hydrophobic nature of the subunit interface in this protein compared to class Sigma GST which has a much more hydrophilic interface and displays sensitivity towards salt due to charge shielding (Stevens *et al.,* 2000). Here an increase in salt results in an increase in the stability of both the dimeric intermediate and the unfolded monomer relative to the native

state (Stevens *et al.,* 1998). Since CLIC1 is a relatively charged molecule it is not surprising that it is sensitive to salt effects.

A point to bear in mind is that CLIC1 functions as a chloride ion channel *in vivo* and shows specificity towards chloride ions (Tulk *et al.*, 2002). Therefore, when analysing the effect of NaCl on the stability of the protein, one must take into account that perhaps either the chloride ions are binding to the positive residues on the protein surface and increasing the stability by screening repulsive interactions, or the negative residues present on the surface of this acidic protein function to repel the negative chloride ions which would be an effective means of selectively channelling these ions through a hydrophilic pore formed by this protein in the membrane. The surface area exposed to the solvent upon denaturation of the intermediate is increased in the presence of NaCl (Table 4). The intermediate state is thus more native-like in nature than it is when in the absence of this salt. This native-like compactness of the intermediate is *not observed under any other conditions at 20^{o}C*. Perhaps NaCl interacts specifically with the protein in that it prevents the possible oligomerisation of the intermediate state? This could have certain implications for how CLIC1 forms chloride channels *in vivo* and whether monomeric or oligomeric forms of the channel are significant. That said, CLIC1 has been shown to exhibit selectivity towards anions in general (Singh and Ashley, 2006), and therefore the chloride anion probably has no specific effect on CLIC1 structure or stability.

4.4.2. CLIC1 Amino Acid Distribution

The fact that ionic strength and pH both have an effect on CLIC1 structure and stability can be explained in terms of the amino acid distribution in this molecule. 24.5% of the protein consists of charged residues, 7.9% of which are in the N-terminal domain. The charged residues of CLIC1 are mostly all exposed to solvent to some extent. However, one face of the molecule, visible when the acidic loop is at the base of the structure and the N-terminal domain

is on the right, is less negatively charged than the opposite face (about 13 exposed Asp & Glu *vs.* about 20) (Figure 70 A).

The negative charges of CLIC1 are therefore asymmetrically distributed across the protein. There are two hotspots of negative charge present in this structure. The first is the *negatively charged loop* region that extends from Pro147 to Gln164 and the second is the *acidic α9 helix* found at the C-terminal end of the protein (Figure 9). The positively charged residues are more evenly distributed over the protein surface. When Tulk *et al.* (2002) incubated CLIC1 in the presence of neutral phospholipids, the protein failed to produce any channel activity and chloride conductance was only evident when the protein was in the presence of lipids with a *net negative charge*. These results imply that the positive residues on the protein surface may, indeed be necessary to interact with the membrane surface before insertion can proceed. There is a patch on the surface of CLIC1 that does not contain any charged residues, however. This "neutral" patch extends from the N-terminal domain across the C-terminal domain but is only present on one face of the protein (Figure 70 A). This implies that the electrostatic effects on the stability of CLIC1 are not distributed equally across the protein and salt and/or pH will affect the one face of the molecule more than the opposite face. This may be significant for the protein's interaction with the negative potential at the membrane surface.

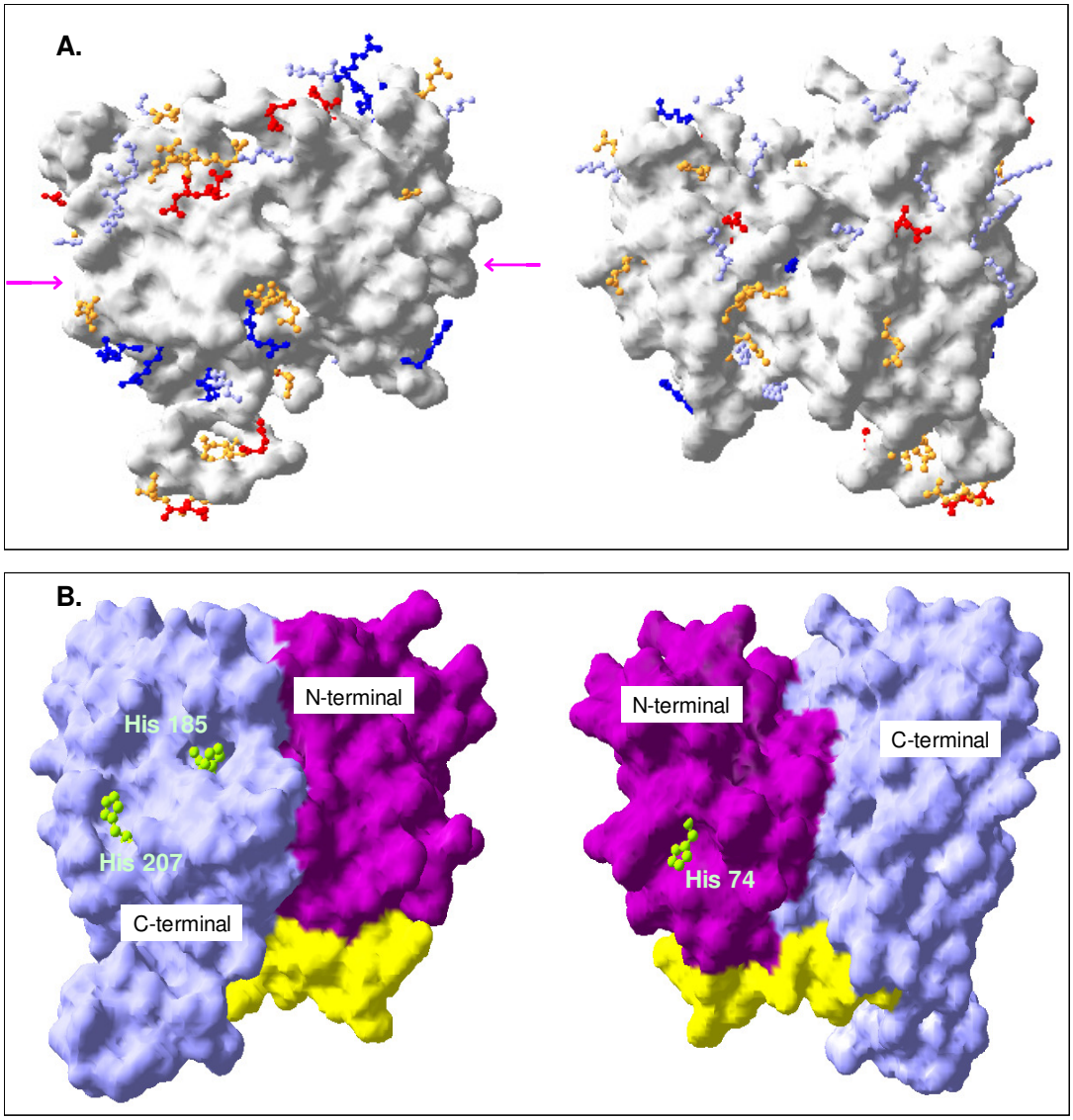


Figure 70: Residue distribution on the surface of CLIC1

(A) Distribution of the charged amino acids on the surface of CLIC1. Both faces of the protein are shown. Aspartate residues are orange, glutamate residues are red, lysines are pale blue and arganines are blue. The uncharged patch on one face is indicated by the arrows in pink. This patch is not visible on the opposite face. **(B)** Distribution of histidine residues on the surface of CLIC1. The N-terminal domain is purple, the C-terminal domain is blue and the linker region is yellow. The images were rendered using Swiss PDB viewer, (Guex and Peitsch, 1997) The PDB code 1k0m was used.

Histidine, with a pK_a of 6.1 in model compounds is the only amino acid that has a functional group with a pK_a within the physiological pH range. This means that at pH 7.0 the histidines of CLIC1 should be neutral, while at pH 5.5 they should be positively charged. Lee *et al.*, (2002) studied the effect of salt on the pK_a values of histidines in myoglobin and staphylococcal nuclease. They concluded that the salt dependence of the pK_a values of these residues was caused by a shift in the equilibrium between charged and neutral forms of histidine in favour of the charged form at high salt concentrations. They surmised that this effect was driven by attractive electrostatic interactions between the charged His^+ and counterions. Generally, as the salt concentration increases, so the pK_a of the histidine residues is increased (Kao *et al.*, 2000).

Therefore, it is possible that in the presence of high concentrations of NaCl, the histidines of CLIC1 remain positively charged at pH 7.0 although histidine residues that are in an environment where there is a high imbalance of charge may have greatly depressed pK_a values due to the repulsive electrostatic forces that are likely to be present. The addition of salt to these residues will simply normalise the pK_a values by attenuating these repulsive interactions.

CLIC1 contains three histidine residues (Figure 70 B) all of which are particularly exposed to the solvent and all of which are sensitive to the concentration of salt via screening by counterions: His74 is the only histidine found in the N-terminal region of the protein. It is in the vicinity of seven negatively charged residues and only one positively charged residue. The high imbalance of charge surrounding this residue would mean that it is extremely sensitive to the salt concentration of the solution (Lee *et al*, 2002). His185 and His207 are located in the C-terminal domain. His185 is within 10 Å of the six negatively charged residues in the C-terminus of CLIC1. It is also in the vicinity of three positive residues. Thus the net charge surrounding this residue is -3. This electronegative environment means the pK_a of His185 is also susceptible to changes in salt concentration. His207 has a net charge of +2 in its local environment, making it the least salt-sensitive of the three histidines of

CLIC1. As the ionic strength is increased, so the attractive Coulombic interactions between His^+ and the negative residues in its vicinity will be attenuated. This will result in stabilisation of the protein at pH 5.5 when the histidines are inherently positively charged. At pH 7.0, the intrinsic charge on the histidine residues should be neutral. Therefore these residues should not form medium- and long-range interactions with the charged residues of the protein at this pH. Thus an increase in the salt concentration and the accompanying screening of these charges should not affect the histidines to the same extent as at pH 5.5, ergo the lower salt sensitivity of CLIC1 stability at pH 7.0.

4.4.3. Na_2SO_4 and KSCN Stabilise the Intermediate State

Using equation 3, the ionic strength of a sodium sulphate solution is double the ionic strength of a sodium chloride solution. However, while chloride ions lie in the neutral region of the Hofmeister series (Figure 2), the large sulphate anion interacts more readily with proteins through both electrostatic and hydrogen bonding interactions. Therefore the screening effects of the chloride anions can be more freely interpreted in terms of the ionic strength of the solution than the specific effects of sulphate anions.

In this case, the presence of the stabilising sulphate anions unexpectedly does not stabilise native CLIC1 at pH 7.0 / 20°C or pH 5.5 / 20°C! The stability and *m*-value obtained from the two-state fit are actually reduced compared to when in the absence of salt (Table 4) despite the fact that the C_m is shifted to higher urea concentrations (Figure 44). However, what is interesting is that an ANS-binding hydrophobic intermediate species with a blue shifted fluorescence λ_{max} is detectable in the presence of 6 M to 7 M urea (pre-transition region) at pH 7.0 / 20°C (Figure 44). This is the *only instance* where the wild type CLIC1 equilibrium intermediate species is detectable at pH 7.0 / 20°C. Similarly the pre-transition intermediate at pH 5.5 / 20°C is stabilised by the presence of

sodium sulphate. This could be because of the interaction of the basic residues with the SO_4^- anions. These interactions could stabilise the intermediate state by decreasing unfavourable electrostatic interactions between the charges on the surface of this molten globule-like structure. This shielding effect of the salt on the intermediate state would result in a decrease in its net charge. This would cause the volume occupied by water in the immediate vicinity of the intermediate to increase thereby decreasing the volume occupied by the protein and hence likely making it more stable.

The difference in the effect of NaCl and Na_2SO_4 on CLIC1 is that Na_2SO_4 exerts its stabilising effects by *interacting specifically with the protein molecule.* Therefore, since the intermediate state is stabilised relative to both the native and denatured states when in the presence of Na_2SO_4, these results confirm that the intermediate species is, indeed a different state of CLIC1 and is not an aggregated state. These results also show that while the increase in the stability of the native state of CLIC1 at pH 5.5 / 20^{o}C when in the presence of NaCl is due entirely to the increased ionic strength of the solution, the increase in the stability of the intermediate state in the presence of Na_2SO_4 could be due rather to specific interactions between this salt and the intermediate species.

The tryptophan fluorescence of CLIC1 decreases with increasing concentrations of Na_2SO_4 (Figure 25). This is due to the quenching nature of the sulphate anion when it interacts with the protein. The secondary structure and hydrodynamic size of CLIC1 increase when the protein is in the presence of up to 0.4 M Na_2SO_4 (Figure 24 and Figure 26). These results could be due to oligomerisation of CLIC1 under these conditions. A more likely explanation, however is that the protein exists in a more "relaxed" and somewhat flexible conformation when in the presence of sodium sulphate, while still retaining its *native monomeric structure*. This could be due to destabilising repulsive electrostatic interactions on the protein surface that become enhanced when the concentration of the salt is increased, resulting in a destabilised native state and a consequently stabilised intermediate species.

Potassium thiocyanate is a chaotropic salt as seen by its position far in the denaturing region of the Hofmeister series (Figure 2). The presence of increasing concentrations (1 M – 4 M) of this salt at both pH 7.0 / 20^{o}C and pH 5.5 / 20^{o}C cause the protein to retract to a state where the λ_{max} is blue shifted from that of the native state (Figure 45). The question is: is the KSCN-induced state equivalent to the intermediate state populated in the presence of mild concentrations of urea? It is likely that this mild denaturing salt creates a state that is *similar although not identical to the urea-induced intermediate state*. It is interesting, though that pH does not affect this conversion and mild concentrations of KSCN produce the intermediate-like species at both pH 7.0 and pH 5.5. Therefore an increase in the SCN^- concentration may be involved *in vivo* in the transformation of CLIC1 to a membrane-competent state.

4.4.4. NaF Interacts Specifically with CLIC1

The effect that NaF has on CLIC1 is most fascinating. This salt was not anticipated to cause the protein to behave differently to when in the presence of NaCl. Both chloride and fluoride ions lie in the neutral region of the Hofmeister series (Figure 2) and therefore, unlike the case with Na_2SO_4 and KSCN, changes in the stability of the protein as measured by NaCl and NaF should report on the effect of a change in the ionic strength of the solution and not on particular interactions of the salt with the protein. However, NaF appears to do exactly that and undergoes specific interactions with CLIC1 that are most pronounced at low pH.

At pH 7.0 / 20^{o}C NaF increases the α-helical nature of the secondary structure of CLIC1 while the tertiary and quaternary structures are not appreciably affected by NaF (Figure 24 and Figure 25). NaCl has been shown to have no significant effect on the native structure of CLIC1 so the fact that NaF affects the secondary structure means that the fluoride ions as opposed to the chloride

ions are *interacting specifically with the protein*, most likely with the positive residues, stabilising the hydrogen bonds that result in helix formation. NaF has an even more pronounced effect on the native state of CLIC1 at pH 5.5 / 20^{o}C. Over and above a prominent increase in the α-helical secondary structure (Figure 24), it also causes an increase in the fluorescence emission intensity (Figure 25) and an increase in the hydrodynamic volume occupied by the protein (Figure 26). Furthermore, and most noteworthy, is the fact that the *native state binds ANS considerably* when in the presence of 0.5 M NaF at pH 5.5 / 20^{o}C (Figure 50). In fact the intensity of the ANS binding to the native state is far more enhanced than when it binds to the urea-induced intermediate species under any condition. A similar effect is observed with the native state of the M32A mutant form of CLIC1 at pH 7.0 / 20^{o}C when in the presence of NaF (Stoychev PHD thesis, in preparation). NaF thus causes considerable alterations to the structure of the native state so much so that it even substantially increases the hydrophobic surface of this protein.

The stability of CLIC1 is also affected by NaF (Figure 44 and Table 4). The most pronounced change is a drop in the *m*-value at pH 7.0 / 20^{o}C and the explicit three-state nature of the unfolding curves observed at pH 5.5 / 20^{o}C due to stabilisation of the intermediate species (Figure 44). At pH 7.0 / 20^{o}C, the cooperativity of unfolding is reduced when in the presence of NaF and the native state is perhaps less compact than when in the absence of NaF. Furthermore while the E_{222}- and F_{max}-monitored transitions are superimposable, the C_m for the λ_{max}-monitored transition is shifted to higher urea concentrations (Figure 44) implying the likelihood of an undetectable intermediate being present at equilibrium at pH 7.0 / 20^{o}C when in the presence of NaF. At pH 5.5 / 20^{o}C the presence of NaF confers an enormous amount of stability to the intermediate state, so much so that it is detectable even by circular dichroism. The intermediate is stabilised at pH 5.5 / 20^{o}C relative to both the native and denatured states when in the presence of NaF. The native state is thus destabilised by the presence of NaF at pH 5.5 / 20^{o}C. This is confirmed by both equilibrium and kinetic data. *NaF increases the rate of unfolding of CLIC1* by

a large amount which verifies its reduced stability in the presence of this salt. However, only 4.2% of the surface area is exposed in the transition state upon unfolding (Table 5). This means that the transition state is exceptionally native-like in terms of its compactness. This result simply confirms the presence of the equilibrium intermediate under these conditions. Conversely, at pH 7.0 / 20^{o}C, the native state is stabilised by NaF in a similar way to when in the presence of NaCl (Figure 60). A relatively large amount of surface area (~20%) is exposed in the transition state upon unfolding under these conditions and the unfolding rate is decreased (Table 5). This means that if intermediate species are present at pH 7.0 / 20^{o}C when in the presence of NaF they are extremely sparsely populated compared to at pH 5.5 / 20^{o}C. It is therefore plausible that the presence of NaF decreases the stability of the native state while concurrently increasing the stability of the equilibrium intermediate species especially at low pH. The specific effect that this salt has on the structure of both the native and intermediate states of CLIC1 is unknown but may be related to the specificity of this protein towards anions in its biological function as a membrane channel protein. Furthermore CLIC1 has been shown to exhibit higher ion selectivity towards F^- and SCN^-, even more so than towards Cl^- (Singh and Ashley, 2006) despite being a chloride ion channel as its name implies.

NaF therefore *enjoys specific interactions with the native and intermediate states of CLIC1*, *resulting in stabilisation of the intermediate species*. It is not known whether this specific effect is physiologically relevant or whether it is merely an experimental artefact. Furthermore the specific interaction of NaF with a protein or an intermediate species has not been observed in any other proteins to date. Nevertheless, this NaF-stabilised intermediate state certainly is useful for studying the properties of the CLIC1 intermediate such as the kinetics of its formation.

The rate of formation of the intermediate in the presence of NaF (Figure 60) is not significantly different to when in the absence of the salt (Figure 54). Once

again it occurs in two phases as detected by fluorescence. The only difference is that the slow phase that most likely represents the formation of the intermediate species occurs at a faster rate in the absence of urea when in the presence of NaF (Table 5). This is because the intermediate species is stabilised relative to the native state when in the presence of this salt. A greater amount of surface area is exposed when the intermediate is formed from the native state at equilibrium than when the intermediate is denatured (Table 4). This could be because of the potentially oligomeric nature of this intermediate.

4.4.5. A Decrease in the Polarity Increases the Helical Content of CLIC1

The polarity of the environment at the membrane surface is low compared to the aqueous environment within the cytoplasm. In order to mimic the reduced polarity of the membrane surface, increasing concentrations of tri-fluoroethanol (TFE) were used. This organic solvent has a lower dielectric constant than water (Llinas *et al.,* 1975) and thus imitates the polarity of the membrane (Bychkova *et al.,* 1996). It is interesting that of all alcohols used to increase α-helicity in proteins; those that contain fluorine such as TFE or hexafluoroisopropanol (HFIP) are the most effective, implying that the F atom must be important in the helix-enhancing process although the reason for this is still not clear (Hirota *et al.,* 1997; Konno *et al.,* 2000; Fatima *et al.,* 2006).

1% to 10% TFE causes the α-helical nature of the protein to increase at pH 7.0 / 20^{o}C (Figure 33). Similarly at pH 5.5 / 20^{o}C, 1% to 6% TFE increases the α-helical secondary structure (Figure 33). This is a known and reported effect of TFE on the structure of proteins (Kamatari *et al.,* 1996 and Fatima *et al.,* 2006). The alcohol decreases the polarity of the environment, weakens non-local hydrophobic interactions and strengthens local polar interactions such as hydrogen bonds thereby stabilising helical structures where the polar amide groups are shielded from the solvent (Thomas and Dill, 1993; Luo and

Baldwin, 1997). TFE has a different mechanism of interaction with the protein to that of Na_2SO_4 which interacts specifically with residues on the protein surface (Otzen and Oliveberg, 1999) although both conditions cause an increase in the helical secondary structure of CLIC1 (Figure 24 and Figure 33).

What is interesting is that further increases in the TFE concentration at pH 7.0 / 20^{o}C do not cause complete denaturation or aggregation of the protein as happens at pH 5.5 / 20^{o}C due to exposed hydrophobic patches. Instead CLIC1 becomes trapped in a state that contains a degree of secondary structure, a similar effect to when the protein is exposed to extremely high temperatures (Figure 28). These results once again confirm the high stability and relative rigidity of the native state of the protein when at pH 7.0 / 20^{o}C compared to at low pH; which means that it is intrinsically stabilised against unfolding when in its "cytosolic" state.

These results simply prove that when the polarity of the solution is lowered, the drop in pH to 5.5 decreases the stability of the protein, possibly by increasing the flexibility or even by reducing its globular nature (Shiraki *et al.,* 1995) and hence making it easier for exposed hydrophobic surfaces to come together and form aggregates. *In vivo* the effect of the drop in polarity at the surface of the membrane simply acts to destabilise the protein further so as to facilitate its partial unfolding and to improve in the exposure of hydrophobic residues which is necessary to assist in localising the protein to the membrane surface. The increased helix-forming propensity of the protein in the low dielectric environment could assist the membrane-spanning domain of the protein in forming the transmembrane helix.

4.4.6. The Absence of Reducing Conditions has a Major Impact on the Structure and Stability of CLIC1

The cytoplasmic environment is highly reducing, containing a ratio of GSH to GSSG that ranges from 30:1 to as high as 100:1 with the physiological concentration of GSH ranging from 1 mM to 10 mM (Hwang *et al.,* 1992). These conditions are far too reducing for proteins to form disulphide bonds (Hwang *et al.,* 1992) and that is why all experiments so far have been conducted on CLIC1 in the presence of 1 mM of the reducing agent, DTT. That said; CLIC1 has been shown to be extremely sensitive to the oxidising or reducing nature of its environment, potentially forming a dimer under oxidising conditions (Littler *et al.*, 2004). The relatively high proportion of cysteines in the CLIC1 sequence means that it will be particularly susceptible to the formation of intrachain or intersubunit disulphide bonds. Furthermore the redox nature of its environment has been shown to be important for membrane insertion and for channel conductance (Singh and Ashley 2006). Therefore it would not be thourough to ignore the structure and stability of the protein when in the absence of reducing conditions.

When in the absence of reducing conditions there is no doubt that CLIC1 behaves in an exceedingly different manner to when in the presence of a reducing agent. The native state itself is altered as seen by the drop in α-helical secondary structure (Figure 30), the quenched fluorescence, the blue shift in the λ_{max} (Figure 31); the increased hydrodynamic diameter (Figure 32) and the increased capacity to bind ANS (Figure 52). All these factors indicate an astonishing resemblance between the *native state of CLIC1 in the absence of reducing conditions* and the *equilibrium intermediate species* that is detected in the presence of DTT at pH 5.5 / 20^{o}C and pH 7.0 / 37^{o}C when under mild denaturing conditions!

Does this resemblance between the native state under non-reducing conditions and the intermediate state imply that formation of the intermediate involves the

formation of disulphide bonds? Or at least that it involves the cysteine residues to some extent? This is unlikely since DTT maintains the reduced state of the cysteines under the conditions in which the intermediate forms. However there is a possibility that the two states have similar functional and perhaps even structural significance. If disulphide bonds are being formed in the absence of reducing conditions, they could either be intramolecular bonds formed *between the four exposed cysteines* in a single molecule or they could be intermolecular disulphide bonds resulting in *oligomerisation* of the protein. Since the hydrodynamic size of the protein increases substantially in the absence of DTT (Figure 32) it is likely that the disulphide bonds are intermolecular. This could result in an oligomeric molecule that is comparable with, although in no way identical to the one formed through interacting hydrophobic surfaces.

It is interesting to note here that CLIC4 has been crystallised in the absence of reducing conditions as a homotrimer (Li *et al.,* 2006) while when it is crystallised in the presence of DTT it is monomeric (Littler *et al.,* 2005) (Figure 6). The CLIC4 trimer formed under non-reducing conditions is not formed by disulphide bonds as is the case with the oxidised CLIC1 dimer (Littler *et al.,* 2004). Instead the CLIC4 molecule is assembled via hydrophobic and hydrogen bonding interactions. It is interesting though that like the CLIC1 dimer, the CLIC4 trimer oligomerises at the α2 helix in the N-terminal domain. Therefore the flexibility of the N-terminal domain and particularly the α2 helix may be a pivotal structural element for the redox-controlled oligomerisation observed in the CLIC proteins.

The native state of CLIC1 under non-reducing conditions is certainly different from that present in the highly reducing environment of the cytoplasm. For one thing, the native state of CLIC1 is considerably more hydrophobic when under non-reducing conditions (Figure 52). This ANS-binding state formed in the absence of DTT may therefore be oligomeric and hence bind to ANS near the interfaces of the monomers as does the dimeric GSTs (Sayed *et al.,* 2002; Dirr *et al.,* 2005). This would also explain why the DLS results show the

hydrodynamic diameter of the protein in the absence of DTT to be larger than when in the presence of the reducing agent. Non-reducing conditions therefore possibly result in a similar dimeric structure to the one observed by Littler *et al.* (2004) when under oxidising conditions. They reported on an intramolecular disulphide bond being formed between Cys24 and Cys59 in the N-terminal domain. However it must be noted that Littler *et al.* reported an increase in the α-helical nature of their dimeric structure whereas this structure of CLIC1 detected under non-reducing conditions has less defined helical structure which would imply a more flexible and on the whole, less structured native state (Figure 30).

Is a non-reducing environment required for CLIC1 to insert into the membrane? Not if the equilibrium intermediate species detected under reducing conditions is the true membrane-competent form of the protein. We cannot exclude the possibility, however, that the membrane-competent form is a combination of the equilibrium intermediate state and some disulphide bond-containing state formed under non-reducing or possibly even oxidising conditions. However, it is important to remember that the environment within the cell is strongly reducing so unless some oxidising signal is present it is unlikely that the state of CLIC1 under non-reducing conditions is significant. It is very interesting, though, that theoretically the enhanced hydrophobicity of the CLIC1 native state observed under non-reducing conditions would attract the molecule to the lipid membrane. Furthermore binding of CLIC4 to the membrane has been shown to be enhanced by oxidation (Littler *et al.,* 2005) and thus a similar effect could be occurring in CLIC1 due to the augmented hydrophobicity of the molecule when exposed to non-reducing and thus perhaps oxidising conditions.

The most fascinating observation when studying CLIC1 under non-reducing conditions is that *pH no longer has an effect on the structure or stability of the protein* (Figure 47). Thus whether the protein is at pH 7.0 in the cytoplasm or whether it is at the lower pH at the membrane surface, the effect of non-

reducing, or perhaps even oxidising conditions, on its structure and stability will be identical. The equilibrium unfolding curves are superimposable at pH 7.0 / 20^{o}C and pH 5.5 / 20^{o}C when under non-reducing conditions (Figure 47). However the curves are in no way superimposable with those obtained under reducing conditions and nor are the curves as monitored by different probes by any means superimposable. This result as well as the inexplicably low recorded stability (Table 4), means that the transition is arguably no longer two-state in nature and implies the presence of intermediate species at equilibrium, species that are most likely formed due to the exposed sulphyldryls of the cysteine residues which form disulphide bonds either intra- or intermolecularly. The possibility of a dimer being formed under oxidising conditions is therefore certainly not revoked by this study. In addition these disulphide bonds may cause incomplete unfolding of the native state even when in the presence of 8 M urea. This would also explain the dubiously low $\Delta G(H_2O)$ value.

The *rate of unfolding* of the protein under non-reducing conditions is not significantly different from the unfolding rate under reducing conditions except that it is slightly faster (Figure 62). The potential formation of disulphide bonds, therefore, does not prevent the protein from unfolding, but in fact, makes it more susceptible to the unfolding process. Thus it is possible that an oxidising signal is required *in vivo* to stimulate the rapid unfolding and perhaps oligomerisation of the protein prior to its insertion into the membrane. A burst phase is detectable in the unfolding transitions in the absence of DTT, especially those monitored using circular dichroism as a probe (Figure 62). This implies the presence of intermediate species along the unfolding pathway of the protein when under non-reducing conditions. These intermediate species are not detectable under reducing conditions and therefore ought to be due to disulphide bond formation. The burst phase detected in the N → D transition when under non-reducing conditions can be compared with the burst phase detected in the I → D transition under reducing conditions. These results provide further evidence supporting the similarity between the urea-induced

intermediate state under reducing conditions and the native state present in the absence of reducing agent.

The results of this study show that the redox potential of the environment of CLIC1 is indeed, extremely important to its structure and stability. However, pH no longer affects the structure or behaviour of the protein when in the absence of reducing conditions. Therefore it can be concluded that the oxidising nature of the environment may not affect the soluble-to membrane-bound transition of CLIC1 where pH is an integral factor but rather could potentially be involved in other processes, possibly concerned with channel activity (Singh and Ashley, 2006).

4.5. Implications for CLIC1 Function

4.5.1. Is the Intermediate a Membrane-Competent Form?

By now it is clear that CLIC1 forms a non-native, potentially oligomeric state under certain conditions. However what is the functional significance of this state? Is it merely an experimental artefact or is this state crucial to CLIC1 functionality *in vivo*?

The most obvious role for the intermediate state is establishment of a so-called "membrane-competent" form of the protein. This membrane-competent form is the state that the protein assumes that permits its insertion into the membrane so that it can take on its membrane-bound structure. The membrane-competent state therefore lowers the energy barrier towards insertion of a protein into the membrane. The membrane-competent state is liable to be extremely flexible and partially denatured with exposed hydrophobic surfaces that have an affinity for the lipid membrane. The membrane-competent state has not surprisingly therefore, been observed in many pore-forming toxins as a molten globule state (reviewed in Parker and Feil, 2005). Thus the detected hydrophobic molten

globule-like intermediate state of CLIC1 is truly a prospective representation of the membrane-competent state of the protein.

4.5.2. Linkage Between Stability and Membrane Cooperativity

The chloride channel activity of CLIC1 has been shown to exhibit a strong pH dependence (Tulk *et al*., 2002; Warton *et al*., 2002), with lowest activity recorded at pH 7.0 and greater activity recorded at both lower and higher pH values. Warton *et al*. (2002) observed a threshold between pH 6.5 and pH 6.0 in which the protein drastically improves in its ability to insert into artificial bilayers (observed by a substantial reduction in the time taken to form a chloride ion channel). In combination with this data, the results from this study suggest that *CLIC1 channel activity is strongest when the protein is less stable*. A similar correlation has been observed with some of the forming toxins for example α-toxin (Bortoleto and Ward, 1999). This pH dependence implies that protonation of the ionisable groups on the surface of CLIC1, which reduces its structural stability, may have a positive effect on the interaction of this protein with the membrane surface and possibly on its ability to insert into the hydrophobic lipid interior. Furthermore, the conductance of CLIC1 channels has been shown to decline with increasing salt concentrations (Singh and Ashley, 2006). This result further complements the theory that the channel activity decreases when the stability increases since it is shown in this work that salts increase the stability of CLIC1 (Table 4). However, since no work was done in the presence of membranes in this study, these conclusions are mere speculations based on the observed correlation between the stability of CLIC1 in the absence of membrane and its channel forming activity at different pH. It can be speculated, nevertheless, that the reduced stability at the low pH lowers the free energy barrier to the formation of the intermediate species that assists the protein in inserting into the membrane.

4.5.3. Proposed Mechanism of Membrane Insertion

A schematic representation of the proposed mechanism of CLIC1 insertion into the membrane is given in Figure 71. Once again it is stressed that no membrane work has been done in this study and the mechanism put forward in this thesis is simply a suggestion centred on the way the protein behaves under conditions representative of the cytoplasm and the membrane surface as well as on information from the literature.

CLIC1 exists in the cytoplasm or the nucleoplasm of cells as a soluble monomeric globular protein with a 45% α-helical content, a strong dipole moment and a net negative charge. The molecule is stabilised by salt bridges and hydrogen bonds on its surface and displays resistance to temperature denaturation.

An unknown signal causes the protein to localise to the membrane. Perhaps this signal is an oxidising signal that occurs during a certain phase in the cell cycle and alters the reducing nature of the immediate environment of the protein? The oxidising signal would result in the native state of the protein becoming far more hydrophobic. CLIC1 will display molten globule-like characteristics under these conditions; will have reduced secondary structure and a far more flexible, less rigid tertiary structure. The protein may form a tryptophan-burying oligomeric state under these conditions either via the formation of disulphide bonds or via the exposed hydrophobic surfaces. Alternative signals that could modify the structure of the native state in a similar way may include an increase in the concentration of F^- or SCN^- ions, both of which interact specifically with the native state.

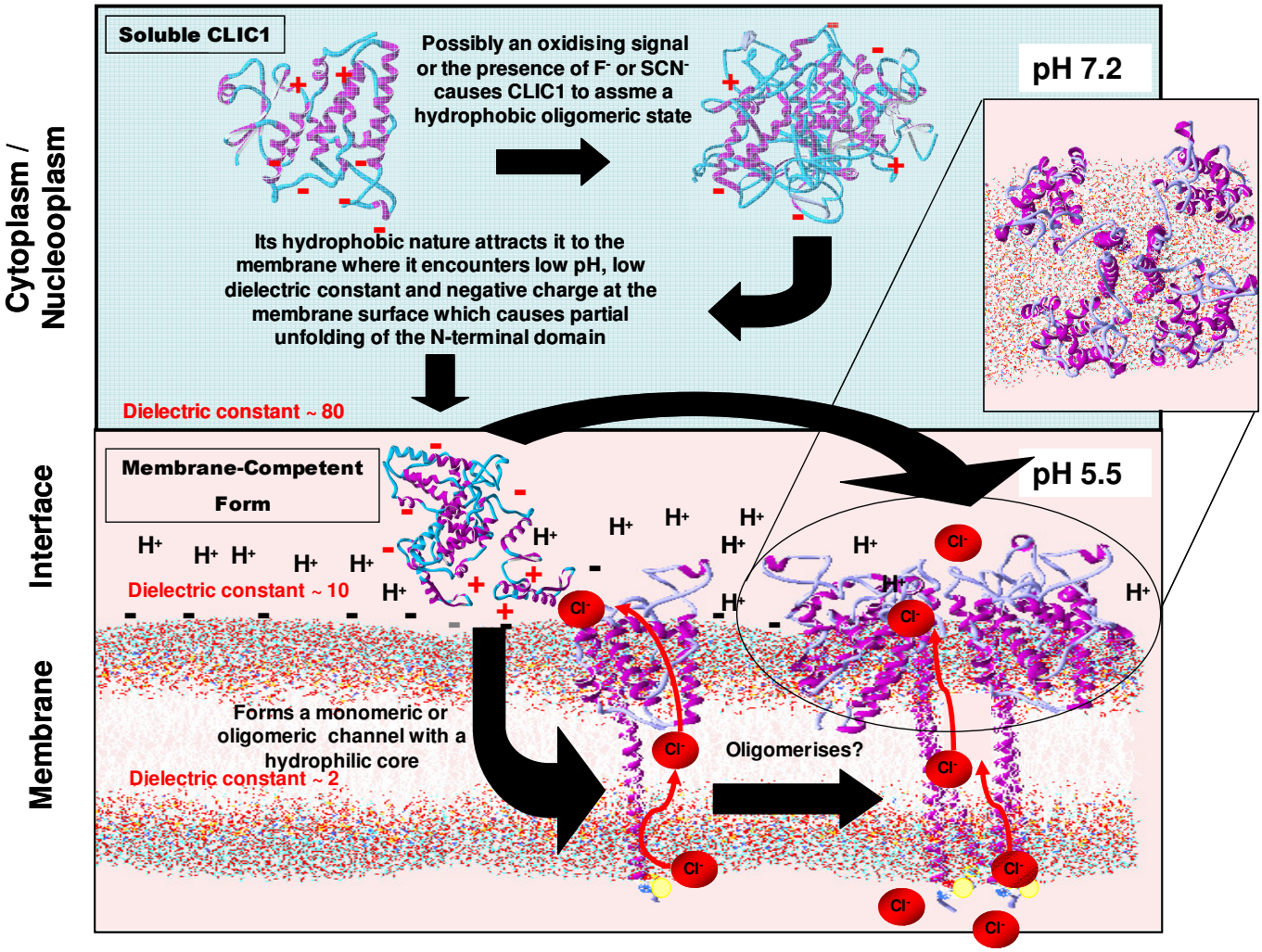


Figure 71: Schematic illustrating CLIC1 interaction with the membrane

In the cytoplasm at physiological temperature and neutral pH, CLIC1 is a soluble protein, displaying a dipole moment and a net negative charge. An unknown signal, which could possibly be oxidation or an increase in the local concentration of F^- or SCN^- ions, increases the hydrophobic surface and causes the protein to localise to the membrane. Here it encounters the electrostatically complex membrane interface including a lower pH and a negative electrostatic potential at the membrane surface. These charges will interact with the charges on the surface of the protein and, together with the low dielectric constant at the membrane surface will decrease the stability of the protein to such an extent that CLIC1 will partially unfold to its flexible molten globule conformation, exposing the hydrophobic helix from the N-terminal domain which will then be able to partition the membrane. It is possible that CLIC1 oligomerises to form a large channel consisting of a tetrameric assembly of CLIC1 subunits. This oligomerisation is possibly promoted by the increased concentration of anions surrounding the protein channel. **The inset** shows a transverse section of a hypothetical tetrameric transmembrane channel. The membrane coordinates are the gel coordinates taken from Heller *et al.,* 1993.

The thus modified native state, a charged molecule bearing a high degree of hydrophobic surface, will be attracted to the electrostatically complex membrane interface environment. Here the polarity is reduced compared to in the cytoplasm, the pH is lowered resulting in an increased proportion of hydrogen ions, the dielectric constant is low, the negative potential of the environment is increased by the negatively charged phospholipids and the extremely hydrophobic lipid membrane is in close proximity.

When CLIC1 comes into contact with this multifaceted environment at the physiological body temperature of 37^{o}C, the stability of the native state will decline and the molten globule-like state will become energetically favoured over the native state. The already flexible N-terminal domain will unfold so as to expose the transmembrane region while the C-terminal domain will remain essentially unchanged, albeit in a potentially more collapsed state with reduced α-helical structure. This state in which CLIC1 exists at the membrane surface is its *membrane-competent form*, which can be detected experimentally in the absence of lipid as an intermediate species in the urea-induced equilibrium unfolding process of the protein.

The residues Pro25 to Val46 are believed to form the ~70 Ǻ long helical transmembrane domain of CLIC1 (Figure 12) (Harrop *et al.,* 2001; Littler *et al.,* 2004; Berry and Hobert, 2006; Singh and Ashley, 2006; Nathaniel PHD thesis, in preparation). Furthermore AGADIR analysis has revealed that these residues have a high propensity to form a helix in the CLIC1 native structure (Nathaniel PHD thesis, in preparation). The hydrophobic nature of the molten globule-like membrane-competent state means that it will be attracted to the lipid membrane surface and the energy barrier to insertion of the protein into the membrane interior is lowered. This enables CLIC1 to partition the membrane and insert the proposed transmembrane region into the lipid interior.

The single tryptophan residue, Trp35 will become embedded within the membrane and the reactive Cys24 will be present on the membrane extremity of the short transmembrane portion of the protein (Singh and Ashley, 2006) as indicated by the yellow spheres in Figure 71. Only positive residues are present within the transmembrane region, instigating the anion specificity of this channel protein.

CLIC1 has been proved capable of forming monomeric channels that can independently conduct chloride ions into the nucleus (Tulk *et al.*, 2002) although the results of this work surely point towards oligomeric channels. The reason for this result could be the lack of lipid *in vitro* into which the membrane-competent state could insert which results in its oligomerisation. Perhaps the membrane-competent structure of the protein exists *in vivo* in both monomeric and oligomeric form and hence is capable of creating monomeric or oligomeric channels? The oligomeric channel may be more efficient at transporting the anions across the membrane, however. Therefore the membrane-competent state may insert directly as an oligomer or else monomeric channels could convert to the oligomeric structure once within the membrane. Singh and Ashley, 2006 support the case of an oligomeric channel. They suggest that *in vivo* functional CLIC1 channels are made up of a minimum of 16 subunits encompassing four tetrameric pores with a single transmembrane domain each and they do not discredit the idea that the protein could form even larger oligomeric structures. It is likely that CLIC1 may even adopt more than one oligomeric state when in the membrane as is the case with Bcl-$_{XL}$ (Antonsson *et al.,* 2001; Thuduppathy *et al.,* 2006). This oligomerisation may be stimulated by the accumulation of anions within the vicinity of the channels. The radius of the pore of the CLIC1 channel must be at least 1.81 Å since this is the radius of a single chloride anion (Dutzler *et al.,* 2002). However, since CLIC1 appears to form a far less specific membrane-pore than was initially assumed (Singh and Ashley, 2006); it is likely that the radius of the channel pore is as large as 7 Å since this is the size of a non-specific anion channel in brain endoplasmic reticulum (Clark *et al.,* 1997).

Chapter 5. Conclusions

The focus of this study has been to examine the various environmental conditions encountered by CLIC1 *in vivo* and to determine their effects on the structure, stability and unfolding kinetics of the protein so as to propose a mechanism whereby this exceptional molecule can exist in a soluble state within the cytoplasm as well as in a membrane bound state. The conditions to which soluble CLIC1 was exposed *in vitro* include: a range of pH, a range of temperature, different salts and different polarity in addition to reducing and non-reducing conditions. The effects are summarised in Figure 72.

It was found that CLIC1 is more stable and less flexible at pH 7.0 / 20^{o}C than at pH 5.5 / 20^{o}C. This is because while unfolding is cooperative at pH 7.0 / 20^{o}C, a stable intermediate species is populated at equilibrium at pH 5.5 / 20^{o}C. Furthermore, at pH 5.5 / 20^{o}C or at pH 7.0 / 37^{o}C certain stabilising interactions on the surface of CLIC1 have been broken rendering the protein more flexible. Likely correlated with its stability, CLIC1 unfolds significantly slower at pH 7.0 / 20^{o}C than at pH 5.5 / 20^{o}C and there is possibly some form of kinetic barrier towards unfolding hidden within the structure of the protein at pH 7.0 / 20^{o}C that most likely prevents spontaneous unfolding within the cytoplasm. This barrier is in the form of hydrogen bonds and salt bridges which also confer a degree of thermal stability upon the molecule under these conditions.

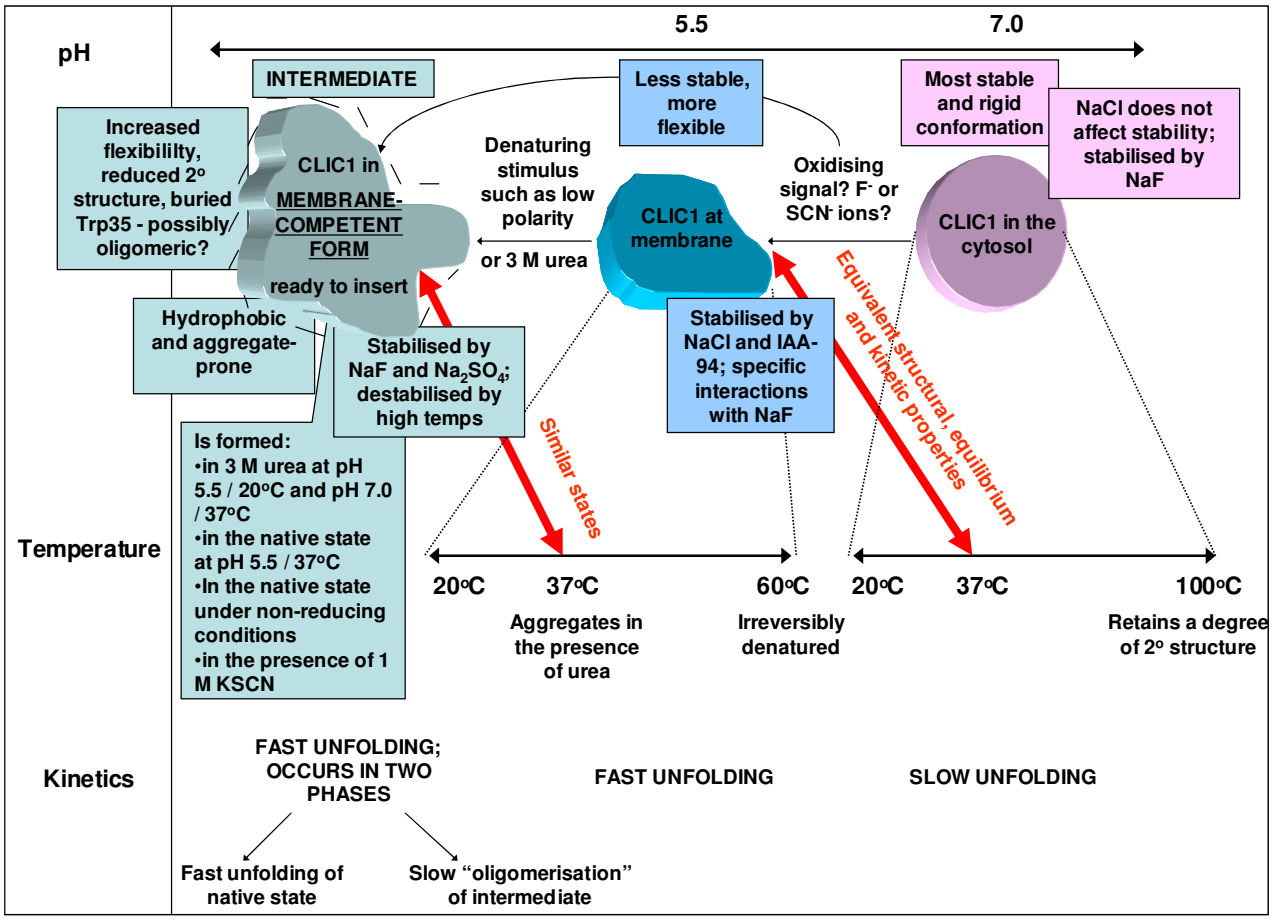


Figure 72: Summary of the effect of different environmental conditions on the structure, stability and unfolding kinetics of CLIC1

The conditions under which the membrane-competent intermediate state forms are shown. The structure and stability of CLIC1 is compared under the different environmental conditions.

An oxidising signal is possibly required by the protein to achieve a state that is attracted to the membrane surface. When CLIC1 exists under non-reducing conditions it assumes an altered, possibly oligomeric native state with exposed hydrophobic surface which would attract it to the lipid membrane. A similar although not identical hydrophobic native state is formed in the presence of F^- ions at pH 5.5 / 20^{o}C or SCN^- ions at pH 7.0 / 20^{o}C and pH 5.5 / 20^{o}C.

When CLIC1 comes into the vicinity of the lower pH, lower dielectric constant and negative charge at the membrane surface at the physiological temperature of 37^{o}C, the kinetic barrier to unfolding is removed and the N-terminal domain is able to unfold relatively quickly to a partially denatured state which may then cause the protein to oligomerise. This molten globule-like state can form rapidly because of the lack of tertiary interactions and it is of sufficient hydrophobicity to insert into and hence traverse the membrane and refold to its new membrane-bound form.

There is an amount of evidence from this work that supports the idea that the membrane-competent intermediate state of the protein is oligomeric. Firstly the lone tryptophan residue in the monomeric structure becomes more buried in the intermediate state. Secondly the blue shift in the fluorescence λ_{max} implies that this burial is not of the same magnitude depending on the condition. The λ_{max} ranges from 343 nm to 339 nm. This implies that perhaps the number of monomers making up the oligomer differs depending on the condition. Thirdly a greater amount of surface area is exposed when the intermediate is formed from the native state at equilibrium than when the intermediate is denatured, implying that the intermediate state is larger than the native state and may be oligomeric. And fourthly the protein unfolds from the native state to the intermediate state in two distinct phases, one of which is slow and exposes a large amount of surface area in the transition state and could conceivably represent oligomerisation.

Salts are seen to have a stabilising effect on the membrane-competent form of the protein. This could mean that an increase in the concentration of anions in the vicinity of the protein at the low pH at the membrane surface could promote the formation of the membrane-competent state or even its oligomerisation within the membrane to create larger channels which would have increased efficiency at transporting the anions across the membrane. An increased concentration of CLIC1 at the membrane interface may have a similar outcome.

It is likely that the molten globule-like state results from an unfolding of the N-terminal domain and a refolding into a similar helical conformation to that observed by Littler *et al.* (2004). CLIC1 is proven to be capable of forming channels in membranes in its monomeric form (Tulk *et al.,* 2002). However this work suggests the membrane-competent state formed at the low pH and electrostatically intricate membrane interface environment is as a result of reduced electrostatic repulsion effects between monomeric subunits and the formation of an oligomeric ion channel is certainly the favoured possibility. Thus, *in vivo* CLIC1 likely oligomerises into a channel possibly made of four monomeric subunits as suggested by Warton *et al.,* 2002 and Singh and Ashley, 2006, where it effectively functions to conduct anions out of the nucleus so as to assist in the process of cell division. In this way CLIC1 has its own small but significant part to play in the many intricate reactions that sustain life.

Chapter 6. References

Abe, Y., Ueda, I., Iwashita, H., Hashimoto, Y., Motoshima, H., Tanaka, Y. and Imoto, T. (1995) Effect of salt concentration on the pK_a of acidic residues in lysozyme. *J. Biochem.* **118,** 946-952

Alberts, B., Bray, D., Lewis, J., Raff, M., Roberts, K., Watson, J.D. (1994) Molecular biology of the cell pp508, Garland publishing, USA

Ali, V., Prakash, K., Kulkarni, S., Ahmad, A., Madhusudan, K.P., and Bhakuni, V. (1999) 8-anilino-1-nahthalene sulfonic acid (ANS) induces folding of acid unfolded cytochrome *c* to molten globule state as a result of electrostatic interactions. *Biochemistry* **38,** 13635-13642

Anfinsen, C.B. (1973) Principles that govern the folding of protein chains *Science* **181,** 2203-230

Antonsson, B., Montessuit, S., Sanchez, B. and Martinou, J-C. (2001) Bax is present as a high molecular weight oligomer/complex in the mitochondrial membrane of apoptotic cells. *J. Biol. Chem.* **276,** 11615-11623

Ashley, R.H. (2003) Challenging accepted ion channel biology: p64 and the CLIC family of putative intracellular anion channel proteins. *Mol. Membr. Biol.,* **20**, 1-11

Baldwin, R.L. (1994) Protein folding: matching speed and stability. *Nature* **369,** 183-184

Baldwin, R.L. (1996) How Hofmeister ion interactions affect protein stability. *Biophys. J.* **71,** 2056-2063

Baldwin, R.L. (2003) In search of the energetic role of peptide hydrogen bonds. *J. Biol. Chem.* **278,** 17581-17588

Baňuelos, S. and Muga, A. (1995) Binding of molten globule-like conformations to lipid bilayers: structure of native and partially folded α-lactalbumin bound to model membranes. *J. Biol. Chem.* **270,** 29910-29915

Barlow, D.J. and Thornton, J.M. (1983) Ion-pairs in proteins. *J. Mol. Biol.* **169,** 867-885

Barrick, D., and Baldwin, R.L. (1993a) The molten globule intermediate of apomyoglobin and the process of protein folding. *Protein Sci.* **2**, 869-876

Barrick, D. and Baldwin, R.L. (1993b) Three-state analysis of sperm whale apomyoglobin folding. *Biochemistry* **32,** 3790-3796

Baskakov, I.V., and Bolen, D.W. (1998) Monitoring the sizes of denatured ensembles of staphylococcal nuclease proteins: implications involving *m*-values, intermediates and thermodynamics. *Biochemistry* **37**, 18010-18017

Bechinger, B. (1996) Towards membrane protein design: pH-sensitive topology of Histidine-containing polypeptides. *J. Mol. Biol.* **263**, 768-775

Beerman ofm cap, B.B., Hinz, H-J., Hofmann, A. and Huber, R. (1998) Acid induced unfolding of annexin V wild type shows two intermediate states. *FEBS Lett.* **423,** 265-269

Bell, C.E., Poon, P.H., Schumaker, V.N. and Eisenberg, D. (1997) Oligomerisation of a 45 kilodalton fragment of diphtheria toxin at pH 5 to a molecule of 20-24 subunits. *Biochemistry* **36,** 15201-15207

Bennett, M.J., Choe, S., and Eisenberg, D. (1994) Refined structure of dimeric diphtheria toxin at 2.0 Å resolution. *Protein Sci.* **3**, 1444-1463

Bennion, B.J. and Daggett, V. (2003) The molecular basis for the chemical denaturation of proteins by urea. *Proc. Natl. Acad. Sci.* **100 (9)**, 5142-5147

Berman, H.M., Westbrook, J, Feng, Z., Gilliland, G., Bhat, T.N., Weissig, H., Shindyalov, I.N., and Bourne, P.E. (2000) The Protein Data Bank *Nucleic Acids Res*. **28**, 235-242

Berne, S., Sepcic, K., Anderluh, G., Turk, T., Macek, P. and Ulrih, N.P. (2005) Effect of pH on the pore forming activity and conformational stability of ostreolysin, a lipid raft-binding protein from the edible mushroom. *Biochemistry* **44,** 11137-11147

Berry, K.L., Bülow, H.E., Hall, D.H. and Hobert, O. A (2003) A *C. elegans* CLIC-like protein required for intracellular tube formation and maintenance. *Science* **302**, 2134-2137

Berry, K.L. and Hobert, O. A. (2006) Mapping functional domains of chloride intracellular channel (CLIC) proteins *in vivo*. *J. Mol. Biol.* **359,** 1316-1333

Berryman, M. A. and Bretsher, A. (2000) Identification of a novel member of the chloride intracellular gene family (CLIC5) that associates with the actin cytoskeleton of placental microvilli. *Mol. Biol. Cell* **11**, 1509-1521

Berryman, M.A. and Goldenring, J.R. (2003) CLIC4 is enriched at cell-cell junctions and colocalizes with AKAP350 at the centrosome and midbody of cultured mammalian cells. *Cell Motil. Cytoskeleton.* **56,** 159-172

Berryman, M. A., Bruno, J., Price, J., and Edwards, J.C. (2004) CLIC-5A functions as a chloride channel *in vitro* and associates with the cortical actin cytoskeleton *in vitro* and *in vivo. J. Biol. Chem.* **279,** 34794-34801

Bhuyan, A.K. and Udgaonkar, J.B. (1998) Multiple kinetic intermediates accumulate during the unfolding of horse cytochrome *c* in the oxidised state. *Biochemistry* **37,** 9147-9155

Bhuyan, A.K. and Udgaonkar, J. B (2001) Folding of horse cytochrome *c* in the reduced state. *J. Mol. Biol.* **312,** 1135-1160

Bjornestedt ,R., Stenberg, G., Widersten, M., Board, P.G., Sinning, I., Jones, T.A. and Mannervik, B. (1995) Functional significance of arginine-15 in the active site of human class Alpha glutathione transferase A1-1. *J. Mol. Biol.* **247,** 765-773

Blewitt, M.G., Chung, L.A. and London, E. (1985) Effect of pH on the conformation of diphtheria toxin and its implications for membrane penetration. *Biochemistry* **24,** 5458-5464

Board, P.G., Coggan, M., Chelvanayagam, G., Easteal, S., Jermiin, L.S., Schulte, G.K., Danley, D.E., Hoth, L.R., Griffor, M.C., Kamath, A.V., Rosner, M. H., Chrunyk, B.A., Perregaux, D.E., Gabel, C.A., Geoghegan, K.F., and Pandit, J. (2000) Identification, characterisation, and crystal structure of the Omega class glutathione transferases. *J. Biol. Chem.* **275**, 24798-24806

Board, P.G., Coggan, M., Watson, S., Gage, P.W., and Dulhunty, A.F. (2004) CLIC-2 modulates cardiac ryanodine receptor Ca^{2+} release channels. *Int. J. Biochem. Cell Biol.* **36,** 1599-1612

Bolen, D.W. and Santoro, M.M (1988) Unfolding free energy changes determined by the linear extrapolation method 2. Incorporation of ΔG^{o}_{N-U} values in a thermodynamic cycle. *Biochemistry* **27**, 8069-8074

Born, M. (1920) Volume and heat of hydration of ions. *Z. Phys.* **1,** 45-48

Bortoleto, R.K. and Ward, R.J. (1999) A stability transition at mildly acidic pH in the alpha-hemolysin (alpha toxin) from *Staphylococcus aureus. FEBS Lett.* **459,** 438-442

Bousset, L., Belrhali, H., Melki, R. and Morera, S. (2001) Crystal structures of the yeast prion Ure2p functional region in complex with glutathione and related compounds. *Biochemistry* **40,** 13564-13573

Brockwell, D.J., Smith, D.A. and Radford, S.E. (2000) Protein folding mechanisms: new methods and emerging ideas. *Curr. Opin. Struct. Biol.* **10**, 16-25

Bychkova, V.E., Pain, R.H. and Ptitsyn, O.B. (1988) The "molten globule" state is involved in the translocation of proteins across membranes? *FEBS Lett.* **238,** 231-234

Bychkova, V.E., Dujsekina, A.E., Kleni, S.I., Tiktopulo, E.I., Uversky, V.N. and Ptitsyn, O.B. (1996) Molten globule-like state of cytochrome *c* under conditions simulating those near the membrane surface. *Biochemistry* **35,** 6058-6063

Caccuri, A.M., Antonini, G., Allocati, N., Di Ilio, C., De Maria, F., Innocenti, F., Parker, M.W., Masulli, M., Lo Bello, M., Turella, P., Federici, G., and Ricci, G. (2002) GSTB1-1 from *Protleus mirabilis*: a snapshot of an enzyme in the evolutionary pathway from a redox enzyme to a conjugating enzyme. *J. Biol. Chem.* **277**, 18777-18784

Carbonnaux, C., Ries-Kautt, M., and Ducruix, A. (1995) Relative effectiveness of various anions on the solubility of acidic hypoderma lineatum collagenase at pH 7.2. *Protein Sci.* **4,** 2123-2128

Carra, J.H., Anderson, E.A and Privalov, P.L., (1994) Three-state thermodynamic analysis of the denaturation of staphylococcal nuclease mutants. *Biochemistry* **33**, 10842-10850

Celej, M.S., Montich, G.G., and Fidelio, G.D. (2003) Protein stability induced by ligand binding correlates with changes in protein flexibility. *Protein Sci.* **12,** 1496-1506

Chakravarty, S., Bhinge, A., and Varadarajan, R. (2002) A procedure for detection and quantitation of cavity volumes in proteins. *J. Biol. Chem.* **277,** 31345-31353

Chalikian, T.V., Gindikin, V.S. and Breslauer, K.J. (1995) Volumetric characterisations of the native, molten globule and unfolded states of cytochrome *c* at acidic pH. *J. Mol. Biol.* **250,** 291-306

Chan, H.S., Bromberg, S and Dill, K.A. (1995) Models of Cooperativity in protein folding. *Phil. Trans. Soc. London* **348**, 61-70

Chenal, A., Savarin, P., Nizard, P., Guillain, F., Gillet, D. and Forge, V. (2002) Membrane protein insertion regulated by bringing electrostatic and hydrophobic interactions into play: A case study with the translocation domain of the diphtheria toxin. *J. Biol. Chem.* **277,** 43425-43432

Chin, C-N., von Heijne, G. and de Gier, J.W.L. (2002) Membrane proteins: shaping up. *Trends. Biochem. Sci.* **27,** 231-234

Cho, S.G., Lee, Y.H., Park, H.S., Ryoo, K., Kang, K.W., Park, J., Eom, S.J., Kim, M.J., Chang, T.S., Choi, S.Y., Shim, J., Kim, Y., Dong, M.S., Lee, M.J., Kim, S.G., Ichijo, H. and Choi, E.J. (2001) Glutathione S-transferase Mu modulates the stress activated signals by suppressing apoptosis signal regulating kinase1. *J. Biol. Chem.* **276**, 12749-12755

Choe, S., Bennett, M.J., Fujii, G., Curmi, P.M., Kanterdjieff, K.A., Collier, R.J. and Eisenberg, D. (1992) The crystal structure of diphtheria toxin. *Nature* **357,** 216-222

Chou, J.J., Li, H.L., Salvesen, G.S., Yuan, J.Y., and Wagner, G. (1999) Solution structure of BID, an intracellular amplifier of apoptotic signalling. *Cell* **96,** 615-624

Chuang, J.Z., Milner, T.A., Zhu, M., and Sung, C.H. (1999) A 29 kDa intracellular chloride channel p64H1 is associated with large dense-core vesicles in rat hippocampal neurons. *J. Neurosci.* **19,** 2919-2928

Clark, A.G., Murray, D. and Ashley, R.H. (1997) Single-channel properties of a rat brain endoplasmic reticulum anion channel. *Biophys. J.* **73,** 168-178

Clark, P.L. (2004) Protein folding in the cell: reshaping the folding funnel. *Trends Biochem. Sci.* **29,** 527-534

Clementi, C., Nymeyer, H., and Onuchic, J.N. (2000) Topological and energetic factors: what determines the structural details of the transition state ensemble and "en-route" intermediates for protein folding? An investigation for small globular proteins. *J. Mol. Biol.* **298,** 937-953

Cobos, E.S. and Radford, S.E. (2006) Sulfate-induced effects in the on-pathway intermediate of the bacterial immunity protein Im7. *Biochemistry* **45,** 2274-2282

COMPARER on-line: structure-based sequence alignment tool: http://www-cryst.bioc.cam.ac.uk/~robert/cpgs/COMPARER/comparer.html

Cromer, B.A., Morton, C.J., Board, P.G., and Parker, M. (2002) From glutathione transferase to pore in a CLIC. *Eur. Biophys. J.* **31**, 356-364

Daggett, V. and Fersht, A.R. (2000) in *Mechanisms of Protein Folding,* second edition (Pain, R. H., ed) pp 175-211, Oxford University Press, Great Britain

Darwin, O., Alonso, V., and Dill, K.A. (1991) Solvent denaturation and stabilization of globular proteins. *Biochemistry* **30**, 5974-5985

Debye, P., and Hückel, E. (1923) Zur theorie der electrolyte. I. Gefrierpunktserniedrigung und verwandte erscheinungen (The interionic attraction theory of deviations from ideal behaviour in solution). *Physik. Z.*, **24,** 185-206

De Young, L.R., Burton, L.E., Liu, J., Powell, M.F., Schmeizer, C.H. and Skelton, N.J. (1996) RhNGF slow unfolding is not due to proline isomerisation: possibility of a cysteine knot loop-threading mechanism. *Protein Sci.* **5,** 1554-1566

Dill, K.A. (1990) Dominant forces in protein folding. *Biochemistry* **29,** 7133-7153

Dill, K.A. and Stigter, D. (1995) Modelling protein stability as heteropolymer collapse. *Adv. Prot. Chem.* **45**, 59-104

Dill, K.A. and Chan, H.S. (1997) From Levinthal to pathways to funnels. *Nat. Struct. Biol.* **4**, 10-19

Dirr, H.W., and Reinemer, P. (1991) Equilibrium unfolding of class Pi glutathione- S transferase. *Biochem. Biophys. Res. Comm.* **180**, 294-300

Dirr, H.W., Reinemer, P. and Huber, R. (1994) X-ray crystal structures of cytosolic glutathione S-transferases. Implications for protein architecture, substrate recognition and catalytic function. *Eur. J. Biochem.***220**, 645-661

Dirr, H.W. and Wallace, L.A. (1999) Role of the C terminal helix 9 in the stability and ligandin function of class α glutathione transferase A1-1. *Biochemistry* **38**, 15631-15640

Dirr, H.W., Little, T., Kuhnert, D.C. and Sayed, Y. (2005) A conserved N-capping motif contributes significantly to the stabilisation and dynamics of the C-terminal region of class Alpha glutathione S-transferases. *J. Biol. Chem.* **280,** 19480-19487

Dobson, C.M., Sali, A. and Karplus, M. (1998) Protein folding: a perspective from theory and experiment. *Angew. Chem. Int. Edit.* **37,** 868-893

Dobson, C.M., and Karplus, M. (1999) The fundamentals of protein folding: bringing together theory and experiment. *Curr. Opin. Struct. Biol.* **9**, 92-101

Dobson, C.M. (2000) in *Mechanisms of Protein Folding* second edition (Pain, R. H., ed) pp 1-33, Oxford University Press, Great Britain

Dobson, C.M. (2004) Principles of protein folding, misfolding and aggregation. *Sem. Cell Dev. Biol.* **15**, 3-16

Doyle, D.F., Waldner, J.C., Parkh, S., Alcazar-Roman, L. and Pielak, G.J. (1996) Changing the transition state for protein (un) folding. *Biochemistry* **35,** 7403-7411

Dulhunty, A., Gage, P., Curtis, S., Chelvanayagam, G., and Board, P. (2001) The glutathione transferase structural family includes a nuclear chloride channel and a ryanodine receptor calcium release channel modulator. *J. Biol. Chem.* **276**, 3319-3323

Dulhunty, A. F., Pouliquin, P., Coggan, M., Gage, P.W. and Board, P.G. (2005) A recently identified member of the glutathione transferase structural family modifies cardiac RyR2 substate activity, coupled gating and activation by Ca^{2+} and ATP. *Biochem. J.* **390** 333-343

Duncan, R.R., Westwood, P.K., Boyd, A., and Ashley, R.H. (1997) Rat brain p64H1, expression of a new member of the p64 chloride channel protein family in endoplasmic reticulum. *J. Biol. Chem.* **272,** 23880-23886

Dutzler, R., Campbell, E.B., Cadene, M., Chait, B.T. and MacKinnon, R. (2002) X-ray structure of a ClC chloride channel at 3.0 Å reveals the molecular basis of anion selectivity. *Nature* **415,** 287-294

Dutzler, R. (2006) The ClC family of chloride channels and transporters. *Curr. Opin. Struct. Biol.* **16,** 439-446

Duy, C. and Fitter, J. (2005) Thermostability of irreversible unfolding α-amylases analysed by unfolding kinetics. *J. Biol. Chem.* **280,** 37360-37365

Edelhoch, H. (1967) Spectroscopic determination of tryptophan and tyrosine in proteins. *Biochemistry* **6,** 1948-1954

Edwards, J.C. (2000) A novel p64-related Cl^- channel: subcellular distribution and nephron segment-specific expression. *Am. J. Physiol.* **276,** F398-F408

Edwards, J.C., and Kapadia, S. (2000) Regulation of the bovine kidney microsomal chloride channel p64 by p59fyn, a Src family tyrosine kinase. *J. Biol. Chem.* **275,** 31826-31832

Edwards, J.C., Cohen, C., Xu, C.W. and Schlesinger, P.H. (2006) *C*-Src control of chloride channel support for osteoclast HCL transport and bone resorption. *J. Biol. Chem.* **281,** 28011-28022

Ellis, R.J., and Hartl, F.U. (1999) Principles of protein folding in the cellular environment. *Curr. Opin. Struct. Biol.* **9**, 102-110

Endo, T., and Schatz, G. (1988) Latent membrane perturbation activity of a mitochondrial precursor protein is exposed by unfolding. *EMBO J.* **7,** 1153-1158

Engelhard, M. and Evans, P.A. (1995) Kinetics of interaction of partially folded proteins with a hydrophobic dye: evidence that molten globule character is maximal in early folding intermediates. *Protein Sci.* 1553-1562

Englander, S.W. (2000) Protein foldinh intermediates and pathways studied by hydrogen exchange. *Annu. Rev. Biophys. Biomol. Struct.* **29,** 213-238

Erhardt, J., and Dirr, H. (1995) Native dimer stabilises the subunit tertiary structure of porcine class Pi glutathione S-transferase. *Eur. J. Biochem.* **230**, 614-620

Fatima, S., Ahmad, B. and Khan, R.H. (2006) Fluoroalcohols induced unfolding of Succinylated Con A: Native like β-structure in partially folded intermediate and α-helix in molten globule like state. *Arch. Biochem. Biophys.* **454**, 170-180

Fernandez-Salas, E., Sagar, M., Cheng, C., Yuspa, S.H., and Weinberg, W.C. (1999) p53 and tumour necrosis factor alpha regulate the expression of a mitochondrial chloride channel protein. *J. Biol. Chem.* **274,** 36488-36497

Fernandez-Salas, E., Suh, K.S., Speransky, V.V., Bowers, W.L., Levy, J.M., Adams, T., Pathak, K.R., Edwards, L.E., Hayes, D.D., Cheng, C., Steven, A.C., Weinberg, W.C., and Yuspa, S.H. (2002) mtCLIC/CLIC4, an organellular chloride channel protein is increased by DNA damage and participates in the apoptotic response to p53. *Mol. Cell Biol.* **22**, 3610-3620

Fersht, A.R. (2000) Transition-state structure as a unifying basis in protein-folding mechanisms: contact order, chain topology, stability, and the extended nucleus mechanism. *Proc. Natl. Acad. Sci. USA* **97,** 1525-1529

Fink, A.L., Calciano, L.J., Goto, Y., Kurotsu, T. and Palleros, P.R. (1994) Classification of acid denaturation of proteins: intermediates and unfolded states. *Biochemistry* **34,** 12504-12511

Fink, A.L. (1995) in *Methods in Molecular Biology, Vol 40: Protein Stability and Folding: Theory and Practice* (Shirley, B. A., ed) pp 343-360, Humana Press Inc., Totowa, NJ

Fink, A.L. (1998) Protein aggregation: folding aggregates, inclusion bodies and amyloid. *Fold. Des.* **3**, R9-R23

Friedli, M., Guipponi, M., Bertrand, S., Bertrand, D., Neerman-Arbez, M., Scott, H.S. and Antonarakis, S.E. (2003) Identification of a novel member of the CLIC family, CLIC6, mapping to 21q22.12. *Gene.* **320,** 31-40

Fujiwara, Arai, M., Shimizu, A., Ikeguchi, M., Kuwajima, K., and Sugai, S. (1999) Folding-unfolding equilibrium and kinetics of equine β-lactoglobulin: equivalence between the equilibrium molten globule state and a burst-phase folding intermediate. *Biochemistry* **38**, 4455-4463

García-Moreno, E., Dwyer, J.J., Gittis, A.G., Lattman, E.E., Spencer, D.S., and Stites, W.E. (1997) Experimental measurement of the effective dielectric in the hydrophobic core of a protein. *Biophys. Chem.* **64,** 211-224

García-Sáez, A.J., Mingarro, I., Pérez-Payá, E., and Salgado, J. (2004) Membrane-insertion fragments of Bcl-x_L, Bax and Bid. *Biochemistry* **43,** 10930-10943

Gonzalez-Mondragon, E., Zubillaga, R.A., and Hernandez-Arana, A. (2006) Effect of a specific inhibitor on the unfolding and refolding kinetics of dimeric triosephosphate isomerase: establishing the dimeric and similarly structured nature of the main transition states on the forward and backward reactions. *Biophys. Chem.* In press.

Goto, Y., Calciano, L.J., and Fink, A.L. (1990) Acid-induced folding of proteins. *Proc. Natl. Acad. Sci.* **87,** 573-577

Gouaux, E. (1997) Channel-forming toxins: tales of transformation. *Curr. Opin. Struct. Biol.* **7,** 566-573

Govindarajan, S. and Goldstein, R.A. (1998) On the thermodynamic hypothesis of protein folding. *Proc. Natl. Acad. Sci.* **95,** 5545-5549

Grantcharova, V., Alm, E.J., Baker, P., and Horwich, A.L. (2001) Mechanisms of protein folding. *Curr. Opin. Struct. Biol.* **11,** 70-82

Greene, R.F.Jr., and Pace, C.N. (1973) Urea and guanidine hydrochloride denaturation of ribonuclease, lysozyme, α-chymotrypsin and β-lactoglobulin. *J. Biol. Chem.* **249,** 5388-5393

Greenfield, N.J. (1996) Methods to estimate the conformation of proteins and polypeptides from circular dichroism data. *Anal. Biochem.* **235,** 1-10

Griffon, N., Jeanneteau, F., Prieur, F., Diaz, J. and Sokoloff, P. (2003) CLIC6, a member of the intracellular chloride channel family interacts with dopamine D(2)-like receptors. *Brain Res. Mol. Brain Res.* **117,** 47-57

Grochulski, P., Masson, L., Borisova, S., Pusztai-Carey, M., Schwartz, J.L., Brosseau, R., and Cygler, M. (1995) *Bacillus thuringiensis* CryIA(a) insecticidal toxin: crystal structure and chemical formation. *J. Mol. Biol.* **254**, 447-464

Gross, A., McDonnell, J.M., and Korsmeyer, S.J. (1999) BCL-2 family members and the mitochondria in apoptosis. *Genes Dev.* **13,** 1899-1911

Guex, N. and Peitsch, M.C. (1997) SWISS-MODEL and the Swiss-PDB viewer: an environment for cooperative protein modelling. *Electrophoresis* **18**, 2714-2723

Guha, S. and Bhattacharyya, B. (1995) A partially folded intermediate during tubulin unfolding: its detection and spectroscopic characterisation. *Biochemistry* **34**, 6925-6931

Gustafsson, A., Etahadieh, M., Jemth, P. and Mannervik, B. (1999) The C-terminal region of human glutathione transferase A1-1 affects the rate of glutathione binding and the ionisation of active-site Tyr9. *Biochemistry* **38,** 16268-16275

Haltia, T. and Freire, E. (1995) Forces and factors that contribute to the structural stability of membrane proteins *Biochim. Biophys. Acta* **1241**, 295-322

Harrop, S.J., De Maere, M.Z., Fairlie, W.D., Rezstsova, T., Valenzuela, S.M., Mazzanti, M., Tonini, R., Qiu, M.R., Jankova, L., Warton, K., Bauskin, A.R., Wu, W.M., Pankhurst, S., Campbell, T.J., Breit, S.N., and Curmi, P.M.G (2001) Crystal structure of a soluble form of the intracellular chloride ion channel CLIC1 (NCC27) at 1.4Å resolution. *J. Biol. Chem.* **276**, 44993-45000

Heiss, N.S., Poustka, A. (1997) Genomic structure of a novel chloride channel gene CLIC2 in Xq28. *Genomics* **45**, 224-228

Heller, H., Schaefer, M. and Schulten, K. (1993) Molecular dynamics simulation of a bilayer of 200~lipids in the gel and in the liquid crystal phases. *J. Phys. Chem.* **97,** 8343-8360

Henderson, P.J.F., (1993) the 12-transmembrane helix transporters. *Curr. Opin. Cell Biol.* **5**, 708-721

Hendsch, Z.S. and Tidor, B. (1994) Do salt bridges stabilise proteins? A continuum electrostatic analysis. *Protein Sci.* **3,** 211-226

Herbert, H., Schmidt-Krey, L., Morgenstern, R., Murata, K., Hirai, T., Mitsuoka, K., and Fujiyoshi, Y. (1997) The 3.0 angstrom projection structure of microsomal glutathione transferase as determined by electron crystallography of p2(1)2(1)2 two-dimensional crystals. *J. Mol. Biol.* **271,** 751-758

Hirota, N., Mizuno, K. and Goto, Y. (1997) Cooperative α-helix formation of β-lactoglobulin and melittin induced by hexafluoroisopropanol. *Protein Sci.* **6,** 416-421

Hofmeister, F. (1888) Zur lehre von der wirkung der salze. Zweite mittheilung. *Arch. Exp. Pathol. Pharmakol.* **24,** 247-260

Holmgren, A. (1985) Thioredoxin. *Ann. Rev. Biochem.* **54**, 237-271

Holmgren, A. (1995) Thioredoxin structure and mechanism: conformational changes on oxidation of the active-site sulphyldryls to a disulfide. *Structure* **3**: 239-243

Hong, H. and Tamm, L.K. (2004) Elastic coupling of integral membrane protein stability to lipid bilayer forces. *Proc. Natl. Acad. Sci.* **101,** 4065-4070

Honig, B.H., Hubbell, W.L. and Flewelling, R.F. (1986) Electrostatic interactions in membranes and proteins. *Annu. Rev. Biophys. Biophys. Chem.* **15,** 163-193

Hornby, J.A.**,** Luo, J.K., Stevens, J.M., Wallace, L.A., Kaplan, W., Armstrong, R.N., and Dirr, H.W. (2000) Equilibrium folding of dimeric class Mu glutathione transferases involves a stable monomeric intermediate. *Biochemistry* **39**, 12336-12344

Howell, S., Duncan, R.R., and Ashley, R.H. (1996) Identification and characterisation of a homologue of p64 in rat tissues. *FEBS Lett.,* **390,** 207-210

Hsu, Y-T., Wolter, K.G. and Youle, R.J. (1997) Cytosol-to-membrane redistribution of Bax and Bcl-$_{XL}$ during apoptosis. *Proc. Natl. Acad. Sci.* **94,** 3668-3672

Huang, G.S., and Oas, T.G. (1995) Submillisecond folding of monomeric λ-repressor. *Proc. Natl. Acad. Sci.* **92,** 6878-6882

Hwang, C., Sinskey, A.J. and Lodish, H.F. (1992) Oxidised redox state of glutathione in the endoplasmic reticulum. *Science* **257,** 1496-1502

Ionescu, R.M., Smith, V.F., O'Neill, J.C. Jr., and Matthews, C.R. (2000) Multistate equilibrium unfolding of *Escherichia coli* dihydrofolate reductase: thermodynamic and spectroscopic description of the native, intermediate and unfolded ensembles. *Biochemistry* **39**, 9540-9550

Jackson, G.S., Hill, A.F., Joseph, C., Hosszu, L., Power, A., Waltho, J.P., Clarke, A.R. and Collinge, J. (1999) Multiple folding pathways for heterologously expressed human prion protein. *Biochim. Biophys. Acta.* **1431,** 1-13

Jacobs, R.E. and White, S.H. (1989) The nature of the hydrophobic binding of small peptides at the bilayer interface: implications for the insertion of transbilayer helices. *Biochemistry* **28**: 3421-3437

Jaenicke, R. and Bohm, G. (1998) The stability of proteins in extreme environments. *Curr. Opin. Struct. Biol.* **8**, 738-748

Jakobsson, P-J., Morgenstern, R., Mancini, J., Ford-Hutchinson, A., and Persson, B. (1999) Common structural features of MAPEG- a widespread superfamily of membrane associated proteins with highly divergent functions in eicosanoid and glutathione metabolism. *Protein Sci.* **8,** 689-692

Janiak, F., Leber, B. and Andrews, D.W. (1994) Assembly of Bcl-2 into microsomal and outer mitochondrial membranes. *J. Biol. Chem.* **269,** 9842-9849

Jemth, P., Gianni, S., Day, R., Li, B., Johnson, C.M., Daggett, V. and Fersht, A.R. (2004) Demonstration of a low energy on-pathway intermediate in a fast-folding protein by kinetics, protein engineering, and simulation. *Proc. Natl. Acad. Sci.* **101,** 6450-6455

Jentsch, T.J., Stein. V., Weinreich, F. and Zdebik, A.A. (2001) Molecular structure and physiological function of chloride channels. *Physiol. Rev.* **82**, 503-568

Jeppesen, P., Ortiz, P., Shepard, W., Kinzy, T.G., Nyborg, J. and Andersen, G.R. (2003) The crystal structure of the glutathione S-transferase-like domain of elongation factor 1B (gamma) from *Saccharomyces cerevisiae. J. Biol. Chem.* **278,** 47190-47198

Jiang, J.X., and London, E. (1990) Involvement of denaturation-like changes in *Pseudomonas* exotoxin A hydrophobicity and membrane penetration determined by characterisation of pH and thermal transitions. Roles of two distinct conformationally altered states. *J. Biol. Chem.* **265,** 8636-8641

Jiang, J.X., Abrams, F.S., and London, E. (1991) Folding changes in membrane-inserted diphtheria toxin that play important roles in its translocation. *Biochemistry* **30**, 3857-3864

Kamatari, Y.O., Konno, T., Kataoka, M. and Akasaka, K. (1996) The methanol-induced globular and expanded denatured states of cytochrome c: a study by CD, fluorescence, NMR and small angle X-ray scattering. *J. Mol. Biol.* **259,** 512-523

Kao, Y-H., Fitch, C.A., Bhattacharya, S. Sarkisian, C.J., Lecomte, J.T.J and García-Moreno, B. E. (2000) Salt effects on ionisation equilibria of histidines in myoglobin. *Biophys. J.* **79**, 1637-1654

Kaplan, W., Hüsler, P., Klump, H., Erhardt, J., Sluis-Cremer, N., and Dirr, H.W. (1997) Conformational stability of pGEX-expressed *Schistosoma japonicum* glutathione S-transferase: a detoxification enzyme and fusion-protein affinity tag. *Protein Sci.* **6**, 399-406

Karp, D.A., Gittis, A.G., Stahley, M.R., Fitch, C.A., Stites, W.E. and Garcia-Moreno, E.B. (2007) High apparent dielectric constant inside a protein reflects structural reorganization coupled to the ionization of an internal asp. *Biophys. J.* **92,** 2041-2053

Kauzmann, W. (1959) Some factors in the interpretation of protein denaturation. *Adv. Protein Chem.* **14,** 1-63

Kharakoz, D.P. and Bychkova, V. E. (1997) Molten globule of human alpha-lactalbumin: hydration, density, and compressibility of the interior. *Biochemistry* **36,** 1882-1890

Kiefhaber, T. (1995) in *Methods in Molecular Biology, Vol 40: Protein Stability and Folding: Theory and Practice* (Shirley, B. A., ed) pp 313-342, Humana Press Inc., Totowa, NJ

Kim, D.H., Jang, D.S., Nam, G.H., Yun, S., Cho, J.H., Choi, J.H., Choi, G., Lee, H.C. and Choi, K.Y. (2000) Equilibrium and kinetic analysis of folding of ketosteroid isomerase from Comamoms testosteroni. *Biochemistry* **39,** 13084-13092

Kim, P.S., and Baldwin, R.L. (1990) Intermediates in the folding reactions of small proteins. *Annu. Rev. Biochem.* **59,** 631-660

Kleinschmidt, J.H., and Tamm, L.K. (1996) Folding intermediates of a β-barrel membrane protein. Kinetic evidence for a multi-step membrane insertion mechanism. *Biochemistry* **35,** 12993-13000

Klotz, I.M. (1996) Equilibrium constants and free energies in unfolding of proteins in urea solutions. *Proc. Natl. Acad. Sci.* **93,** 14411-14415

Kohn, W.D., Kay, C.M., and Hodges, R.S. (1997) Salt effects on protein stability: two-stranded α-helical coiled coils containing inter- or intra- helical ion pairs. *J. Mol. Biol.* **267,** 1039-1052

Konno, T., Iwashita, J., and Nagayama, K. (2000) Fluorinated alcohol, the third group of co solvents that stabilise the molten globule state relative to the highly denatured state of cytochrome c. *Protein Sci.* **9,** 564-569

Kraayenhof, R., Sterk, G.J. and Sang, H.W. (1993) Probing biomembrane interfacial potential and pH profiles with a new type of float-like fluorophores positioned at varying distance from the membrane surface. *Biochemistry* **32,** 10057-10066

Krantz, B.A., Srivastava, A.K., Nauli, S., Baker, D., Sauer, R.T. and Sosnick, T.R. (2002) Understanding protein hydrogen bond formation with kinetic H/D amide isotope effects. *Nat. Struct. Biol.* **9,** 458-463

Krishna, M.M.G. and Englander, S.W. (2007) A unified mechanism of protein folding: predetermined pathways with optional errors. *Protein Sci.* **16,** 449-464

Kuhlman, B., Luisi, D.L., Evans, P.A., and Raleigh, D.P. (1998) Global analysis of the effects of temperature and denaturant on the folding and unfolding kinetics of the N-terminal domain of the protein L9. *J. Mol. Biol.* **284,** 1661-1670

Kuhlman, B., Luisi, D.L., Young, P., and Raleigh, D.P. (1999) pK_a values and the pH dependent stability of the N-terminal domain of L9 as probes of electrostatic interactions in the denatured state. Differentiation between local and non local interactions. *Biochemistry* **38**, 4896-4903

Kumar, S. and Nussinov, R. (2002) Relationship between ion pair geometries and electrostatic strengths in proteins. *Biophys. J.* **83,** 1595-1612

Kuwajima, K. (1996) The molten globule state of α-lactalbumin. *FASEB J.* **10,** 102-109

Kuwajima, K., Yamaya, H., and Sugai, S. (1996) The burst-phase intermediate in the refolding of β-lactoglobulin studied by stopped-flow circular dichroism and absorbance spectroscopy. *J. Mol. Biol.* **264,** 806-822

Kuwajima, K. and Arai, M. (2000) in *Mechanisms of Protein Folding,* second edition (Pain, R. H., ed) pp 139-174, Oxford University Press, Great Britain

Kyte, J., and Doolittle, R.F. (1982) A simple method for displaying the hydropathic character of a protein. *J. Mol. Biol.* **157,** 105-132

Lacroix, E., Viguera, A.R. and Serrano, L. (1998) Elucidating the folding problem of alpha-helices: local motifs, long-range electrostatics, ionic strength dependence and prediction of NMR parameters. *J. Mol. Biol.*, **248**, 173-191

Ladner, J.E., Parsons, J.F., Rife, C.L., Gilliland, G.L., and Armstrong, R.N. (2004) Parallel evolutionary pathways for glutathione transferases: structure and mechanism of the mitochondria class Kappa enzyme rGST K1-1. *Biochemistry* **43,** 352-361

Laemmli, U.K., (1970) Cleavage of structural proteins during the assembly of the head of bacteriophage T4. *Nature* **227**, 680-685

Lakowicz, J.R. (1999) *Principles of fluorescence spectroscopy*. Plenum Press, New York.

Landry, D., Sullivan, S., Nicolaides, M., Redhead, C., Edelman, A., Field, M., Al-Awqati, Q., and Edwards, J. (1993) Molecular cloning and characterisation of p64, a chloride channel protein from kidney microsomes. *J. Biol. Chem.* **268,** 14948-14955

Landry, D.W., Reitman, M., Cragoe, E.J.Jr. and Al-Awqati, Q. (1997) Epithelial chloride channel: development of inhibitory ligands. *J. Gen. Physiol.* **90,** 779-798

Laskowski, R. A., Hutchinson, E. G., Michie, A. D., Wallace, A. C., Jones, M. L., and Thornton, J. M. (1997) PDBsum: A Web-based database of summaries and analyses of all PDB structures. *Trends Biochem. Sci.* **22**, 488-490

Laurents, D.V., and Baldwin, R.L. (1998) Protein folding: Matching theory and experiment. *Biophys. J.* **75**, 428-434

Lazdunski, C.J., Baty, D., Geli, V., Cavard, D., Morton, J., Lloubes, R., Howard, S.P., Knibiehler, M., Chartier, M., Varenne, S. *et al.* (1988) The membrane channel-forming colicin A: synthesis, secretion, structure, action and immunity. *Biochim. Biophys. Acta* **947,** 445-464

Lee, K.K., Fitch, C.A., Lecomte, J.T.J, and García-Moreno, B. E, (2002) Electrostatic effects in highly charged proteins: salt sensitivity of pK_a values of histidines in staphylococcal nuclease. *Biochemistry* **41**, 5656-5667

Levinthal, C. (1968) Are there pathways for protein folding? *J. Chim. Phys. Phys.-Chim. Biol.* **65,** 44-45

Li, J., Carrol, J., Eller, D.J. (1991) Crystal structure of insecticidal delta-endotoxin from *Bacillus thuringiensis* at 2.5 Å resolution. *Nature* **353**, 815-821

Li, Y.F., Li, D.F., Zang, Z.H. and Wang, D.C. (2006) Trimeric structure of the wild soluble chloride intracellular ion channel CLIC4 observed in crystals. *Biochem. Biophys. Res. Comm.* **343,** 1272-1278

Lindeberg, M., Zakharov, S.D. and Cramer, W.A. (2000) Unfolding pathway of the colicin E1 channel protein on a membrane surface. *J. Mol. Biol.* **295,** 679-692

Linderstrøm-Lang, K. (1924) *Compt. Rend. Trav. Lab. Carlsberg* **15**, 7

Littler, D.R., Harrop, S.J., Fairlie, D., Brown, L.J., Pankhurst, G.J., Pankhurst, S., DeMaere, M.Z., Campbell, T.J., Bauskin, A.R., Tonini, R., Mazzanti, M., Breit, S.N., and Curmi, P.M.G. (2004) The intracellular chloride ion channel protein CLIC1 undergoes a redox-controlled structural transition. *J. Biol. Chem.* **279,** 9298-9305

Littler, D. R., Assaad, N.N., Harrop, S.J., Brown, L.J., Pankhurst, G.J., Luciani, P., Aguilar, M-I., Mazzanti, M., Berryman, M.A., and Breit, S.N. (2005) Crystal structure of the soluble form of the redox-regulated chloride ion channel protein CLIC4. *FEBS J.* **272,** 4996-5007

Llinas, M. and Klein, M.P. (1975) Charge relay at the peptide bond. A proton magnetic resonance study of solvation effects on the amide electron density distribution. *J. Am. Chem. Soc.* **97**, 731-737

London, E. (1992) Diphtheria toxin: membrane interaction and membrane translocation. *Biochim. Biophys. Acta.* **1113,** 25-51

Luo, J-K., Hornby, J.A.T., Wallace, L.A., Chen, J., Armstrong, R.N., and Dirr, H.W. (2002) Impact of domain interchange on conformational stability and equilibrium folding of dimeric class μ glutathione transferases. *Protein Sci.* **11,** 2208-2217

Luo, P. and Baldwin, R.L. (1997) Mechanism of helix induction by trifluoroethanol: a framework for extrapolating the helix-forming properties of peptides from trifluoroethanol / water mixtures back to water. *Biochemistry* **36,** 8413-8421

Luque, I., Leavtt, S.A., and Freire, E. (2002) The linkage between protein folding and functional cooperativity: two sides of the same coin? *Annu. Rev. Biophys. Biomol. Struct.* **31**, 235-256

Lusitani, D. Menhart, N., Keiderling, T.A., Fung, L.W-M (1998) Ionic strength effect on the thermal unfolding of alpha-spectrin peptides. *Biochemistry* **37**, 1656-1654

Makarov, D.E., Keller, C.A., Plaxco, K.W. and Metiu, H. (2001) How the folding rate constant of simple, single domain proteins depends on the number of native contacts. *Proc. Natl. Acad. Sci.* **99,** 3535-3539

Makhatadze, G.I., Lopez, M.M., Richardson III, J.M., and Thomas, S.T. (1998) Anion binding to the ubiquitin molecule. *Protein Sci.* **7**, 689-697

Manceva, S.D., Pusztai-Carey, M. and Butko, P. (2004) Effect of pH and ionic strength on the cytolytic toxin Cyt1A: a fluorescence spectroscopy study. *Biochim. Biophys. Acta* **1699,** 123-130

Maniatis, T. and Fristsch, E.F. (1982) Sambrook *J. Mol. Cloning*: a laboratory manual. Cold Spring Harbor, N.Y.: Cold Spring Harbor Laboratory Publications

Marqusee, S., Robbins, V.H. and Baldwin, R.L. (1989) Unusually stable helix formation in short alanine-based peptides. *Proc. Natl. Acad. Sci.* **86,** 5286-5290

Martin, J.L. (1995) Thioredoxin- a fold for all reasons. *Structure* **3**, 245-250

Matthew, J.B. (1985) Electrostatic effects in proteins. *Ann. Rev. Biophys. Biophys. Chem.* **14,** 387-417

Mathews, C. K. and van Holde, K.E. (1995) *Biochemistry* 2nd edition: The matrix of life: weak interactions that make up the aqueous environment, pp 25-54, The Benjamin/Cummings publishing company, inc, Menlo Park, CA.

Matouschek, A., Otzen, D.E., Itzhaki, L.S., Jackson, S.E. and Fersht. A.R. (1995) Movement of the position of the transition state in protein folding. *Biochemistry* **34**, 13656-13662

Matulis, D. and Lovrein, R. (1998) 1-anilino-8-naphthalene-sulphonate anion-protein binding depends primarily on ion pair formation. *Biophys. J.* **74,** 422-429

Mauring, K., Deich, J., Rosell, F.I., McAnaney, T.B., Moerner, W.E. and Boxer, S.G. (2005) Enhancement of the blue fluorescent proteins by high pressure or low temperature. *J. Phys. Chem.* **109,** 12976-12981

McLaughlin, S. (1989) The electrostatic properties of membranes. *Annu. Rev. Biophys. Biophys. Chem.* **18,** 113-136

Menestrina, G., Forti, S., and Gambale, F. (1989) Interaction of tetanus toxin with lipid vesicles. Effects of pH, surface charge, and transmembrane potential on the kinetics of channel formation. *Biophys J.* **55,** 393-405

Minn, A.J., Velez, P., Schendel, S.L., Liang, H., Muchmore, S.W., Fesik, S.W., Fill, M., and Thompson, C.B. (1997) Bcl-x_L forms an ion channel in synthetic lipid membranes. *Nature* **385,** 353-357

Mirsky, A.E., and Pauling, L. (1936) On the structure of native, denatured and coagulated proteins. *Proc. Natl. Acad. Sci.* **22,** 439-447

Money, T.T., King, R.G., Wong, M.H., Stevenson, J.L., Kalionis, B., Erwich, J.J., Huisman, M.A., Timmer, A., Hiden, U., Desoye, G. and Gude, N.M. (2006) Expression and cellular localisation of chloride intracellular channel 3 in human placenta and fetal membranes. *Placenta* in press

Muchmore, S.W., Sattlen, M., Liang, H., Meadows, R.P., Harlan, J.E., Yoon, H.s., Nettesheim, D., Chang, B.S., Thompson, C.B., Wong, S.L., Ng, S.L., and Fesik, S.W. (1996) X-ray and NMR structure of human Bcl-xL, an inhibitor of programmed cell death. *Nature* **381,** 335-341

Mukaiyama, A., Takano, K., Haruki, M., Morikawa, M. and Kanaya, S. (2004) Kinetically robust monomeric protein from a hyperthermophile. *Biochemistry* **43,** 13859-13866

Murphy, K.P. (1995) in *Protein Stability and Folding Theory and Practice* (Shirley, B.A., Ed.) pp 1-34, Boehringer Ingelheim Pharmaceuticals, Inc., Ridgefield, CT

Murray, D., Arbuzova, A., Hangyas-Mihalyne, G., Gambhir, A., Ben-Tal, N., Honig, B. and McLaughlin, S. (1999) Electrostatic properties of membranes containing acidic lipids and adsorbed basic peptides: Theory and experiment. *Biophys. J.* **77,** 3176-3188

Murzin, A.G., Brenner, S. E., Hubbard, T., Chothia, C. (1995). SCOP: a structural classification of proteins database for the investigation of sequences and structures. *J. Mol. Biol.* **247**, 536-540 http://scop.mrc-lmb.cam.ac.uk/scop/

Myers, J.K., Pace, C.N. and Scholtz, J.M. (1995) Denaturant *m*-values and heat capacity changes: relation to changes in accessible surface areas of protein unfolding. *Protein Sci.* **4**, 2138-2148

Myers, J.K. and Oas, T.G. (2001) Preorganized secondary structure as an important determinant of fast protein folding. *Nat. Struct. Biol.* **8,** 552-558

Myers, K., Somanlath, P.R., Berryman, M. and Visavaraghavan, S. (2004) Identification of chloride intracellular channel proteins in spermatozoa. *FEBS Lett.* **566,** 136-140

Neet, K.E., and Timm, D.E. (1994) Conformational stability of dimeric proteins: Quantitative studies by equilibrium denaturation. *Protein Sci.* **3**, 2167-2174

Nishii, I., Kataoka, M. and Goto, Y. (1995) Thermodynamic stability of the molten globule states of apomyoglobin (1995) *J. Mol. Biol.* **250,** 223-238

Nishizawa, T., Nago, T., Iwatsubo, T., Forte, J.G., and Urshidani, T. (2000) Molecular cloning and characterisation of a novel chloride intracellular channel-related protein, parchorin expressed in water secreting cells. *J. Biol. Chem.* **275**, 11164-11173

Novarino, G., Fabrizi, C., Tonini, R., Denti, M.A., Malchiodi-Albedi, F., Lauro, G.M., Sacchetti, B., Paradisi, S., Ferroni, A., Curmi, P.M., Breit, S.N. and Mazzanti, M. (2004) Involvement of the intracellular ion channel CLIC1 in microglia-mediated β-amyloid-induced neurotoxicity. *J. Neurosci.* **24,** 5322-5330

Oakley, A.J., Rossjohn, J., Lo Bello, M., Caccuri, A.M., Federici, D., and Parker, M.W. (1997) The three dimensional structure of the human Pi class glutathione transferase P1-1 in complex with the inhibitor ethacrynic acid and its glutathione conjugate. *Biochemistry* **36**, 576-585

Oakley, A.J. (2005) Glutathione transferases: new functions. *Curr. Opin. Struct. Biol.* **15,** 716-723

Ogasahara, K., Matsushita, E., and Yutani, K. (1993) Further examination of the intermediate state in the denaturation of the tryptophan synthase α subunit:

evidence that the equilibrium denaturation intermediate is a molten globule. *J. Biol. Chem.* **234,** 1197-1206

Ogasahara, K., and Yutani, K. (1994) Unfolding-refolding kinetics of the tryptophan synthase α subunit by CD and fluorescence measurements. *J. Mol. Biol.* **236,** 1227-1240

Oliveberg, M., Vuilleumier, S., and Fersht, A.R. (1994) Thermodynamic study of the acid denaturation of Barnase and its dependence on ionic strength: evidence for residual electrostatic interactions in the acid/thermally denatured state. *Biochemistry* **33**, 8826-8832

Otzen, D.E. and Oliveberg, M. (1999) Salt-induced detour through compact regions of the protein folding landscape. *Proc. Natl. Acad. Sci.* **96**, 11746-11751

Ozkan, S.B., Dill, K.A., and Bahar, I. (2002) Fast folding protein kinetics, hidden intermediates and the sequential stabilisation model. *Protein Sci.* **11,** 1958-1970

Pace, C.N. and Tanford, C. (1968) Thermodynamics of the unfolding of beta lactoglobulin A in aqueous urea solutions between 5 and 55 degrees. *Biochemistry* **7,** 198-208

Pace, C.N., (1986a) Determination and analysis of urea and guanidine hydrochloride denaturation curves. *Methods in Enzymology* **131**, 266-280

Pace, C.N., (1986b) in *Enzyme structure*, *Part L* (Hirs, C.H.W., and Timasheff, S.N., Eds.) pp 266-280, Academic Press, Inc.

Pace, C.N., Shirley, B.A., McNutt, M., Gajiwala, K. (1996) Forces contributing to the conformational stability of proteins. *FASEB J.* **10,** 75-83

Pace, C.N. and Scholtz, J.M. (1997) in *Protein Structure: a practical approach* (Creighton, T.E. ed.) 2nd edition, pp 299-321, IRL Press, Oxford University Press, Oxford.

Pace, C.N., Alston, R.W. and Shaw, K.L. (2000) Charge-charge interactions influence the denatured state ensemble and contribute to protein stability. *Protein Sci.* **9,** 1395-1398

Pagliari, L.J., Kuwana, T., Bonzon, C., Newmeyer, D.D., Tu, S., Beere, H.M. and Green, D.R. (2005) The multidomain proapoptotic molecules Bax and Bak are directly activated by heat. *Proc. Natl. Acad. Sci.* **102,** 17975-17980

Pande, V.S. (2003) Meeting halfway on the bridge between protein folding theory and experiment. *Proc. Natl. Acad. Sci.* **100,** 3555-3556

Parker, M.J. and Marqusee, S. (1999) The cooperativity of burst phase reactions explored. *J. Mol. Biol.* **293,** 1195-1210

Parker, M.W., Postma, J.P.M., Pattus, F., Tucker, A.D. and Tsernoglou, P. (1992) Refined structure of the pore-forming domain of Colicin A at 2.4Å resolution *J. Mol. Biol.* **224**, 639-657

Parker, M.W., and Pattus, F. (1993) Rendering a membrane protein soluble in water: a common packing motif in bacterial protein toxins. *Trends in Biochem. Sci.* **18**, 391-395

Parker, M.W. and Feil, S.C. (2005) Pore-forming protein toxin: from structure to function. *Prog. Biophys. Mol. Biol.* **88**, 91-142

PDBsum database of the known 3D structures of proteins and nucleic acids http://www.biochem.ucl.ac.uk/bsm/pdbsum/

Peitzsch, R.M, Eisenberg, M., Sharp, K.A. and McLaughlin, S. (1995) Calculations of the electrical potential adjacent to model phospholipid bilayers. *Biophys. J.* **68,** 729-738

Perrett, S., Freeman, S.J., Butler, P.J.G., and Fersht, A.R. (1999) Equilibrium folding properties of the yeast prion protein determinant Ure2. *J. Mol. Biol.* **290,** 331-345

Plaxco, K.W., Simons, K.T. and Baker, D. (1998) Contact order, transition state placement and the refolding rates of single domain proteins. *J. Mol. Biol.* **277,** 985-994

Plaxco, K.W., Simons, K.T., Ruczinski, I. and Baker, D. (2000) Topology, stability, sequence and length: defining the determinants of two-state protein folding kinetics. *Biochemistry* **39,** 11177-11183

Plaxco, K.W., and Gross, M. (2001) Unfolded, yes but random? Never! *Nat Struct. Biol.* **8,** 659-660

Prajapati, S., Bhakuni, V., Abu, K.R., and Jain, S. (1998) Alkaline unfolding and salt-induced folding of bovine liver catalase at high pH. *Eur. J. Biochem.* **255,** 178-184

Prats, M., Teissie, J. and Tocanne, J-F. (1986) Lateral proton conduction at lipid-water interfaces and its implications for the chemiosmotic hypothesis. *Nature* **322,** 756-758

Privalov, P.L. (1992) in *Protein Folding* (Creighton, T.E. ed.) pp 83-126, W. H. Freeman and Company, New York

Promdonkoy, B., and Ellar, D.J. (2003) Investigation of the pore-forming mechanism of a cytolytic δ-endotoxin from *Bacillus thuringiensis. Biochem. J.* **374,** 255-259

Proutski, I., Karoulias, N., and Ashley, R.H. (2002) Over-expressed chloride intracellular channel protein CLIC4 (p64H1) is an essential component of novel plasma membrane anion channels. *Biochem. Biophys. Res. Commun.* **297,** 317-322

Qi, P.X., Sosnick, T.R. and Englander, S.W. (1998) The burst phase in ribonuclease a folding and solvent dependence of the unfolded state. *Nature Struct. Biol.* **5,** 882-884

Qian, Z., Okuhara, D., Abe, M., and Rosner, M.R., (1999) Molecular cloning and characterization of a mitogen-activated protein kinase associated intracellular chloride channel. *J. Biol. Chem.* **274**, 1621-7

Ragone, R. (2001) Hydrogen-bonding classes in proteins and their contribution to the unfolding reaction. *Protein Sci.* **10,** 2075-2082

Rausell, C., Pardo-Lopez, L., Sanchez, J., Munoz-Garay, C., Morera, C., Soberon, M. and Bravo, A. (2004) Unfolding events in the water-soluble monomeric Cry1Ab toxin during transition to oligomeric pre-pore and membrane-inserted pore channel. *J. Biol. Chem.* **279,** 55168-55175

Redhead, C.R., Edelman, A.E., Brown, D., Landry, D.W., al-Awqati, Q. (1992) A ubiquitous 64-kDa protein is a component of a chloride channel of plasma and intracellular membranes. *Proc. Natl. Acad. Sci.* **89,** 3716-3720

Roder, H., and Colón, W. (1997) Kinetic role of early intermediates in protein folding. *Curr. Opin. Struct. Biol.* **7,** 15-28

Roder, H., Előve, G.A., and Shastry, M.C.R., (2000) in *Mechanisms of Protein Folding,* second edition (Pain, R. H., ed) pp 65-104, Oxford University Press, Great Britain

Rossjohn, J., Polekhina, G., Feil, S.C., Allocati, N., Masulli, M., Di Ilio, C. and Parker, M.W. (1998) A mixed disulphide bond in bacterial glutathione transferase: functional and evolutionary implications. *Structure* **6**, 721-734

Royer, C.A. (1995) in *Methods in Molecular Biology, Vol 40: Protein Stability and Folding: Theory and Practice* (Shirley, B. A., ed) pp 65-89, Humana Press Inc., Totowa, NJ

Rumbley, J., Hoang, L., Mayne, L. and Englander, S.W. (2001) An amino acid code for protein folding. *Proc. Natl. Acad. Sci.* **98,** 105-112

Sacchetta, P., Aceto, A., Bucciarelli, T., Dragani, B., Santarone, S., Allocati, N., and Di Ilio C. (1993) Multiphasic denaturation of glutathione transferase B1-1 by guanidinium chloride. Role of the dimeric structure on the flexibility of the active site. *Eur. J. Biochem.* **215**, 741-745

Sadeghi, M., Naderi-Manesh, H., Zarrabi, M. and Ranjbar, B. (2006) Effective factors in thermostability of thermophilic proteins. *Biophys. Chem.* **119,** 256-270

Saeki, K., Yasug, E., Okuma, E., Breit, S.N., Nakamura, M., Toda, T., Kaburagi, Y. and You, A. (2005) Proteomic analysis on insulin signalling in human hematopoietic cells: identification of CLIC1 and SRp20 as novel downstream effectors of insulin. *Am. J. Physiol. Endocrinol. Metab.* **289,** E419-E428

Sakai, K., Sakurai, K., Sakai, M., Hoshino, M. and Goto, Y. (2000) Conformation and stability of thiol-modified bovine β-lactoglobulin. *Protein Sci.* **9,** 1719-1729

Santoro, M.M., and Bolen, D.W. (1992) A test of the linear extrapolation of unfolding free energy changes over an extended denaturant concentration range. *Biochemistry* **31,** 4901-4907

Sayed, Y., Hornby, J.A.F., Lopez, M., and Dirr, H. (2002) Thermodynamics of the ligandin function of human class Alpha glutathione transferase A1-1: energetics of organic anion ligand binding. *Biochem. J* **363,** 341-346

Scandurra, R., Consalvi, V., Ciaraluce, R., Politi, L. and Engel, P.C. (1998) Protein thermostability in extremophiles. *Biochimie* **80,** 933-941

Schendel, S.L., Xie, Z., Montal, M.O., Matsyama, S., Montal, M. and Reed, J.C. (1997) Channel formation by antiapoptotic protein Bcl-2. *Proc. Natl. Acad. Sci.* **94,** 5113-5118

Schindler, T., Herrler, M., Marahiel, M.A., Schmid, F.X. (1995) Extremely rapid protein folding in the absence of intermediates. *Nat. Struct. Biol.* **2,** 663-673

Schlesinger, P.H., Blair, H.C., Teitelbaum, S.T., and Edwards, J.C. (1997) Characterisation of the osteoclast ruffled border chloride channel and its role on bone resorption. *J. Biol. Chem.* **272,** 18636-18643

Semisotnov, G.V., Rodionova, N.A., Razgulyaev, O.I., Uversky, V.N., Gripas, A.F., and Gilmanshin, R.I. (1991) Study of the "molten globule" intermediate state in protein folding by a hydrophobic fluorescence probe. *Biopolymers* **31,** 119-128

Setterdahl, A.T., Chivers, P.T., Hirasawa, M., Lemaire, S.D., Keryer, E., Miginiac-Maslow, M., Kim, S-K., Mason, J., Jaquot, J-P., Longbine, C.C., de Lamotte-Guery, F., and Knaff, D.B. (2003) Effect of pH on the oxidation-reduction properties of thioredoxins. *Biochemistry* **42,** 14877-14884

Shakhonovich, E.I. and Finkelstein, A.V. (1989) Theory of cooperative transitions in protein molecules I. Why denaturation of globular proteins is a first order phase transition. *Biopolymers* **28**, 1667-1680

Shanks, R.A., Larocca, M.C., Berryman, M., Edwards, J.C., Urushidani, T., Navarre, J., and Goldenring, J.R. (2002) AKAP350 at the Golgi apparatus. II. Association of AKAP350 with a novel chloride intracellular channel (CLIC) family member. *J. Biol. Chem.* **277,** 40973-40980

Shastry, M.C. and Roder, H. (1998) Evidence for barrier-limited protein folding kinetics on the microsecond timescale. *Nature Struct. Biol.* **5,** 358-392

Shaw, K.L., Grimsley, G.R., Yakolev, G.I., Makarov, A.A. and Pace, C.N. (2001) The effect of net charge on the solubility, activity and stability of ribonuclease Sa. *Protein Sci.* **10,** 1206-1215

Sheehan, D., Meade, G., Foley, V.M. and Dowd, C.A. (2001) Structure function and evolution of glutathione transferases: implications for classification of non-mammalian members of an ancient enzyme superfamily. *Biochem. J.* **360,** 1-16

Shimizu, S. and Chan, H.S. (2002) Origins of protein denatured state compactness and hydrophobic clustering in aqueous urea: inferences from nonpolar potentials of mean force. *Proteins, Struct. Funct. Genet.* **49**, 560-566

Shiraki, K., Nishikawa, K. and Goto, Y. (1995) Trifluoroethanol-induced stabilisation of the α-helical structure of β-lactoglobulin: implication for non-hierarchical protein folding. *J. Mol. Biol.* **245,** 180-194

Shirley, B.A., (1995) in *Methods in Molecular Biology, Vol 40: Protein Stability and Folding: Theory and Practice* (Shirley, B. A., ed) pp 177-190, Humana Press Inc., Totowa, NJ

Shorning, B.Y., Wilson, D.B., Meehan, R.R., and Ashley, R.H. (2003) Molecular cloning and developmental expression of two Chloride Intracellular Channel (CLIC) genes in *Xenopus laevis. Dev. Genes Evol.* **213,** 514-514

Shortle, D., and Ackerman, M.S. (2001) Persistence of native-like topology in a denatured protein in 8 M urea. *Science* **293,** 487-489

Singh, H. and Ashley, R.H. (2006) Redox regulation of CLIC1 by cysteine residues associated with the putative channel pore. *Biophys J.* **90,** 1628-1638

Sinning, I., Kleywegt, G.J., Cowan, S.W., Reinemer, P., Dirr, H.W., Huber, R., Gilliland, G.L., Armstrong, R.N., Ji, X., Board, P.G., Ohin, B., Mannervik, B. and Jones, T.A. (1993) Structure determination and refinement of human Alpha class glutathione transferase A1-1 and a comparison with the Mu and Pi class enzymes. *J. Mol. Biol.* **232,** 192-212

Soulages, J.L. (1998) Chemical denaturation: Potential impact of undetected intermediates in the free energy of unfolding and *m*-values obtained from a two-state assumption. *Biophys. J.* **75**, 484-492

Spooner, R.A., Watson, P.D., Marsden, C.J., Smith, D.C., Moore, K.A., Cook, J.P., Lord, J.M. and Roberts, L.M. (2004) Protein disulphide-isomerase reduces ricin to it's a and B chains in the endoplasmic reticulum. *Biochemistry* **383,** 285-293

Spolar, R.S. and Record, M.T. (1994) Coupling of local folding to site-specific binding of proteins to DNA. *Science* **263,** 777-784

Spudich, G. and Marqusee, S. (2000) A change in the apparent *m*-value reveals a populated intermediate under equilibrium conditions in *Escherichia coli* ribonuclease H1. *Biochemistry* **39,** 11677-11683

Stevens, J.M., Hornby, J.A.T., Armstrong, R.N., and Dirr, H.W. (1998) Class Sigma glutathione transferase unfolds via a dimeric and a monomeric

intermediate: impact of subunit interface on conformational stability in the superfamily. *Biochemistry* **37**, 15534-15541

Stevens, J.M., Armstrong, R.N., and Dirr, H.W. (2000) Electrostatic interactions affecting the active site of class Sigma glutathione S-transferase. *Biochem. J.* **347,** 193-197

Stigter, D. and Dill, K.A. (1990) Charge effects on folded and unfolded proteins. *Biochemistry* **29,** 1262-1271

Strippoli, P., D'Addabbo, P., Lenzi, L., Giannone, S., Canaider, S., Casedei, R., Vitale, L., Carinci, P. and Zannotti, M. (2002) Segmental paralogy in the human genome: a large-scale triplication on 1p, 6p and 21q. *Mamm. Genome.* **13,** 456-462

Strop, P., and Mayo, S.L. (2000) Contribution of surface salt bridges to protein stability. *Biochemistry* **39,** 1251-1255

Stryler, L. (1965) The interaction of a naphthalene dye with apomyoglobin and apohemoglobin. A fluorescent probe of non-polar binding sites. *J. Mol. Biol.* **13,** 482-495

Suginta, W., Karoulias, N., Aitken, A. and Ashley, R.H. (2001) Chloride intracellular channel protein CLIC4 (p64H1) binds directly to brain dynamin I in a complex containing actin, tubulin and 14-3-3 isoforms. *Biochem. J.* **359,** 55-64

Suh, K.S., Mutoh, M., Nagashima, K., Fernandez-Salas, E., Edwards, L.E. and Hayed, D.D. (2005) Antisense suppression of the chloride intracellular family induces apoptosis, enhances tumour necrosis factor α-induced apoptosis, and inhibits tumour growth. *Cancer Res.* **65,** 562-571

Suzuki, M., Youle, R.J., and Tjandra, N. (2000) Structure of Bax. Co regulation of dimer formation and intracellular localization. *Cell* **103**, 645-654

Swietnicki, W., Peterson, R., Gambetti, P., and Surewicz, W.K. (1997) pH-dependent stability and conformation of the recombinant human prion protein PrP (90-231). *J. Biol. Chem.* **272,** 27517-27520

Szeltner, Z. and Polgar, L. (1996) Conformational stability and catalytic activity of HIV-1 protease are both enhanced at high salt concentration. *J. Biol. Chem.* **271,** 5458-5463

Takano, K., Yamagata, Y., Funahashi, J., Hioki, Y., Kuramitsu, S. and Yutani, K. (1999) Contribution of intra- and intermolecular hydrogen bond to the conformational stability of human lysozyme. *Biochemistry* **38,** 12698-12708

Takano, K., Tsuchimori, K., Yamagata, Y. and Yutani, K. (2000) Contribution of salt bridges near the surface of a protein to the conformational stability. *Biochemistry* **39,** 12375-12381

Takano, K., Scholtz, J.M., Sacchettini, J.C., and Pace, C.N. (2003) The contribution of polar group burial to protein stability is strongly context-dependent. *J. Biol. Chem.,* **278,** 31790-31795

Tan, Y.J., Oliveberg, M., Davis, B. and Fersht, A.R. (1995) Perturbed pK_a-values of the denatured states of proteins. *J. Mol. Biol.* **254**, 980-992

Tanford, C. (1961) Physical chemistry of macromolecules. John Wiley and Sons, Inc., New York

Tanford, C., Kawahara, K., and Lapanje, S. (1967) Proteins as random coils. I. Intrinsic viscosities and sedimentation coefficients in concentrated guanidine hydrochloride. *J. Am. Chem. Soc.* **89**, 729-736.

Tanford, C. (1970) Protein denaturation C. Theoretical models for the mechanism of denaturation *Adv. Protein Chem.* **24,** 1-95

Tejuca, M., Dalla Serra, M., Ferreras, M., Lanio, M. E. and Menestrina, G. (1996) Mechanism of membrane permeabilisation of sticholysin I, a cytolysin isolated from the venom of the sea anemone *Stichodactyla helianthus. J. Membr. Biol.* **183,** 125-135

Thomas, P.P., and Dill, K.A. (1993) Local and non-local interaction in globular proteins and methods of alcohol denaturation. *Protein Sci.* **2,** 2050-2065

Thompson, L.C., Walters, J., Burke, J., Parsons, J.F., Armstrong, R.N. and Dirr, H.W. (2006) Double mutation at the subunit interface of glutathione transferase rGSTM1-1 results in a stable, folded monomer. *Biochemistry* **45,** 2267-2273

Thual, C., Bousset, L., Komar, A.A., Walter, S., Buchner, J., Cullin, C., and Melki, R. (2001) Stability, folding, dimerisation and assembly properties of the yeast prion Ure2p. *Biochemistry* **40,** 1764-1773

Thuduppathy, G.R., and Hill, R.B. (2005) Acid destabilisation of the solution conformation of Bcl-$_{XL}$ does not drive its pH-dependent insertion into membranes. *Protein Sci.* **15,** 1-10

Thuduppathy, G.R., Craig, J.W., Kholodenko, V., Schon, A. and Hill, B. (2006) Evidence that membrane insertion of the cytosolic domain of Bcl-$_{XL}$ is governed by an electrostatic mechanism. *J. Mol. Biol.* **359,** 1045-1058

Tilley, S.J. and Saibil, H. R. (2006) The mechanism of pore formation by bacterial toxins. *Curr. Opin. Struct. Biol.* **16,** 230-236

Tonini, R., Ferroni, A., Valenzuela, S.M., Warton, K., Campbell, T.J., Breit, S.N. and Mazzanti, M. (2000) Functional characterisation of the NCC27 nuclear protein in stable transfected CHO-K1 cells. *FASEB J.* **14,** 1171-1178

Torchinsky, Y.M. (1981) Sulphur in proteins. Pergamon press, Oxford

Tory, M.C. and Merrill, A.R. (1999) Adventures in membrane protein topology. A study of the membrane bound state of colicin E1. *J. Biol. Chem.* **274,** 24539-24549

Tulk, B.M., and Edwards, J.C. (1998) NCC27, a homologue of intracellular chloride channel p64, is expressed in brush border of renal proximal tubule. *Am. J. Physiol.* **274,** F1140-F1149

Tulk, B.M., Schlesinger, P.H., Kapadia, S.A., and Edwards, J.C. (2000) CLIC-1 functions as a chloride channel when expressed and purified from bacteria. *J. Biol. Chem.* **275**, 26986-26998

Tulk, B.M., Kapadia, S., and Edwards, J.C. (2002) CLIC1 inserts from the aqueous phase into phospholipid membranes, where it functions as an anion channel. *Am. J. Physiol. Cell Physiol.* **282**, C1103-C1112

Uchiyama, H., Perez-Prat, E.M., Watanabe, K., Kumagai. And Kuwajima, K. (1995) Effects of amino acid substitutions in the hydrophobic core of α-lactalbumin on the stability of the molten globule state. *Protein Eng.* **8,** 1153-1161

Ulrih, N.P., Anderluh, G., Maček, P. and Chalikian, T.V. (2004) Salt-induced oligomerisation of partially folded intermediates of equinatoxin II. *Biochemistry* **43,** 9536-9545

Urushidani, T., Chow, D., and Forte, J.G. (1999) Redistribution of a 120kDa phosphoprotein in the parietal cell associated with stimulation. *J. Membr. Biol.* **168,** 209-220

Valenzuela, S.M., Martin, D.K., Por, S.B., Robbins, J.M., Warton, K., Bootcov, M.R., Schofield, P.R., Campbell, T.J., and Breit, S.N. (1997) Molecular cloning and expression of a chloride ion channel of cell nuclei. *J. Biol. Chem.* **272**, 12575-12582

Valenzuela, S.M., Mazzanti, M., Tonini, R., Qui, M.R., Warton, K., Musgrove, E.A., Campbell, T.J., and Breit, S.N. (2000) The nuclear chloride ion channel NCC27 is involved in regulation of the cell cycle. *J. Physiol.* **529,** 541-552

Van der Goot, F.G., González-Manãs, J.M., Lakey, J.H., and Pattus, F. (1991) A 'molten-globule' membrane-insertion intermediate of the pore-forming domain of colicin A. *Nature* **354,** 408-410

Van der Vies, S.M., Viitanen, P.V, Gatenby, A.A., Lorimer, G.H. and Jaenicke, R. (1992) Conformational states of ribulosebishosphate carboxylase and their interaction with chaperonin 60. *Biochemistry* **31,** 3635-3644

Van Meer, G. (1989) Lipid traffic in animal cells. *Annu. Rev. Cell Biol.* **5**, 247-275

Vassilenko, K.S. and Uversky, V.N. (2002) Native-like secondary structure of molten globules. *Biochim. Biophys. Acta.* **1594,** 168-177

Vaz, W.L., Nisksch, A. and Jahnig, F. (1978) Electrostatic interactions at charged lipid membranes. Measurement of surface pH with fluorescence lipoid pH indicators. *Eur. J. Biochem.* **83,** 299-305

Vecsey-Semjen, B., Mollby, R. and Van der Goot, F.G. (1996) Partial C-terminal unfolding is required for channel formation by Staphylococcal α-toxin. *J. Biol. Chem.* **271,** 8655-8660

Vendruscolo, M., Paci, E., Dobson, C.M. and Karplus, M. (2001) Three key residues form a critical contact network in a transition state for protein folding. *Nature* **409,** 641-646

Vogt, G., Woell, S. and Argos, P. (1997) Protein thermal stability, hydrogen bonds and ion pairs. *J. Mol. Biol.* **269,** 631-643

Vu, D.M., Myers, J.K., Oas, T.G., and Dyer, R.B. (2004) Probing the folding and unfolding dynamics of secondary and tertiary structures in a three-helix bundle protein. *Biochemistry* **43**, 3582-3589

Wallace, L.A., Blatch, G.L., and Dirr, H.W. (1998a) A topologically conserved aliphatic residue in alpha-helix 6 stabilises the hydrophobic core of domain II of glutathione transferases and is a structural determinant for the unfolding pathway. *Biochem. J.* **336**, 413-418

Wallace, L.A., Sluis-Cremer, N. and Dirr, H.W. (1998b) Equilibrium and kinetic unfolding properties of dimeric human glutathione transferase A1-1. *Biochemistry* **37**, 5320-5328

Wallace, L.A., and Dirr, H.W. (1999) Folding and assembly of dimeric human glutathione transferase A1-1. *Biochemistry* **38**, 16686-16694

Wallace, L.A., Burke, J., and Dirr, H.W. (2000) Domain-domain interface packing at conserved Trp-20 in class α glutathione transferase impacts on protein stability. *Biochim. Biophys. Acta* **1478,** 325-332.

Wallace, L.A., and Matthews, C.R. (2002) Sequential vs. parallel protein-folding mechanisms: experimental tests for complex folding reactions. *Biophys. Chem.* **101-102,** 113-131

Wallace, L.A., and Dirr, H.W. (in preparation) Complex folding landscapes for homologous dimeric glutathione transferases and glutaredoxin-2, a monomeric variant, share common mechanistic features

Warton, K., Tonini, R., Fairlie, W.D., Mathews, J.M., Valenzuela, S.M., Qiu, M.R., Wu, W.M., Pankhurst, S., Bauskin, A.R., Harrop, S.J., Campbell, T.J., Curmi, P.M.G., Breit, S.N., and Mazzanti, M. (2002) Recombinant CLIC1 (NCC27) assembles in lipid bilayers via a pH-dependent two-state process to form chloride ion channels with identical characteristics to those observed in Chinese hamster ovary cells expressing CLIC1. *J. Biol. Chem.* **277**, 26003-26011

Warwicker, J. (1999) Simplified methods for pK_a and acid pH-dependent stability estimation in proteins: removing dielectric and counterion boundaries. *Protein Sci.* **8,** 418-425

Wedekind, J.E., Trame, C.B., Dorywalska, M., Koehl, P., Raschke, T.M., Mckee, M. Fitzgerald, D., Collier, R.J., and Mckay, D.B. (2001) Refined crystallographic structure of *Pseudomonas aeruginosa* exotoxin a and its implications for the molecular mechanism of toxicity. *J. Mol. Biol.* **314,** 823-829

Wei, Z. and Song, J. (2005) Molecular mechanism underlying the thermal stability and pH-induced unfolding of CHABII. *J. Mol. Biol.* **348,** 205-218

Weinreich, F. and Jentsch, T.J. (2001) Pores formed by single subunits in mixed dimers of different ClC chloride channels. *J. Biol. Chem.* **276,** 2347-2353

White, S.H. and Wimley, W.C. (1994) Peptides in lipid bilayers: Structural and thermodynamic basis for partitioning and folding. *Curr. Opin. Struct. Biol.* **24,** 113-117

White, S.H. and Wimley, W. C. (1999) Membrane protein folding and stability: physical principles. *Annu. Rev. Biophys. Biomol. Struct.* **28**, 319-65

White, S.H., Ladokhin, A.S., Jayasinghe, S. and Hristova, K. (2001) How membranes shape protein structure. *J. Biol. Chem.* **276,** 32395-32398

White, S.H. (2003) Translocons, thermodynamics, and the folding of membrane proteins. *FEBS. Lett.* **555,** 116-121

Whitten, S.T., and García-Moreno, B.E. (2000) pH dependence of stability of staphylococcal nuclease: evidence of substantial electrostatic interactions in the denatured state. *Biochemistry* **39**, 14292-14304

Whitten, S.T., Wooll, J.O., Razeghifard, R., Garcia-Moreno, E. and Hilser, V.J. (2001) The origin of pH-dependent changes in *m*-values for the denaturant-induced unfolding of proteins. *J. Mol. Biol.* **309**, 1165-1175

Whitten, S.T., Garcia-Moreno, B.E. and Hilser, V.J. (2005) Local conformational fluctuations can modulate the coupling between proton binding and global structural transitions in proteins. *Proc. Natl. Acad. Sci.* **102**, 4282-4287

Wittung-Stafshede, P. (2004) Slow unfolding explains high stability of thermostable ferredoxins: common mechanism governing thermostability. *Biochim. Biophys. Acta* **1700**, 1-4

Wojtasek, H. and Leal, W.S. (1999) Conformational change in the pheromone-binding protein from *Bombyx mori* induced by pH and by interaction with membranes. *J. Biol. Chem.* **274,** 30950-30956

Wolter, K.G., Hsu, Y.T., Smith, C.L., Nechushtan, A., Xi, X.G., and Youle, R.J. (1997) Movement of Bax from the cytosol to mitochondria during apoptosis. *J. Cell Biol.* **139,** 1281-1292

Wolynes, P.G., Onuchic, J.N. and Thirumalai, D. (1995) Navigating the folding routes. *Science* **267,** 1619-1623

Woody, R.W. (1995) Circular dichroism. *Methods in Enzymology* **246**, 34-71

Wu, L.C. and Kim, P.S. (1998) A specific hydrophobic core in the α-lactalbumin molten globule. *J. Mol. Biol.* **280,** 175-182

Xia, B., Vlamis-Gardikas, A., Holmgren, A., Write, P.E., and Dyson, J. (2001) Solution structure of *Escherichia coli* glutaredoxin2 shows similarity to mammalian glutathione S- transferases *J. Mol. Biol.* **310**, 907-918

Xie, Z., Schendel, S., Matsuyama, S. and Reed, J.C. (1998) Acidic pH promotes dimerization of Bcl-2 family proteins. *Biochemistry* **37,** 6410-6418

Yao, M. and Bolen, D.W. (1995) How valid are denaturant-induced unfolding free energy measurements? Level of conformance to common assumptions over an extended range of ribonuclease A stability. *Biochemistry* **34**, 3771-3781

Yassin, Z., Clemente-Jiménez, M.J., Téllez-Sanz, R. and García-Fuentes, L. (2003) Salt influence on glutathione-*Schistosoma japonicum* glutathione S-transferase binding. *Int. J. Biol. Macromol.* **31,** 155-162

Yau, W-M., Wimley, W.C., Gawrisch, K. and White, S.H. (1998) Preference of tryptophan for membrane interfaces. *Biochemistry* **37,** 14713-14718

Yethon, J.A., Epand, R.F., Leber, B., Epand, R.M. and Andrews, D.W. (2003) Interaction with a membrane surface triggers a reversible conformational change in Bax normally associated with induction of apoptosis. *J. Biol. Chem.* **278,** 48935-48941

Zakharov, S.D. and Cramer, WA. (2002) Colicin crystal structures: pathways and mechanisms for colicin insertion into membranes. *Biochim. Biophys. Acta* **1565,** 333-346

Zakharov, S.D., Kotova, E.A., Antonenko, Y.N., and Cramer, W.A. (2004) On the role of lipid in colicin pore formation. *Biochim. Biophys. Acta* **1666,** 239-249

Zavodszky, P., Kardos, J., Svingor, A. and Petsko, G.A. (1998) Adjustment of conformational flexibility is a key event in the thermal adaptation of proteins. *Proc. Natl. Acad. Sci.* **95,** 7406-7411

Zhao, J-M., and London, E. (1986) Similarity of the conformation of diphtheria toxin at high temperature to that in the membrane-penetrating low-pH state. *Proc. Natl. Acad. Sci.* **83,** 2002-2006